UNIVERSITÀ DEGLI STUDI
DI SASSARI

FACOLTÀ DI AGRARIA

DIPARTIMENTO DI ECONOMIA E SISTEMI ARBOREI

Scuola di Dottorato di Ricerca in

Scienze dei Sistemi Agrari e Forestali e delle Produzioni Alimentari

Indirizzo di:

Agrometeorologia ed Ecofisiologia dei Sistemi Agrari e Forestali

XXII ciclo

CLIMATE CHANGE IMPACT ON DURUM WHEAT IN SARDINIA

Docenti guida:

Prof. Donatella Spano
Dr. Carla Cesaraccio

Coordinatore di Indirizzo

Prof. Donatella Spano

Direttore della Scuola:

Chiar.mo Prof. Piero Deidda

Dottorando:

Dr. Valentina Mereu

Anno Accademico 2008/2009

La nostra conoscenza,

se paragonata alla realtà, è primitiva e infantile.

Eppure è il bene più grande di cui disponiamo.

Albert Einstein

CONTENTS

ABSTRACT

The high sensitivity of agriculture to climate conditions and the great uncertainty on the combined effects of increasing in CO_2 concentration and changes in temperature and rainfall patterns on crops growth and development, reveal the crucial importance of focusing researches in this field. While individual effects of higher temperatures, elevated CO_2 and changed rainfall patterns on agriculture are relatively well known, very few studies have adressed the issue of interactions between different effects of climate change, which is pivotal in improving the ability of evaluating climate change impact on crops.

Moreover, developing our understanding of the climate change science and its impacts is necessary both to identify the most appropriate adaptation strategies and actions for territorial planning, and to search more effective mitigation strategies to cope with climate change.

Furthermore, considering the socio-economic importance of agriculture for food security, it is essential to undertake assessments of how future climate change could affect crop yields, so as to provide necessary information to implement appropriate adaptation strategies.

In this perspective, the aim of this study was to assess potential climate change impact and changing in ambient carbon dioxide (CO_2) levels on production and phenology for two of the most important varieties of durum wheat at four experimental sites in Sardinia, differents for soil, climate conditions and management practices, and provide directions for possible adaptation strategies.

The CERES-Wheat model in combination with a stochastic Weather Generator (WG) were used to quantify the climate change impacts on wheat growth and production. The synthetic weather series, representing the future climates, are generated by modifying the WG parameters according to the features of a set of GCM-based climate change scenarios. Twenty-seven climate change scenarios were generated, for each experimental site, by pattern scaling thecnique, considering three values of climate sensitivity and four emission scenarios.

The use of this approach allowed to explore a wide range of possible future change in climate and give a more likely crop impact assessment.

The results obtained show changes in wheat yield and phenology differents for climate change scenarios, varieties and locations analysed. As in other similar studies, it is projected that the interaction of multiple factors, that seem to cancel each other out, may diluite the climate change impacts. The adaptation strategy considered (shift in planting date) seems a usefull strategy in response to climate change.

RIASSUNTO

L'elevata sensibilità dell'agricoltura alle condizioni climatiche e la grande incertezza relativa agli effetti combinati che le variazioni di temperatura e precipitazioni previste per i periodi futuri assieme all'incremento nella concentrazione atmosferica di CO_2 possono avere sulla crescita e lo sviluppo delle colture, rivelano l'importanza cruciale di concentrare le ricerche in questo campo. Mentre i singoli effetti di incremento delle temperature, riduzione delle precipitazioni e variazioni nella concentrazione atmosferica di CO_2 sulle colture sono relativamente ben conosciuti, ancora pochi studi hanno valutato le interazioni tra i diversi effetti del cambiamento climatico, che è fondamentale conoscere per migliorare la capacità di previsione dell'impatto dei cambiamenti climatici sulle colture.

Inoltre, conoscere meglio i potenziali impatti dei cambiamenti climatici sulle colture è di fondamentale importanza sia per individuare le più adeguate strategie di adattamento e prodisporre anche opportune azioni di pianificazione territoriale, sia per la ricerca di strategie di mitigazione più efficaci per far fronte ai cambiamenti climatici.

Considerando infatti l'importanza socio-economica del settore agricolo per la sicurezza alimentare, è indispensabile effettuare valutazioni di impatto finalizzate a fornire le informazioni necessarie per implementare adeguate strategie di adattamento.

In quest'ottica si inserisce il presente studio, con il principale obiettivo di effettuare la valutazione del potenziale impatto del cambiamento climatico e dell'aumentata concentrazione di biossido di carbonio (CO_2) in atmosfera, su produzione e fenologia di due delle varietà più importanti di grano duro (Simeto e Iride), per quattro siti sperimentali in Sardegna, differenti per il suolo, condizioni climatiche e pratiche di gestione, e di possibili strategie di adattamento in risposta al cambiamento climatico.

Il modello di simulazione colturale CERES-Wheat in combinazione con un generatore stocastico di dati meteorologici (WG) è stato utilizzato per quantificare l'effetto delle incertezze di scenari di cambiamento climatico sulla sviluppo e la produzione del frumento. Modificando i parametri del WG in base alle caratteristiche di una serie di scenari di cambiamento climatico basati sugli output di tre GCMs, sono state prodotte ventisette combinazioni di scenari di cambiamento climatico per ogni sito, utilizzando la tecnica di Pattern scaling, in considerazione di tre valori di climate sensitivity e di quattro scenari di emissione.

L'utilizzo di questo approccio permette di esplorare una vasta gamma di possibili cambiamenti futuri del clima e di dare di conseguenza una valutazione più probabile dell' impatto che tali variazioni potranno avere sulla coltura.

I risultati ottenuti mostrano che la resa a la fenologia del frumento variano in base allo scenario di cambiamento climatico, alle varietà e alla località considerate. In linea con altre ricerche analoghe, si è osservato che l'interazione di molteplici fattori, che sembrano annullarsi a

vicenda, può ridurre l'impatto dei cambiamenti climatici. Inoltre l'applicazione di alcune strategie di adattamento, quali ad esempio l'anticipo della data di semina, può consentire non solo di ridurre gli effetti negati dell'impatto del cambiamento climatico ma anche di giovare degli aspetti positivi ad esso associati.

INTRODUCTION

There is great attention and concern for the impact of climate change and its variability worldwide. The Intergovernmental Panel on Climate Change (IPCC) Fourth Assessment Report defines the climate change as a change in the state of the climate that can be identified (e.g. using statistical tests) by changes in the mean and/or the variability of its properties, and that persists for an extended period, typically decades or longer. It refers to any change in climate over time, whether due to natural variability or as a result of human activity. This definition differs from that one reported in the United Nations Framework Convention on Climate Change (UNFCCC), where climate change refers to a change of climate that is attributed directly or indirectly to human activity that alters the composition of the global atmosphere and that is in addition to natural climate variability observed over comparable time periods (IPCC, 2007).

Both at policy (UNFCCC) and science level (IPCC) climate change represent one of the priorities for action.

Climate system warming is unequivocal, as it is now evident from the observed increases in the global average air and ocean temperatures, the widespread melting of snow and ice and the rising global average sea level. There is a substantial new evidence that suggest that changes in terrestrial, marine and freshwater systems are now strongly influenced by observed recent global warming. A wide range of species and communities in terrestrial ecosystems is already strongly affecyed by recent changes in the climate system (IPCC, 2007).

Changes in the atmospheric concentrations of greenhouse gases (GHGs) and aerosols, land cover and solar radiation alter the energy balance of the climate system and are drivers of climate change. They affect the absorption, scattering and emission of radiation within the atmosphere and at the Earth's surface. The resulting positive or negative changes in energy balance due to these factors are expressed as radiative forcing[1], which is used to compare warming or cooling influences on global climate. The radiative forcing of the climate system is dominated by the long-lived GHGs.

Human activities result in emissions of four long-lived GHGs: carbon dioxide (CO_2), methane (CH_4), nitrous oxide (N_2O) and halocarbons (a group of gases containing fluorine, chlorine or bromine) (Figg. 1a, 1b). The global GHG emissions due to human activities have grown since pre-industrial times, with an increase of 70% (from 28.7 to 49.0 $GtCO_2$-eq) between 1970 and 2004. The atmospheric concentrations of GHGs increase when emissions are larger than removal processes.

[1] Radiative forcing is a measure of the influence a factor has in altering the balance of incoming and outgoing energy in the Earth-atmosphere system and is an index of the importance of the factor as a potential climate change mechanism. The radiative forcing values are expressed in watts per square metre (W/m2)(IPCC, 2007).

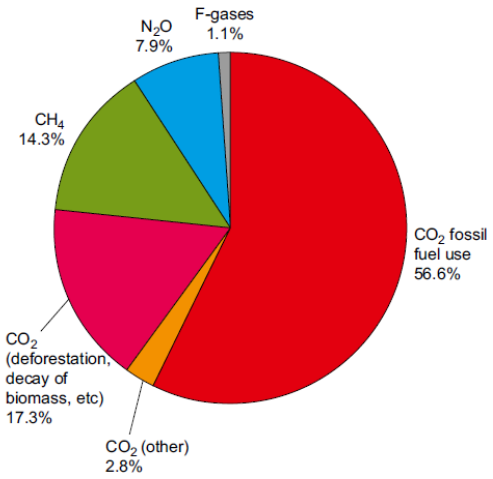

Figure 1a. Global anthropogenic greenhousegas emissions in 2004 (IPCC, 2007).

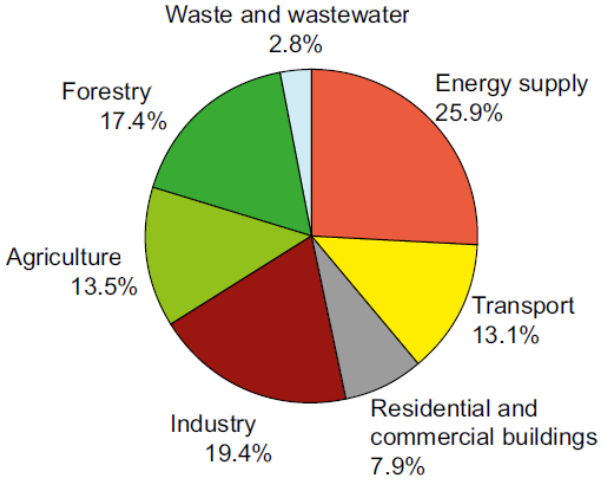

Figure 1b. Global anthropogenic greenhousegas emissions by sector in 2004 (IPCC, 2007).

Global Warming Potential (GWP) is a measure of how much a given mass of greenhouse gas is estimated to contribute to global warming, i.e. how much a given greenhouse gas contributes to Earth's radiative forcing. It is a simple measure whose calculation is based on a relative scale which compares the gas in question to that of the same mass of carbon dioxide. Carbon dioxide has a GWP of 1, by definition. A GWP is calculated over a specific time interval so the length of this time interval must be stated to make the value meaningful.

Global Warming Potentials (GWPs) are one type of simplified index based upon radiative properties that can be used to estimate the potential future impacts of emissions of different gases upon the climate system in a relative sense. GWP is based on a number of factors, including the radiative efficiency (infrared-absorbing ability) of each gas relative to that of carbon dioxide, as well as the decay rate of each gas (the amount removed from the atmosphere over a given number of years) relative to that of carbon dioxide.

An exact definition of how GWP is calculated is reported in the IPCC's 2001a Third Assessment Report. The GWP is defined as the ratio of the time-integrated radiative forcing from the instantaneous release of 1 kg of a trace substance relative to that of 1 kg of a reference gas:

$$GWP\,(x) = \frac{\int_0^{TH} a_x \cdot [x(t)]\,dt}{\int_0^{TH} a_r \cdot [r(t)]\,dt}$$

where *TH* is the time horizon over which the calculation is considered; a_x is the radiative efficiency due to a unit increase in atmospheric abundance of the substance (i.e., Wm^{-2} kg^{-1}) and [*x(t)*] is the time-dependent decay in abundance of the substance following an instantaneous release of it at time t=0. The denominator contains the corresponding quantities for the reference gas (i.e. CO_2). The radiative efficiencies a_x and a_r are not necessarily constant over time. While the absorption of infrared radiation by many greenhouse gases varies linearly with their abundance, a

few important ones display non-linear behaviour for current and likely future abundances (e.g., CO_2, CH_4, and N_2O). For those gases, the relative radiative forcing will depend upon abundance and hence upon the future scenario adopted.

A schematic framework representing anthropogenic drivers, impacts of and responses to climate change, and their linkages, is shown in Figure 2.

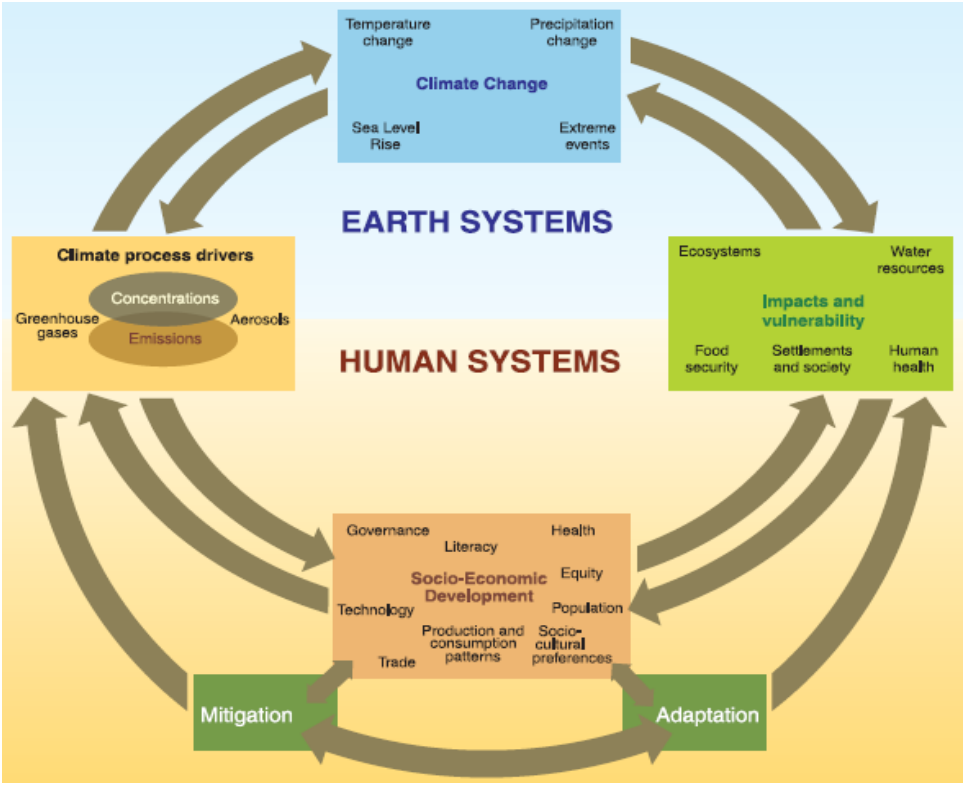

Figure 2. Schematic framework representing anthropogenic drivers, impacts of and responses to climate change, and their linkages (IPCC, 2007).

GHGs differ in their warming influence (radiative forcing) on the global climate system due to their different radiative properties and lifetimes in the atmosphere. These warming influences may be expressed through a common metric based on the radiative forcing of CO_2 that is the most important anthropogenic GHG and represents 77% of total anthropogenic GHG emissions in 2004 (IPCC, 2007).

Climate change due to greenhouse gas emissions is expected to increase temperature and modify frequency of extreme events, possibly leading to more drought and floods. These changes will in turn alter the availability of water resources, productivity of grazing lands and livestock, and the distribution of agricultural pests and diseases.

High uncertainty is related to climate sensitivity. The climate sensitivity is a measure of the climate system response to sustained radiative forcing. It is defined as the equilibrium global

average surface warming following a doubling of CO_2 concentration. Now the climate sensitivity is likely to be in the range of 2 to 4.5°C with a best estimate of about 3°C, and it is very unlikely to be less than 1.5°C. Values substantially higher than 4.5°C cannot be excluded, but agreement of models with observations is not as good for those values (IPCC, 2007).

Evaluation of evidence on observed changes related to climate change is made difficult because the observed responses of systems and sectors are influenced by many other factors. Non climatic drivers can influence systems and sectors directly and/or indirectly through their effects on climate variables such as reflected solar radiation and evaporation. Socioeconomic processes, including land-use change (e.g., agriculture to urban area), land-cover modification (e.g., ecosystem degradation), technological change, pollution, and invasive species constitute some of the important non-climate drivers.

Climate change impacts can be roughly divided into two groups (FAO, 2007):

- *biophysical impacts:*

■ sea level rise, changes to ocean salinity;
■ sea temperature rise causing fish to inhabit different ranges;
■ changes in land, soil and water resources (quantity, quality);
■ physiological effects on crops, pasture, forests and livestock (quantity, quality);
■ increased weed and pest challenges;
■ shifts in spatial and temporal distribution of impacts;

- *socio-economic impacts:*

■ decline in yields and production;
■ reduced marginal GDP (Gross Domestic Product) from agriculture;
■ fluctuations in world market prices;
■ changes in geographical distribution of trade regimes;
■ increased number of people at risk of hunger and food insecurity;
■ migration and civil unrest.

Altered frequencies and intensities of extreme weather, together with sea level rise, are expected to have mostly adverse effects on natural and human systems. Examples for selected extremes and sectors are shown in Table 1.

Table 1. Examples of possible impacts of climate change due to changes in extreme weather and climate events, based on projections to the mid- to late 21st century. These do not take into account any changes or developments in adaptive capacity. The likelihood estimates in column two relate to the phenomena listed in column one (IPCC, 2007).

Phenomenon and direction of trend	**Likelihood of direction of trend future trends based on projections for 21st century using SRES scenarios**	**Examples of major projected impacts by sector**			
		Agriculture, forestry and ecosystems {WGII 4.4, 5.4}	**Water resources {WGII 3.4}**	**Human health {WGII 8.2, 8.4}**	**Industry, settlement and society {WGII 7.4}**
Over most land areas, warmer and fewer cold days and nights, warmer and more frequent hot days and nights	Virtually certain	Increased yields in colder environment; decreased yields in warmer environment; increased insect outbreaks	Effects on water resources relying on snowmelt; effects on some water supplies	Reduced human mortality from decreased cold exposure	Reduced energy demand for heating; increased demand for cooling; declining air quality in cities; reduced disruption to transport due to snow, ice; effects on winter tourism
Warm spells/heat waves. Frequency increases over most land areas	Very likely	Reduced yields in warmer regions due to heat stress; increased danger of wildfire	Increased water demand; water quality problems, e.g. algal blooms	Increased risk of heat-related mortality, especially for the elderly, chronically sick, very young and socially isolated	Reduction in quality of life for people in warm areas without appropriate housing; impacts on the elderly, very young and poor
Heavy precipitation events. Frequency increases over most areas	Very likely	Damage to crops; soil erosion, inability to cultivate land due to waterlogging of soils	Adverse effects on quality of surface and groundwater; contamination of water supply; water scarcity may be relieved	Increased risk of deaths, injuries and infectious, respiratory and skin diseases	Disruption of settlements, commerce, transport and societies due to flooding: pressures on urban and rural infrastructures; loss of property
Area affected by drought increases	Likely	Land degradation; lower yields/crop damage and failure; increased livestock deaths; increased risk of wildfire	More widespread water stress	Increased risk of food and water shortage; increased risk of malnutrition; increased risk of water- and food-borne diseases	Water shortage for settlements, industry and societies; reduced hydropower generation potentials; potential for population migration
Intense tropical cyclone activity increases	Likely	Damage to crops; windthrow (uprooting) of trees; damage to coral reefs	Power outages causing disruption of public water supply	Increased risk of deaths, injuries, water- and food-borne diseases; post-traumatic stress disorders	Disruption by flood and high winds; withdrawal of risk coverage in vulnerable areas by private insurers; potential for population migrations; loss of property
Increased incidence of extreme high sea level (excludes tsunamis)	Likely	Salinisation of irrigation water, estuaries and fresh- water systems	Decreased fresh-water availability due to saltwater intrusion	Increased risk of deaths and injuries by drowning in floods; migration-related health effects	Costs of coastal protection versus costs of land-use relocation; potential for movement of populations and infrastructure; also see tropical cyclones above

In particular for the agro-ecosystems, a changing climate will affect them in heterogeneous ways, with either benefits or negative consequences dominating in different agricultural regions (Fig. 3).

There is significant concern about the impacts of climate change and its variability on agricultural production worldwide.

Agriculture is inherently sensitive to climate conditions, and is one of the sectors most vulnerable to the risks and impacts of global climate change (Reilly, 1995; Smith and Skinner, 2002). Vulnerability can be viewed as a function of the sensitivity of agriculture to changes in climate, the adaptive capacity of the system, and the degree of exposure to climate hazards (IPCC, 2001*b*).

These characteristics determine a highly differentiated regional vulnerability to climate change. For instance, Africa and India face larger climate impacts due to impacts on health and catastrophic events, respectively.

Climate change is expected to affect agriculture around the world, but very differently in different parts of the world (Parry *et al.*, 2004).

Rising atmospheric CO_2 concentration, higher temperature, changing patterns of precipitation, and altered frequencies of extreme events will have significant effects on crop production, with associated consequences for water resources and pest/disease distributions. It will probably combine to depress yields and increase production risks in many world regions, widening the gap between rich and poor countries (IPCC, 2007).

The resulting effects depend on current climatic and soil conditions, the direction of change and the availability of resources and infrastructure to cope with change.

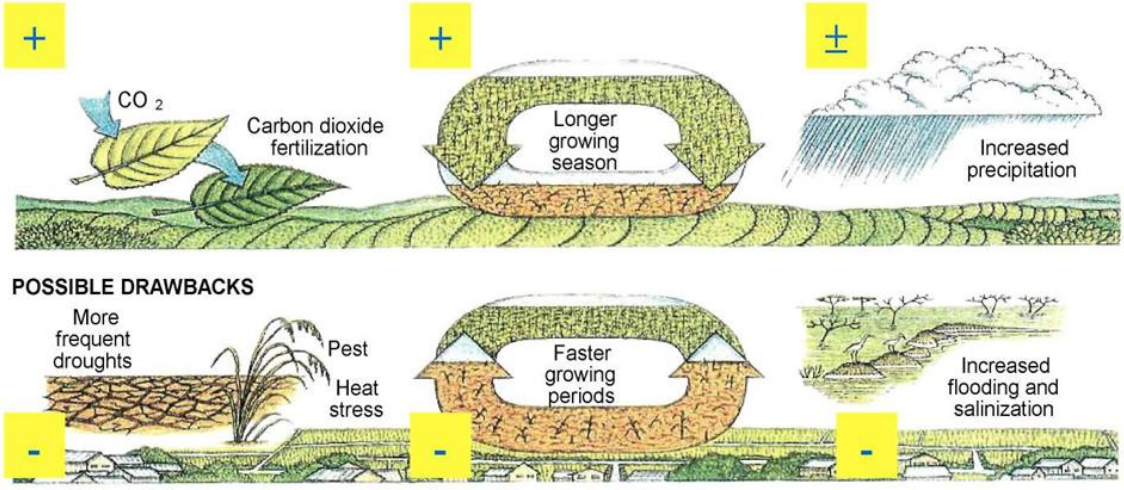

Figure 3. Agro-ecosystem processes and a changing climate (from: Bongaarts, 1994).

A changing climate will alter the hydrological regime, the timing of seasons, the arrival of pollinators and the prevalence, extent, type of crop diseases and pests, and so productivity of crop

species and their geographic distribution. Globalization and intensification techniques may also contribute to new configurations of plant-pest relationships that affect cultivated and wild plants.

A number and variety of environmental factors may lead to crop yield changes. Weather is one of the key components that controls agricultural production. In some cases, it has been stated that as much as 80% of the variability of agricultural production is due to the variability in weather conditions, especially for rainfed production systems (Petr, 1991; Fageria, 1992).

One of the most important factors is the direct effect of CO_2 enrichment on plant growth and development, also called the CO_2 fertilization effect, which, generally, has a positive effect on crop yields (Idso and Idso, 1994). Current research confirms that crops would respond positively to elevated CO_2 in the absence of climate change (e.g. Kimball *et al.*, 2002; Jablonski *et al.*, 2002; Ainsworth & Long, 2005). Many experiments show that crop yields increase on average by 30% for a doubling of CO_2 concentration (particularly C3 plants) (Acock and Allen, 1985; Cure and Acock, 1986; Kimball, 1983; Poorter, 1993; Hsiao and Jackson, 1999). C3 species (wheat, rice, soybeans, etc..) respond very positively to high CO_2 concentrations in contrast to the C4 species (maize, sorghum, sugar cane, millet, etc.) that are photosynthetically more efficient and so less sensitive to increased CO_2 concentration.

Crop responses to elevated CO_2 have been shown to be modulated by environmental and management factors. For instance, relative crop yield response to elevated CO_2, compared to ambient CO_2 levels, is greater in rain-fed than in irrigated crops, due to a combination of increased water-use efficiency and root water-uptake capacity (Tubiello and Ewert, 2002). Increased CO_2 levels reduce stomatal conductance and transpiration rates. High-temperature and salinity stress may also increase relative crop response, at least in the short term. Conversely, low fertilizer N applications tend to depress crop responses to elevated CO_2 (Kimball and Idso, 1983; Kimball *et al.*, 2002).

It remains uncertain whether many of the effects of CO_2 enrichment observed in controlled environments will prevail in farmers' fields in the future. Under these more typical conditions, many existing limiting factors – such as soil and water quality, weed-crop competition, weed and pest interactions – as well as their unknown evolution under elevated CO_2 and a changing climate might suppress the yield gains seen in current experiments (e.g., Rosenzweig and Hillel, 1998; Tubiello and Ewert, 2002).

Increased CO_2 accelerates crop development due to increased leaf temperature resulting from reduced transpiration, reducing the efficiency of biomass or seed production. The content of non-structural carbohydrates generally increases under high CO_2, while the concentration of mineral nutrients and proteins is reduced.

It is important to consider that while crops could respond positively to elevated CO_2 in the absence of climate change, the associated impacts of high temperatures, altered patterns of

precipitation, and possibly increased frequency of extreme events such as droughts and floods will likely combine to depress yields and increase production risks in many regions over time.

Increasing in ambient air temperature is another important factor related to climate change. Air temperature is the main weather variable that regulates the rate of vegetative and reproductive development (Hodges, 1991). In most cases, an increase in temperature causes an increase in the developmental rates. At extremely high temperatures, the inverse occurs, and developmental rates slow down as the temperature further increases. Temperature, through its influence on the acceleration of maturation time and on heat stress, usually leads to a decrease in crop yields. However, in certain cases, a temperature increase may allow crops to get closer to their optimal growth thermal range and can be beneficial to crop yields (Nonhebel, 1996; Singh *et al.*, 1998; Southworth *et al.*, 2000). Recently observed temperature increases could induce likely shifts in the optimal zonation of crops and may extend crop-growing seasons in many regions. For instance, Chmielewski *et al.* (2004) found that in Germany, for the period 1961–1990, the beginning of the growing season advanced by 2.3 days per decade, following increases in mean annual air temperature of 0.36 °C per decade. Over the same period, warmer temperatures advanced the beginning of stem elongation in rye by 2.9 days per decade; the beginning of cherry tree blossom by 2 days per decade; and the beginning of apple tree blossom by 2.2 days per decade.

The climate warming is expected to expand the area of cereal cultivation (e.g. wheat and maize) northwards (Kenny *et al.*, 1993; Harrison *et al.*, 1995; Carter *et al.*, 1996). For wheat, an increment of temperature will probably lead to a small yield reduction, whereas an increase in CO_2 will probably cause a large yield increase and the net effect of both for a moderate climate change is a large yield increase (Harrison and Butterfield, 2000; Nonhebel, 1996).

For indeterminate energy crops that are favoured by the longer growing season and by increased water use efficiency due to higher CO_2 levels, higher temperatures and CO_2 concentrations would generally be favourable.

For seed crops, the duration to maturity depends on temperature and day length. A temperature increase will therefore shorten the length of the growing period and possibly reduce yields (Peiris *et al.*, 1996). At the same time, the cropping area of the cooler season seed crops (e.g. pea, faba bean and oil seed rape) will probably expand northwards leading to increased productivity of seed crops there. There will also be a northward expansion of warmer season seed crops (e.g. soybean and sunflower). Harrison *et al.* (1995) estimated this northward expansion for sunflower, but also found a general decrease in water-limited yield of sunflower in many regions.

Vegetable responses to changes in temperature and CO_2 vary among species, mainly depending on the type of yield component and the response of phenological development to temperature change. For determinate crops such as onions warming will reduce the duration of crop growth and hence yield (Harrison *et al.*, 1995), whereas warming stimulates growth and yield in indeterminate crops such as carrots (Wheeler *et al.*, 1996). Onion yields are sensitive to the degree

of warming (Harrison *et al.*, 1995), with a yield decrease for warmer future climate scenarios and a yield increase for cooler future climate scenarios. Root and tuber crops are expected to show a large response to rising atmospheric CO_2 due to their large underground sinks for carbon and apoplastic mechanisms of phloem loading (Farrar, 1996; Komor *et al.*, 1996).

Perennial crops are in general sensitive to the greater precocity of phenological stages: compared to arable crops they are in fact less likely to adapt through a revised timetable for tending operations. Many fruit's species are susceptible to spring frosts during the flowering period and winter temperatures have an important role in productivity. The rising temperatures will advance both the last spring frost so that the bloom is likely that the risk of harm remains virtually unchanged. Probably will decrease the risk of damage caused by early autumn frosts, and will increase the demand for water. For example, for the wine sector is expected to increase the risk of frost, shortening the ripening period, increasing in water stress, damage at maturity, and changes in having pests and plant diseases.

For olive, it was shown that in $2 \times CO_2$ case, the suitable area for olive cultivation could be enlarged due to changes in temperature and precipitation patterns (Bindi *et al.*, 1992).

For the European region is expected an increase of areas suitable for grapevines and olives cultivation in particular for the northern and eastern.

Precipitation does not directly control any of the plant processes. It is considered to be a modifier that indirectly affects many of the plant growth and developmental processes.

However drier conditions and increasing temperatures may lead to lower yields and the need for new varieties and cultivation methods (Alexandrov, 1997; Sirotenko *et al.*, 1997).

Decreases in precipitation and soil moisture are an important factor leading to declining crop production, although increasing atmospheric CO_2 may make crops less sensitive to water stress (Brown and Rosenberg, 1997; Singh *et al.*, 1998). Furthermore, sufficient nutrient supply may be necessary for crop yields to fully derive the benefits of CO_2 enrichment (Wolf, 1996).

Another important agrometeorological variable associated with agricultural production is the solar radiation, which provides the energy for the processes that drive photosynthesis, affecting carbohydrate partitioning and biomass growth of the individual plant components (Boote and Loomis, 1991). Photosynthesis is normally represented through an asymptotic response function, with a linear response at low light levels.

Increasing solar radiation stimulates the leaf assimilation, thereby increasing the yields. However, as the increased solar radiation stimulates evapotraspiration, the yields may decrease due to a deepened water stress if the water supply is at its critical level.

Furthermore climate change may be characterized by an increase in climate variability and it is predicted that some extreme events will increase in frequency as a result of it (McCarthy, 2001).

The predicted increase in extreme weather events, e.g., spells of high temperature and droughts (Meehl and Tebaldi, 2004; Schär *et al.,* 2004; Beniston *et al.,* 2007), is expected to increase yield variability (Jones *et al.,* 2003) and to reduce average yield (Trnka *et al.,* 2004). In particular, in the European-Mediterranean region, increases in the frequency of extreme climate events during specific critical crop development stages (e.g., heat stress or late frosts during flowering period, rainy days during sowing time), together with higher rainfall intensity and longer dry spells, are likely to reduce the yield of summer crops (e.g., sunflower).

Increases in temperature and precipitation variability will put pressure on crops growth on their marginal climate ranges: for instance, increases in temperature variability in southern wheat-growing areas may limit yields through lack of cold hardening and increased winterkill.

Precipitation extremes (i.e., droughts or floods) are detrimental to crop productivity.

Higher heavy precipitation and flooding regimes could increase crop damage in some areas, due to soil water-logging, physical plant damage, and pest infestation (Rosenzweig *et al.* 2002a, b). At the opposite extreme, greater drought frequency and increased evaporative demands may increase the need for irrigation in specific regions, further straining competition for water with other sectors (Rosenzweig *et al.* 2004). In regions lacking additional water resources, entire cropping systems may go out of production.

Drought stress in plants is a result of a combination of factors, such as potential evapotranspiration, extractable soil moisture in the rooting zone, root distribution, canopy size, and other plant and environmental factors. Drought can cause an increase or decrease in developmental rates, depending on the stage of development. In many cases, the response to drought stress is also a function of species or cultivar, depending on their drought-tolerance. Drought can also reduce gross carbon assimilation through stomatal closure, causing a modification of biomass partitioning to the different plant components.

Water logging stress is caused by flooding or intense rainfall events. It can cause a lack of oxygen in the rooting zone, which is required for root growth and respiration. A decrease in oxygen content in the soil can result in a decrease in root activities, causing increase in root senescence and root death rates. The overall effect of water logging is a reduction in water uptake; the ultimate impact is similar to the drought stress effects discussed earlier (Hoogenboom, 2000).

Sequential extreme events can severely affect crops. Droughts, followed by intense rain, for example, can reduce soil water absorption and increase the potential for flooding, thereby creating conditions favoring fungal infestations of leaf, root and tuber crops in runoff areas (Rosenzweig *et al.,* 2005).

In coastal agricultural regions, sea-level rise and associated saltwater intrusion and storm-surge flooding can damage crops through diminished soil aeration, salinization, and direct damage. This could be most serious in countries with major crop-growing areas in low-lying coastal regions.

The extreme events will endanger especially perennial crops (e.g. grapevine, olive and energy crops) because their production capacity can be negatively affected for many years.

An example of extreme events was the severe heat wave over large parts of Europe that started in June 2003 and continued through July until mid-August, raising summer temperatures by 3 to 5 °C from Northern Spain to the Czech Republic and from Germany to Italy (Schär *et al.*, 2004). Extreme maximum temperatures of 35 to 40 °C were repeatedly recorded in July and to a larger extent in August in most of the Southern and Central European countries from Germany to Turkey. This extreme weather was caused by an anti-cyclone firmly anchored over the western European land mass holding back the rain-bearing depressions that usually enter the continent from the Atlantic Ocean. This situation was exceptional in the extended length of time (over 20 days), during which it conveyed very hot dry air up from south of the Mediterranean Sea (Olesen and Bindi, 2004).

As reported by Olesen and Bindi (2004), the low precipitation during this period failed to compensate for the accumulated evapotranspiration of almost 400 mm in the Mediterranean area, creating a cumulative water balance deficit of up to 380 mm in South Europe and of 200 mm over France, Germany, western Czech Republic, Hungary and southern Romania and the extreme weather conditions decreased the quantity and quality of the harvests, particularly in Central and Southern European agricultural areas; threatening a large proportion of harvests, and increasing production costs (Figure 4). For instance, the reduction in cereal production in EU reached more than 23 million tonnes (MT) compared to that one of 2002.

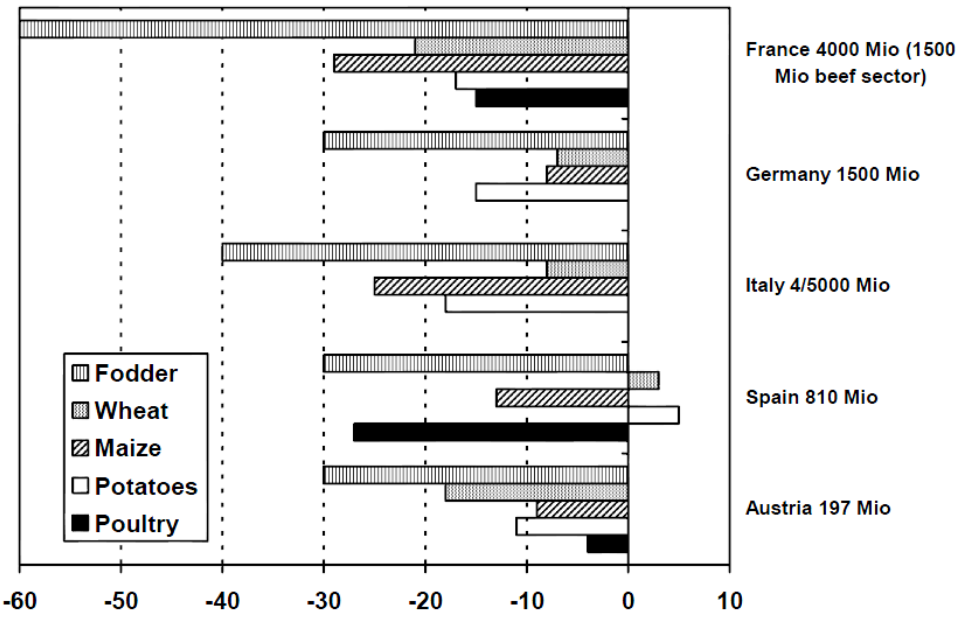

Figure 4: Impact of the summer 2003 heat wave and drought on agriculture (production (% reduction) and financial costs (mio. €) for 2003 relative to 2002) in 5 selected countries (Source: COPA-COGECA, 2003).

The heat wave that began in early June accelerated crop development by 10 to 20 days, thus advancing ripening and maturity. The very high air temperature and solar radiation, especially from the second part of July to the beginning of August, resulted in a notable increase in the crops' water consumption. This, together with the particularly dry summer, resulted in an acute depletion of soil water and lowered crop yields.

The summer drought of 2003 has been taken in many parts of the society as an indicator of the climate change that might come, and as such it may be used as an eye-opener for the agricultural community of the adaptations that will need to be taken as a result of climate change.

Finally, other factors such as stratospheric ozone depletion (Bender *et al.*, 1999) and pathological agents (Manning and Tiedemann, 1995) could have significant effects on agricultural production under a changing climate. Elevated concentrations of ground level ozone have been found to have large effects on crop yields. Experimental evidence suggests that growing season mean ozone concentrations of 30-45 ppb could see crop yield losses of 10-40 per cent for sensitive varieties of wheat, rice and legumes.

The range of plant pathogens and insect pests are constrained by temperature and the frequency and severity of weather events affects the timing, intensity and nature of outbreaks of most organisms. milder winters and warmer nights allow increased winter survival of many plant pests and pathogens, accelerate vector and pathogen life cycles, and increase sporulation and infectiousness of foliar fungi, because climate change will allow survival of plants and pathogens outside their historic ranges, models consistently indicate northward (and southward in the Southern Hemisphere) range shifts in insect pests and diseases with warming (Coakley *et al.*, 1999).

Despite uncertainties about the rate and magnitude of climate change, recent assessment studies have consistently shown that agricultural production systems in the mid and high latitudes are likely to benefit in the near term (approximately to mid-century), while production systems in the low-latitudes may decline over the coming few decades. Since most of the developing countries are located in lower-latitude regions, increased divergence in climate vulnerability between these groups of nations is expected (IPCC, 2001*b*). The combination of greater climate vulnerability and lower adaptive capacity may create additional challenges to developing countries as they confront global warming in the coming decades.

Indeed, while in many parts of the world producers have the physical, agricultural, economic and social resources to moderate, or adapt to, the impacts of climate variability on food production systems, in other parts of the world, for instance in Africa, there aren't enough resources to address climate change and agricultural systems will be particularly vulnerable (Haile, 2005). This is in part because a large fraction of Africa's crop production depends directly on rainfall. For example, 89% of cereals in sub-Saharan Africa are rainfed (Cooper, 2004). In many

parts of the world, climate is already a key driver of food security (Gregory *et al.,* 2005; Verdin *et al.,* 2005).

While, at EU level, several studies indicate that the projected climate change in the media will be beneficial for agricultural production over the next three decades. They presuppose, however, more serious adverse effects by mid-century because of extreme weather events.

However, in the coming decades, agriculture will suffer the influence of climate change even in areas where the level of technology has advanced and agriculture will necessarily develop in a context of growing uncertainty.

Agriculture, however, is also the largest source of methane (CH_4) and nitrous oxide (N_2O) emissions. The main sources of methane are wetlands, rice fields, livestock. Its ability to retain heat is 30 times more than carbon dioxide, its radiation forcing is 15%. The average air concentration was 1.6 ppm in 1975, now has reached and exceeded the value of 1.7 ppm and is increasing by an average annual rate assessed between 1.1% and 1.4%.

Nitrous oxide emissions grew by about 50%, due mainly to increased use of fertilizer and the growth of agriculture (IPCC, 2007). Its ability to retain heat is about 300 times more than carbon dioxide. The average concentration is already higher than the value of 0.3 ppm and is increasing by an annual rate of nearly 0.3%, which is surely less than the increase in other greenhouse gases, but the average time of persistence is about 120 years.

For these reasons agriculture is involved not only in the adoption of strategies to adapt at climate change but also in the adoption of practices for climate change mitigation.

Under future climate and socio-economic pressures, land managers and farmers will be faced with challenges in regard to selecting those mitigation and adaptation strategies that together meet food, fibre and climate policy requirements (Rosenzweig and Tubiello, 2007).

1. FOOD SECURITY (RISK OF HUNGER)

Since the 1980s various definitions of food security have emerged, both in academic literature and in national and multi-lateral policy documents. Also field programs on food security have greatly contributed to a more comprehensive view on the issue. This has led to a definition of food security, accepted in the late 1980s, and reconfirmed at the World Food Summit (WFS) in 1996: Food security represents "a state when all people at all times have physical and economic access to safe and nutritious food to meet their dietary needs and food preferences for an active and healthy life" (World Food Summit 1996). In a food-secure region the land would have the biophysical capability to produce food of the quality and quantity required by the people, its farmers would have access to capital, credit, and technology, and consumers would have enough purchasing power to acquire food (Aggarwal *et al.* 2001; ACC/SCN, 2004; Heidhues *et al.*, 2004; Falcon and Naylor, 2005).

1.1 Food production and food security

Climate change may have significant effects on food supply, i.e., how much food is produced, as well as food security, i.e., how much food is available to people. How much, where, and when food supply and security will be affected by climate change are questions that many scientists and policy-makers are examining.

Food production will be particularly sensitive to climate change, because crop yields depend in large part on prevailing climate conditions (temperature and rainfall patterns). Also increased intensity and frequency of storms, drought and flooding, altered hydrological cycles may have implications for future food availability.

Agriculture currently accounts for 24% of world output, employs 22% of the global population, and occupies 40% of the land area. 75% of the poorest people in the world (the one billion people who live on less than $1 a day) live in rural areas and rely on agriculture for their livelihood (Bruinsma, 2003).

The projections obtained for different future scenarios foresee an overall reduction of food supply and an increased level malnutrition, more than a linear trend of climate change, and may have far-reaching consequences (Fischer *et al.*, 2005).

Warming of several degrees Celsius is projected to alter production significantly and increase food prices globally, increasing the risk of hunger in vulnerable populations (Houghton *et al.*, 2001).

Some regions may improve production, while others suffer yield losses. For example, for regions at high and mid-latitudes, yield increases lead to production increases, a trend that may be enhanced by the countries' greater adaptive capacity as in Canada and Europe. In contrast, yield

decreases at lower latitudes, and especially in the arid and sub-humid tropics, leading to production decreases with increases in the risk of hunger. Reduction of food supplies will be a serious problem particularly for South Asia and Africa (Parry *et al*., 2005).

These effects may be exacerbated where adaptive capacity is lower than the global average. Demand for world grain from North America (on the order of 80% of the global marketable surplus) has increased the sensitivity of world food supply to climate. Different climate models project similar changes in the shifts of agricultural production zones around the world.

In addition, developing countries are more vulnerable to climate change than developed countries, because of the predominance of agriculture in their economies, the scarcity of capital for adaptation measures, their warmer baseline climates and their heightened exposure to extreme events (Parry *et al.,* 2001).

Thus, climate change may have particularly serious consequences in the developing world, where some 800 million people are undernourished. Of great concern is a group of more than 40 'least-developed' countries, mostly in sub-Saharan Africa, where domestic per capita food production declined by 10% in the last 20 years (Fisher *et al.,* 2005).

Therefore, while some parts of the world will benefit from climate change (at least in the short term), developing regions will suffer a reduction in food supply and thus a potential increase in malnutrition. For example, in Africa, it is estimated that cereal productivity, under the HadCM2 greenhouse gas only scenario, will be reduced by about 10% from the reference case by 2080; the consequent risk of hunger in the region would increase by 20% (Rosenzweig *et al.,* 2001).

The impacts of climate change, therefore, will fall disproportionately upon developing countries and on the poorest within all countries, exacerbating inequities in health status and access to food, clean water and other basic resources. Shortages in food supply could generate distortions in international trade at regional and global levels, and disparities and disputes could become more pronounced over time (Houghton *et al.,* 2001).

Many interactive processes determine the dynamics of world food demand and supply: agro-climatic conditions, land resources and their management are clearly a key component, but they are critically affected by distinct socio-economic pressures. These include current and projected trends in population growth, changes in dietary habits (meat needing much more land to produce than cereals), availability and access to technology and development, food policies, and demand for energy, including biofuels, which can compete with food production for a limited land supply.

A number of studies have quantified the impacts of climate change on food security at regional and global scales (e.g., Fischer *et al.,* 2002*b*, 2005; Parry *et al.,* 2004, 2005; Tubiello and Fischer, 2006). These projections are based on complex modelling frameworks that integrate the outputs of GCMs, agro-ecological zone data and/or dynamic crop models, and socio-economic models. In these systems, impacts of climate change on agronomic production potentials are first

computed; then consequences for food supply, demand and consumption at regional to global levels are computed, taking into account different socio-economic futures (typically SRES scenarios). A number of limitations, however, make these model projections highly uncertain. In fact these estimates are limited to the impacts of climate change mainly on food availability; they do not cover potential changes in the stability of food supplies, for instance, in the face of changes to climate and/or socioeconomic variability. The projections are based on a limited number of crop models, and only one economic model the latter lacking sufficient evaluation against observations, and thus in need of further improvements. Despite these limitations and uncertainties, these studies show that climate change is likely to increase the number of people at risk of hunger compared with reference scenarios with no climate change. However, impacts will depend strongly on projected socio-economic developments. For instance, Fischer *et al.* (2002*a*, 2005) estimate that climate change will increase the number of undernourished people in 2080 by 5-26%, relative to the no climate change case, or by between 5-10 million (SRES B1) and 120-170 million people (SRES A2). The within-SRES ranges are across several GCM climate projections. Using only one GCM scenario, Parry *et al.* (2004, 2005) estimated small reductions by 2080, i.e., –5% (– 10 [B1] to –30 [A2] million people), and slight increases of +13-26% (10 [B2] to 30 [A1] million people) (IPCC, 2007).

Climate change may thus result in 5-170 million people additionally at risk of hunger by 2100, depending on assumed socio-economic scenario . Among developing countries, sub-Saharan Africa may be the most negatively affected, due to and decreased quality of land and water resources and an increasing share of people at risk of hunger. Mediterranean countries are expected to experience severe droughts, leading to abandonment of agricultural land and desertification (Tubiello and Rosenzweig, 2008).

Under current climate, Fischer *et al.*, 2005, with AEZ (Agro-Ecological Zoning) methodology, computes that two-thirds of the global land surface (about 8.9 billion hectare) suffer severe constraints for crop cultivation: 13.2% is too cold, 26.5% is too dry, 4.6% is too steep, 2.0% is too wet and 19.8% has poor soils. Climate change will have positive and negative impacts, as some constraints will be alleviated while others may increase. The results for the Hadley HadCM3 climate model and the IPCC A1F1 scenario, representing a high-emission scenario, indicate that with rapid climate change these constraints may change respectively to 5.2, 29.0, 1.1, 5.7 and 24.5%. The agro-ecological changes due to climate change will result in water deficits in some areas and surplus in others as well as increased or reduced infestation of disease pathogens and parasites.

Under climate change and by the 2080s, regional analyses of AEZ results indicate expansions of land area with severe constraints as follows: Central America and Caribbean (1–3% increase; AEZ simulations for current climate: 270 million hectares); Oceania and Polynesia (0.5–4.5%), northern Africa (2–3.5%; AEZ simulations for current climate: 550 million hectares) and

Western Asia (up to 1%; AEZ simulations for current climate: 435 million hectares). In southern Africa, AEZ projects up to an additional 11% of a total land area of 265 million hectares to be at risk of being severely constrained for crop agriculture.

Therefore, in consequence of the projected decline in cultivated area per capita, increase in yield growth may well be necessary to compensate for losses of land to other uses, especially if we also consider the projections of population growth.

The median population growth projection for 2025 is 7.8 billion, compared to the present 6.4 billion; the high variant comes to 8.3 and the low variant to 7.3 billion. For the year 2050, the central projection is around 9 billion. In Asia, the population will grow by 650 million people between now and 2025, i.e., an annual growth rate of approximately 1% (Roetter and Van Keulen, 2008).

Adequate knowledge about the food demand side is essential for judging the effort that will be required to increase yield and optimize resource use efficiencies.

Consequences of the adaptation measures which may be taken in some countries are not so obvious for other countries and would need to be further explored. Some regions should see new opportunities to produce, or yields increase, but others may see output under pressure. In establishing a country's food balance for a particular time period (in the form of food balance sheets), many assumptions and uncertainties on food supply are introduced, especially in low-income countries (Roetter and Van Keulen, 2008).

Finally, it is important to consider the reduction of available land to food production in respect to energy production through the widespread cultivation of bioenergy crops (Tuck *et al.*, 2006).

There is a risk of greater fluctuations in productivity with the risk of more volatile agricultural prices, with economic and social effects.

The reduction in the entity of the global crops production will necessarily impact on prices which tend to have more than proportionate increases in respect on the availability of such products. The impacts on world food prices are difficult to predict, due to uncertainties over future demand, emergence of new cultivars and production technologies, there is a general expectation that world food prices will tend to rise in response to a warmer climate.

The price of agricultural commodities is a good all-around quantity to reflect the net consequences of climate change for the regional or global supply-demand balance and on food security.

With unmitigated climate change, declines in yields in low-latitude regions (where many developing countries are located) are projected to require that net imports of cereals increase. Higher grain prices will affect the number of people at risk of hunger. The number of hungry people in developing countries will increase by ~1% for every 2-2.5% increase in prices. This means that the number of people at risk of hunger grows by 10-60% in the scenarios tested,

resulting an increase estimated between 60 to 350 million people in this condition (Rosenzweig and Parry, 1994).

Impacts of climate change on world food prices are summarized in Figure 5. Overall, the effects of higher global mean temperatures (GMTs) on food prices follow the expected changes in crop and livestock production. Higher output associated with a moderate increase in the GMT likely results in a small decline in real world food (cereals) prices, while GMT changes in the range of 5.5°C or more could lead to a pronounced increase in food prices of, on average, 30% (IPCC, 2007).

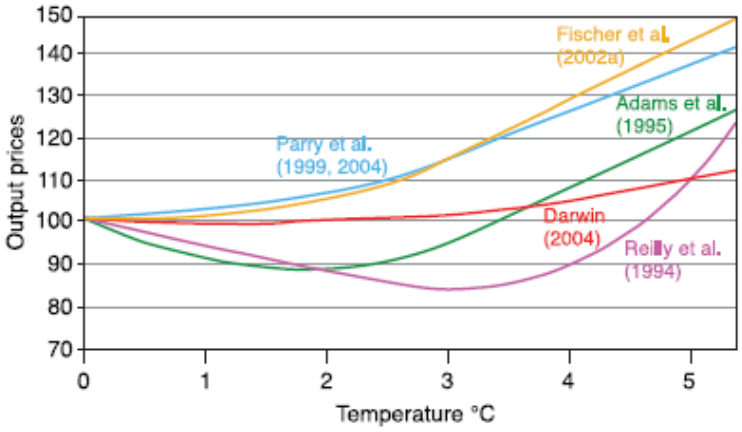

Figure 5. Cereal prices (percent of baseline) versus global mean temperature change for major modelling studies. Prices interpolated from point estimates of temperature effects (IPCC, 2007).

A recent study (Fischer *et al.*, 2005) shows that under some scenarios and models, there could be significant declines in agricultural productivity in many world regions, increasing the incentive to farm new areas, and to generally increase farming intensity, which will put pressure on the environment. Crop price changes under climate change are moderate, due to relatively small net global impacts on crop-production potentials. For the range of scenarios, in the case of HadCM3 climate projections, cereal prices increase 2–20% (scenario B1 to A1FI); for CSIRO the increase is 4–10%, in comparison to baselines period projections.

The simulation results suggest also that the climate change impacts on agricultural GDP are small at global level, i.e. between -1.5% (in HadCM3-A1FI scenario) and +2.6% (in NCAR-A2 scenario), in comparison to total global GDP of agriculture for baseline projections. At the same time, the results from Fischer analysis indicated that agriculture in developed countries as a group would benefit under climate change. Among developed regions, simulations indicate that North America gains in all GCM scenarios (in particular, 3–13% under SRES A2, for different GCM projections); agricultural GDP mostly increases in the Former Soviet Union (up to 23% in scenario A2); while only Western Europe loses agricultural GDP, across all GCM scenarios (-6 to -18% under SRES A2). By contrast, the results indicated decreases in agricultural GDP in most

developing regions, with the exception of Latin America. For Asia, by 2080, agricultural GDP losses amount to about -4%, under SRES A1 and A2, and HadCM3 and CSIRO climate. Aggregate projections for Africa are also negative, -2 to -8% for HadCM3 and -7 to -9% for CSIRO (Fischer *et al*., 2005).

It's necessary also to consider that the degradation of the natural resource base for agriculture, especially soil and water quality, is one of the major future challenges for global food security. Those processes are likely to be intensified by adverse changes in temperature and precipitation. Land use and management have been shown to have a greater impact on soil conditions than the direct effects of climate change, thus adaptation has the potential to significantly mitigate but may, in some cases, intensify degradation. Such environmental damage may raise the costs of adaptation.

1.2 World Cereal Production

Cereals are the base of world agriculture and therefore they are a key element for food security. Currently, the global area planted with cereals amounts to nearly 700 million hectares for a total production of 2.2 billion tonnes (FAO, 2009).

Figure 6 shows, on the left, the evolution of global cereal production for the last few years and, on the right, the world cereal production divided by main type.

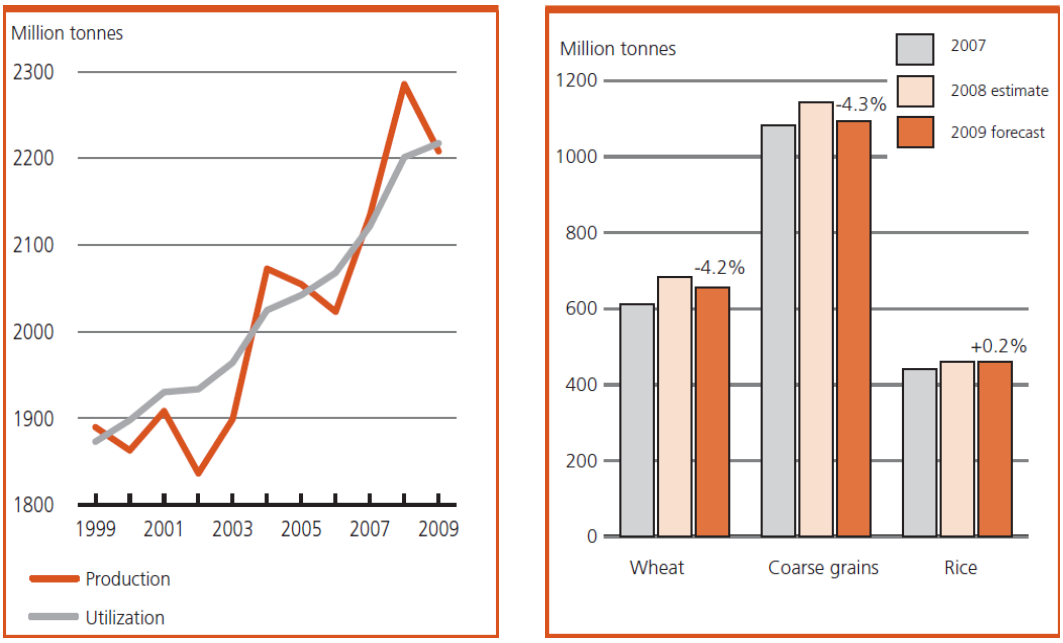

Figure 6. World cereal production and utilization (on the left), World cereal production by type (on the right) (FAO, 2009).

Rice, wheat and maize are the main cereal cultivated in the world, with respectively 660, 600 and 790 million tonnes produced in 2007 (FAO, 2009).

Hafner (2003) found for the major cereals at global scale (based on data from 188 nations) substantial growth in yields per unit area. For instance, the 40-year (1962-2002) average annual yield increases were 62 kg ha^{-1} for grain maize and 43 kg ha^{-1} for wheat. In Europe, the annual yield increase was even considerably higher with 145 kg ha^{-1} for grain maize and 77 kg ha^{-1} for wheat.

However, climate change may have different effects on future cereal production, altering the extention and localization of suitable areas for their cultivation and the future yield.

A warming of 1°C is estimated to decrease wheat, rice and corn yields by 10% (Brown, 2002).

In general for cereals are expected a loss of production globally for 2080, compared to the current period, from -2.1 to -4% depending on the models used (Parry *et al.*, 2005). These reductions, apparently small, are important issues for the food supply.

The impacts will differ depending on the geographic areas and types of cereals considered.

Models for cereal crops indicate that, in some temperate areas, potential yields increase with small temperature increases, but decrease with large temperature rises. In most tropical and subtropical regions, however, potential yields are projected to decrease under all projected temperature changes, especially for dryland/rainfed regions where rainfall decreases substantially (Rosenzweig *et al.*, 2005).

For instance, for wheat and for maize, a climatic warming will expand the area of cultivation northwards. In particular for wheat, a rise in temperature will lead to a small yield reduction, whereas an increase in CO_2 will cause a large yield increase; for maize, future climate scenario analyses led to result of increases in yield for northern areas and decreases in southern areas (Wolf and van Diepen, 1995). This is due to a small effect of increased CO_2 concentration on growth (maize is a C4 plant which responds less positively to CO_2 increases than C3 plants such as wheat and barley) and a negative effect of temperature on the duration of growing season. This latter effect, however, can largely be prevented by growing other maize varieties (Wolf and van Diepen, 1995). Projections for a range of SRES scenarios show a 30 to 50% increase in the area suitable for grain maize production in Europe by the end of the 21st century, including Ireland, Scotland, southern Sweden and Finland (Hildén *et al.*, 2005; Olesen *et al.*, 2007).

Fischer et al., 2005 using the AEZ methodology show that the result indicated, under all climate change scenarios, that declines in cereal-productivity potentials of more than 5% will be realized by 2080 in a group of more than 40 countries worldwide, with mean losses of about -15%.

It is also important to consider that cereal crops may feel the climate change impact but may also influence the climate change entity as a result of management practices adopted.

A specific example is rice, which is both impacted by and impacts climate. Climate change is expected to significantly impact the productivity of rice systems and thus the nutrition and livelihood of millions of people. Rice varieties have different abilities to tolerate high temperature, salinity, drought and floods. Rice varieties with salinity tolerance have been used to expedite the recovery of production in areas damaged by the 2004 Asian tsunami. The selection of appropriate rice varieties deserves consideration for adaptation to climate change taking into account more than high yielding potential. Emission of methane from flooded rice soils has been identified as a contributor to global warming. Water regimes, organic matter management, temperature and soil properties as well as rice plant are factors determining the production and flux of methane (CH4) in rice fields. Varietal differences could be used to lessen the methane emission in rice production. Also, intermittent irrigation and/or alternating dry-wet irrigation could reduce methane emission from rice fields, while the transfer and adoption of the Rice Integrated Crop Management (RICM) system would increase the efficiency of nitrogen fertilizer in rice production, thus reducing the nitrous oxide (a greenhouse gas) emission. Upland rice cultivation under slash-and-burn shifting cultivation, especially in sub- Saharan Africa, has resulted in destruction of forest vegetation. The development of wetland rice in sub-Saharan Africa could reduce deforestation in these areas (FAO, 2007).

It is also important to consider that a large proportion of cereal production could be used to produce bio fuels (as happened in recent years), and could be not available as a food to people and livestock, and therefore prices could tend increase.

Land used for the production of biofuels and their by-products is projected by the IEA (International Energy Agency) to expand three- to four-fold at the global level, depending on policies pursued, over the next few decades, and even more rapidly in Europe and North America. OECD–FAO (2008) projections suggest that this land will come from a global shift towards cereals over the next decade. The additional land needed will come from non-cereal croplands in Australia, Canada and the United States of America; set-aside lands in the EU or the United States Conservation Reserve Program; and new, currently uncultivated land, especially in Latin America.

1.3 Wheat Production

Wheat production has high importance for the global economy. With over 200 hectares and 600 million tonnes produced is the third most cultivated cereal in the world, after maize and rice (Tab. 2). Europe is the second largest producer after Asia, providing one third of total world production on an area of over 50 million hectares (FAO, 2009).

Wheat is an important crop not only today, it may well have influenced human history. Wheat was a key factor enabling the emergence of civilization because it was one of the first crops that could be easily cultivated on a large scale, and had the additional advantage of yielding a

harvest that provides long-term storage of food. Today, there are different classes and uses of wheat. Although, it is mainly used as a staple food to make flour for leavened, flat and steamed breads, wheat can also be used as livestock feed, for fermentation to make beer and other alcoholic liquids, and recently, as a source of bio-energy (Mergoum *et al.,* 2009).

Table 2. Leading countries/groups for wheat production in the world (million metric tons)(from: Mergoum *et al.,* 2009).

S. No.	Country	2005–2006	2006–2007	2007–2008 (estimate)
1	European Union	122.7	124.8	127.3
2	China	97.5	103.5	100.0
3	Former Soviet Union	92.2	85.9	84.6
4	India	69.0	69.0	73.7
5	USA	57.3	49.3	59.0
6	Canada	26.8	27.3	24.5
7	Australia	24.5	10.5	22.1
8	Argentina	13.8	14.2	14.0
	Worldwide	622.0	594.0	610.2

Global wheat production must increase at about 2% annually to meet future demands. The potential of increasing the global arable land is limited; hence, future increases in wheat production must be achieved by enhancing the wheat productivity to the land already in use. The objectives of most breeding programs include: high and stable yields, superior end-use quality, desirable agronomic characteristics, biotic (mainly, pests) resistance, and abiotic (environmental stresses) tolerance. While it is virtually impossible to combine all these characteristics into a single ‘‘perfect’’ variety, continuous breeding efforts toward achieving these objectives will ensure that new varieties possess as many desirable and economic traits as possible (Mergoum *et al.,* 2009).

The two main commercial types of wheat are durum (*Triticum durum L.,* 2n = 4x = 28) and common (*Triticum aestivum L.,* 2n = 6x = 42) wheat, the latter being the more widely grown.

Wheat has three growth habits, namely *winter* (wheat grown primarily during the winter months, that requires vernalization to flower, and can withstand prolonged periods of below freezing temperatures), *facultative* (wheat grown primarily during the winter months in mild climates, that may or may not require vernalization to flower, and cannot withstand prolonged periods of below freezing temperatures), and *spring* (wheat grown primarily during the spring and summer months, that normally do not require vernalization to flower, and cannot withstand moderate periods of below freezing temperatures). Growth habit should be viewed as a continuum from winter wheat to facultative wheat to spring wheat, because wheat can be grown through the winter or summer, is very drought tolerant, and is used primarily for human consumption, it is the most widely grown crop in the world (Baenziger *et al.,* 2009).

Winter wheat is primarily common wheat (2n = 6x = 42) which has extensive germplasm resources that are used in breeding, often for disease and insect resistance. Though wheat can be

used as a forage crop and its grain for animal feed, the primary uses of common wheat are to make products used for human consumption; hence end-use quality is also a major breeding objective. The quality characteristics of these products are often associated with kernel hardness which affects milling, kernel color, and specific climatic zones or regions. For instance, the *soft red* and *white* wheat cultivars are generally used to make breakfast cereals, cookies, cakes, and crackers. The *hard red* and *white* wheat cultivars are used predominantly for leavened products such as bread and the *soft white* wheat cultivars of the Pacific Northwest are often exported and used to make noodles or steam breads (Baenziger *et al.*, 2009).

Spring wheat is the largest component of the worldwide wheat production followed by winter wheat. Based on genomic constitution, commercially grown wheat is of two main classes (i) durum wheat, a tetraploid with AABB genomes and (ii) common wheat, a hexaploid with AABBDD genomes. Based on kernel color, endosperm hardness, and other quality characteristics spring wheat is classified into three distinct classes (Mergoum *et al.*, 2009):

- *Hard red spring (HRS) wheat:* Contains the highest percentage of protein of the wheat classes, making it excellent for bread wheat with superior milling and baking characteristics.

- *Soft white (SW) wheat:* Contains low protein content but is high yielding. It produces flour for baking cakes, crackers, cookies, pastries, quick breads, muffins, and snack foods.

- *Hard white spring (HWS) wheat:* The newest class of wheat, closely related to red wheats (except for color genes), has a milder, sweeter flavour, equal fibre and similar milling and baking properties. Flour from HWS wheat is used mainly in the production of yeast breads, hard rolls, bulgur, tortillas, and oriental noodles. HWS wheat is used primarily in domestic markets, although it is also exported in limited quantities.

Climate change may have positive or negative effects on future wheat production in relation to many factors such as entity of climate change, wheat species and varieties, geographical area, crop management techniques and technological development.

Some studies conducted to assess the impact of climate change on wheat shows that a temperature rise will lead to a small yield reduction, because the increase in temperature can accelerate the crop cycle, reducing the time of light and water assimilation and consequently a decrease in the efficiency of water and light use (Whetton *et al.*, 1993). For example, an increase by 1 °C during grain fill reduces the length of this phase by 5%, and yield declines by a similar amount (Olesen *et al.*, 2000).

On the other hand an increase in CO_2 will cause a significant increases in production in the autumn-winter cereals in conditions of optimum temperature (Mitchell *et al.*, 1993) because of increased CO_2 leads to an increase in productivity due to greater efficiency of use of light, water, and nutrients (phosphorus in particular). A higher CO_2 concentration reduce stomatal aperture and stomatal density, which causes a reduction in stomatal conductance and thus transpiration (Olesen

and Bindi, 2002). An average reduction of 20% of stomatal conductance has been found with a doubling of the current CO_2 concentration (Gifford *et al.*, 2000, Drake *et al.*, 1997, Barrett and Gifford, 1999). Another important effect of enrichment of the current CO_2 concentration is the reduction of dark respiration. The maintenance respiration has been found to be reduced by 20% for a doubling of the current CO_2 concentration (Drake *et al.*, 1997).

The resulting effects of these crop responses to rising CO_2 concentration are increasing resources use efficiencies for radiation, water and nitrogen, but the highest effect is seen for water use efficiency which is positively affected by all three factors and for wheat can increase by about 50 to 60% for a doubling of current CO_2 concentration (Dowing *et al.*, 2000).

The net effect of both (temperature and CO_2 effects) for a moderate climate change is a possible yield increase (Harrison and Butterfield, 2000; Nonhebel, 1996), but in conditions of high temperature, the positive effect of CO_2 might not be sufficient to counterbalance the negative stress and reduce the grain filling period.

In the figure 7 it is possible to see the changes in potentially attainable wheat production predicted by AEZ under different GCM climate change scenarios, versus CO_2 concentration (Fischer *et al.*, 2005). For wheat production in 2080s, AEZ projects substantial decrease in attainable yield in the order of 15-45%. Specifically, AEZ computed decreases in South Asia (20–75%); Southeast Asia (10–95%); and in South America (12–27%); the same simulation results suggest that land suitable for wheat production might virtually disappear in Africa.

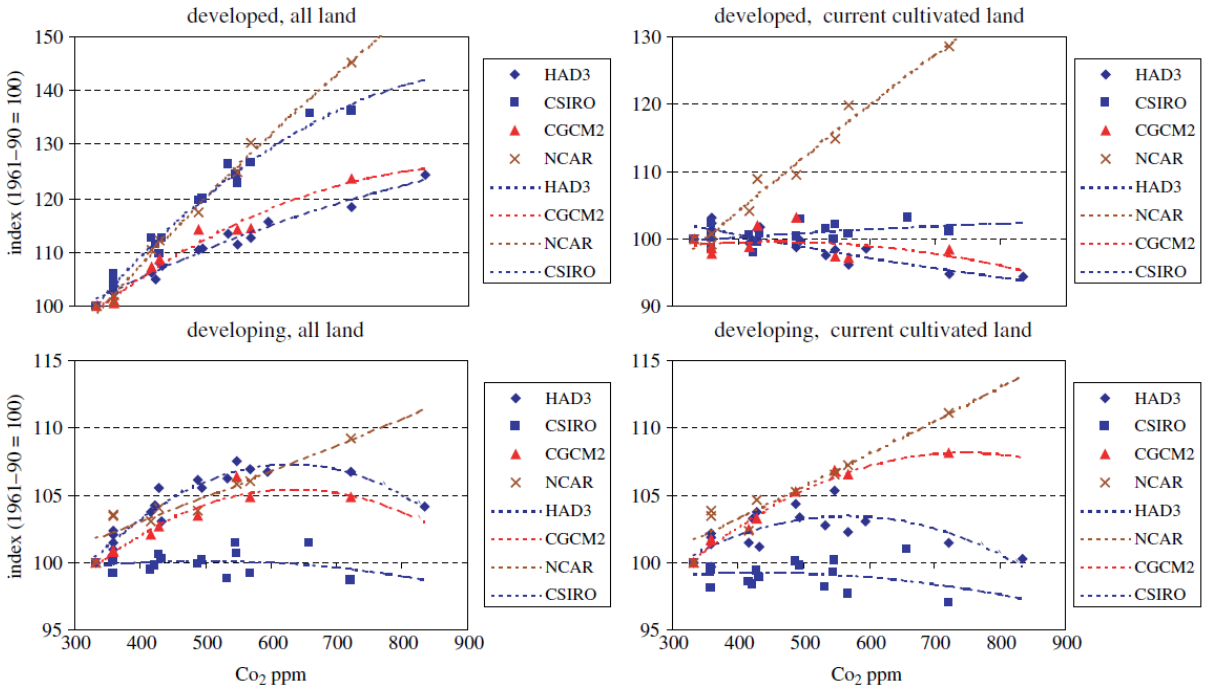

Figure 7. Changes in potentially attainable wheat production predicted by AEZ under different GCM climate change scenarios, versus CO2 concentration. Projections are for either current cultivated land (right), or all available under future climates (left), and pooled into developed (top) and developing (bottom) countries. Results are expressed against an index of climate change (Z100 in 1990), a proxy for time from 1990 to 2080 (from: Fischer *et al.*, 2005).

Anyway the net effect of increased CO_2 and climate change on crop yields will closely depend on local conditions and management practices, such as the type and levels of water and nutrient application. It is well-know that water limitation tend to enhance the positive crop response to elevated CO_2, compared to well-watered conditions. The contrary is true for nitrogen limitation: well-fertilised crops respond more positively to CO_2 than less fertilised ones (Tubiello *et al.*, 2000).

Ghaffari et al. (2002) reported that elevated CO_2 increased dry weight accumulation by 28% (low-N) to 103% (high-N).

Recent studies show increases on wheat yield by 2050 could range from 37% under the B2 scenario to 101% under the A1 scenario (Ewert *et al.*, 2005). Climate-related increases in crop yields are expected for wheat mainly in northern Europe: +2 to +9% by 2020, +8 to +25% by 2050, +10 to +30% by 2080 (Alexandrov *et al.*, 2002; Ewert *et al.*, 2005; Audsley *et al.*, 2006; Olesen *et al.*, 2007) probably due to a CO_2 increase.

The experiments made in controlled environment indicate that the winter wheat growth and biomass production might increase up to 33± 6% at doubled ambient CO_2 (Cure and Acock, 1986). Some studies also showed that the variability in these wheat responses to CO_2 enrichment is very high (Bender *et al.*, 1999). Recent review of 156 experiments with winter wheat (Amthor, 2001) that were carried out during 1976-2001 supports these results. Those experiments that were undertaken in controlled environment show 12-14% yield increase per 100 ppm of additional ambient CO_2 concentration while for the field experiments the reported increase is only 8.0-8.6% per 100 ppm of CO_2 (Trnka *et al.*, 2004).

A study (Tubiello *et al.*, 2000) conducted in Italy, more precisely in Modena and Foggia, shows how the effects of reducing production in conditions of rising temperatures, have been more marked than those induced by the increase in positive CO_2. In Modena there were losses in wheat production in the order of 5-15%. Similarly in Foggia, where wheat is subjected to water stress in the current conditions, climate change simulated induced a reduction in the production of the order of 30-50%.

Another study carried out in the south Sardinia, without consider CO_2, showed that an increase in temperature from 1 to 6 ° C, and a decrease in precipitation from 5 to 30%, will lead to early flowering stage from 2.5 to 12 days and a yield reduction from -2.2 to -38.5% (Cesaraccio *et al.*, 2008).

A study conducted at national and regional Italian level, based on AEZ methodology (FAO/IIASA, 2005), shows an expansions of suitable land area for wheat, for all future scenarios and GCMs considered and a forecasts to 2080 show increases for areas suited, especially in parts of northern Italy, and a decrease of area with severe constraints until the 2080s. The scenarios showed also an increase of potential yield in particular for the northern (Mereu *et al.*, 2008).

1.3.1 Durum wheat

Durum wheat [*Triticum turgidum* ssp. turgidum convar. durum (Desf.) MacKey] is one of the oldest cultivated cereal species in the world. It is of great importance in cereal areas of the Mediterranean Basin and North America, where the great bulk of world production of this crop and land under cultivation with it are concentrated (Table 3).

Table 3. Area, yields, and production of durum wheat in the world in 2004 and 2005.

Country	Area (000 ha)		Yield (t/ha)		Production (000 t)	
Year	2004	2005	2004	2005	2004	2005
Algeria	1,369	1,000	1.33	1.00	1,816	1,000
Argentina	57	54	3.16	2.96	180	160
Australia	200	200	2.00	2.00	400	400
Austria	15	15	4.00	4.00	60	60
Canada	2,141	2,200	2.32	2.16	4,962	4,750
France	406	415	5.05	3.98	2,050	1,650
Germany	8	8	6.25	5.75	50	46
Greece	500	500	2.00	2.00	1,000	1,000
India	450	450	2.67	2.67	1,200	1,200
Italy	1,870	1,450	3.05	2.41	5,700	3,500
Kazakhstan	100	100	1.00	1.00	100	100
Mexico	230	240	5.22	5.00	1,200	1,200
Morocco	1,111	1,050	1.82	0.71	2,025	750
Portugal	145	120	1.14	0.58	165	70
Russia	1,000	1,000	1.00	1.20	1,000	1,200
Spain	910	850	3.10	1.18	2,825	1,000
Syria	830	830	2.53	2.53	2,100	2,100
Tunisia	830	750	1.69	1.53	1,400	1,150
Turkey	1,100	1,100	2.18	2.09	2,400	2,300
UK	1	1	6.00	6.00	6	6
USA	956	993	2.56	2.58	2,450	2,560
World	14,229	13,326	2.33	1.97	33,089	26,202

Source: USDA (http://www.fas.usda.gov/pecad/highlights/2005/07/durum2005/).

The area annually planted with durum wheat worldwide is estimated to be about 13.5 million ha, though it has shown a decreasing tendency since the 1970s when it was close to 18 million ha (Belaid, 2000). The European Union devotes around 3.5 million ha to its cultivation, with a production of around 9.2 million metric tons. Canada is the second largest producer in the world and the greatest exporter. Average global yields have increased from 1.4 t ha^{-1} during the 1970s to more than 2 t ha^{-1} in recent years, leading to a great increase in total production. However, a reduction in global production occurred in 2005 due to lower plantings in the major EU durum

weath producing countries (Italy and Spain), combined with a severe drought affecting growing areas in the Mediterranean Basin (Royo *et al.,* 2009).

In the SEWANA region (South Europe, West Asia, and North Africa), durum wheat is mainly grown under rainfed conditions. Drought and heat during the grain filling period, nutrient deficiencies, soil problems, diseases, and pests are the main yield constraints.

The Mediterranean Basin is also the largest consumer of durum wheat products (pasta, couscous, bulgur, frekeh, etc.), and the most significant import market.

Durum wheat originated and became diversified in the Middle and Near East and in North Africa (MacKey, 2005). On the basis of the geographic origin and ecophysiological characterization of a number of Mediterranean and West Asian durum wheat landraces, the species *T. turgidum* L. ssp. *durum* (Desf.) Husn was subdivided during the last century into three botanical sections, namely mediterranea, syriaca, and europea (Grignac, 1965). Recent studies indicate that the genetic diversity in durum wheat seems to be structured, at least in part, according to a geographical pattern (Moragues *et al.,* 2006, 2007; Maccaferri *et al.,* 2005).

Durum wheat landraces, which were widely cultivated in the early twentieth century, were later increasingly replaced by improved varieties. The introduction of productive semi-dwarf cultivars resulted in the abandon of the genetically diverse, locally well-adapted but unimproved landraces, and the extinction of on-farm genetic variability. It has been suggested that the level of genetic diversity underlying the successful modern varieties may have fallen due to the limited number of ancestors, the relative uniformity of the pursued ideotype (Autrique *et al.,* 1996; Pecetti and Annicchiarico, 1998), the high selection pressure applied in breeding programs, and the relatively small number of varieties currently in cultivation (Skovmand *et al.,* 2005).

The main risk of a narrowing of the genetic background of the modern genetic pool is one of increased vulnerability to diseases and pests (Frankel *et al.,* 1995) and a fall in the abiotic stress tolerance, particularly to the drought and high temperatures that are typical of many regions growing durum wheat.

However, the results of several studies not only do not evidence an overall decrease in the genetic diversity of durum wheat due to past breeding activities but even reveal that it is increasing over time as a result of the introgression of genetic variability (Autrique *et al.,* 1996; Maccaferri *et al.,* 2003; Martynov *et al.,* 2005). CIMMYT and ICARDA, the two international centres operating with durum wheat, have largely helped to widen the genetic pool of current cultivars; shuttle breeding and germplasm exchange all around the world have been key factors in creating the current overall variation in durum wheat.

Around 79,000 tetraploid and 253,000 unspecified Triticum accessions are currently available in gene bank collections around the world (Skovmand *et al.,* 2005). The characterization of germplasm maintained in gene banks is crucial for exploiting the existing genetic variability for

traits of economic importance such as yield, yield stability, grain quality, and tolerance to biotic and abiotic stresses.

1.3.1.1 The Italian Pool

Durum wheat is the primary cereal crop of southern peninsular Italy, Sicily and Sardinia.

Figure 8 shows the trend in the durum wheat production in Italy from 1961 to 2000. The Italian production had an upward trend over the past 40 years. Areas of the South Italy were declined from the years 1981-1990 and the trend remains the same for the period 1991-2000 with a reduction rate of about 11.4 and 5% respectively. Otherwise, both the Center and North areas have maintained a rising trend throughout the period examined.

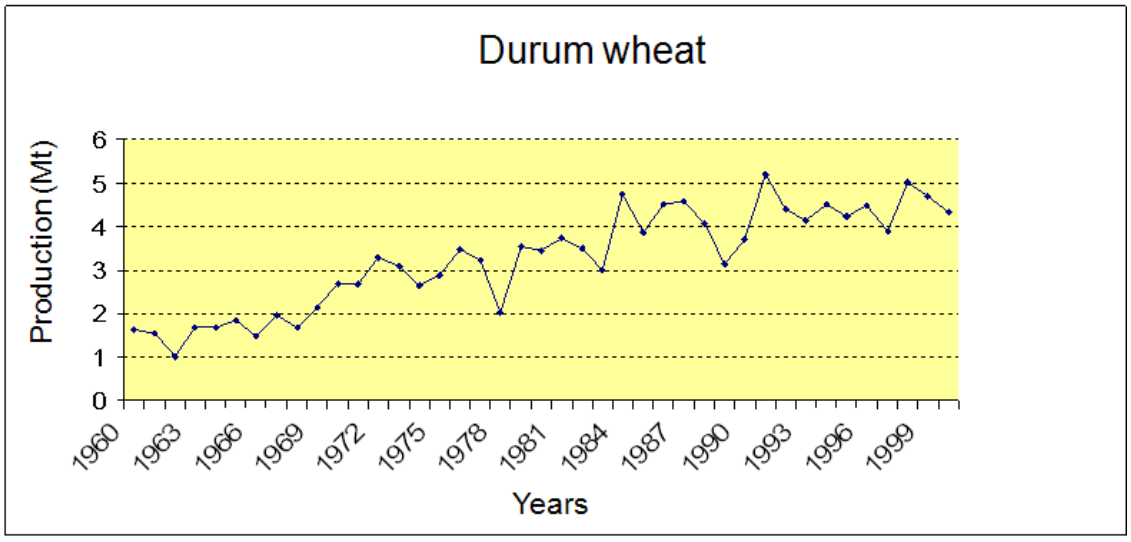

Figure 8. Trend in the durum wheat production in Italy from 1961 to 2000 (data provided by ISTAT).

Sardinia contributes to the Italian durum wheat production with 5.4% of the surface harvested and 3.3% of the total production. Figure 9 shows the historical evolution of production and the sowing area under wheat in Sardinia from the period 1960-2001 (source: ISTAT). The data are presented at intervals of seven years.

Cagliari's province is by far the most important, accounting for 59.6% of cultivated area and for 52.7% of production. Oristano's province is the second important province with values of 18.0% and 24.5% of cultivated area and production respectively, followed by the province of Sassari with 14.0% and 16.7%, and the province of Nuoro with 4.0% and 6.1%.

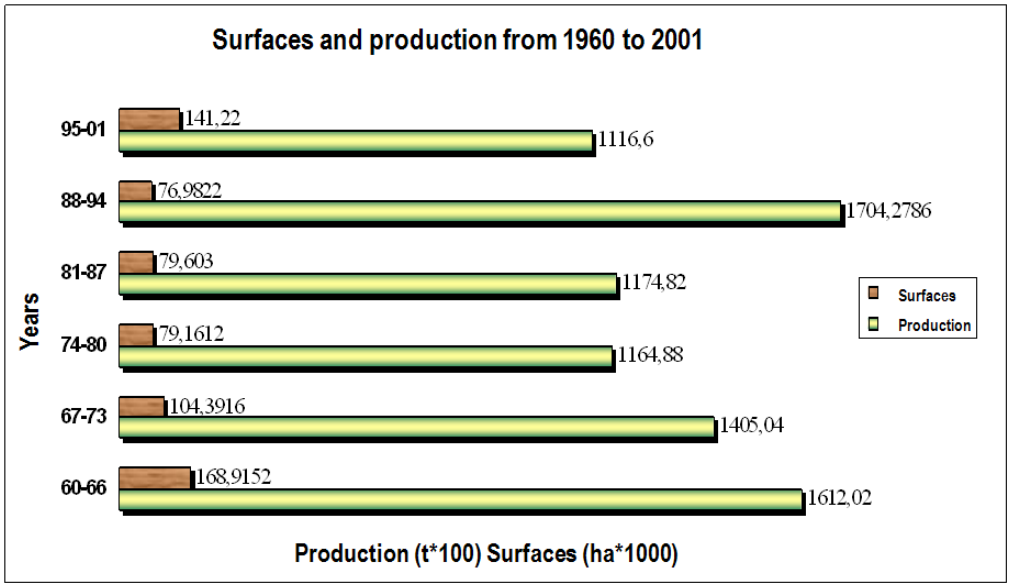

Figure 9. Historical evolution of production and sowing area under wheat in Sardinia for the period 1960-2001 (data provided by ISTAT).

Thanks to its economic importance, durum wheat in Italy it has enjoyed many years of intensive breeding, which has generated germplasm grown widely both inside and outside Italy (Bagnara and Scarascia Mugnozza, 1975).

The importance of durum wheat in Italy and the noteworthy breeding efforts devoted from the beginning of the twentieth century to improve this species, make the Italian pool one of the most representative within the Mediterranean Basin. Although other countries conducted breeding programs in the early decades of the last century, Italy may be considered as a pioneer in durum wheat improvement.

Numerous selections were obtained by Italian breeders during the early decades of the twentieth century from a very large pool of Mediterranean landraces (Di Fonzo *et al.*, 2005). One of the most widely spread was the variety 'Senatore Capelli', an 'africanum' type selected from the population 'Jean Retifah' from Algeria that was released in 1915, used in further crosses and is still grown in some areas (Di Fonzo *et al.*, 2005). However, only small-yield increases were achieved at the early times since most landraces were tall and very sensitive to lodging.

Breeding efforts resulted in the release of a number of improved varieties from 1950 to 1975. 'Appulo' and 'Trinakria' were two of the most outstanding varieties, due to their yielding ability, quality, and good adaptation to drought. The varieties 'Viscardo Montarani', 'Carlo Jucci', and 'Giovani Raineri' were obtained from crosses with hexaploid wheat aiming to enhance the number of fertile florets per spikelet. Research on mutation breeding as a way to induce shorter plants with strong straw resulted in the selection of lines with higher yielding ability and short straw such as 'Castelporziano' and 'Castelfusano', derived from the cultivar 'Capelli' (Scarascia-Mugnozza *et al.*, 1972). The gap between durum and bread wheat yield potential was filled by the

release in 1974 of ‘Creso’, a high-quality variety derived from a cross between a CIMMYT dwarf line and cv. ‘Castelfusano’.

During the last few decades, the Italian pool has been enriched with the incorporation of new gene pools, mainly from CIMMYT germplasm. The varieties ‘Simeto’, ‘Duilio’, ‘Iride’, ‘Arcangelo’, ‘Creso’, ‘Colosseo’, ‘Ciccio’, ‘Ofanto’, ‘Grazia’, ‘Appulo’, ‘Rusticano’, ‘Radioso’, ‘Appio’, ‘Svevo’, ‘Neodur’, ‘Zenit’, and ‘Meridiano’ are among the ones most cultivated by Italian farmers (Di Fonzo *et al.*, 2005).

2. ADAPTATIONS AND MITIGATIONS STRATEGIES

If greenhouse gas emissions are not abated, crop production likely will decline towards the end of this century, and in many regions it could be seriously compromised.

A large amount of literature shows also that without mitigation and adaptation, climate change will be problematic in some regions for agricultural production and communities. However, the detrimental climate impacts can be reduced and numerous opportunities can be created by changing climatic conditions (Smith and Wandel, 2006; Adger *et al.,* 2005; Alexandrov and Hoogenboom, 2000; Bellocchi *et al.,* 2002; Carbone *et al.,* 2003; Gbetibouo and Hassan, 2005; Challinor *et al.,* 2007*a*; Salinger *et al.,* 2000). However climate extreme events will probably be the most challenging for farmers and society in general under future climate change (Rosenzweig *et al.,* 2001). In the shorter term, trade liberalization, new demand for land for biofuels and the global food market will affect trade and production (van Meijl *et al.,* 2006). Farmers can and do adapt to climate change in the context of globalization and changing policies in order to reduce negative impacts.

Hence it's very important to focus the attention on the potential roles of adaptation and mitigation strategies, and their interactions, in responding to climate change.

Article 4.1b of the United Nations Framework Convention on Climate Change (UNFCCC, 1992) states that parties are 'committed to formulate and implement national and, where appropriate, regional programs containing measures to mitigate climate change and measures to facilitate adequate adaptation to climate change.' The Kyoto Protocol (Article 10) further commits parties to promote and facilitate adaptation, and deploy adaptation technologies to address climate change (UNFCCC, 1998).

The mitigation, indeed, needs to be necessarily coupled with adaptation actions. These, either anticipatory or reactive, represent the only viable option to cope with unavoidable climate change impacts that mitigation cannot eliminate.

2.1 Adaptation strategies

Adaptation is an important component of climate change impact and vulnerability assessment, and is one of the policy options in response to climate change impacts (Fankhauser, 1996; Smith and Lenhart, 1996; Smit *et al.,* 1999) that has been recognized internationally by government. The majority of countries recognizes adaptation as an important component of its climate change response strategy and is exploring adaptation options in several sectors.

Adaptation includes all the initiatives and measures to reduce the vulnerability of natural and human systems against actual or expected climate change effects. Various types of adaptation

exist, e.g. *anticipatory* and *reactive*, *private* and *public*, and *autonomous* and *planned*, etc. Examples are raising river or coastal dikes, the substitution of more temperature-shock resistant plants for sensitive ones, etc. (IPCC, 2007).

The IPCC (2001 *b*) defines *autonomous* adaptation as: "adaptation that does not constitute a conscious response to climatic stimuli but is triggered by ecological changes in natural systems and by market or welfare changes in human systems" and *planned* adaptation as: "adaptation that is the result of a deliberate policy decision based on an awareness that conditions have changed or are about to change and that action is required to return to, maintain, or achieve a desired state".

Private adaptation include actions taken by individual actors and *public* adaptation include actions put in place by regional, national and international policies in order to complement, enhance and/or facilitate responses by single and organizations.

Another important distinction is the one based on the timing of adaptation actions which distinguishes between *anticipatory* or proactive adaptation and *reactive* or responsive adaptation. They are defined by the IPCC (2001 *b*) as: "adaptation that takes place before and after impacts of climate change are observed", respectively. There can be circumstances when an anticipatory intervention is less costly and more effective than a reactive action (typical example is that of flood or coastal protection), and this is particularly relevant for planned adaptation. Reactive adaptation is a major characteristic of unmanaged natural system and of autonomous adaptation reactions of social economic systems.

Agriculture is among the most vulnerable sectors to the risks and impacts of global climate change (Parry and Carter, 1989; Reilly, 1995) and adaptation is certainly an important component of any policy response to climate change in this sector (Mizina *et al.,* 1999; Reilly and Schimmelpfennig, 1999).

Agricultural adaptation, defined as "the adjustment in agricultural systems in response to actual or expected climatic stimuli or their effects, to moderate harm or exploit beneficial opportunities" (IPCC, 2001 *b*), becomes a key element in climate change policy that must be studied in depth.

Studies show that without adaptation, climate change is generally problematic for agricultural production and for agricultural economies and communities, while with adaptation, vulnerability can be significantly reduced (Easterling *et al.,* 1993; Rosenzwieg and Parry, 1994; Fankhauser, 1996; Smith *et al.,*1996; Wheaton and McIver, 1999).

Adaptations in agriculture vary with respect to the climatic stimuli to which adjustments are made (i.e. various attributes of climate change, including variability and extreme events) and according to the differing farm types and locations, and the economic, political and institutional circumstances in which the climatic stimuli are experienced and management decisions are made (Chiotti and Johnston, 1995; Tol *et al.*, 1998; Smit *et al.*, 1999; Bryant *et al.*, 2000).

Many potential agricultural adaptation options have been suggested, representing measures or practices that might be adopted to alleviate expected adverse impacts. They encompass a wide range of forms (technical, financial, managerial), scales (global, regional, local) and participants (governments, industries, farmers) (Smithers and Smit ,1997; Skinner *et al.*, 2001). Most of these represent possible or potential or adaptation measures, rather than ones actually adopted.

Adaptation in agriculture has always been the norm rather than the exception. In addition to changes driven by several socio-economic factors (chiefly market conditions and policy frameworks), farmers always have to adapt to the vagaries of weather, on weekly, seasonal, annual and longer timescales.

The problem in the coming decades will be the rate and nature of climate change compared to the adaptation capacity of farmers.

Adaptive capacity of a system, in the context of climate change, can be viewed as the full set of system skills (i.e., technical solutions available to farmers in order to respond to climate stresses) as determined by the socio-economic and cultural settings, plus institutional and policy context, prevalent in the region of interest. The concept of adaptive capacity is a theoretical one, i.e., it is not easily measurable, while the actual adaptation responses can be measured in a cost-benefit fashion or some other monetary or non-monetary approach (Tubiello and Rosenzweig, 2008).

Recent studies have also emphasized the concept of vulnerability of agricultural system as a function of exposure of that system to climate hazards, its intrinsic sensitivity to that exposure, and its adaptive capacity (Tubiello and Rosenzweig, 2008):

Vulnerability= *f* (Exposure, Sensitivity (Exposure), Adaptive Capacity).

As reported by many studies, if future changes are relatively moderate, farmers may successfully adapt to changing climates by applying a variety of agronomic techniques that already work well under current climates, such as adjusting the timing of planting and harvesting operations, and substituting cultivars.

These changes in agronomic practices in agriculture are defined as the autonomous adaptation strategies, while planned adaptation strategies include conscious policy options or response strategies, often multisectoral in nature, aimed at altering the adaptive capacity of the agricultural system or facilitating specific adaptations.

The agronomic strategies available include both short-term adjustments and long-term adaptations (Easterling, 1996).

Short-term adjustments are seen as autonomous in the sense that no other sectors (e.g. policy, research etc.) are needed in their development and implementation. Examples of short-term adjustments are changes in varieties, sowing dates and fertiliser and pesticide use.

Long-term adaptations are major structural changes to overcome adversity such as changes in land-use to maximize yield under new conditions, application of new technologies, breeding of crop varieties, new land management techniques, and water-use efficiency related techniques.

Most of the short-term adjustments involve relatively little cost for the farmers, since they are often just extensions of the existing schemes to deal with climatic variability. However, long-term adaptations and changes in farming systems, institutions, land use etc. may carry considerably higher costs. Some of these costs can be reduced, if timely action is taken (Stern, 2006). However, there is a need at regional, national and international levels to analyze the needs for such planned adaptation options, their costs and their time horizon.

Reilly and Schimmelpfennig (1999) define the following "major classes of adaptation":

- seasonal changes and sowing dates;
- different variety or species;
- water supply and irrigation system;
- other inputs (fertilizer, tillage methods, grain drying, other field operations);
- new crop varieties;
- forest fire management, promotion of agroforestry, adaptive management with suitable species and silvicultural practices.

Accordingly, types of responses include:

- reduction of food security risk;
- identifying present vulnerabilities;
- adjusting agricultural research priorities;
- protecting genetic resources and intellectual property rights;
- strengthening agricultural extension and communication systems;
- adjustment in commodity and trade policy;
- increased training and education;
- identification and promotion of (micro-) climatic benefits and environmental services of trees and forests (FAO, 2005).

Adaptation strategies will vary with agricultural systems, location, and scenarios of climate change considered and so the responses to specific adaptation strategies for given cropping systems can still vary considerably, as a function of these factors.

For cereals, different adaptation strategies are needed for fall sown crops, such as winter wheat and barley, compared to spring crops, such as maize and spring wheat.

For spring crops, climate warming will allow earlier planting or sowing than at present. Earlier planting in spring increases the length of the growing season; thus earlier planting using long season cultivars will increase yield potential, if soil moisture is adequate and the risk of heat

stress is low. Otherwise, earlier planting combined with a short-season cultivar would give the best assurance of avoiding heat and water stresses (Tubiello *et al.,* 2000). For winter crops (i.e. cereals), a specific growth stage has to be reached before the onset of winter to ensure winter survival, thus they are often sown when temperatures approach the time when vernalization is most effective (Harrison *et al.,* 1995).

For winter cereal, it could be possible the use of longer-maturing cultivars, but these require enough precipitation over the extended growing season to sustain grain filling. If the particular climate scenario considered consists of both warmer and drier conditions, such an adaptation strategy will likely not work. Additionally, such a strategy might not work at southern sites, regardless of the climate scenario considered, because farmers there already plant cultivars having low vernalization requirements and maturity times in the upper range of those available. In such cases, effective adaptation might not be possible without further breeding programs, a process that typically takes a decade or longer before newly adapted cultivars can be distributed to farmers (Rosenzweig and Tubiello, 2007).

In addition to changing planting strategies and cultivar type, land management systems could be adapted to new climate conditions. The introduction of optimal agricultural technology (machine, fertiliser, fungicide, etc.) may be considered as a fundamental strategy for adapting agriculture to climate change. Shifts from rainfed to irrigated agriculture could be the simplest solution, but issues of water availability, cost, and competition from other sectors need to be considered (i.e., Reilly *et al.,* 2003; Tubiello *et al.,* 2002; Rosenzweig *et al.,* 2004). At higher levels of adaptation, cropping systems and crop types could be changed altogether in addition to field management adjustments (i.e., Reilly *et al.,* 2003), or cultivation areas could shift geographically, following the creation of new agricultural zonations determined by a changing climate (e.g., Fischer *et al.,* 2001).

Furthermore changes of land use may be used as adaptation strategies to the differential response of crops to climate change. Changes in land allocation may also be used to stabilize production or for the conservation of soil moisture.

About climate variability there are strong indications that climate change will also bring about pronounced changes in climate variability (IPCC, 2007). Several studies have indicated that specific scenarios with mean warmer and wetter conditions might be associated with increased frequency of heavy precipitation events (i.e., Milly *et al.,* 2002), with potential implications for increased crop losses. For example, Rosenzweig *et al.* (2002 *a, b*) computed that agricultural losses in the U.S. due to heavy precipitation and excess soil moisture could double by 2030.

As opposed to adaptation to changes in mean conditions, which require adjustments in agronomic techniques, adaptation to future changes, likely an increase, in climate variability may require an attention to stability and resilience of production, rather than to improving its absolute levels. Crop management and cropping systems have evolved to provide farmers with stability of

production and thus steady income in the face of uncertain weather. The coefficient of variation (CV) of yield in given areas may be used as a measure of system stability, providing insight into superior cropping techniques at given sites. For example, cropping rotations, integrated pest management, soil conservation and fallow techniques, that produce lower CVs and higher long-term yields because of reductions in crop-failure probabilities, are examples of management practices that contribute to stability of farm production and income (Rosenzweig and Tubiello, 2007).

Some adaptations will likely be successful (e.g., change in planting dates to avoid heat stress), while other attempted adaptations (e.g., changing varieties and breeds, altered crop rotations, development of new agricultural areas) may not always be effective in avoiding the negative effects of droughts or floods on crop production. Importantly, there are additional dimensions to adaptation, related to social and cultural aspects, that might either favor or hinder adoption of new techniques by farmers, depending on community dynamics (Smith *et al.*, 2003; Smit and Skinner, 2002).

To be effective, many of these adaptations, including spending on agricultural research and outreach programmes, and the selection and breeding of new hybrids and cultivars, would require an active role by government. It is important to recognise that changes in increasing atmospheric CO_2 concentration and global warming are likely to alter the phenological response of certain crops, thereby putting current crop–weather relationships in doubt (Challinor *et al.*, 2007*b*).

Although the breeding of new cultivars with improved yields under future climate is a potentially crucial adaptation option, the basis on which any new cultivars are developed will depend on the nature and extent of climate change in any specific region or cropping system (Tingem and Rivington, 2009).

Climate change adaptation for agricultural cropping systems requires a higher resilience against both excess of water (due to high intensity rainfall) and lack of water (due to extended drought periods). A key element to respond to both problems is soil organic matter, which improves and stabilizes the soil structure so that the soils can absorb higher amounts of water without causing surface run off, which could result in soil erosion and, further downstream, in flooding. Soil organic matter also improves the water absorption capacity of the soil for during extended drought (FAO, 2007).

While intensive soil tillage reduces soil organic matter through aerobic mineralization, low tillage and the maintenance of a permanent soil cover (through crops, crop residues or cover crops and the introduction of diversified crop rotations) increases soil organic matter. A no- or low-tilled soil conserves the structure of soil for fauna and related macrospores (earthworms, termites and root channels) to serve as drainage channels for excess water. Surface mulch cover protects soil from excess temperatures and evaporation losses and can reduce crop water requirements by 30% (FAO, 2007).

It is important to consider the need to conserve the biodiversity, because the biodiversity in all its components (e.g. genes, species, ecosystem) increases resilience to changing environmental conditions and stresses. Genetically-diverse populations and species-rich ecosystems have greater potential to adapt to climate change. FAO promotes use of indigenous and locally-adapted plants and animals as well as the selection and multiplication of crop varieties and autochthonous races adapted or resistant to adverse conditions (FAO, 2007).

The agricultural cost (both to producers and consumers) of responding to climate change will mostly be for the implementation of measures to adapt. At the individual farm level, these costs will reflect changes in revenues, while at national and global levels they will reflect changes in prices paid by consumers. Crop producers who possess adequate levels of capital and technology should be capable of adapting to climate change, although changes in types of crops that are grown may be required.

At the global level, adaptation is expected to result in small percentage changes in income. These changes are expected to be generally positive for small to moderate amounts of warming, account taken for CO_2 effects (Easterling and Apps, 2005).

2.2 Mitigation strategies

Mitigation can be defined as the anthropogenic intervention to reduce the sources or enhance the sinks of greenhouse gases (IPCC, 2001*a*).

The Kyoto Protocol under the UN Framework Convention on Climate Change (UNFCCC) commits industrialised signatory countries to reduce their emissions to below the level in 1990.

While agriculture stands to be greatly affected by projected climate change, it has historically been and it is, a major source of greenhouse gases to the atmosphere, thus itself contributing to climate change.

Management of land for food and livestock production over the past century was responsible for cumulative carbon emissions of about 150 GT C, compared to 300 GT C from fossil fuels (LULUCF, 2000). At present, agriculture and associated land use change such as deforestation contributes to, respectively, 13 and 17% of total anthropogenic greenhouse gas emission (GHG). While carbon dioxide emission from agriculture are relatively small (about a quarter of the carbon dioxide annually released into the atmosphere by human activities) the sector accounts for about 60% of all nitrous oxide (mainly from fertilizer applications and manure management) and about 50% of methane (emitted mainly from livestock and rice cultivation). The GHG impact through radiative forcing of NO_2 is 300 times that of CO_2. Methane and nitrous oxide emissions are projected to further increase by 35 to 60 % by 2030, driven by growing nitrogen fertilizer use and increased livestock production in response to growing food demand.

Modifying current management of agricultural systems could therefore greatly help to mitigate global anthropogenic emissions.

The emissions occurred in past decades have shown the planet to a certain degree of climate change, so all actions taken today carry out their effectiveness in the second half of this century (Milly *et al.,* 2002).

Mitigation of climate change is a global responsibility.

IPCC estimates that the global technical mitigation potential for agriculture will be between 5500 and 6000 Mt CO_2-equivalent per year by 2030, 89% of which are assumed to be from carbon sequestration in soils.

IPCC also estimates that reductions of agricultural GHG mitigation options are cost-competitive with non-agricultural options for achieving long-term climate objectives. Soil carbon sequestration could indeed take effect very quickly and is very cost-effective in agriculture. A successful approach could be achieved by paying farmers for carbon sequestration (building soil organic matter) which sets up a scenario where: CO_2 is removed from the atmosphere (mitigation); higher organic matter levels in soil increase agroecosystem resilience (adaptation); and improved soil fertility leads to better yields (production and income generation). Therefore farmers could

increase their income by selling carbon-emission credits to other carbon-emitting sectors. However, sequestration of CO_2 in soils is not included in the Clean Development Mechanism (CDM) agreed to in Kyoto. The scope of the successor of the CDM could be enhanced with a view to increase carbon sinks in soil and in above- and below-ground biomass, and thus contribute to removing methodological barriers to operationalising soil carbon sequestration under the Post-2012 climate change regime (FAO, 2008).

Possible mitigation approaches in agriculture concentrate on either (or both) of the following key factors:

- carbon sequestration from the atmosphere and its storage in the soil by increasing the stock of organic carbon;
- adoption of management practices to reduce emissions of greenhouse gases resulting on farming.

It is important to remark how these two options differ. Indeed, carbon sequestration in soil (by increasing carbon inputs into the soil and reducing the decay rate of soil organic matter) is limited, while management changes, aimed at reducing carbon fluxes from agricultural activities, may last for an indefinite period, as long as the new management system is sustainable in both energy and ecological terms.

Of the 150 GT C that were lost in the last century due to land conversion to agriculture and subsequent production, about two thirds were lost due to deforestation and one-third, roughly 50 GT C, due to cultivation of current agricultural soils and exports as food products (LULUCF, 2000).

Crop management and conservation tillage practices can improve soil quality and raise Soil Organic Carbon (SOC) levels, while enhancing sustainability and resilience of agricultural systems. 'Best practice' farming techniques (i.e. use of cover crops and/or nitrogen fixers in rotation cycles, appropriate use of fertilizers and organic amendments, soil water management improvements to irrigation and drainage and improved varieties with high biomass production) are included in both systems.

Over the next four decades, such best practices could store about 8 GT C in agricultural soils. Currently, the fossil fuel used to mechanically sow, irrigate, harvest and dry crops, including fertilizer manufacture, is responsible for atmospheric emissions of about 150– 200 MT C yr^{-1}. As total cropland covers about 1.5 G ha of global ice-free land, this figure is equal to a global average emission rate of 100–130 kg C ha^{-1} yr^{-1} (Rosenzweig and Tubiello, 2007).

Recently, a study (West and Marland, 2002) on intensive agriculture (corn, wheat, and soybean rotation systems) in the US Midwest, showed that reduced-tillage agriculture gave better results than conventional tillage, either in terms of its direct benefits, and of indirect effects, resulting in reduced C emissions from reduced requirements for field operations and inputs.

Indirect reductions were obtained despite the increased use of pesticides and herbicides, being machinery and labour for soil preparation lower in reduced-tillage systems.

Generally, direct benefits of carbon sequestration in reduced tillage systems have a limited duration (20–40 years), while those arising from reduced C emissions can last as long as the relative management changes are in place. Therefore, even though flux reductions may appear small compared to total anthropogenic emissions, they may mitigate sectoral emissions. (Rosenzweig and Tubiello, 2007).

Furthermore, agriculture may help to mitigate anthropogenic greenhouse emissions through the production of bio-fuels. If available marginal land was used for energy crops, the IPCC projects a significant displacement of fossil fuels, globally up to 3–4 GT C yr^{-1} by mid century through conversion of about 200 M ha of marginal land to bio-fuel production (IPCC, 2001*c*). However, issues of input availability, especially water, have not been considered in previous studies and need to be further investigated.

Because of the greater global warming potential of CH_4 and N_2O compared to CO_2, mitigation of non-CO_2 greenhouse gases in agriculture can be quite significant and achieved via the development of more efficient rice (for methane) and livestock production systems (for both methane and nitrous-dioxide). In intensive agricultural systems with crops and livestock production, direct CO_2 emissions are predominantly connected to field crop production and are typically in the range of 150– 200 kg C ha^{-1} yr^{-1} (West and Marland, 2002; Flessa *et al.*, 2002). Greenhouse gas analyses of different farm systems in Europe have recently shown that such CO_2 emissions represent only 10–15% of farm total, with methane and N_2O corresponding respectively to 25–30% and 60% of total greenhouse gas emissions from farm activities. N_2O input results from N volatilization from fertilized fields and animal waste, and effective mitigation strategies for N_2O emissions are harder to identify, given the heterogeneity of emissions in space and time and the difficulty of timing fertilizer applications and/or manure management. Uncertain data on emission factors also cause difficulties in the assessment of efficient N_2O-reduction. Current techniques are focusing on the reduction of absolute amounts of fertilizer N applied to fields (Rosenzweig and Tubiello, 2007).

By analyzing all components of farm activities, Flessa *et al.* (2002) suggested that overall emissions of the non-CO_2 gases could be reduced by about 25% by shifting to less intensive, organic production systems. Given the higher global warming potential of both CH_4 and N_2O compared to that of CO_2 however, overall farm emissions could still be significant even in organic systems. A possibly viable strategy to mitigating non-CO_2 gases in intensive mixed crop-livestock farming systems, such as those in place in both Europe and North America, might be a change in human diet towards a lower meat consumption level, thus reducing livestock numbers, as well as grain production for feed (Flessa *et al.*, 2002).

There are a number of possibilities for reducing emissions of methane and nitrous oxide emissions through improving management practices and introducing new technologies (Weiske *et al.,* 2006). Advantage should be taken of the fact that some of the measures simultaneously may reduce the net emission of several greenhouse gases. Such measures may be combined with land management measures to sequester soil carbon too. A number of options exist to reduce or even reverse the emissions of greenhouse gases from agriculture. These options can be grouped according to gases and modes of action:

• Reduction in direct energy use (fuel, electricity, heating) and indirect energy use (e.g. fertilisers).

• Substitution of fossil energy through biofuel production and anaerobic digestion of manure etc.

• Increased carbon storage in soils through higher inputs (straw incorporation, manure, cover crops, grass in rotation) and reduced soil organic matter turnover (minimum and no-tillage).

• Reduced methane emissions through improved diets for ruminant animals and through improved handling and storage of manures (including anaerobic digestion).

• Reduced nitrous oxide emissions through tighter nitrogen cycling and through technical measures to reduce emissions from manure stores and from manures and fertilisers applied to soil.

In general, most of these management methods and technologies need to be further developed, if they are to be applied in a cost-effective manner. However, some of these methods provide additional social and environmental benefits, which need to be considered.

Literature provides relatively low mitigation costs, both at global and European level. A common finding in the climate-economy literature (IPCC and the Stern Review, 2007) is that stabilization of atmospheric GHG concentrations at a "safe" level in 2100 is achievable at a limited economic penalty for the society, between 1% and 2% of Gross World Product (GWP).

A report recently published by McKinsey (2009) confirms those findings, reporting a GDP (Gross Domestic Product) loss less than 1% in 2030, equivalent to 200 and 350 EUR Billion. To comply with a stringent climate policy aimed at 450 CO_2 only stabilization, World Energy Outlook (2008) estimates an average annual increase in zero or low carbon technologies investments equal to 0.55% of GWP between 2010 and 2030.

2.3 Links between adaptation and mitigation strategies

The Third Assessment Report of the IPCC (TAR) demonstrated that the level of climate change impacts, and whether or not this level is dangerous, is determined by both adaptation and mitigation efforts (Smit *et al.,* 2001). Adaptation and mitigation are both viable strategies to combat damages due to climate change. However, they tackle the problem from completely different angles. Adaptation can be seen as direct damage prevention, while mitigation would be indirect damage prevention (Verheyen, 2005).

Mitigation and adaptation work at different spatial and time scales. Mitigation is "global" and "long term" while adaptation is "local" and "shorter term" (Fussel and Klein, 2006; Tol, 2005; Wilbanks, 2005). This has several important implications.

Firstly, mitigation can be considered as a "permanent" solution to anthropogenic climate change. In contrast, adaptation is more temporary as it typically addresses current or expected damages.

Secondly, the effects of mitigation and adaptation occur at different times (Wilbanks, 2005; Fussel and Klein, 2006). That is, emission reductions today will translate in a lower temperature increase and ultimately lower damage only in the (far) future, whereas adaptation measures, once implemented, are immediately effective in reducing the damage. This differentiation is particularly relevant under the policy making perspective: probably, the stronger reason for the scarce appeal of mitigation policies is their "certain" and "present" cost facing a future and thus uncertain benefit.

Thirdly, mitigation provides a "global", whereas adaptation provides a "local" response to anthropogenic climate change. The benefits induced by a ton of carbon abated are experienced irrespectively of where this ton has been abated. Differently, adaptation entails measures implemented locally whose benefits advantage primarily the local communities targeted (Bosello *et al*, 2009).

However, only recently policy-makers have expressed an interest in exploring interrelationships between adaptation and mitigation. Recognizing the dual need for adaptation and mitigation, as well as the need to explore trade-offs and synergies between the two responses, they are faced with an array of questions (GAIM Task Force, 2002; Clark et al., 2004; see also Figure 9): (1) How much adaptation and mitigation would be optimal, when, and in which combination? (2) Are adaptation and mitigation substitutes or are they complementary to one another? (3) When and where is it best to invest in adaptation, and when and where in mitigation? (4) How do their costs and effectiveness vary over time? The up-to-date relevant literature does not provide clear answers to the above questions (IPCC, 2007). In other words, decision maker needs to place herself somewhere inside the decision space represented by the triangle of Figure 10: verteces are possible, but unlikely.

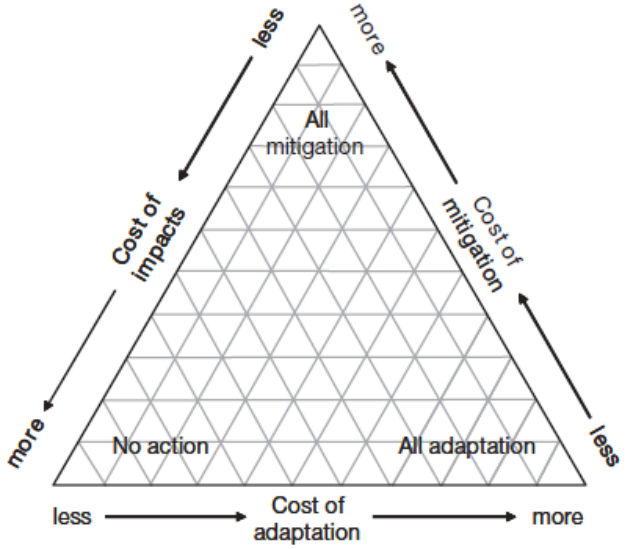

Figure 10. A schematic overview of inter-relationships between adaptation, mitigation and impacts, based on Holdridge's life-zone classification scheme (Holdridge, 1947, 1967; M.L. Parry, personal communication).

On the one hand, agriculture is one the main human sectors that will be affected by climate change over the next decades, which will consequently require adaptation measures. But agriculture represents also a major source of greenhouse gas emissions into the atmosphere. Therefore, synergies need to be identified between adaptation and mitigation strategies, in order to face climate and social challenges over the next decades. Hence, farmers and other stakeholders in this sector will have to cope with the dual task of contributing to global reductions of carbon dioxide and other greenhouse gas emissions, while having to manage an already changing climate.

Both mitigation and adaptation are needed in responding to risks of impacts from climate change in agriculture and both are necessary, recognizing that each has its limits.

Mitigation and adaptation are also related in more action-specific ways. For instance, individual mitigation and adaptation actions often have the potential to interact with each other. In some cases, they offer alternatives, in others, they reinforce each other. In either case, the actions are also related to other aspects of sustainable development pathways as well. Considering mitigation and adaptation as parts of an integrated portfolio of strategies, policies, and actions is complicated, however, by the fact that adaptation is in many ways more complex than mitigation—e.g., it can be both anticipatory and reactive and it often depends on a mosaic of local circumstances—but it has received less research attention, especially where costs are concerned (Wilbanks *et al.*, 2007).

Mitigation and adaptation measures tend to differ in the timing of the efforts (mitigation benefits are lagged in time, unlike some adaptation benefits), the geographical pattern of their effects (mitigation benefits are more global; adaptation benefits are more localized), and the

sectoral focus of their responses (mitigation focuses on greenhouse gas emitters and sinks; adaptation focuses on sectors and activities sensitive to climate impacts) (Wilbanks *et al.,* 2007).

In the first place, interactions between adaptation strategies and the mitigation potential of the adapted system should be considered. Some specific adaptation practices might not be conducive to mitigation: e.g., as agricultural zonation shifts the earth's potential agricultural limits polewards, increased cultivation in previously marginal lands may result in significant losses of SOC in formerly untouched areas.Yet, some adaptation practices currently implemented in agricultural areas may positively reinforce land mitigation potentials under specific conditions: e.g., increased irrigation and fertilization to keep production in semi-arid regions under climate change conditions may also enhance soils potential to sequester carbon in those areas, as in the case of sub-Saharan Africa, where even small improvements in irrigation efficiency may have remarkable effects on biomass production of crops (Solomon *et al.,* 2000) and, thus, on soil inputs.

Yields and SOC levels will both be affected by climate change impacts on agriculture, as well as farming soils, with relatively positive or adverse results. Elevated CO_2 will have positive effects on soil carbon storage, as it increases above- and below-ground biomass production in the agro-ecosystem. In the same way, an extended growing season under warmer climates will allow for increased carbon inputs into soils. However, warmer temperatures may have adverse effects on SOC by increasing decomposition rates, reducing inputs and, thus, shortening crop life cycles. Increased variability and frequency of extreme events will adversely impact soil carbon storage, either by decreasing local production levels and by worsening soil quality (Rosenzweig and Tubiello, 2007).

Mitigation strategies and adaptation measures may reveal important interactions. These interactions between mitigation and adaptation can be mutually re-enforcing, especially in view of increased climate variability under climate change. By increasing the soils ability to hold moisture and to face erosion, and by enriching ecosystem biodiversity through diversified cropping systems, many mitigation techniques implemented for carbon sequestration may also help cropping systems to better withstand droughts and/or floods, whose frequency and severity is projected to increase in future warmer climates (Rosenzweig and Tubiello, 2007).

The efficacy of agronomic adaptation strategies under climate change in a variety of production systems for given regions and different possible levels of climate change may be tested within the support of dynamic crop models.

However, first it is necessary to consider the range of emission scenarios and climate models that can be used to estimate the magnitude of future climate changes.

3. CLIMATE MODELS AND PROJECTIONS

3.1 Emission scenarios

In order to determine how the climate may change in the future the attention has been focused on the evolution of greenhouse gases emissions, considered unequivocally responsible for the temperature increase since the post-industrial civilization (IPCC, 2007).

The emissions scenarios (SRES[2], 2000) developed by IPCC have been constructed to explore socio-economic development and related pressures on the global environment in this century, with special reference to emissions of greenhouse gases into the atmosphere. Emissions of greenhouse gases are linked to the behaviour of different systems (social productive natural) rather complex, which are influenced by socio-economic, demographic and technological changes, economic activity, energy use and land use change. Future emissions and the evolution of their underlying driving forces are highly uncertain, as reflected in the very wide range of future emissions paths in the literature that is also captured by the SRES emission scenarios. The use of scenarios addresses the uncertainties related to known factors. Uncertainties related to unknown factors can of course never be persuasively captured by any approach. As the prediction of future anthropogenic GHG emissions is impossible, alternative GHG emissions scenarios become a major tool for analyzing potential long-range developments of the socio-economic system and corresponding emission sources.

Scenarios are images of the future, or alternative futures. They are neither predictions nor forecasts. Rather, each scenario is one alternative image of how the future might unfold. As such they enhance our understanding of how systems behave, evolve and interact. They are useful tools for scientific assessments, learning about complex systems behavior and for policymaking and assist in climate change analysis, including climate modeling and the assessment of impacts, adaptation and mitigation (IPCC, 2007).

The choice of scenarios is important because it can determine the outcome of a climate impact assessment. Extreme scenarios can produce extreme impacts; moderate scenarios may produce more modest effects (Smith and Hulme, 1998). It follows that the selection of scenarios can also be controversial, unless the fundamental uncertainties inherent in future projections are properly addressed in the impact analysis. So, in choosing the set of scenarios for use in the given climate impact analysis, the set should represent the uncertainties.

[2] SRES-Special Report on Emission Scenarios, Working Group III-IPCC, 2000.

The scenarios are based on an extensive assessment of driving forces and emissions in the scenario literature, alternative modelling approaches, and an "open process"[3] that solicited wide participation and feedback.

Four different narrative storylines (A1, A2, B1 and B2) were developed to describe consistently the relationships between emission driving forces and their evolution and add context for the scenario quantification (Fig. 11). Each storyline explore alternative development pathways, covering a wide range of demographic, economic and technological driving forces and resulting GHG emissions.

After determining the basic features and driving forces for each of the four storylines, have been developed 40 SRES scenarios by six modelling teams using different modelling approaches to examine the range of outcomes arising from a range of models that use similar assumptions about driving forces. Each scenario represents a specific quantitative interpretation of one of four storylines. All the interpretations and quantifications associated with a single storyline are called a scenario "family".

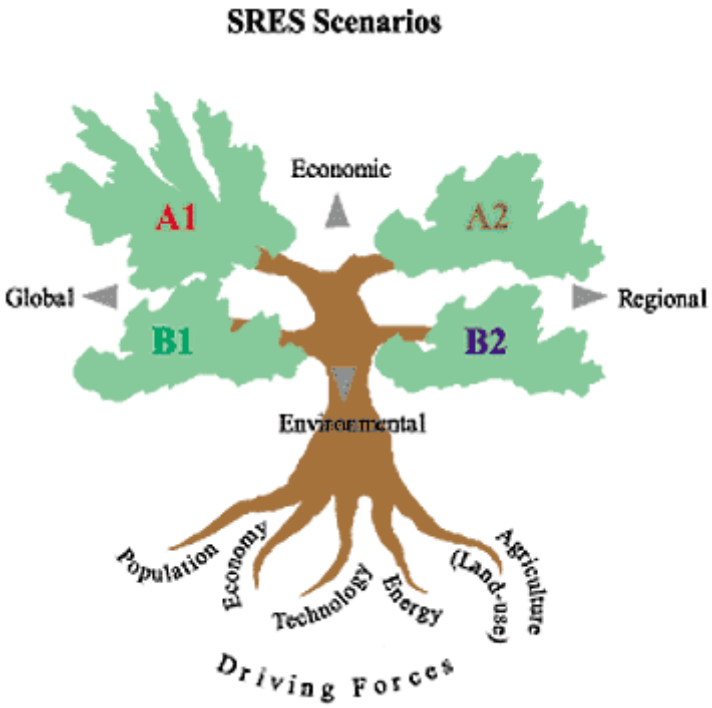

Figure 11. Schematic illustration of SRES scenarios. The four scenario "families" are illustrated, very simplistically, as branches of a two-dimensional tree. In reality, the four scenario families share a space of a much higher dimensionality given the numerous assumptions needed to define any given scenario in a particular modeling approach. The schematic diagram illustrates that the scenarios build on the main driving forces of GHG emissions. Each scenario family is based on a common specification of some of the main driving forces (IPCC, 2007).

[3] The open process defined in the Special Report on Emissions Scenarios (SRES) Terms of Reference calls for the use of multiple models, seeking inputs from a wide community as well as making scenario results widely available for comments and review. These objectives were fulfilled by the SRES multi-model approach and the open SRES website.

The set of scenarios consists of six scenario groups drawn from the four families: one group each in A2, B1, B2, and three groups within the A1 family, characterizing alternative developments of energy technologies: A1FI (fossil fuel intensive), A1B (balanced), and A1T (predominantly non-fossil fuel). Within each family and group of scenarios, some share "harmonized" assumptions on global population, gross world product, and final energy. These are marked as "HS" for harmonized scenarios. "OS" denotes scenarios that explore uncertainties in driving forces beyond those of the harmonized scenarios (SRES, 2000) (Fig. 12).

The SRES scenarios do not include additional climate policies above current ones. The emissions projections are widely used in the assessments of future climate change, and their underlying assumptions with respect to socio-economic, demographic and technological change serve as inputs to many recent climate change vulnerability and impact assessments.

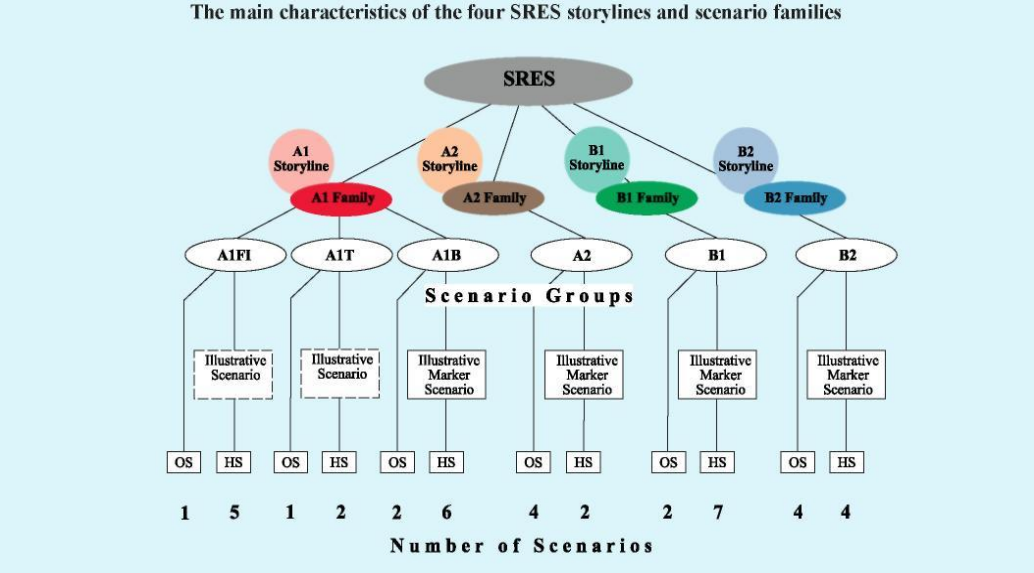

Figure 12. The main characteristics of the four SRES storylines and scenario families.

In particular:

The **A1** storyline and scenario family describes a future world of very rapid economic growth, global population that peaks in mid-century and declines thereafter, and the rapid introduction of new and more efficient technologies. Major underlying themes are convergence among regions, capacity building, and increased cultural and social interactions, with a substantial reduction in regional differences in per capita income. The A1 scenario family is diveded into three groups that describe alternative directions of technological change in the energy system: fossil intensive (A1FI), non-fossil energy sources (A1T), or a balance across all sources (A1B).

The **A2** storyline and scenario family describes a very heterogeneous world. The underlying theme is self-reliance and preservation of local identities. Fertility patterns across regions converge very slowly, which results in continuously increasing global population. Economic development is primarily regionally oriented and per capita economic growth and technological changes are more fragmented and slower than in other storylines.

The **B1** storyline and scenario family describes a convergent world with the same global population that peaks in mid-century and declines thereafter, as in the A1 storyline, but with rapid changes in economic structures toward a service and information economy, with reductions in material intensity, and the introduction of clean and resource-efficient technologies. The emphasis is on global solutions to economic, social, and environmental sustainability, including improved equity, but without additional climate initiatives.

The **B2** storyline and scenario family describes a world in which the emphasis is on local solutions to economic, social, and environmental sustainability. It is a world with continuously increasing global population at a rate lower than A2, intermediate levels of economic development, and less rapid and more diverse technological change than in the B1 and A1 storylines. While the scenario is also oriented toward environmental protection and social equity, it focuses on local and regional levels.

3.2 General Circulation Models

Emissions of greenhouse gases connected to specific SRES scenarios are translated into projections of climate change over this century by using General Circulation Models (GCMs).

General Circulation Models, which represent physical processes in the atmosphere, ocean, cryosphere and land surface, are the most advanced tools currently available for simulating the response of the global climate system to increasing greenhouse gas concentrations.

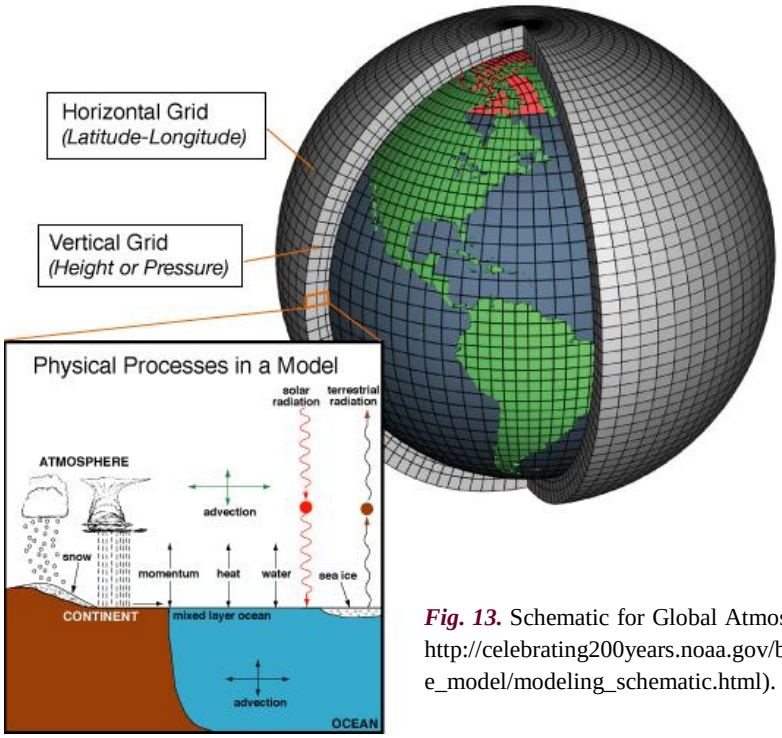

Fig. 13. Schematic for Global Atmospheric Model (from http://celebrating200years.noaa.gov/breakthroughs/climate_model/modeling_schematic.html).

The most recent versions of GCMs, termed atmosphere-ocean general circulation models, couple comprehensive 3-D atmospheric GCMs with ocean GCMs, sea-ice models, and models of land-surface processes. In climate change projections, the GCMs are run with varying environmental conditions, which most commonly reflect changes in concentration of greenhouse gases.

Their use in climate-change impact assessment studies is widespread (IPCC, 2007). Five criteria that should be met by climate scenarios to be useful for impact researchers and policy makers are:

Criterion 1: Consistency with global projections. They should be consistent with a broad range of global warming projections based on increased concentrations of greenhouse gases. This range is variously cited as 1.4°C to 5.8°C by 2100, or 1.5°C to 4.5°C for a doubling of atmospheric CO_2 concentration (ca 560 ppm) (otherwise known as the "equilibrium climate sensitivity").

Criterion 2: Physical plausibility. They should be physically plausible; that is, they should not violate the basic laws of physics. Hence, changes in one region should be physically consistent with those in another region and globally. In addition, the combination of changes in different variables (which are often correlated with each other) should be physically consistent.

Criterion 3: Applicability in impact assessments. They should describe changes in a sufficient number of variables on a spatial and temporal scale that allows for impact assessment. For example, impact models may require input data on variables such as precipitation, solar radiation, temperature, humidity and windspeed at spatial scales ranging from global to site and at temporal scales ranging from annual means to daily or hourly values.

Criterion 4: Representative. They should be representative of the potential range of future regional climate change. Only in this way can a realistic range of possible impacts be estimated.

Criterion 5: Accessibility. They should be straightforward to obtain, interpret and apply for impact assessment. Many impact assessment projects include a separate scenario development component which specifically aims to address this last point.

While simpler models have also been used to provide globally- or regionally-averaged estimates of the climate response, only GCMs, possibly in conjunction with nested regional models, have the potential to provide geographically and physically consistent estimates of regional climate change which are required in impact analysis, thus fulfilling criterion 2 (IPCC, 2007).

GCMs depict the climate using a three dimensional grid over the globe (see Fig. 13 and Fig.14), typically having a horizontal resolution of between 250 and 600 km, 10 to 20 vertical layers in the atmosphere and sometimes as many as 30 layers in the oceans. Their resolution is thus quite coarse relative to the scale of exposure units in most impact assessments, hence only partially fulfilling criterion 3. Moreover, many physical processes, such as those related to clouds, also occur at smaller scales and cannot be properly modelled. Instead, their known properties must be averaged over the larger scale in a technique known as parameterization.

This is one source of uncertainty in GCM-based simulations of future climate. Others relate to the simulation of various feedback mechanisms in models concerning, for example, water vapor and warming, clouds and radiation, ocean circulation and ice and snow albedo. For this reason, GCMs may simulate quite different responses to the same forcing, simply because of the way certain processes and feedbacks are modelled.

However, while these differences in response are usually consistent with the climate sensitivity range described in criterion 1, they are unlikely to satisfy criterion 4 concerning the uncertainty range of regional projections. Even the selection of all the available GCM experiments would not guarantee a representative range, due to other uncertainties that GCMs do not fully address, especially the range in estimates of future atmospheric composition (IPCC, 2007).

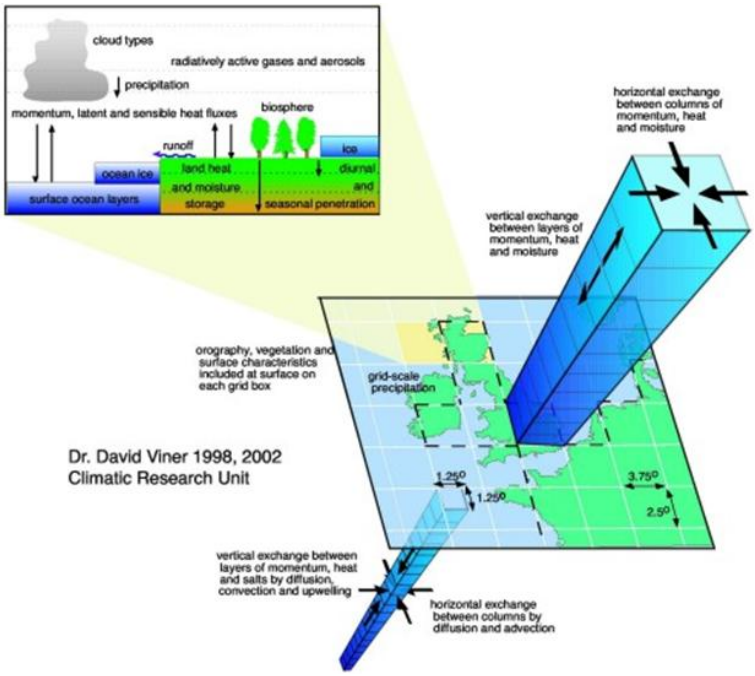

Figure 14. GCMs three-dimensional grid (from IPCC web site).

Here is a brief description of the most widely used GCM:

HadCM3: is a coupled atmosphere-ocean general circulation model developed at the Hadley Center in the UK and described by Gordon *et al.* (2000). It has a stable control climatology and does not use flux adjustment.

The atmospheric component of the model has 19 levels with a horizontal resolution of 2.5 degrees of latitude by 3.75 degrees of longitude, which produces a global grid of 96 x 73 cells. This is equivalent to a surface resolution of about 417 km x 278 km at the equator reducing to 295 km x 278 km at 45 degrees of latitude. The oceanic component of the model has 20 levels with a horizontal resolution of 1.25 x 1.25 degrees. At this resolution it is possible to represent important details in oceanic current structures.

ECHAM-5: is the fifth generation atmospheric general circulation model (ECHAM) developed at the Max Planck Institute for Meteorology (MPIM). It is the most recent version in a series of ECHAM models evolving originally from the spectral weather prediction model of the European Centre for Medium Range Weather Forecasts (ECMWF; Simmons *et al.*, 1989), significantly modified to make it suitable for climate simulations. The dynamical core of ECHAM5 solves prognostic equations for vorticity, divergence, logarithm of surface pressure and temperature, water vapour and water in the clouds which are expressed in the horizontal by spectral coefficients.

In its standard configuration, the model has 19 or 31 vertical layers with the top level at 10 hPa. The middle-atmosphere version is currently available with either 39 or 90 layers (top level at 0.01 hPa). Horizontal resolutions employed so far are T21, T31, T42, T63, T85, T106 and T159 (where "T" is the spectral resolution).

NCAR-PCM: The PCM is a fully coupled climate system model and includes numerical models of the atmosphere, land, ocean, and sea ice. The early target architecture of the PCM was the Cray T3E900 at the National Energy Research Supercomputing Center (NERSC). After initial tests on the T3E, it became apparent that SGI Origin 2000/128 (O2K) systems would be available at NCAR and the Los Alamos National Laboratory (LANL). The atmospheric model is the NCAR Community Climate Model, Version 3.2, which is used with a horizontal resolution of T42 (equivalent to a grid spacing of about 3 degrees) and 18 vertical levels. The land model is currently embedded in CCM3.

The ocean model is the LANL Parallel Ocean Program (POP)with a horizontal grid resolution of approximately 2/3 degree and 32 levels in the vertical.

The model of sea ice consists of both ice thermodynamics and full dynamics. Physically, the model is two-dimensional with a stereographic grid over each pole at a horizontal resolution of 27 km. The flux coupler is the connecting mechanism between the component models which facilitates the exchange of information (i.e., state variables as well as heat, water and momentum fluxes). The process involves the conservative mapping of data from one grid to another, averaging in space and time as needed, and scaling the fluxes such that total energy is conserved.

INGV-SXG: is an Atmosphere Ocean sea-ice General Circulation Model (AOGCM) developed at INGV (National Institute of Geophysics and Volcanology) with the aim of investigating the features and the mechanisms of the climate variability and change. The model is an evolution of SINTEX and SINTEX-F (Gualdi *et al.* 2003a, 2003b; Guilyardi *et al.*, 2003). The new model (INGV-SXG) includes a thermodynamic-dynamic sea-ice model and the capabilities to use external radiative forcings (Ozone, Sulfate Aerosols, Greenhouse Gases like CO2, CH4, N2O and CFCs).

The model is composed of four parts: Atmosphere, Ocean, Sea–Ice and Coupler.

The atmospheric component is ECHAM4 whit a horizontal resolution about 1.125 x1.125 degrees and vertical resolution with 19 hybrid sigma-pressure levels; top level at 10 hPa; 7 layers above 200 hPa, 5 layers below 850 hPa.

The ocean component is OPA 8.2 (Madec *et al.*, 1999) in ORCA2 configuration: 2°x2° cos (latitude). Vertical resolution with 31 vertical levels, with 14 levels lying in the top 150 meters.

The sea-ice model is an evolution of the sea-ice is described by the LIM (Louvain-La-Neuve sea-ice model) (Timmerman *et al.*, 2005), which is a thermodynamic-dynamic snow sea-ice model. Horizontal resolution is the same as the ocean model (2° in longitude and roughly 2° cos(phi) in latitude and vertical resolution with 3 layers: 1 in snow and 2 in ice.

The software used to couple ocean and atmospheric components is OASIS 2.4 (Valke *et al.*, 2000). Its main tasks are the synchronization of the models being coupled, and the treatment and interpolation of the fields exchanged between the models.

CSIRO: is a coupled ocean-atmosphere-ice circulation model developed in Australia by the Commonwealth Scientific and Industrial Research Organization (CSIRO) and described by Gordon and O'Farell (1997). The model uses flux correction.

The atmosphere model has 9 levels in the vertical and horizontal resolution of spectral R21 (approximately 5.6 by 3.2 degrees, about 625 km x 350 km). The oceanic component of the model has the same horizontal resolution with 21 levels.

3.3 Downscaling techniques

The use of GCMs data for agricultural impact studies presents limitations due to its coarser resolution which determines a serious mismatch of scale between the available climate change scenarios and the spatial resolution required in agricultural impact studies. This was particularly evident in those areas where complex topography, which cannot be fully reproduced by GCMs, plays an important role in climate patterns (Moriondo and Bindi, 2006). Moreover, GCMs simulated climate variability is highly dependent on the physical parameterizations (Kharin and Zwiers, 2000), which limit the capability of GCMs to reproduce climate extreme events, which play a fundamental role in assessing climate change impacts in agriculture.

To fill the gap between what is simulated by GCMs and what is required by the impact models, downscaling techniques have been developed: the dynamical downscaling-RCMs (Regional Climate Models) and empirical/statistical downscaling.

3.3.1 Dynamical downscaling – Regional Climate Models

Dynamical downscaling consists in simulation of atmospheric processes and interactions between components of the climate system with use of complete meteorological equations. This simulation results in weather variables and fluxes (Temperature, Precipitation, Relative Humidity, Wind, Radiation, Latent and Sensible Heat, Soil Moisture, Runoff, …) and requires a large amount

of computational and data storage resources. It can be performed by explicit solving of process-based physical dynamics of the regional climate system.

The GCM large-scale fields are used as driving initial and time-dependent lateral boundary conditions (e.g., 6-hourly) for the RCM and it is possible to produce detailed simulations for selected regions by nesting a Regional Climate Model (RCM) into a global GCM. Dynamic downscaling explicitly simulates both large scale and sub-grid-scale processes; it delivers meteorologically-consistent downscaled variable response to large-scale forcing.

The transition from a model run on a large domain (GCM) with low resolution to another run one on a smaller domain with high spatial resolution (RCM) is done by *Nesting*.

Two Nesting strategies are possible:

- *1 way nesting:* the information goes only from the coarse grid model to the fine grid model (the first one provide initial and boundary conditions). The 1 way nesting can be asynchronous and the two models can be completely different.
- *2 way nesting:* results of the fine model are "passed" to the coarse one, for a better evaluation of the subgrid phenomena. 2 way nesting is synchronous. It is possible to analyze of the sub-grid processes (explicitly solved) and the large scale ones.

Dynamic downscaling seems to be one of the most promising techniques.

It should be stressed that this spatial resolution may result still too coarse especially for morphological complex region (Moriondo and Bindi, 2005) and also the dynamic downscaling techniques are complex and require long times for data processing and high costs. Moreover it fails to take into account the uncertainty and non-unique nature of the solution; it is limited by parameterization techniques.

Regional Climate Models

There is an intermediate level between GCMs and field scale, as shown in figure 15, which is composed of Regional Climate Models (RCMs), global models with variable spatial resolution or high-resolution global models.

Regional Climate Models represent dynamic downscaling techniques (see section 3.3).

Regional climate modelling has received increased attention in recent years. This is due to the fact that the low resolution of GCMs cannot well represent the subgrid-scale weather phenomena as well as the spatial variability of climatic characteristics within individual grid boxes.

The high spatial variability of the climate conditions makes it necessary to analyze the impacts of climate change on a regional scale or for specific sites. Spatially highly resolved

simulations of possible future climate developments are therefore needed as a basis for such impact studies.

A common approach to obtain the high resolution climate data required as an input to the impact models (e.g. crop simulation models) is to downscale output from Global Circulation Models (GCMs), typically operating on horizontal resolutions of 100–200 km, into a finer gridded data (resolution being, say, 10-25 km using the dynamical downscaling by applying the Regional Climate Models), or into the specific locations (represented, e.g., by meteorological stations) using statistical downscaling.

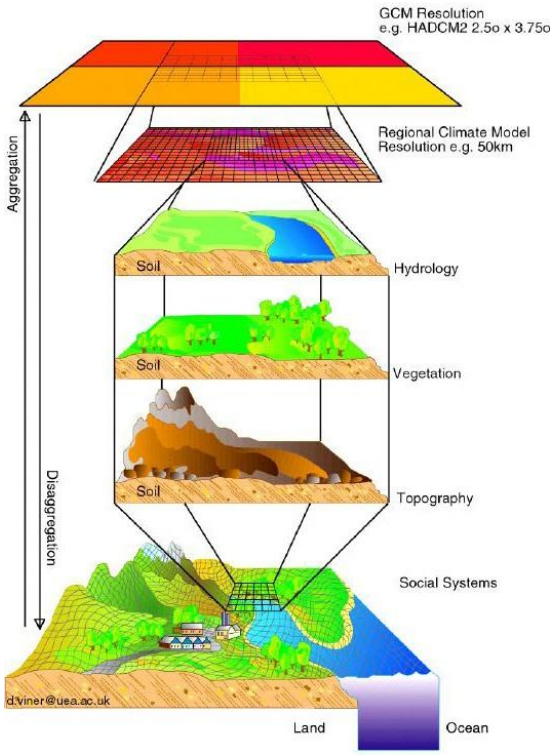

Figure 15. Scheme of downscaling (from web site: http://www.cccsn.ca/Help_and_Contact/Downscaling_html_m5385e5b8.jpg).

RCMs model physical processes as GCMs do, but on a finer spatial and temporal scale. Usually, GCM output defines the boundary conditions for these simulations. Recently, RCMs have improved substantially and are more and more frequently used to produce climate change scenarios for impact studies. On the other hand, this general applicability is somewhat limited by the intrinsic parameterizations of sub-scale processes, which are often based on observational data statistics.

3.3.2 Statistical downscaling – empirical models

Empirical/statistical downscaling develop statistical relationships that link the large-scale atmospheric variables (or *"predictors"*) with local/regional climate variables (or *"predictands"*).

Then the large scale output of a GCM simulation is fed into this statistical model to estimate the corresponding local and regional characteristics. One of the primary advantages of these techniques is that they are computationally inexpensive and thus can be easily applied to output from different GCM experiments. Another advantage is that they can be used to provide site-specific information, which can be critical for many climate change impact studies. The major theoretical weakness of statistical downscaling methods is that their basic assumption in not verifiable, i.e., that statistical relationships developed for the present day climate also hold under the different forcing condition of possible future climate (a limitation that also applies to the physical parameterization of dynamical models). In all cases, the quality of the downscaled product depends on the quality of the driving model.

The empirical downscaling of GCM on existing meteorological stations may reduce the gap between large scale and global scale. In a simplest way, differences in temperature, rainfall and radiation between present and future GCM scenarios for a region may be applied directly to observed meteorological data in that region to reproduce future climate (Delta approach) (Arnell *et al.,* 1998). However in this case the future meteorological data do not incorporate change in climatic variability, so that possible changes in climate extreme events are not simulated.

Statistical downscaling assumes stationarity of the projected climate system and cannot capture higher moments, it is computationally inexpensive and many representations can be generated quickly.

In statistical downscaling, three different strategies can be identified: (1) transfer functions, making use of functional dependencies between explanatory and dependent variables (e.g., Murphy, 1999; von Storch and Zwiers, 1999; Zorita and von Storch, 1999); (2) weather generators, which exploit stochastic models for variables of interest and generate simulated series by sampling from them (e.g., Semenov and Barrow, 1997; Wilks, 1999); and (3) weather type schemes, using relationships between large-scale circulation regimes and local weather, which allow for the translation of changes in circulation regime statistics into changes of weather statistics. All schemes rely on observed time series and aim at generating simulated series for a period of interest.

The first strategy allows estimating local surface surface weather *(Y=predictand)* from the larger-scale free-atmosphere characteristics *(X=predictors)* via transfer function *f* derived from observations:

$$Y = f(X)$$

The basic assumptions and requirements for statistical downscaling are the following:

1. model representation: predictors must be simulated successfully by GCM;

2. strong relationship between predictor(s) and predictand: predictor(s) explain large enough portion of predictands's variance and reflecting a physical mechanism;

3. stationarity: predictor-predictand relationship is constant in time (and it holds in a future climate);

4. description of change: predictor bear the signal of the change.

The choice of variables to be downscaled (= predictands) is driven by the need of the "impact" model used. The most common are temperature and precipitation amount, others are cloudiness, sunshine duration, cloud ceiling height, humidity variables, sea level, snow cover, wind speed and direction, precipitation probability, extreme values and various parameters of the statistical distribution.

The spatial resolution can be: station (site-specific), well defined area (river basin) or gridbox (of various size).

Different predictands require different predictors. Possible predictors are:

– height of pressure levels at low and middle troposphere,

– temperature of lower troposphere (~ 850 hPa),

– thickness of 1000/500 hPa layer,

– vorticity and humidity (for precipitation).

Can be choice one or more levels and the spatial representation can be closest grid(s), average within larger area, representing spatial variability: several gridpoints, or spatial pattern characteristics.

Transfer function *f* is calibrated using the "real-world" (=observed/measured data and often "re-analysis data") and then applied to the "model" world (mostly GCM output).

The scheme in figure 16 shows the calibration step and the scheme in figure 17 shows the steps for statistical downscaling.

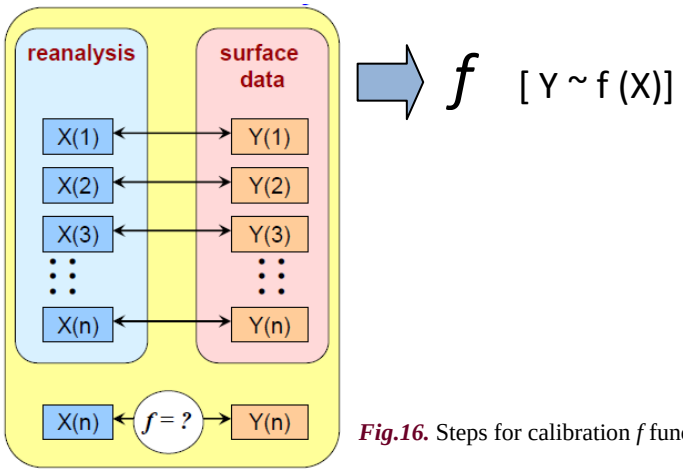

Fig.16. Steps for calibration *f* function (from Dubrovsky, 2009).

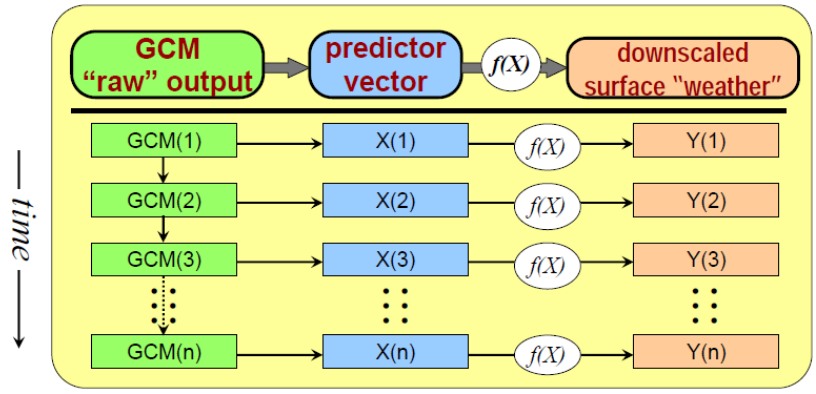

Fig.17. Steps for statistical downscaling using transfer functions(from Dubrovsky, 2009).

About the second strategy, that considers the use of weather generator, see the section 3.4.

The third strategy considers weather type schemes in statistical downscaling, using relationships between large-scale circulation regimes and local weather (Fig. 18). Different transfer functions are used for different weather types. Surface weather characteristics are closely related to large-scale circulation. This may be characterized by a small number of weather types or by a vector of scores (weights) giving contributions of specific circulation types. If the circulation pattern cannot explain climate change signal should be added other predictors, which would bear the climate change signal.

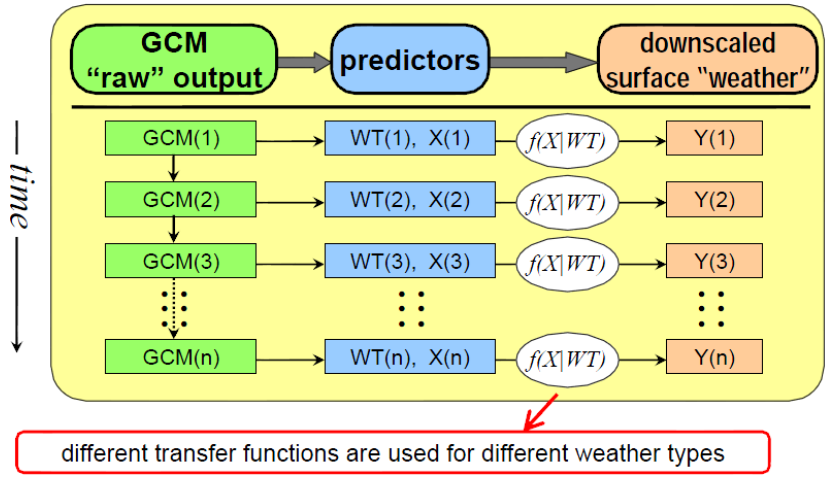

Fig.18. Steps for statistical downscaling using transfer functions for weather type (WT)(from Dubrovsky, 2009).

Stochastic Weather Generator

Stochastic Weather Generators (WG) are considered as one of the Statistical downscaling techniques. The similarities are that it relies on statistics (rather than physics-based equations used in GCMs and RCMs) and that it produces site specific (or area-specific) surface weather series. The differences are that to calibrate WG are necessary only observed variables required by the impact model, so that it does not need circulation characteristics (it rather relies on a fact that the

circulation regime is inherently reflected in a structure of surface weather series) and stress on the stochastic structure of the surface weather series.

A stochastic weather generator is a mathematical model, which produces synthetic time series of weather data of unlimited length for a location based on the statistical characteristics of observed weather at that location.

The generators employ statistical models to generate arbitrarily long synthetic weather series which resemble (in terms of the statistical characteristics) the real world weather series. Parameters of the generator use to be derived from the observed weather series or they may be interpolated from the surrounding stations (Guenni, 1994). To generate series representing the changed climate, the parameters of the generator are modified according to the GCM-based climate change scenario or according to the user's choice. As the generators use to have only modest demands on computer resources, one may generate a set of long synthetic weather series representing a broad range of climate scenarios. This makes the generators helpful not only in evaluating a response of the weather-dependent processes to anticipated climate change, but also in performing detailed sensitivity analysis to changes in individual climate variables (Dubrovsky *et al.*, 2004).

Depending on the processes being modelled, weather generators differ in time resolution (daily step, hourly step, continuous in time), spatial resolution (single site, multiple sites, continuous in space) and number of variables (single-variate, multi-variate). The choice of the underlying statistical model aims to achieve the best fit between the stochastic structure of the observed and synthetic weather series.

Models for generating stochastic weather data are conventionally developed in two steps. The first step is to model daily precipitation and the second step is to model the remaining variables of interest, such as daily maximum and minimum temperature, solar radiation, humidity and wind speed conditional on precipitation occurrence. Different model parameters are usually required for each month, to reflect seasonal variations both in the values of the variables themselves and in their cross-correlations (IPCC, 2007).

Perhaps the best known approach for developing weather generators was introduced by Richardson (1981), and since then the WGs based on this approach are often referred to as the "Richardson-type". At the first step, the estimation of precipitation involves first modelling the occurrence of wet and dry days using a Markov procedure, and then modelling the amount of precipitation falling on wet days using a functional estimate of the precipitation frequency distribution. The remaining variables are then computed based on their correlations with each other and with the wet or dry status of each day. The Richardson-type of generator has been used very successfully in a range of applications in hydrology, agriculture and environmental management.

One criticism of the Richardson-type WG is its failure to describe adequately the length of dry and wet series (i.e. persistent events such as drought and prolonged rainfall). These can be very important in some applications (e.g. agricultural impacts). For this reason an alternative, "serial approach" has been developed (Racsko *et al.*, 1991), which first models the sequence of dry and wet series of days and then models other weather variables like precipitation amount and temperature as dependent on the wet or dry series.

Stochastic weather generators are often used in climate-change impact studies to provide synthetic weather series for present or changed climate conditions (Riha *et al.*, 1996; Mearns *et al.*, 1997; Semenov and Barrow, 1997; Dubrovsky *et al.*, 2004; Tubiello *et al.*, 2000; Trnka *et al.*, 2004), used as inputs to simulation models (crop growth models, rainfall-runoff models, etc.) and the impacts are thereafter assessed by comparing the results obtained with the weather series representing present and changed climates.

The decision to apply a weather generator in an impact assessment may be determined by one or more of the following requirements:

- long time series of daily weather, which are not available from observational records;
- daily weather data in a region of data sparsity;
- gridded daily weather data for spatial analysis (e.g. of risk);
- the ability to investigate changes in both the mean climate and its inter-daily variability.

These models, in fact, consider the predicted changes, obtained from GCMs, both in terms of climate means and variability to be applied the weather generator parameters.

One of the main advantages of SWGs is that long synthetic weather series that resemble the observed ones in selected statistical characteristics may be simulated. This feature is particularly advantageous when the analysis concerns extreme events, whose probabilities may be estimated from these long runs with a smaller uncertainty than using short runs and/or observed weather series.

All weather generators require some type of local climate data as input to define the monthly mean values and associated variability over time for each weather variable (rainfall, maximum and minimum temperatures, and solar radiation).

Several steps of analysis are required to parameterise and test the WG:

Data collection - observed daily climatological data for the variables and site(s) of interest should be collected, quality controlled and correctly formatted. If the WG is to be parameterised for a 1961-1990 baseline period, as much data as possible from this period will be required. On the

other hand, if it important to model low frequency, high magnitude events, it will be desirable to obtain the longest possible observed time series. The long series are also required to make the sampling error in estimating WG parameters as low as possible. For spatial applications, between-site consistency of the observational time period may also be important.

Parameterisation - the parameters of the model are estimated using methods documented for the weather generator. If spatial analysis is also being undertaken, this will require parameter estimation at many sites and subsequent interpolation of the parameters to a grid or other spatial field. Some WG programs have automatic procedures for parameter estimation.

Model testing - time series of weather are generated and their statistics analysed and compared with the observed data (*direct validation*) on which they were based. The significance of any discrepancies between the WG-derived and observed series can be assessed by running both series through an impact model (*indirect validation*). Again, automatic model testing procedures are built in to some public domain WG programs.

The *direct validation* experiments are usually focused on reproduction of characteristics representing the distribution of the variables (means, standard deviations and higher-order moments), their interdiurnal variability, and correlations among them. The differences between the characteristics derived from the observed and synthetic series should not differ statistically significantly. However, no generator may obviously fit all characteristics of the observed series. Unfortunately, some of the characteristics, which are not reproduced with satisfactory accuracy, may crucially affect output from the models fed by the synthetic weather series. For example, the low-frequency variability, which is often underestimated by the generators, has an effect on the crop yields. Generally, nearly any insufficiency of the generator in reproducing stochastic structure of the weather series may be reduced by suitable modification of the underlying model. However, this usually leads to greater complexity of the model (with more parameters), and thereby to lower accuracy of parameters derived from the learning sample of given limited size (lower 'stability' of the model) (Dubrovsky *et al.*, 2004).

Before modifying the model of the generator, it is therefore reasonable to perform the indirect validation, which may show whether the generator is applicable in a given application.

The *indirect validation* is made by comparing statistical properties of output characteristics (e.g., crop yields) simulated with observed vs. synthetic weather series. The results of the indirect validation may show that the weather series created by a simpler generator, which fails in some direct validation tests, serves satisfactorily as an input for some simulation models (Dubrovsky *et al.*, 2004).

Climate scenarios - to generate weather series for future climate, the parameters of the WG derived from the observed data (representing the present climate) are modified according to climate change scenarios, which define increments in individual climate characteristics. These increments

(additive or multiplicative) are derived from outputs of GCMs or RCMs or using the statistical downscaling method.

Weather generators using different approaches have been tested and applied in climate impact assessment (e.g. Wallis and Griffiths, 1995; Harrison *et al.*, 1995), and the approaches have also been compared (e.g. Johnson *et al.*, 1996; Semenov *et al.*, 1998). While they are most commonly applied as single-site weather generators (producing the single-site weather series and ignoring observed spatial correlations of climate characteristics), the multi-site weather generators have also been developed to simulate weather series for a larger area, facilitating spatial analysis (e.g. of risk).

The following example demonstrates the limited value of using the single site weather generator for spatial impact assessments: a WG may simulate the occurrence of 3 prolonged droughts in a 30 year time series at location A. It may also simulate the same number of droughts at a nearby location B, but in different years. On the other hand, the observed climate at both locations may also show three drought years, but it is likely that these are the same years at both locations, since drought is commonly a widespread phenomenon. Thus, while the WG may provide an accurate statistical representation of the observed situation at each individual site (i.e. the risk of drought and its local impact), taken together, the droughts are not simultaneous and the aggregate impact (e.g. on water resources or agriculture) is likely to be less severe than in the real situation, where widespread drought affects a large area.

The most common weather generators that have been used include WGEN (Richardson, 1981, 1985), Simmeteo (Geng *et al.*, 1986), CLIGEN (Johnson *et al.*, 1996) as well as various other weather simulation models (Peiris and McNicol, 1996; Dubrovsky, 1997; Friend, 1998; Semenov *et al.*, 1998). The accurate generation of precipitation, both the occurrence of an event as well as the amount, is the most difficult task, especially for tropical and sub-tropical regions (Arnold and Elliot, 1996; Schmidt *et al.*, 1996; Jimoh and Webster, 1997). Several improvements of existing simulators that include a higher order Markov model to account for the high variability of tropical precipitation have been developed (Jones and Thornton, 1997; Schmidt *et al.*, 1997).

Several weather generators have been integrated in weather utility programs that analyze and prepare weather data for model applications, such as WeatherMan (Pickering *et al.*, 1994). They have also been incorporated in several simulation software such as the DSSAT (Decision Support System for Agrotechnology Transfer) or others decision support system (Tsuji *et al.*, 1994; Baffaut *et al.*, 1996).

4. CROP SIMULATION MODELS

Crop simulation models have been used as a tool for studing the impacts of climate change on crop growth and development and for evaluating possible adaptation strategies.

Models are a mathematical representation of a real-world system. Actually, they are simplifications of a real-world system, because it is impossible to include all the interactions between the environment and the growth and development processes of crops in a model. Thus, a model might include many assumptions and simplifications, especially when information that describes the interactions of the system is inadequate or does not exist (Hoogenboom, 2000; Wallach, 2006).

Depending on the scientific discipline, there are different types of models, ranging from very simple models, which are based on one equation, to extremely advanced models that include thousands of equations related to each other.

Agriculture involves biological factors for which, in many cases, the interactions with the environment are unknown. The science of plants and crops represents an integration of the disciplines of biology, physics, and chemistry. Plant and crop simulation models are a mathematical representation of this system.

Ritchie *et al.* (1985) defined the crop simulation models as a combination of mathematical equations and logic that conceptually represent a simplified crop production system.

One of the main goals of crop simulation models is to estimate agricultural production as a function of weather and soil conditions as well as crop management (Hoogenboom, 2000). The weather variables, such as air temperature, precipitation, and solar radiation, are, therefore, key input variables for the simulation models.

4.1 Modelling approaches

Crop models, in general, integrate current knowledge from various disciplines, including agrometeorology, soil physics, soil chemistry, crop physiology, plant breeding, and agronomy, into a set of mathematical equations to predict growth, development and yields.

Crop simulation models are conventionally distinguished between mechanistic, in which all quantified processes have physical or physiological basis, and empirical models, consisting of functions that are chosen, often arbitrarily, to fit measurements from field and laboratory (Monteith, 1996).

Empirical models are direct description of the observed data and are defined by estimating the parameters of a multiple regression. They provide a description of observed system and relations between system and its variables, but they not provide an explanation, and do not add knowledge to the system studied.

Mechanistic models include an explanation of relationships between system modelled and explanatory variables.

Crop models are generally a compromise between mechanistic and empirical models because of the complexity in reproducing biological systems, that precludes the possibility to encompass all hierarchical levels in one model. This not because of computer limitations but because a model that begins with the recognition and formulation of a problem focuses on a specific hierarchical level (e.g., crop) the moment the problem is defined (Sinclair and Seligman, 2000).

Models can also be distinguished between dynamic or static depending on the time factor is or not considered (Donatelli, 1995).

Crop growth models are physiologically based, because they calculate the causal relationships between the various plant functions and the environment. The opposite would be a statistical approach, primarily using correlative relations between all processes (Hoogenboom, 2000).

Crop models are simulation models, in that they use one or more sets of differential equations, and calculate both rate and state variables over time, normally from planting until maturity or harvest.

Crop models can also be identified as being deterministic, when they make an exact calculation or prediction. In this case, the opposite would be stochastic or probabilistic models, which provide a different answer for each calculation (Hoogenboom, 2000).

Deterministic models use mathematical representations of the underlying regularities that are produced by the entities being modelled and generate theoretically perfect data. Parameters and variables are not subject to random fluctuations. They are fixed, so the system is at any time entirely defined by the initial conditions, in contrast with a stochastic model. Deterministic models can be solved by numerical analysis or computer simulation. They are often described by sets of differential equations. Deterministic models are appropriate when large numbers of individuals of species are involved, and it can safely be supposed that the importance of statistical variations in the average behaviour of the system are relatively unimportant. For many biological systems, however, this assumption may not be valid.

Stochastic models use computational elements that represent the entities and processes and they take into consideration the presence of some randomness in one or more of its parameters or variables. Model predictions, therefore, do not give a single point estimate, but a probability distribution of possible estimates. Stochastic models should be used where either the number of individuals is small or there is a reason to expect random events to have an important influence on the system behaviour. Often, a stochastic model will be more appropriate when we need to take account of species as discrete units rather than as continuous variables. It may also be necessary to take account of events occurring at random times.

Crop models are, in general, dynamic system models. They are dynamic as they describe how the state variables evolve over time, and they describe a system as in a crop model there are several state variables that interact (Wallach, 2006).

The first simulation models date back to the activity of de Wit (1965) who introduced the theory of systems and approaches for the simulation of the dynamics of these in plant physiology. The school of de Wit developed a large number of simulation models of crop growth and development at various levels of complexity and elaboration. The attention shifted from the first simple cognitive aspects of plant physiology to more practical aspects, with particular reference to production. Therefore specific models were developed for different species grown under two levels of production: potential production and production constrained by limiting factors, as water and nitrogen inputs. The contributions of the school of de Wit have been essential in the development of simulation models that, from a physiological approach, have applications in the general field of agroecosystems. Since the 90s were introduced models with a mechanistic approach more distinctly, with greater emphasis on the components of an agricultural nature. Among them are cited CROPGRO (Hoogenboom *et al.,* 1992, Boote *et al.,* 1997) and APSIM (Agricultural Production System Simulator) (McCown *et al.,* 1996). Some of these models were included within the so-called decision support systems (Decision Support System, DSS).

The 'School of De Wit' (de Wit and Goudriaan, 1974; Bouman *et al.,* 1996) defines four different levels or facets with respect to the evolution of plant growth models (Penning de Vries and van Laar, 1982; Penning de Vries *et al.,* 1989).

In Phase 1, temperature and solar radiation are used as inputs to simulate growth and development and to calculate potential production. Growth in this case only includes the simulation of the plant carbon balance.

In Phase 2, precipitation and irrigation are added as an input, and the soil and plant water balances are simulated.

In Phase 3, soil nitrogen is added as an input to simulate growth and development, the soil and plant water balance, and the soil and plant nitrogen balance.

In Phase 4, other soil minerals are added as inputs as well as pests, diseases, and weeds. In this phase, the complete soil–plant–atmosphere system is simulated, including interactions with most of the biotic and abiotic components.

Only few models include one or more processes at Level 4; several models also include the option to simulate the impact of pest and disease damage.

Several models have been used to simulate crop growth.

Most of the widely used crop simulation models are those included in APSIM, and in DSSAT (Decision Support System for Agrotechnology Transfer) (e.g. CERES or CROPGRO)

(Jones *et al.*, 1998), the Simulation and Systems Analysis for Rice Production (SARP) models (Riethoven *et al.*, 1995), and the 'School of deWit' crop models (Bouman *et al.*, 1996).

In the table 4 we will briefly describe some of these most used models.

CERES and CROPGRO models placed more emphasis on agronomic objectives and started to include farming practices in the inputs. At the same time, EPIC, the first generic model, was developed in response to agro-environmental concerns including soil erosion, water and nitrogen (Brisson *et al.*, 2006). CropSyst (Stockle *et al.*, 1994) arose out of EPIC. APSIM was derived from CERES, as was CERES-ECG, which is a modification and extension of CERES to include additional environmental concerns such as the soil nitrogen balance (Brisson *et al.*, 2006).

The current trend is towards developing generic and agro-environmental models that take into account farming practices (e.g. STICS model).

As models become more complex by including the simulation of more processes, the requirement to define input data for these new processes also increases (Hunt, 1994). Although model users would like to be able to simulate the complete soil–plant–atmosphere continuum, they normally have a very difficult time in obtaining the input parameters required to simulate these processes (Hunt and Boote, 1998). Computer modellers have a tendency to request input information for their simulation models that, in many cases, is not available. The lack of adequate input data requires that some of these model inputs have to be scaled back to the level at which input data are available (Hoogenboom, 2000).

Generally most of the fields experiments that are normally used in order to evaluate crop models were designed for other purposes, so they often do not contain the complete data set necessary for crop models inputs. These gaps have to be filled either by calculations (e.g. using model in order to calculate daily global solar radiation, or calculating initial available soil water content at planting time from available data) or approximation (as in case of crop residues of the previous crop or initial nitrogen content in the deeper soil layers) (St'astna *et al.*, 2002).

It is also important to keep a balance between all the processes that are simulated by a model, so that they contain the same amount of details (Monteith, 1996). This approach might require different types of models for different applications, depending on the complexity of the problem that is being investigated (Boote *et al.*, 1996).

One recent advancement in model development has been the change towards modularity. Although this concept has originated through object-oriented modelling (Hodges *et al.*, 1992; Waldman and Rickman, 1996; Acock and Reddy, 1997), the trend now seems to have changed towards developing modules that can be exchanged between different modelling systems (Timlin *et al.*, 1996; Acock and Reynolds, 1997). The APSIM system is built on the premise that the user can build a model, based on a selected set of modules that simulate the various plant and soil processes (McCown *et al.*, 1996). A similar approach is also being implemented in the CERES model for

cereals and CROPGRO model for grain legumes (Boote *et al.,* 1997) both implemented into DSSAT.

Crop simulation models can play an important role at different levels of applications, ranging from decision support for crop management at a farm level to advancing understanding of sciences at a research level.

Investigations based on crop simulation models are faster and require less labor and other resources compared to experimental studies alone. Crop models are also helpful with respect to decision-making in sustainable farming systems (Boote *et al.,* 1996).

Crop simulation models that include the dynamics of crop–soil–weather interactions and integrate crop resource capture principles can assist in the evaluation of the impact of specific traits on yield across a range of climates, soil types and seasons (Asseng *et al.,* 2003).

Many agronomic and environmental studies are conducted to determine crop characteristics and agronomic practices for maximizing crop production, optimizing natural resource use and minimizing environmental impact and pollution. The use of crop simulation models is an efficient complement to experimental research. These models can be used for interpretation of results and analysis of the behaviour of agronomic systems under diverse environmental conditions and management options.

Researchers have performed impact assessments and alternatives evaluation following a wide variety of methodologies. Some examples are historical analogs, Ricardian analysis and empirical relationships (Tao *et al.,* 2006; Mendelsohn and Dinar, 1999; Polsky and Easterling, 2001; Webb *et al.,* 2008).

However, the most common approach corresponds to the use of crop simulation models to estimate the potential impacts of projected climatic conditions on agricultural systems (Table 5) because of a reliable assessment of climate change impact or the evaluation of potential adaptation and mitigation strategies cannot be made without the use of a crop simulation model.

Table 4. The main crop growth simulation models used for wheat crop.

Software / Model	**Summary description**	**References**
CERES-Wheat model, implemented into DSSAT (Decision Support System for Agrotechnology Transfer) software.	CERES-Wheat model is a dynamic mechanistic crop growth model that simulates daily phonological development and growth in response to environmental factors (soil and climate) and management (crop variety, planting conditions, nitrogen fertilisation, and irrigation. (More specific details about CERES-Wheat model are given in the section 2.1 of this thesis).	Ritchie *et al.*, 1985. Jones *et al.*, 1998.
CROPSYST (Cropping Systems Simulation Model)	Multiyear, multi-crop, daily time step crop growth simulation model, developed with emphasis on a friendly user interface, and with a link to GIS software and a weather generator.	Stockle C., Donatelli M., 1994.
APSIM (Agricultural Production System sIMulator)	APSIM, is a cropping system modelling environment that simulates the dynamics of soil/plant- management interactions within a single crop or a cropping system in response to the climate and soil conditions and allows the evaluation of management intervention through tillage, irrigation, or fertilisation as well as choice, timing and sequencing of crops either in fixed or flexible rotations. APSIM consists of a central interface Engine connected to a series of plug-in/pull-out modules. It is able to simulate more than 20 different crops as well as grass and trees, and includes crop modules for wheat, maize, sorghum, millet, various grain legumes, sunflower, cotton, sugarcane, and lucerne.	McCown *et al.*, 1996.
SIRIUS	SIRIUS is a wheat simulation model that calculates biomass from intercepted photosynthetically active radiation (PAR) and grain growth from simple partitioning rules. Leaf area index (LAI) is developed from a simple thermal time sub-model. Phenological development is calculated from the mainstem leaf appearance rate and final leaf number, with the latter determined by responses to daylength and vernalisation. Effects of water and N deficits are calculated through their influences on LAI development and radiation-use efficiency.	Jamieson et al., 1998.
STICS	STICS is a daily time step crop model that simulates crop growth as well as soil water and nitrogen balances driven by daily climatic data. It calculates both agricultural variables (yield, input consumption) and environmental variables (water and nitrogen losses).Other specific feature of the model is its consistency and transparency as the required inputs are almost exclusively in form of directly measurable parameters without use of semi-empirical coefficients.	INRA, France. Brisson N. et al., 2003.
WOFOST	WOFOST is a mechanistic generic crop growth model that includes model parameters for: Wheat, Grain Maize, Barley, Rice, Sugar Beet, Potato, Field Bean, Soy Bean, Oilseed Rape and Sunflower. It explains crop growth on the basis of the uderlying processes, such as photosynthesis and respiration, and how these processes are affected by environmental conditions. The model describes crop growth as biomass accumulation in combination with phenological development. It simulates the crop life cycle from sowing or emergence to maturity. Meteorological data (rain, temperature, windspeed, global radiation, air humidity) are needed as input. Other input data include volumetric soil moisture content at various suction levels, and other data on saturated and unsaturated water flow. Also data on site specific soil and crop management are requested. Time step for simulation is one day.	Boogaard, et al.,1998.

Table 5. Some of main recent studies using simulation models for climate change impact assessment on wheat crop (others study references may be found in the text).

Author	Model	Location	Scale	Observation period	Object	Variables
Brassard *et al.*, 2008.	CERES-Wheat	Quebec, Canada.	Regional spatial scale	Current (1961–1990) and future (2040–2069) periods.	Assessment of the potential impacts of greenhouse gas climate change and changing ambient carbon dioxide (CO2) levels on wheat crop.	Yield
Moriondo M. And Bindi M., 2007.	CropSyst	Mediterranean area	Mediterranean basin scale	Baseline (60-90) and future (2070-2100) periods.	Assessment of climate change impact on wheat.	Phenology
Ludwig, F. and Asseng S., 2006.	APSIM	Western Australia	Local scale	Baseline (60-90) and future (2050, 2100) periods.	Assessment of climate change impacts on wheat.	Yield
Rither G.M. and Semenov M.A., 2004.	SIRIUS	England and Wales	Local scale	Baseline (60-90) and future (2020, 2050) periods.	Modelling impacts of Climate Change on wheat crop.	Yield
Trnka *et al.*, 2004.	CERES-Wheat	Seven experimental sites in Czech Republic.	Local scale	Current period (61-90) and three future periods (2025, 2050 and 2100) for SRES emission scenariosA2 and B1.	Quantify the effect of uncertainties in selected climate change scenarios on winter wheat.	Yield
Guerena A. *et al.*, 2001.	CERES-Wheat	Spain	National scale	Current climate (1xCO_2) and future climate (2xCO_2)	Assessment of climate change and CO_2 concentration on wheat production in Spain.	Phenology, yield, biomass
Tubiello *et al.*, 2000.	CropSyst	Two Italian locations, Modena and Foggia	Local scale	Current climate (1xCO_2) and future climate (2xCO_2).	Effects of climate change, elevated CO_2 and adaptation strategies on wheat crop.	Phenology and yield
Iglesias *et al.*, 1999.	CERES-Wheat	Spain	National scale	Current climate (61-90) and future climate (2050s).	Develop of tools for a spatial analysis for agricultural climate change impact studies.	Phenology and yield
Mavromatis T. And Jones P. D., 1999.	CERES-Wheat	Study region in central France	Regional spatial scale	Current observed and derived by GCM climate (61-90).	Evaluation of direct use of daily GCM data in impact assessment studies for wheat crop.	Phenology and yield

OBJECTIVES

The high sensitivity of agriculture to climate conditions and the great uncertainty on the combined effects of increasing in CO_2 concentration and changes in temperature and rainfall patterns on crops growth and development, reveal the crucial importance of focusing researches in this field. While individual effects of higher temperatures, elevated CO_2 and changed rainfall patterns on agriculture are relatively well known, very few studies have addressed the issue of interactions between different effects of climate change, which is critical in improving the ability of evaluating climate change impact on crops.

Moreover, developing our understanding of the climate change science and its impacts is necessary both to identify the most appropriate adaptation strategies and actions for territorial planning, and to search more effective mitigation strategies to cope with climate change.

Considering the socio-economic importance of agriculture for food security, it is essential to undertake assessments of how future climate change could affect crop yields, so as to provide necessary information to implement appropriate adaptation strategies.

The main objectives of this research were to evaluate the effects of climate change and elevated CO_2 on durum wheat production and phenology, at four experimental sites in Sardinia, differents for soil, climate conditions and management practices, and provide directions for possible adaptation strategies.

To achieve these main objectives, the approach used in this study was:

(1) The application and assessment of a coupled climate scenario-crop model method, in which Atmosphere-Ocean General Circulation Models, used to generate future climate scenarios, are integrated into crop models to simulate future crop yields.

(2) The use of a weather generator (WG) to produce long time series of synthetic weather data. Once calibrated the WG from the observed weather series, the synthetic weather series, representing the present climate, are generated. Then, to generate weather series representing the future climate, the WG parameters are modified according to the features of a set of GCM-based climate change scenarios.

(3) The analysis of daily meteorological variables for current climatic conditions and climate change projections. These data are used as input variables for crop simulation models in conjunction with soil parameters and agronomic and management information, to simulate the dynamics of plant growth and development.

(4) The comparison of the results of these simulations for both current and future climatic conditions. Impacts of climate change are then expressed as changes in crop productivity and phenological phases. In addition, some adaptation strategies are explored.

To summarize, the specific aims of the work are:

1. to calibrate and validate CERES-Wheat model and obtain a robust set of genetic coefficients for to of the most important durum wheat varieties cultivated in Sardinia and in southern Italy,
2. to obtain synthetic weather data for current and future climate using WG and GCMs data,
3. to assess the climate change impact on crop yield and phenological crop phases,
4. to suggest same possible adaptation strategies in order to reduce the climate change impact.

The use of this approach not only allows to gain an insight into how future crop yields may change, but also into the nature of the factors responsible for yield changes, and how they may affect crop production and duration of the main phenological phases.

MATERIALS AND METHODS

SCHEME OF METHODOLOGY:

The methodology proposed in this dissertation for estimating the climate changes impact on durum wheat growth and development, includes the following steps (see also Fig. 19 and 25):

I. collection of observed data from the experimental sites located in Sardinia;
II. calibration and validation of CERES-Wheat crop growth model with respect to local conditions (with observed data) (Fig.18);
III. generation of synthetic weather data for present and future climates using a weather generator according to climate change scenarios based on GCMs;
IV. validation of Weather Generator through comparison of crop yields simulated by the model using observed weather data and yields simulated by the model using synthetic weather data;
V. modelling and assessment of impacts of changed CO_2 concentration and the related changed climatic conditions on durum wheat growth and development, linking climate change scenarios with crop model;
VI. adaptation analysis.

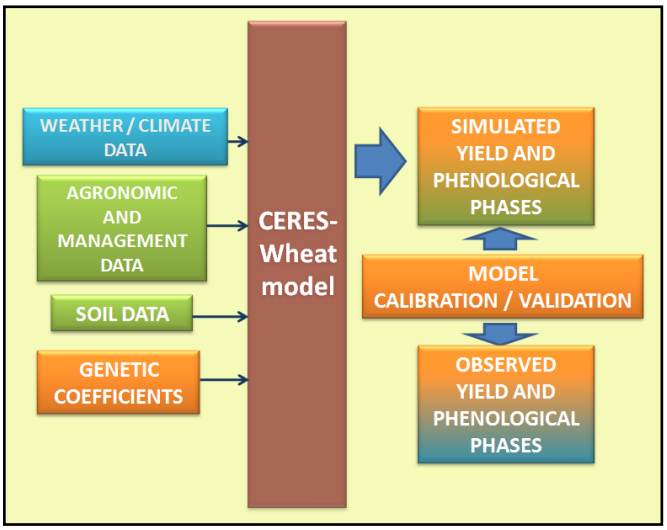

Figure 19. Scheme of methodology for the calibration and validation of CERES-Wheat model.

1. DATA COLLECTION

Soil, climate, agronomic and management data were collected from four experimental sites located in Sardinia (Ussana, Benatzu, Ottava, and Santa Lucia), Italy, for two of the most important varieties of durum wheat for the wheat production in Italy and Sardinia (Simeto and Iride).

1.1 Experimental sites description

A description of the experimental sites is reported in the following sections and Table 6.

Santa Lucia:

'Santa Lucia' is an experimental station (39°58' N; 8°37' E; 15 m a.s.l.) of the Department of Agronomy Sciences and Plant Breeding, University of Sassari. The climate is typically Mediterranean, with a long-term average annual rainfall of 550 mm, mainly occurring between October and April. The soil is a clay-loam and deep with plant available water holding capacity of 250 mm to the maximum rooting depth of 130 cm. Water tables frequently start to perch at about 70 cm soil depth and occasionally reach the surface. The annual mean temperature values range from 24.5°C in August to 9.9 °C in January.

Ottava:

'Ottava' is an experimental station (40°46' N; 8°29' E; 80 m a.s.l.) of the Department of Agronomy Sciences and Plant Breeding, University of Sassari. Also in this location the climate is typically Mediterranean, with a long-term average annual rainfall of 560 mm. The soil is a sandy-clay-loam of depth about 0.6 m overlaid on limestone. The annual mean temperatures range from 24.2°C in August to 9.8 °C in January.

Ussana:

'Ussana' is an experimental station (39°24' N; 9°5' E; 114 m a.s.l.) of the Agricultural Research Agency of Sardinia (AGRIS-DIRVE). The climate is Mediterranean, with warm and dry summer and mild winter. Rainfall events are concentrated during autumn and winter-early spring months. Total mean annual precipitation of the area is 430 mm. The annual mean temperature values range from 25.4°C in August and 9.9°C in January. The soil is sandy-clay-loam, shallow.

Benatzu:

The experimental station 'Benatzu' (39°24' N; 9°5' E; 114 m a.s.l.) of the Agricultural Research Agency of Sardinia (AGRIS-DIRVE) is closed to 'Ussana' but differs for soil type (see Tab. 6). The climate is Mediterranean, with warm and dry summer and mild winter. Rainfall events are concentrated during autumn and winter-early spring months. Total mean annual precipitation of

the area is 430 mm. The annual mean temperature values range from 25.4°C in August and 9.9°C in January. The soil is clay and deep.

1.2 Soil data

Some of tha main soil physical and chemical characteristics of each experimental are reported in Table 6. Basic soil features requested as input by the model are: content in sand (%), silt (%), clay %), total N (%), stone (%), pH, C.S.C. (cmol kg^{-1}), color, run off value, slope and a fertility factor.

Some information relative to initial available soil water content at planting time, initial nitrogen content in the deeper soil layers, and data concerning crop residues of the previous crop were not available. Consequently, initial condition data were approximated: the previous crop was considered to estimate nitrogen content in the soil, the simulation starting date was set on 15 August to allow the model to start the water balance some months before the data of sowing, and estimating the available soil water content about 20% for this date. The water balance routine of the model was run starting at 15th August also without initial conditions to check if this estimated value of soil water content was correct.

1.3 Weather data

The weather data are maximum and minimum daily air temperature (°C) and rainfall daily data (mm), recorded by automatic weather stations located near the study areas, for the period 1974–2008. The weather data of Ottava and Santa Lucia stations were provided by ARPA-Sardegna (Specialist Regional Hydro-weather-climate Department) and data of Ussana and Benatzu stations were provided by Agricultural Research Agency of Sardinia (AGRIS-DIRVE).

Global solar radiation (MJ/m^2) daily data, available only for same years of the whole period were also collected. For the remaining years the solar radiation daily data were estimated.

Estimation of solar radiation

Global solar radiation values was estimated using the software RadEst v. 3.0 (Donatelli *et al.*, 2003).

The RadEst program estimates daily global solar radiation values for a location at a given latitude. Four models, derived from the model proposed by Bristow and Campbell, are available to estimate daily radiation from air temperature data. All the models estimate atmospheric transmissivity of global solar radiation based on the difference between maximum and minimum temperature. The estimated value of radiation is calculated as the product of the estimated transmissivity times the value of potential radiation outside the earth atmosphere.

The model used in this work is the *Campbell-Donatelli model* (Donatelli and Campbell, 1998).

1.4 Agronomic and management data

Durum wheat experimental data, regarding production characteristics and management techniques, were collected for the period 1989-2007.

Initial conditions, such as previous crop, planting depth and dates, row spacing, plant population, fertilizer applications, harvest schedule were collected and then set as input in the model. In each site the varieties considered are grown under the same environmental conditions and are sown the same day. Fertilization and weed control operations are carried out simultaneously using the same type and the same quantity of fertilizer and herbicide. Similarly, the harvest is done the same day. According to this method the differences observed for different genotypes are attributable mainly to genetic differences.

The sowing is carried out on 8 lines per parcel with a line length of 5.9 m and a distance between rows of 0.18 m. The sowing depth is 3-4 cm. The parcels have an area of 10 m^2. The field trials experimental design was a triple lattice according to the procedures of the Italian durum wheat network for cultivar evaluation (http://www.cerealicoltura.it).

1.5 Cultivars description

For this study have been selected two durum wheat varieties: Simeto and Iride, and their characteristics are briefly described below:

Simeto, released in 1988, is an early, short, drought resistant variety of spring durum wheat with high and constant value of potential yield, excellent grain quality and highly resistant to drought. Thanks to these characteristics has spread quickly especially in the southern Italian areas, with particular reference to hot-arid areas of Sicily, and still is the most cultivated varieties of wheat in Europe. Aside from a slight decline in the late '90s, Simeto reaches values of land cultivated for the production of certified seed always higher than 25 thousand hectares with a peak of over 40 thousand in 1996 and 1997. Moreover, the generalized decline in certified seed production that has affected the whole Italian seed production has had more limited impact on this variety that still now (2008) is the first variety in Italy with over 47 thousand tons of certified seed production (http://www.sementi.it/).

Iride is a variety of spring durum wheat with good resistance to cold, early-cycle development and good tillering ability, characteristics that make it suitable for any time of sowing.

Released in 1996, for many years the best durum wheat variety for yield in the Italian trials, with a very good and stable yield in all cultivation areas, very good adaptability and resistance to common diseases, and extraordinary ear fertility. Iride is actually (2008) the second variety in Italy for the production of certified seed with over 38 thousand tons (http://www.sementi.it/).

Table 6. General characteristics of the experimental sites in Sardinia.

Characteristics				
Site	**Santa Lucia**	**Ottava**	**Ussana**	**Benatzu**
Latitude	39°58' N	40°46' N	39°24' N	39°24' N
Longitude	8°37' E	8°29' E	9°5' E	9°5' E
Elevation (m)	14 a.s.l.	80 a.s.l.	114 a.s.l.	80 a.s.l.
Soil type	-	Xerochrepts	Petrocalcic Palexeralf	Vertic Epiaquept
Sand, Silt, Clay (%) for the top layer (40 cm)	51, 14, 35	54, 18, 28	57, 16, 27	39, 30, 31
Color	Brown	Red	Brown	Red
pH in H_2O for the top layer (40 cm)	8.0	7.8	8.3	8.5
Drainage	Moderately well	Moderately well	Moderately well	Moderately well
Mean annual T (°C)	16.6	16.2	16.9	16.9
Mean air T (November-June)	13.8	13.3	13.9	13.9
Main annual precipitation (mm)	550	560	430	430
Mean precipitation (November-June)	420	410	310	310
Mean annual accumulated global solar radiation (MJ/m^2)	5900	5100	5300	5300

2. CROP MODELING

2.1 Crop model description: CERES-Wheat model

The model chosen for this study is the CERES-Wheat (Crop Estimation through Resource and Environment Synthesis) model, version 4.0.2.0.

CERES-Wheat is a yield simulation model that was originally developed under the auspices of the USDA-ARS Wheat Yield Project and the U.S. government multiagency AGRI- STARS program (Ritchie and Otter, 1985). The CERES-Wheat model simulates the impacts of the main environmental factors, such as weather, soil type, and major soil characteristics, and crop management on wheat growth, development, and yield (Ritchie *et al.*, 1998).

The model was chosen for the ability to simulate yield and crop phenology because it was widely evaluated and for the possibility to set ambient CO_2 concentration.

The model is one of the main models that have been incorporated in DSSAT (Decision Support System for Agro technology Transfer).

The DSSAT is a collection of independent programs that operate together; crop simulation models are at its center. Databases describe weather, soil, experiment conditions and measurements, and genotype information for applying the models to different situations (Jones *et al.*, 2003). The DSSAT-CSM (cropping system model) simulates growth, development and yield of a crop growing on a uniform area of land under prescribed or simulated management as well as the changes in soil water, carbon, and nitrogen that take place under the cropping system over time. The DSSAT-CSM is structured using the modular approach described by Jones *et al.* (2001) and Porter *et al.* (2000).

The DSSAT-CSM has a main driver program, a land unit module, and modules for the primary components that make up a land unit in a cropping system (Fig. 20).

The Primary modules are for weather, soil, plant, soil-plant-atmosphere interface, and management components. Collectively, these components describe the time changes in the soil and plants that occur on a single land unit in response to weather and management.

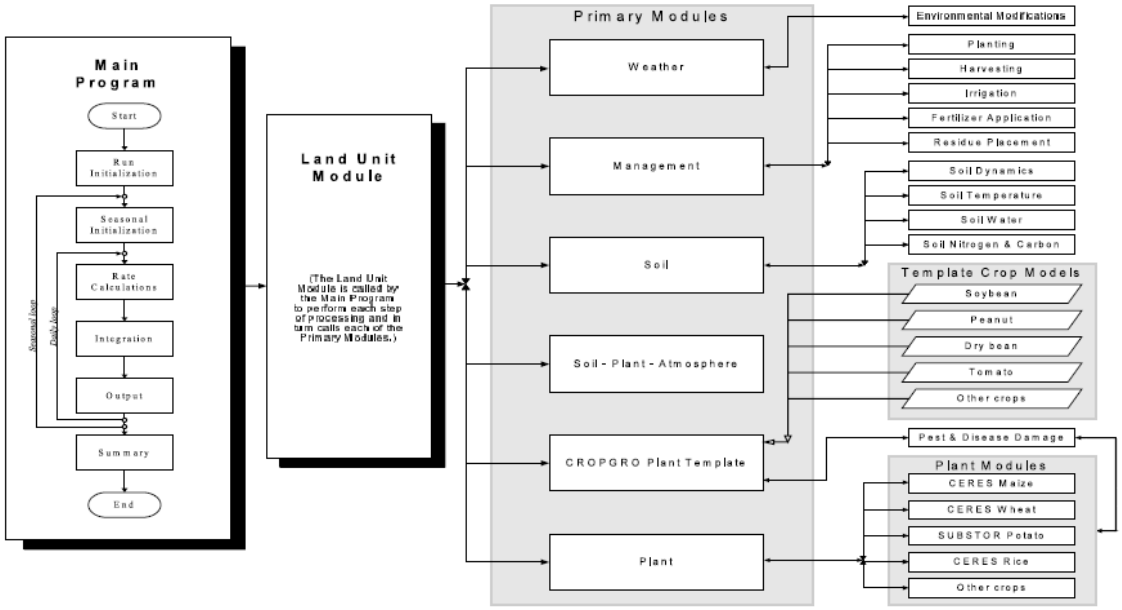

Fig. 20. Overview of the components and modular structure of the DSSAT-CSM.

Table 7 lists the primary and sub modules currently used in the CSM and summarizes their functions. The Land Unit module calls each of the primary cropping system modules each day. At the start of each new crop season, it obtains management information from the DSSAT input file. The Land Unit and Primary modules link to sub modules, and thus are used to aggregate processes and information describing successive components of the cropping system. For example, the Soil module has four sub modules that integrate soil water, soil carbon and nitrogen, soil temperature and soil dynamics processes. The Plant module has sub modules for various crops (Jones *et al.*, 2003).

The CERES- Wheat model was modified for integration into the modular DSSAT-CSM. For CERES-Wheat model the plant life cycle is divided into several phases, which are the following:

- germination,
- emergence,
- terminal spikelet,
- end ear growth,
- beginning grain fill,
- maturity,
- harvest.

Rate of development is governed by thermal time, or growing degree-days (GDD) (see Fig.21), which is computed based on the daily maximum and minimum temperatures. The GDD required to progress from one growth stage to another are either defined as a user input (through genetics coefficients), or are computed internally based on user inputs and assumptions about

duration of intermediate stages. The number of GDD occurring on a calendar day is a function of a triangular or trapezoidal function defined by a base temperature, optimum temperatures, and a maximum temperature above which development does not occur.

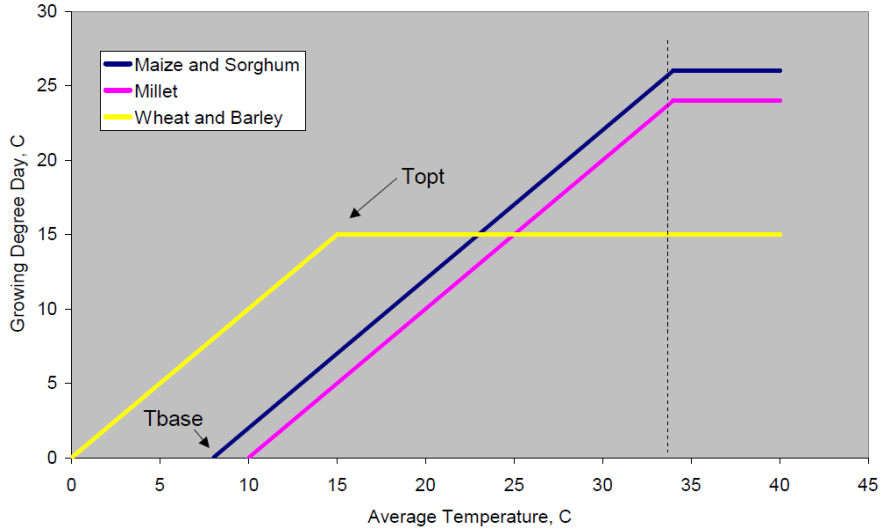

Fig.21. Growing Degree Days for Vegetative Development (Jones *et al.*, 2007).

Daylength may affect the total number of leaves formed by altering the duration of the floral induction phase, and thus, floral initiation. Daylength sensitivity is a cultivar specific user input. Currently, only temperature and, in some cases, daylength, drive the accumulation of GDD; high temperature, drought and nutrient stresses currently have no effect on developement. During the vegetative phase, emergence of new leaves is used to limit leaf area development until after a species-dependent number of leaves have appeared. Thereafter, vegetative branching can occur, and leaf area development depends on the availability of assimilates and specific leaf area. Leaf area expansion is modified by daily temperature GDD, and water and nitrogen stress.

Daily plant growth is computed by converting daily intercepted photosynthetically active radiation into plant dry matter using a crop-specific radiation use efficiency parameter. Light interception is computed as a function of LAI, plant population, and row spacing.

Potential growth rate is estimated by this relation:

$$PCARB = \frac{RUE \cdot PAR}{PLTPOP} \cdot (1 - e^{\{-k \cdot LAI\}}) \cdot CO_2$$

Where:

PCARB - Potential growth rate, g · plant^{-1};

RUE - Radiation Use Efficiency (g Dry Matter · PAR^{-1})

PAR - Photosynthetically Active Radiation (MJm^{-2}d^{-1})

PLTOP - Plant population, pl · m^{-2}

k - Light extinction factor (-0.85 wheat, barley; 0.65 maize; 0.625 rice)

LAI - Leaf area index

CO_2 - CO_2 modification factor

The CO_2 modification factor takes into account the variation in the concentration of CO_2 in the atmosphere and its consequence in photosynthesis: an increase in CO_2 concentration leads to an increase in the efficiency of photosynthesis. Figure 22 shows modification factors depending on the concentration of CO_2. The table shows how the model considers the greater benefit of wheat (C3 plants) compared to maize (C4 plant) with increasing CO_2 concentration.

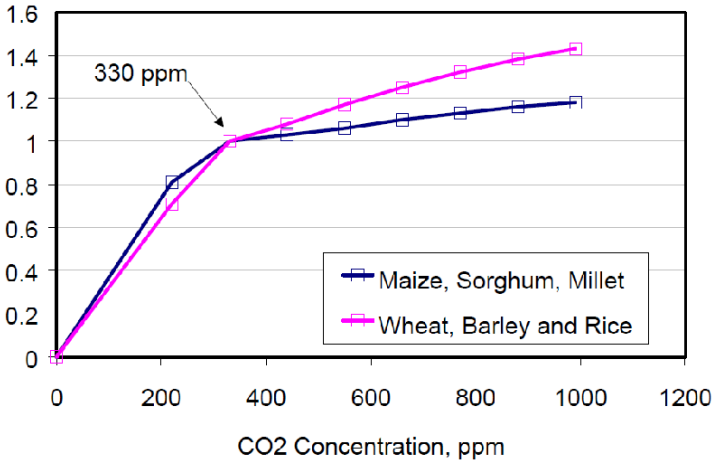

	Wheat	Mais
CO_2 (ppm)	CO_2Y	CO_2Y
0	0	0
220	0.71	0.81
330	1	1
440	1.08	1.03
550	1.17	1.06
660	1.25	1.1
770	1.32	1.13
880	1.38	1.16
990	1.43	1.18

Fig.22. CO_2 modification factor (Jones *et al.*, 2007).

The model also simulates the effects of CO_2 on stomatal resistance by means of a ratio applied to the calculation of transpiration rates that accounts for stomatal closure under higher CO_2 concentration (Hoogemboom, 1995).

The amount of new dry matter available for growth each day may also be modified by the most limiting of water or nitrogen stress, and temperature, and is sensitive to atmospheric CO_2 concentration. Above ground biomass has priority for carbohydrate, and at the end of each day, carbohydrate not used for above ground biomass is allocated to roots. Roots must receive, however, a specified stage-dependent minimum of the daily carbohydrate available for growth. Leaf area is converted into new leaf weight using empirical functions.

Kernel numbers per plant are computed during flowering based on the cultivar's genetic potential, canopy weight, average rate of carbohydrate accumulation during flowering, and temperature, water and nitrogen stresses. Potential kernel number is a user-defined input for specific cultivars.

Once the beginning of grain fill is reached, the model computes daily grain growth rate based on a user-specified cultivar input defined as the potential kernel growth rate (mg/(kernel d)).

Daily growth rate is modified by temperature and assimilate availability. If the daily pool of carbon is insufficient to allow growth at the potential rate, a fraction of carbon can be remobilized from the vegetative to reproductive sinks each day. Kernels are allowed to grow until physiological maturity is reached. If the plant runs out of resources, however, growth is terminated prior to physiological maturity. Likewise, if the grain growth rate is reduced below a threshold value for several days, growth is also terminated (Ritchie and Otter, 1985; Ritchie *et al.*, 1998).

Table 7. Summary description of modules in the DSSAT-CSM.

Modules	Sub modules	Behavior
Main program (DSSAT–CSM)		Controls time loops,, determines which modules to call based on user input switches, controls print timing for all modules
Land unit		Provides a single interface between cropping system behavior and applications that control the use of the cropping system. It serves as a collection point for all components that interact on a homogenous area of land
Weather		Reads or generates daily weather parameters used by the model. Adjusts daily values if required, and computes hourly values
Soil	Soil dynamics	Computes soil structure characteristics by layer. This module currently reads values from a file, but future versions can modify soil properties in response to tillage, etc
	Soil temperature module	Computes soil temperature by layer
	Soil water module	Computes soil water processes including snow accumulation and melt, runoff, infiltration, saturated flow and water table depth. Volumetric soil water content is updated daily for all soil layers. Tipping bucket approach is used
	Soil nitrogen and carbon module	Computes soil nitrogen and carbon processes, including organic and inorganic fertilizer and residue placement, decomposition rates, nutrient fluxes between various pools and soil layers. Soil nitrate and ammonium concentrations are updated on a daily basis for each layer
SPAM		Resolves competition for resources in soil–plant–atmosphere system. Current version computes partitioning of energy and resolves energy balance processes for soil evaporation, transpiration, and root water extraction
CROPGRO Crop Template module		Computes crop growth processes including phenology, photosynthesis, plant nitrogen and carbon demand, growth partitioning, and pest and disease damage for crops modeled using the CROPGRO model Crop Template (soybean, peanut, dry bean, chickpea, cowpea, faba bean, tomato, Macuna, Brachiaria, Bahiagrass)
Individual plant growth modules	CERES-Maize; CERES-Wheat; CERES-Rice; SubStor-Potato; Other plant models	Modules that simulate growth and yield for individual species. Each is a separate module that simulates phenology, daily growth and partitioning, plant nitrogen and carbon demands, senescence of plant material, etc
Management operations module	Planting	Determines planting date based on read-in value or simulated using an input planting window and soil, weather conditions
	Harvesting	Determines harvest date, based on maturity, read-in value or on a harvesting window along with soil, weather conditions
	Irrigation	Determines daily irrigation, based on read-in values or automatic applications based on soil water depletion
	Fertilizer	Determines fertilizer additions, based on read-in values or automatic conditions
	Residue	Application of residues and other organic material (plant, animal) as read-in values or simulated in crop rotations

Input requirements for CERES-Wheat include weather and soil conditions, plant characteristics, and crop management (Hunt *et al.*, 2001).

The minimum weather input requirements of the model are daily solar radiation, maximum and minimum air temperature, and precipitation. These values are usually available at many locations with the exception of solar radiation. However, solar radiation can be estimated from other observations: from sunshine durations using the Angstrom-Prescott formula, from maximum and minimum temperatures using Hargreaves-Samani formula, or other combinations of daily weather characteristics (e.g. Trnka *et al.*, 2007).

Soil inputs include drainage and runoff coefficients, first-stage evaporation and soil albedo, water-holding characteristics for each individual soil layer, and rooting preference coefficients at several depth increments.

The model also requires saturated soil water content and initial soil water content for the first day of simulation.

Required crop genetic inputs are coefficients related to photo- period sensitivity, duration of grain filling, conversion of mass to grain number, grain-filling rates, vernalization requirements, stem size, and cold hardiness (Hunt *et al.*, 1993).

Check management input information includes plant population, planting depth, and date of planting. If the crop is irrigated, the date of application and amount is required.

Latitude is required for calculating day length.

The model can use different weather, soils, genetic, and management information within a growing season or for different seasons in a single model execution.

The model simulates phenological development; biomass accumulation and partitioning; leaf area index LAI); root, stem, leaf, and grain growth; and the soil and plant water and N balance from planting until harvest maturity based on daily time steps.

The model integrates also daily stress effects as feedback on growth and/or development processes.

CERES model can simulate following parameters:

1. Crop and soil status at main development stages: BIOMASS (kg ha^{-1}), LAI, LEAF NUM, ET (mm), RAIN (mm), IRRIG (mm), SWATER (mm), CROPN(kg ha^{-1} as well as %),N and water stress at different dates, crop age and growth stages as per requirement.

2. Main growth and development variables: Flowering date (days after planting – dap), physiological maturity (dap), grain yield (kg ha^{-1}; dry), weight per grain (g; dry), grain number (grain/m2), grains/ear, maximum LAI (m^2/m^2), biomass (kg ha^{-1}) at anthesis, biomass N (kg N ha^{-1}) at anthesis, biomass (kg ha^{-1}) at harvest, stalk weight (kg ha^{-1}) at harvest, harvest index (kg/kg), final leaf number, grain N (kg N ha^{-1}), biomass N (kg N ha^{-1}), stalk N (kg N ha^{-1}) and seed N (%).

3. Environmental and stress factors at different growth stages. Environmental factors are maximum and minimum temperature, solar radiation and photoperiod. Stress factors include water and N stress at different growth stages.

4. Water balance.
5. Nitrogen balance.
6. Organic matter.
7. Phosphorus balance.

In this study anthesis date and grain yield, were considered.

2.2 CERES-Wheat model calibration

CERES-Wheat model was calibrated determining the seven genetic coefficients which characterize each variety. The calibration can be made by direct observation of crop characteristics through experimental trials or by a procedure that minimizes the difference between measured and corresponding simulated data by the genetic parameters of the CERES model.

The seven coefficients present in the CERES-Wheat model are the following:

P1V: Days at optimum vernalizing temperature required to complete vernalization.

This coefficient reflects the differing vernalization requirements of varieties. Vernalization is assumed to occur at temperatures between 0 and 18°C. The optimum temperature for vernalization is assumed to be in the range of 0 to 7°C, with temperature between 7 and 18°C having a decreasing influence in the process. Minimun and maximum daily temperatures are used to calculate a daily vernalization effectiveness factor with a value ranging between 0 and 1. Although there is variability in sensitivity to vernalization between cultivars, 50 vernalization days are assumed to be sufficient to completely vernalize all cultivars. Spring wheat varieties have a low sensitivity to vernalization. They are incorporated in the model in the same way as winter wheat varieties by expressing the differences in vernalization through this genetic coefficient. Spring wheat should have P1V values < 5.

P1D: Percentage reduction in development rate in a photoperiod 10 hour shorter than the threshold relative to that at the threshold. This coefficient is used to describe the sensitivity of varieties to photoperiod. Wheat is a long day plant and minimizes its development during short days. Generally this value ranges between 20 and 100, depending on cultivar.

P5: Grain filling (excluding lag) phase duration (°C d). Grain filling duration is difficult to quantify than visual developments events (e.g. leaf appearance or flowering), and the most accurate determination of the beginning and ending of grain filling requires destructive sampling. This

genetic coefficient is based on the total heat, and for each unit of increasing above 0° C adds 20 degree days at starting value of 430 degree days.

G1: Kernel number per unit canopy weight at anthesis (#/g).

G2: Standard kernel size under optimum conditions (mg).

G3: Standard, non-stressed dry weight (total, including grain) of a single tiller at maturity (g).

PHINT: Interval between successive leaf tip appearances (°C d).

Genetic coefficients were derived partly from literature sources (Dettori, 2006 and Rinaldi, 2004) and were optimized through an iterative procedure, minimizing the difference from observed and simulated data.

The following variables were considered in model calibration: grain yield (kg ha^{-1}) accounting for biomass production and anthesis date (days after planting, dap) regarding phenological development.

In this thesis the calibration was performed for each cultivar using the all set of data from the two experimental sites (Benatzu and Ussana) located in the South of Sardinia and the other two sites located in the North and Centre of Sardinia (Ottava and Santa Lucia) was used to evaluate the performance of the model.

First were calibrated the coefficients related to phenology (P1V, P1D and P5) and then the coefficients related to the grain filling characteristics (G1, G2, G3). PHINT was the last calibrated coefficient.

2.3 CERES-Wheat model validation and evaluation

In the literature, is often used both the term "validation" and "evaluation". A rather common definition is that validation concerns determining whether a model is adequate for its intended purpose or not. This emphasizes the important fact that a model should be judged with reference to an objective (this definition seems to indicate that the result of a validation exercise is "yes"(the model is valid) or "not" (not valid); but it is rarely the case that one makes such a categorical decision). Rather one seeks a diversity of indications about how well the model

represents crop responses. For this reason it would be preferable to use the term "evaluation" (Wallach, 2006).

Model evaluation, in its simplest form, is a comparison between simulated and observed values. Beyond comparisons, there are several statistical measures available to evaluate the association between predicted and observed values, among them are the Pearson correlation coefficient (r) and its square, the coefficient of determination (R^2). Willmott (1982) has pointed out that the main problem with this analysis is that the magnitudes of r and R^2 are not consistently related to the accuracy of prediction where accuracy is defined as the degree to which model predictions approach the magnitudes of their observed counterparts. Further, as R^2 often is unrelated to the sizes of the difference between observed and predicted values, high or statistically significant R^2 may be misleading.

Hence, also other different test criteria, have been used to evaluate the performance of the model, e.g., RMSE, GSD, EF, CRM, MBE, MAE, and *d*-Index, because it is important to use more than one measure in order to bring out different aspects of model agreement.

Statistical analysis

The performance of model was determined using several indexes mainly based on the calculation of correlation and differences between estimated and measured yield and anthesis values. Results obtained from data used for the calibration sites (Benatzu and Ussana) were analyzed calculating the correlation coefficient (*r*) and its square, the coefficient of determination (R^2), the root mean squared error (RMSE), general standard deviation or relative root mean squared error (GSD), modelling efficiency index (EF), coefficient of residual mass (CRM), mean bias error (MBE), mean absolute error (MAE), and Index of agreement (*d*-Index) for the predicted and observed yield and anthesis values. Also the results obtained from data used for the validation sites (S. Lucia and Ottava) were analyzed calculating the same indices.

The Pearson correlation coefficient (*r*) is the correlation coefficient between measured and calculated values defined as:

$$r = \frac{\sum_{i=1}^{n} (E_i - \overline{E}) \cdot (M_i - \overline{M})}{\sqrt{\sum_{i=1}^{n} (E_i - \overline{E})^2 \cdot \sum_{i=1}^{n} (M_i - \overline{M})^2}}$$

The range of r is $-1 \leq r \leq 1$. A value of $r=1$indicates that there exists a perfect linear relationship between simulated and observed values. However this does not necessarily imply that the model is perfect.

The RMSE was used to test the accuracy of the model, which is defined as the variation, expressed in the same unit as the data, between simulated and measured values (Loague and Green, 1991):

$$RMSE = \sqrt{\frac{\sum_{i=1}^{n} E_i - M_i^{\,2}}{n}}$$

where Ei and Mi indicate the simulated and measured annual values of the year i and n the number of annual values. RMSE represents the typical size of model error, with values equaling or near zero indicating perfect or near perfect estimates. The RMSE was also expressed as a coefficient of variation (GSD) by dividing it by the mean of the measured yield or anthesis values ($\overline{M}$):

$$GSD = \sqrt{\frac{\sum_{i=1}^{n} E_i - M_i^{\,2}}{n}} \frac{100}{\overline{M}} = RMSE \frac{100}{\overline{M}}$$

In addition, the accuracy of the model was evaluated using another index based on squared differences, the modelling efficiency index (EF):

$$EF = 1 - \frac{\sum_{i=1}^{n} E_i - M_i^{\,2}}{\sum_{i=1}^{n} M_i - \overline{M}^{\,2}}$$

EF values greater than 0 indicate that the model estimates are better predictors than the average measured value, with negative values indicating the opposite. A EF value equal or near 1 means a perfect or near perfect estimates.

To measure the tendency of the model to overestimate or underestimate the measured values three statistics were used: the coefficient of residual mass (CRM), the mean bias error (MBE) and the mean absolute error (MAE):

$$CRM = 1 - \frac{\sum_{i=1}^{n} E_i}{\sum_{i=1}^{n} M_i}$$

$$MBE = \sum_{i=1}^{n} \frac{E_i - M_i}{n}$$

$$MAE = \sum_{i=1}^{n} \frac{|E_i - M_i|}{n}$$

A negative CRM indicates a tendency of the model toward overestimation (Xevi *et al.*, 1996). A positive bias error indicates a tendency to over predict a variable while a negative bias error implies a tendency to under predict a variable. MAE values near or equal to zero indicate a better match along the 1:1 line comparison of estimated and observed values (Rasse *et al.*, 2000).

Willmott (1981) propose an Index of agreement (*d*) defined as:

$$d = 1 - \frac{\sum_{i=1}^{n} (E_i - M_i)^2}{\sum_{i=1}^{n} \left(|E_i - \overline{M}| + |M_i - \overline{M}| \right)^2}$$

If the model is perfect, then observed values are equal to simulated values and *d*=1. If the model predictions are identical in all cases and equal to the average of the observed values, d=0. These limiting values are the same as for EF, but for other cases, the two criteria will have different values.

3. CLIMATE CHANGE SCENARIOS

Various approaches can be used to produce weather series representing the changed climate. Most of them rely on Global Climate Models (GCMs). However, as GCMs cannot reliably simulate even the present climate conditions (e.g. annual cycles of the means), the direct GCM representation of future climate cannot be used as an input to the impact models. Instead, it is recommended to use climate change scenarios which represent differences or ratios in individual variables between some plausible future climate and the current or control climate (Dubrovsky *et al.*, 2005).

The changes in the climatic variables for a given site can be obtained by interpolation of GCM-simulated values for the 4 corners of the GCM grid box in which the target area lies.

With a climate change scenario, 2 techniques are typically used to construct the weather series representing the changed climate (Dubrovsky *et al.*, 2000): (1) an observed weather series is modified (additively or multiplicatively) by the scenario parameters (e.g. Maytín *et al.*, 1995; Mearns *et al.*, 1992); (2) a weather series is produced by a weather generator whose parameters have been modified according to the scenario (e.g. Dubrovsky *et al.*, 2000, Riha *et al.*, 1996, Semenov and Barrow, 1997). In this thesis the latter technique was chosen.

GCM-based climate change scenarios are affected by many uncertainties. To account for the uncertainties, use of multiple scenarios in climate change impact studies is widely recommended and adopted. This is typically done by using a set of scenarios derived from several GCM simulations (e.g. several GCMs run at one or more emission scenarios, several runs of a single GCM using different initial conditions, and one or more emission scenarios).

Statistical post-processing was applied to develop a 'standardized' scenario from a given GCM transient run. In developing this scenario, it was hypothesized that the climate change pattern (both annual cycle and spatial pattern) is the product of the standardized scenario, which defines the response of the variables to a 1°C rise in T_G (global mean temperature) and ΔT_G. This is the pattern scaling technique (Santer *et al.* 1990) used in the IPCC First Assessment Report (Mitchell *et al.*, 1990) and subsequently widely adopted in constructing the climate change scenario (Dubrovsky *et al.*, 2005).

Use of the pattern scaling technique in constructing the climate change scenarios allows to separate: (1) uncertainties in determining the climate change pattern: (inter-GCM uncertainty /differences between individual GCMs/, internal uncertainty of a given GCM, and uncertainty related to the regression technique used to determine the standardized scenario), and (2) uncertainty in estimating the global mean temperature (T_G), which is often estimated using a simple climate model, e.g. MAGICC/SCENGEN 4.1 model (Harvey *et al.*, 1997; Hulme *et al.*, 2000) which is available from the CRU web page (http://www.cru.uea.ac.uk/~mikeh/software/).

MAGICC/SCENGEN is a coupled gas-cycle/climate model (MAGICC) that drives a spatial climate-change scenario generator (SCENGEN). MAGICC has been the primary model used by IPCC to produce projections of future global-mean temperature and sea level rise and has been used in many impact studies (Goldammer and Price, 1998, Kont *et al.*, 2003).

Applicability of the pattern scaling technique is conditioned by the assumption that changes in climatic variables are proportional to $\Delta T_{G.}$

The climate change scenario for any period and any emission scenario for which ΔT_G can be estimated, is determined as:

$$\Delta X(t) = \Delta X_S \times \Delta T_G(t)$$

where ΔX_S is the standardized change in the variable X and ΔX is the change in X resulting from ΔT_G.

The standardized scenario (ΔX_S) may be determined by dividing the scenario related to a selected period by ΔT_G predicted by a given model for a given period.

$$\Delta X_S = \Delta X_{(tA\text{-}tB)} / \Delta T_{G(tA\text{-}tB)}$$

In a more sophisticated approach, the standardized scenarios are obtained from the transient run by a linear regression (not passing through zero), in which the independent variable *x* is ΔT_G, and the dependent variable *y* is the change of a given variable in a given time, $\Delta X(t)$. Standardized change of climate characteristic X then coincides with the slope parameter in regression equation:

$$\Delta X_S = a \cdot \Delta T_G + b$$

Different GCMs give different standardized scenarios (ΔX_S).

The ΔT_G values were estimated by the MAGICC model. In MAGICC a given emission scenario is converted to GHG and aerosol concentrations and radiative forcing, and the resulting ΔT_G and sea level are estimated assuming chosen value of the climate sensitivity factor.

The overall uncertainty in the change in global mean temperature (ΔT_G) is thus driven by uncertainties in two input parameters of the MAGICC model: choice of an emission scenario and climate sensitivity factor.

The equilibrium climate sensitivity parameter (hereafter referred to as 'climate sensitivity', $\Delta T2\times$) refers to the equilibrium change in T_G following a doubling of the atmospheric (equivalent) CO_2 concentration. Due to the inertia of the climate system, the temperature response of transient GCM simulations to doubled CO_2 generally decreases with increasing rate of CO_2 rise and is therefore always lower than the climate sensitivity. The value of the climate sensitivity factor is the subject of much discussion. According to the IPCC the value is likely to be in the range 1.5°C to 4.5°C (no confidence interval is stated) with 3°C being the best estimate. The IPCC's 4th assessment report assumes the range from 2°C to 4.5°C.

Figure 23 compares the range of ΔT_{global} simulated by a set of GCMs for emission scenario SRES-A2 with the values simulated by MAGICC model run at various climate sensitivities. The figure indicates that the range of GCM-simulated ΔT_{global} values is not representative for uncertainty in climate sensitivity. Therefore it implies, that the set of climate change scenarios determined by the pattern scaling method in which we use different values of ΔTglobal estimated by MAGICC run at various emission scenarios and climate sensitivities will better represent uncertainty in ΔT_{global}.

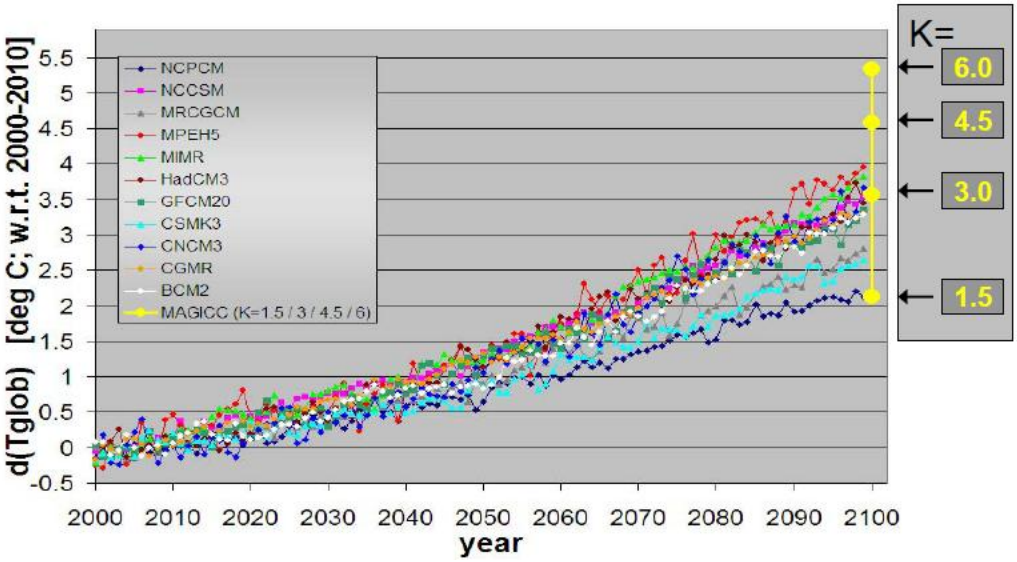

Figure 23. Range of ΔT_{global} simulated for emission scenario SRES-A2 by a set of GCMs from IPCC-AR4 (colour time series) and by MAGICC model run at various climate sensitivities(yellow bar on the right) (Dubrovsky, 2009).

In this thesis, I used a set of 9 climate change scenarios, which results as a combination of three GCMs used to determine the standardised scenarios and three values of ΔT_G (low, intermediate, high) used to scale the standardized scenarios.

The three ΔT_G values are based on following combinations of the emission scenario and climate sensitivity factor (see Table 10): low estimate of ΔT_G is determined as a lowest ΔT_G value of the four main emission scenarios for the low climate sensitivity (1.5°C) and given future period; intermediate estimate of ΔT_G is determined as the average of the two intermediate ΔT_G values for the intermediate climate sensitivity (3°C); high estimate of ΔT_G is determined as a maximum of the four ΔT_G values for the high climate sensitivity (4.5°C). The ΔT_G was estimated for three future period: 2025, 2050 and 2075.

The set of three GCMs used to derive the standardised scenarios include HadCM3, ECHAM5 and NCAR-PCM. These 3 GCM were chosen because of their best ability to simulate

the present climate conditions in Mediterranean regions. Due to the demands of the presently used CERES-Wheat crop growth model, the following 4 variables were used from the GCM outputs:

- precipitation (PREC),
- daily maximum and minimum temperature (TMAX and TMIN),
- solar radiation (SRAD).

The scenarios for impact studies in Sardinia were developed for 3 sites: Ottava (North-West Sardinia), Ussana (South Sardinia) and Santa Lucia (Central-West Sardinia), were the experimental fields are located. Site-specific scenarios were developed from each of the 3 GCMs and for each of the 3 locations. The scenarios consist of changes in monthly means of TMAX, TMIN, PREC and SRAD that were obtained by spatial interpolation of GCM-simulated grid-specific values.

The future values of CO_2 concentration were also based on the MAGICC model simulations (Table 8).

Table 8. Changes in global mean temperature, ΔT_G, calculated by the MAGICC model. Baseline period: 1961–1990; baseline CO_2 level: 333 ppm. Climate sensitivities: low $\Delta T_{2\times}$ = 1.5°C; intermediate $\Delta T_{2\times}$ = 3°C; high $\Delta T_{2\times}$ = 4.5°C.

FUTURE PERIOD	**2025**				**2050**				**2075**			
Climate sensitivity (°C)	**1.5**	**3**	**4.5**	**CO_2 concentration (ppm)**	**1.5**	**3**	**4.5**	**CO_2 concentration (ppm)**	**1.5**	**3**	**4.5**	**CO_2 concentration (ppm)**
SRES B1	**0.4**	**0.66**	**0.84**	**416.0**	**0.68**	**1.17**	**1.51**	**469.8**	**0.93**	**1.64**	**2.17**	**501.0**
SRES B2	**0.45**	**0.74**	**0.93**	**425.7**	**0.8**	**1.35**	**1.74**	**476.1**	**1.14**	**1.97**	**2.59**	**542.2**
SRES A1B	**0.44**	**0.71**	**0.89**	**437.7**	**0.96**	**1.58**	**2.02**	**555.2**	**1.41**	**2.41**	**3.13**	**631.7**
SRES A2	**0.41**	**0.68**	**0.86**	**432.5**	**0.9**	**1.49**	**1.90**	**533.3**	**1.54**	**2.59**	**3.33**	**705.3**
ΔT_G	**0.4**	**0.695**	**0.93**		**0.68**	**1.42**	**2.02**		**0.93**	**2.19**	**3.33**	

In result for each of the three experimental station in Sardinia 27 climate change scenarios are used here: 3 GCMs (HadCM3, ECHAM5 and NCAR), 3 levels of climate sensitivity (1.5, 3 and 4.5 °C) and 3 future periods (2025, 2050 and 2075).

Having the climate change scenarios, the 100-year synthetic daily weather series (values of SRAD, TMAX, TMIN and PREC) were produced by the stochastic weather generator, which was calibrated using the observed weather data and whose parameters was then modified according to the climate change scenario.

3.1 M&Rfi Weather Generator

The weather generator used to produce synthetic weather series for this study is M&Rfi. M&Rfi is a more flexible follower of Met&Roll (M&Rfi = Met&Roll flexible), which is a parametric single-station 4-variate stochastic daily weather generator based on Markov chain,

Gamma distribution and autoregressive model (Dubrovský, 1997; Dubrovský et al., 2000; Dubrovský et al., 2004).

Compared to Met&Roll, which is strictly daily 4-variate generator, the time step in M&Rfi may vary from 1 day to 1 month and a number of variables is optional.

Similarly to Met&Roll, it is based on the first-order autoregressive model, two-state Markov chain (order = 0, 1, 3) and Gamma distribution. The WG may be run either in a non-conditional mode, or in a conditional mode [/C switch]. In the former case, all parameters are modelled by a multivariate AR model (tip: variables may be transformed using a /T switch). In the latter case, the conditioning variable (typically precipitation) is modelled by a Markov chain model (series of occurrence/non-occurrence of above-threshold (=wet in the case of precipitation being the conditioning variable) values), the amount is modelled by Gamma distribution.

Important features of the M&Rfi generator include:

- **spatial resolution:** single-site;
- **optional time step:** 1 day, 2 days, 3 days, 5 days, 1 week, 10 days, half-month, month;
- **transformation** (e.g. logarithmic, exponential power) of input variables;
- the **range checking** is performed during the WG calibration from the input (learning) weather data;
- **climate change scenario** may be used to directly modify input weather series or to modify M&Rfi parameters and then generate synthetic series representing climate change conditions;
- synthetic series may observe the **weather forecast**, which is either probabilistic or deterministic.
- additional weather characteristics (for example solar radiation and evapotranspiration) may be estimated from available weather characteristics.

According to the applied time step and a set of weather characteristics being involved, various settings of the generator may be used. In the present analysis, the M&Rfi's settings corresponds to the latest version of Met&Roll described in Dubrovsky et al. (2004) and used in several recent experiments (e.g. Trnka et al., 2004): Precipitation occurrence is a primary (= generated in the first step) characteristic modelled by a two-state Markov chain (order = 0, 1, 3), precipitation amount is fitted by Gamma, and solar radiation and daily extreme temperatures are modelled by first-order autoregressive model with means and standard deviations being conditioned on precipitation occurrence.

The figure 24 shows the scheme of using the weather generator to produce synthetic weather series representing present and future climate conditions.

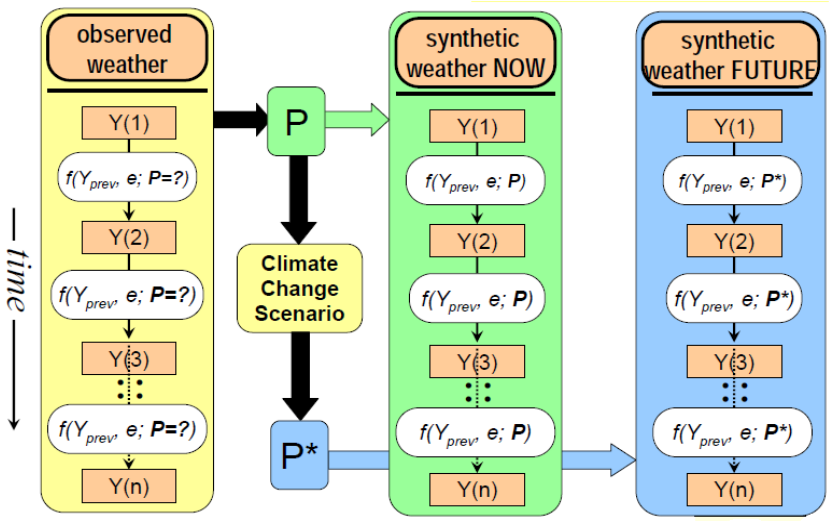

Figure 24. Scheme of using the weather generator Y(t) = weather series; f(.) = underlying model of the weather generator; e = random vector; P = set of WG parameters derived from the observed series; P* = WG parameters representing future climate and obtained by modifying P according to the climate change scenario (from Dubrovsky 2009).

4. CLIMATE CHANGE IMPACT ASSESSMENT

Methodology for the present climate change impact study is summarized graphically in the scheme below (Fig. 25).

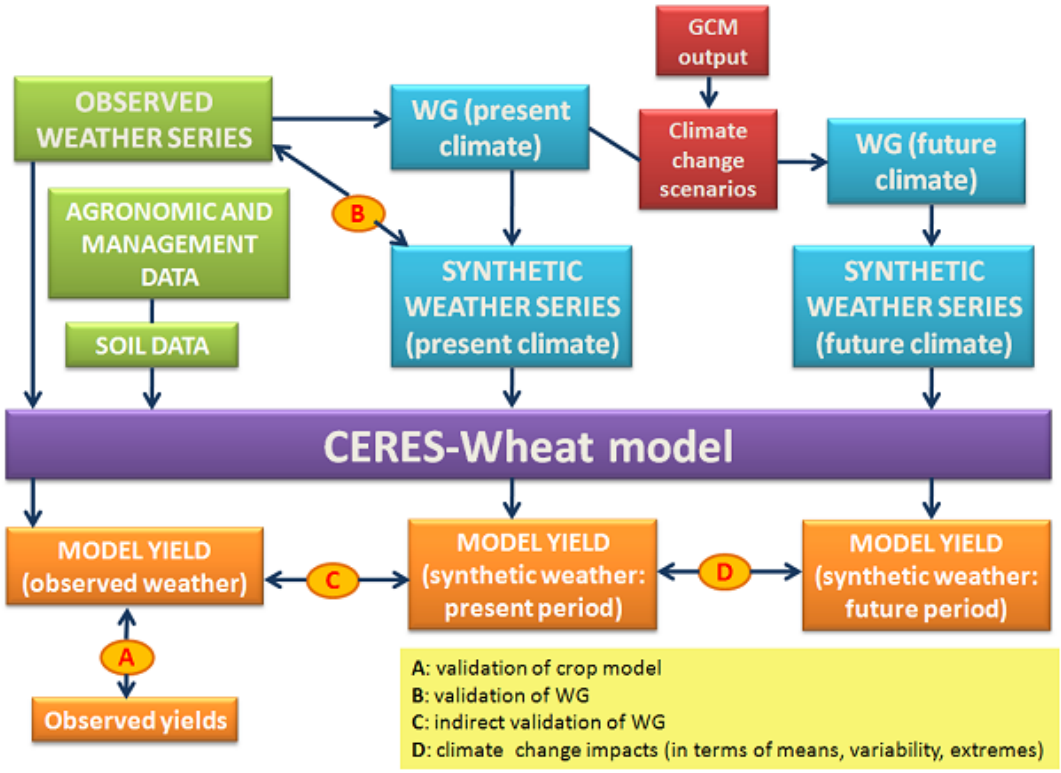

Figure 25. Scheme of Climate Change impact study (modified from: Dubrovsky M., 2009).

Climate change impact assessment

In order to carry out the climate change impact assessment, the method, originally developed by Semenov and Porter (1995), and adapted for other studies (Zalud and Dubrovsky, 2002, Trnka *et al.*, 2004) was applied. The method is based on the comparison of the output from multiple crop growth model runs with synthetic weather series representing the present and changed climates.

The non-meteorological input parameters (cultivar characteristics, soil properties, planting details, fertilization regime) were the same for each site and each future period and reflect the typical values applied in the real crop experiments (Tab.9).

For each experimental site 27 climate change scenarios were used, as low, middle and high versions of 3 GCMs (HadCM3, ECHAM5 and NCAR) for 3 future periods (2025, 2050, 2075).

For each climate scenarios, a 99-year simulation with synthetic series was carried out considering a fixed value of CO_2 (360 ppm) and also considering different future levels of CO_2

concentrations in the atmosphere projected for the three future periods by the different climate change scenarios. Therefore, indirect effect of increased CO_2 concentration (related to changed weather conditions) and effect of both direct (or CO_2-fertilisation effect) and indirect increase in CO_2 concentration on crop yields, was evaluated.

The results of yield and anthesis under climate change scenarios were analyzed using Student-Newman-Keuls (SNK) test, based on a stepwise or layer approach to significance testing (Bechhofer *et al.*, 1995).

Validation of weather generator

Before using the weather generator in the impact study was necessary to evaluate how the imperfection of the weather generator affect results obtained with crop model fed by the synthetic weather series.

The validation of the weather generator was made by comparing statistical properties of crop model output characteristics (crop yield and anthesis) simulated by CERES-Wheat with observed weather data versus outputs obtained with synthetic weather series for actual period, generated by weather generator.

CERES-Wheat model simulations were run for the "representative" years of each experimental site in Sardinia, with 30-year observed weather series and 99-year synthetic weather series.

Table 9. Characteristics of the "representative" years applied at the test sites.

Site	*Ussana*	*Benatzu*	*Ottava*	*Santa Lucia*
Sowing date	3 December	13 December	8 December	14 December
Harvest date	24 June	29 June	26 June	28 June
Total annual value of N and P_2O_5 fertilizer applications (kg ha^{-1})	90 - 75	90 - 75	90 – 90	120 - 90
Initial available soil water and nitrogen (%) at starting simulation (15^{th} August)	20 - 10	20 - 40	20– 20	50 - 60

The model yields simulated with synthetic weather series were compared to those simulated with the observed series using F-test (comparison of the variances) and t-test (comparison of the means) (Mavromatis and Jones, 1998; Dubrovsky *et al.*, 2004). First an F-test was performed. If the P-value was low ($P<0.05$) the variances of the two samples cannot be assumed to be equal and the t-test with a correction for unequal variances was used.

5. ADAPTATION STRATEGIES EVALUATION

The yields may be modified by various management responses, such as adjustment in fertilization and irrigation regimes, shifting the planting date, etc..

In this methodology only the shift of planting date is considered. This is a simple but very useful adaptation solution, because it can offer an immediately available responce for farmers towards climate change, even today.

The 99-year crop model simulations were run for the different climate scenarios and different values of CO_2 at water and nitrogen limited conditions, considering a earlier planting date (D-30 days) and later planting date (D+30 days), where D is the planting date of the "representative year" of each experimental site.

This analysis considered only the middle versions of the 3 GCMs (HadCM3, ECHAM5 and NCAR) for the 3 future periods (2025, 2050, 2075).

RESULTS

In this chapter the results obtained in this study are showed. They can be summarized as follow:

1. Calibration and evaluation of the CERES-Wheat model for two durum wheat varieties (Simeto and Iride) in four experimental sites in Sardinia (Ussana and Benatzu: South of Sardinia, Ottava: North and Santa Lucia: Centre of Sardinia), for an index of production (yield) and a phenological stage (anthesis).
2. Analysis of climate change scenarios obtained for each experimental station, considering three GCMs (Hadley, NCAR and ECHAM), three climate sensitivity levels (1.5, 3 and 4.5 °C) and different emission scenarios (A1B, A2, B1, B2), for three future periods (2025, 2050, 2075). Results observed in terms of change in precipitation, temperature, and solar radiation, are reported.
3. Validation of the Weather Generator used for climate change scenarios production, in terms of crop model output, for each experimental site.
4. Analysis of Climate Change impacts on the two wheat cultivars studied, separately for each experimental site, using the 27 climate change scenarios developed for each site and considering first the indirect effect of increased CO_2 concentration (changes in temperatures, solar radiation and precipitation) and then both indirect and direct effect of increased CO_2 concentration on yield and anthesis.
5. Evaluation of adaptation strategies (sowing date shift) in response to climate change, analyzing the effect of changing in sowing date on yield and anthesis, separately for each cultivar and for each experimental site.

1. CERES-WHEAT MODEL CALIBRATION AND VALIDATION

In this section the results of CERES-Wheat model calibration and validation for Simeto and Iride varieties are shown.

First of all are showed the calibration of Simeto and Iride using dataset from Ussana and Benatzu sites (located in the South of Sardinia). These experimental sites are very different regarding soil characteristics but are located at one kilometer of distance and have the same weather conditions.

Second are showed evaluation and validation of the CERES-Wheat model for the two durum wheat varieties using datasets from Ottava (North of Sardinia) and Santa Lucia (Centre of Sardinia) experimental sites.

In both phases are studied an index of production (yield) and and an index of phenology (anthesis).

1.1 Calibration for Simeto cultivar

The model calibration for Simeto cultivar was performed using data from Benatzu and Ussana experimental sites. Almost the entire available dataset, for the period 1989-2007, was used: thirty-two years of data for yield and thirty-one years for anthesis (two years of this period were not available and two years were excluded from calibration because of outliers).

The statistical results for yield and anthesis calibration are listed in Table 1.1.

Table 1.1 CERES-Wheat calibration results for Benatzu and Ussana experimental sites on grain yield (t ha^{-1}) and anthesis (dap=day after planting) for Simeto cultivar. Mean, standard deviation (SD), minimum, and maximum observed and simulated values are reported. Statistical analysis results are also shown.

SIMETO		YIELD (t ha^{-1})		ANTHESIS (dap)	
		OBS	SIM	OBS	SIM
Mean	**Mean**	3.4	3.9	132	132
Standard deviation	**SD**	1.2	0.8	10	8.4
Minimum	**Min**	0.8	2.5	105	117
Maximum	**Max**	6.8	6.0	164	157
Number of samples	**N**	32		31	
Pearson coefficient	**r**	0.80***		0.90***	
Coefficient of determination	**R^2**	0.63		0.80	
Root Mean Square Error	**RMSE**	0.91		4.44	
General standard Deviation	**GSD (%)**	26		3	
Modeling Efficiency	**EF**	0.46		0.80	
Mean Bias Error	**MBE**	0.49		-0.29	
Mean Absolute Error	**MAE**	0.77		3.45	
Coefficient of Residual Mass	**CRM**	-0.14		0.00	
Index of agreement	**d-Index**	0.81		0.93	

* p≤0.02; **p≤0.01; ***p≤0.001; ns=not significant.

OBS, observed values; SIM, simulated values.

The results show that the mean value for simulated yields is higher than the correspondent mean value of observed yields for the period considered. The value of standard deviation for simulated yields is lower than the standard deviation value for observed yields. This is in accordance withthe fact that the model generally tends to reduce the variability of simulated values and over estimates because of it does not take into account the effect of pest and/or diseases that could affect the production.

The coefficient of Pearson (r), with a value of 0.80, is significant for p <0.001 for a number of samples of 32. The coefficient of determination R^2 explains 63% of the total variation. The Figure 1.1.1 shows the correlation of values for the simulated and observed data. The data show a

good correlation, as demonstrated by the parameters of the equation of the linear regression (y=bx+a) (b = 1.18, a = 1.2) (Fig. 1.1.1).

Taking into account the indices based on differences between expected and measured data there are relatively low values of RMSE (0.9 t ha^{-1}). This confirm the good estimate accuracy of the model, as further demonstrated by the GSD index value of 26%. The predictive efficiency of the model was firther confimed by the EF index value of 0.46. Thus, as regards the mean of estimate values are better than the mean of the observations. The value of CRM is equal to -0.14, this is indicative of the tendency of the model to overestimate the yields. Similarly MBE (0.49 t ha^{-1}) and MAE (0.63) indices confirm the predictive capability of the model and its tendency to overestimate. Finally, the index of agreement between simulated data and measured data (d-Index), showed a rather satisfactory value (0.81).

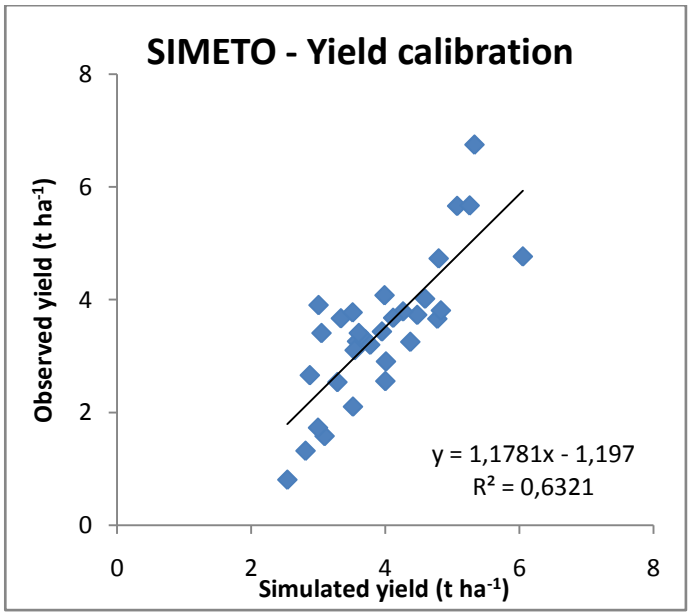

Figure 1.1.1 Calibration of yield for Simeto by comparing observed and simulated values of yield (t ha^{-1}) for Benatzu and Ussana experimental sites.

The results for anthesis calibration show a perfect correspondence between mean values of observed and simulated data, with a little lower standard deviations for simulated values.

Pearson's r value (r = 0.90) is significant for p <0.001. The coefficient of determination R^2 indicates that 80% of the total variation is explained by the model. The comparison between simulated data and observed data is shown in Figure 1.1.2. The equation of the linear regression simulated values vs. observed values indicates a good correlation as confirmed by the values of the slope (b = 1.1) and intercept (a = 10.0).

The RMSE index value is fairly low, moreover, the percentage very low of GSD (3%) indicates how the model works well in the simulation of phenological data. Also the high value of

EF index, equal to 0.80, confirms the predictive ability of the model for anthesis. The CRM index is at optimal value of 0.00. MBE index confirms the goodness of this estimate and a slight tendency to underestimate (-0.29). The d-Index, with a value of 0.93, confirms the good correlation between observed and simulated data.

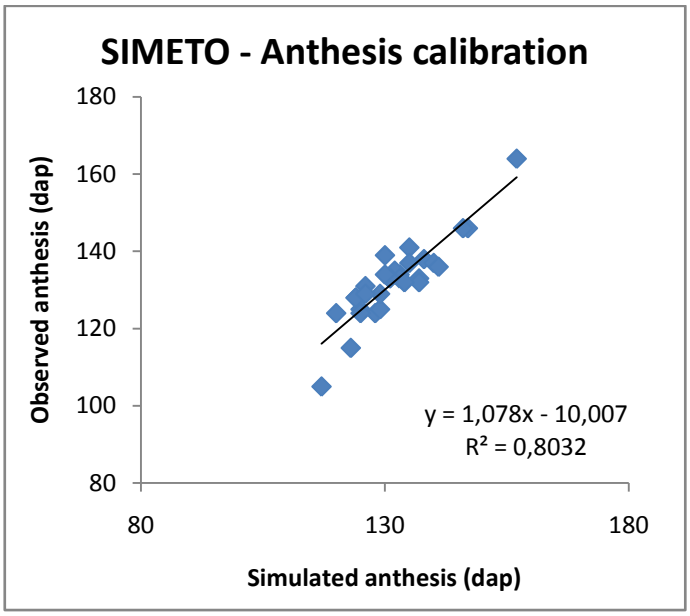

Figure 1.1.2 Calibration of anthesis for Simeto by comparing observed and simulated values of anthesis (dap) for Benatzu and Ussana experimental sites.

1.2 Calibration for Iride cultivar

As for Simeto, the model calibration for yield and anthesis for Iride cultivar was performed using data from Benatzu and Ussana experimental sites. In this case a dataset for the period 1997-2007 was used. Nineteen years of data were used for yield and sixteen years data were used for anthesis: one year was excluded for yield because of outlier and four years data for anthesis were not available.

The statistical results for yield and anthesis calibration are reported in Table 1.2.

Table 1.2 CERES-Wheat calibration results for Benatzu and Ussana experimental sites on grain yield (t ha^{-1}) and anthesis (dap=day after planting) for Iride cultivar. Mean, standard deviation (SD), minimum, and maximum observed and simulated values are reported. Statistical analysis results are also shown.

IRIDE		YIELD (t ha-1)		ANTHESIS (dap)	
		OBS	SIM	OBS	SIM
Mean	**Mean**	4.1	4.2	125	125
Standard deviation	**SD**	1.4	0.9	7.6	9.5
Minimum	**Min**	2.0	3.1	105	98
Maximum	**Max**	6.8	6.1	139	140
Number of samples	**N**	19		16	
Pearson coefficient	**r**	0.82***		0.94***	
Coefficient of determination	**R^2**	0.67		0.89	
Root Mean Square Error	**RMSE**	0.81		3.34	
General standard Deviation	**GSD (%)**	22		3	
Modeling Efficiency	**EF**	0.63		0.77	
Mean Bias Error	**MBE**	0.16		-0.63	
Mean Absolute Error	**MAE**	0.66		2.75	
Coefficient of Residual Mass	**CRM**	-0.04		0.00	
Index of agreement	**d-Index**	0.80		0.97	

*p≤0.02; **p≤0.01; ***p≤0.001; ns=not significant.

OBS, observed values; SIM, simulated values.

The results show that the mean value for simulated yields is very similar in respect to the correspondent mean value of observed yields for the period considered. The value of standard deviation for simulated yields is lower than the standard deviation value for observed yields. This is in according to the fact that the model in general tends to reduce the variability of simulated values.

The coefficient of Pearson (r), with a value of 0.82, is significant for p <0.001 and the coefficient of determination R^2 explains 67% of the total variation. Figure 1.2.1 shows the good

correlation between simulated and observed value for anthesis, as confirmed by the parameters of the equation of the linear regression (b = 1.21, a = 1.01) (Fig.1.2.1).

Also for the variety Iride as for Simeto, for the indices based on differences between expected data and measured data, a relatively low value of RMSE (0.8 t ha^{-1}) is found. The good predictive efficiency of the model is once more confirmed, as further demonstrated by the GSD index value, and EF index, representing respectively 22% and 0.63. Thus, as regards the data predicted by the model for the cultivar Iride, the mean of estimate values are better than the mean of the observations. The low negative value of CRM (-0.04) and the low positive value of MBE (0.16 t ha^{-1}) and MAE (0.66) confirm the good predictive capability of the model and its low tendency to overestimate. Finally, the index of agreement between simulated data and measured data (d-Index), showed a fairly satisfactory value (0.80).

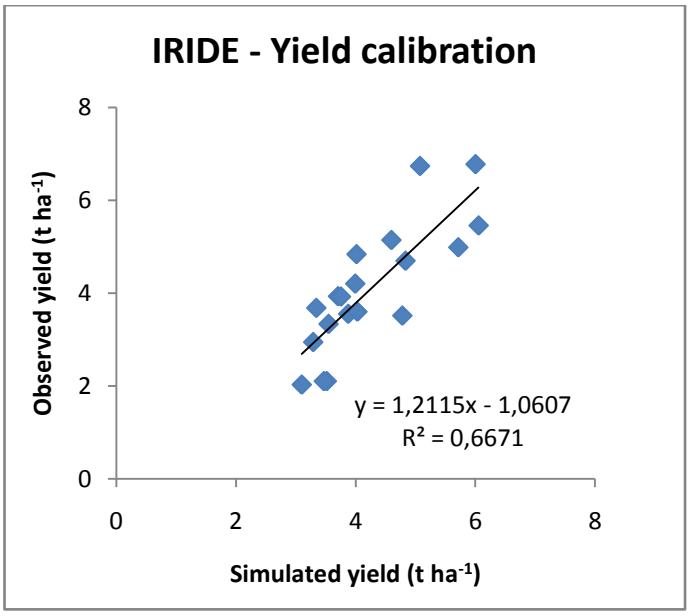

Figure 1.2.1 Calibration of yield for Iride by comparing observed and simulated values of yield (t ha^{-1}) for Benatzu and Ussana experimental sites.

The results for Iride cultivar regarding model anthesis calibration show a perfect correspondence between mean values of observed and simulated data, with a slightly higher standard deviations for simulated values.

The value of Pearson's r (r = 0.94) is significant for p <0.001. The coefficient of determination R^2 indicates that 89% of the total variation is explained by the model. The comparison between simulated data and observed data is shown in Figure 1.2.2. The equation of the linear regression simulated values vs. observed values indicates a good correlation as confirmed by the values of the slope (b = 0.7) and intercept (a = 32).

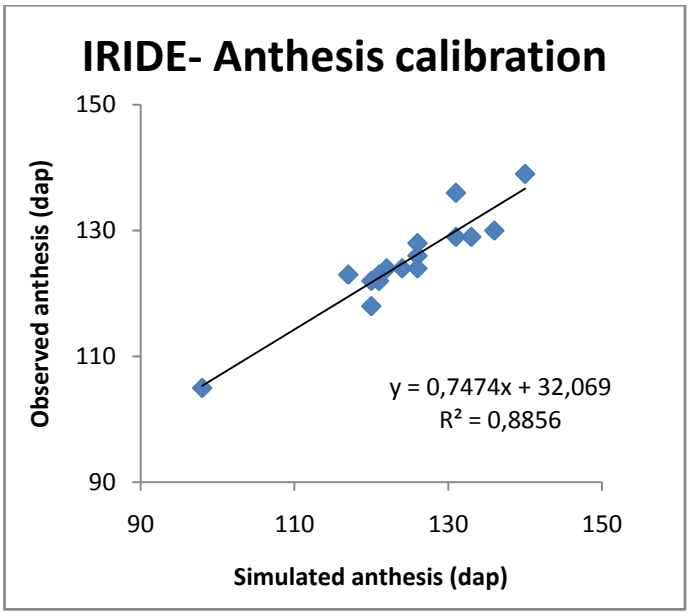

Figure 1.2.2 Calibration of anthesis for Iride by comparing observed and simulated values of anthesis (dap) for Benatzu and Ussana experimental sites.

1.3 Evaluation for Simeto cultivar

As previously explained, the model evaluation for Simeto cultivar was performed for Ottava and Santa Lucia experimental sites. The results of evaluation for yield and anthesis were examined using graphical and statistical analysis.

Ottava

In Table 1.3.1 the results of evaluation for Simeto variety are shown.

Table 1.3.1 CERES-Wheat evaluation results for Ottava experimental site on grain yield (t ha^{-1}) and anthesis (dap=day after planting) for Simeto cultivar. Mean, standard deviation (SD), minimum, and maximum observed and simulated values are reported. Statistical analysis results are also shown.

SIMETO		YIELD (t ha^{-1})		ANTHESIS (dap)	
		OBS	SIM	OBS	SIM
Mean	**Mean**	3.5	4.1	135	137
Standard deviation	**SD**	1.3	1.2	12	10
Minimum	**Min**	1.6	2.5	116	120
Maximum	**Max**	5.6	6.6	152	152
Number of samples	**N**	10		10	
Pearson coefficient	**r**	0.82**		0.93***	
Coefficient of determination	**R^2**	0.67		0.86	
Root Mean Square Error	**RMSE**	0.93		4.8	
General standard Deviation	**GSD (%)**	26		4	
Modeling Efficiency	**EF**	0.42		0.83	
Mean Bias Error	**MBE**	0.59		1.60	
Mean Absolute Error	**MAE**	0.79		4.00	
Coefficient of Residual Mass	**CRM**	-0.17		-0.01	
Index of agreement	**d-Index**	0.86		0.95	

*p≤0.02; **p≤0.01; ***p≤0.001; ns=not significant.

OBS, observed values; SIM, simulated values.

The results for Ottava site show still the tendency of the model to simulate higher values than actual. The mean value for simulated yields is higher than the correspondent mean value of observed yields for the period considered, and the value of standard deviation for simulated yields is a little bit lower than the standard deviation value for observed yields.

The r coefficient of Pearson, with a value of 0.82, is significant for $p < 0.01$. The coefficient of determination R^2 explains 67% of the total variation. The Figure 1.3.1 shows the

correlation of values for the simulated and observed data. The data show a good correlation, as demonstrated by the parameters of the equation of the linear regression (b = 0.85, a = 0.02).

As for all cases of calibration, also for Simeto evaluation there are relatively low values of RMSE (0.9 t ha^{-1}). So the general good accuracy of the model in predicting observed values is confirmed. This is also demonstrated by the GSD index value, and the EF index, representing respectively 26% and 0.42. Thus, as regards the data predicted by the model for the cultivar Simeto, the mean of estimate values are better than the mean of the observations. The CRM index, equal to -0.17, confirms the tendency of the model to overestimate yields. Similarly, the indices MBE (0.59 t ha^{-1}) and MAE (0.79) confirm the predictive capability of the model and its tendency to overestimate. Finally, the high value (0.86) of the d-Index proves the very good agreement between simulated and measured yield data.

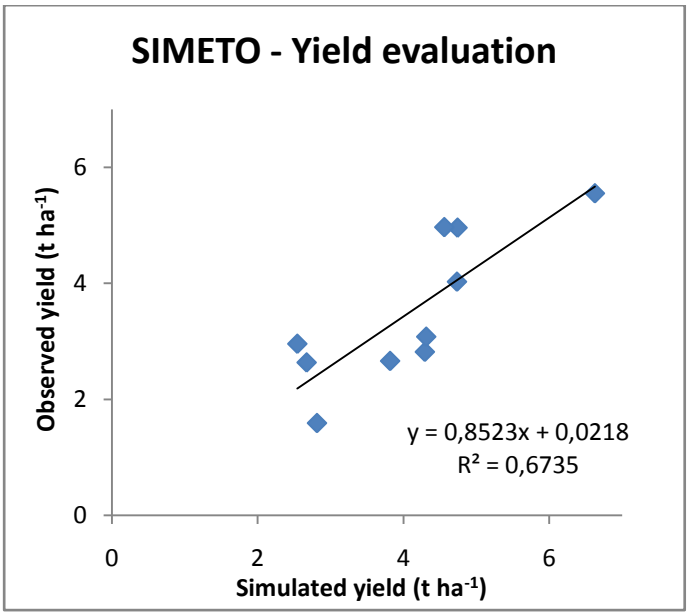

Figure 1.3.1 Evaluation of yield for Simeto by comparing observed and simulated values of yield (t ha^{-1}) for Ottava experimental site.

The results for anthesis model evaluation show a good correspondence between mean values of observed and simulated data, with a little bit lower standard deviations for simulated values.

The value of Pearson's r (r = 0.93) is significant for p <0.001. The coefficient of determination R^2 indicates that 86% of the total variation is explained by the model. The comparison between simulated data and observed data is shown in Figure 1.3.2. The equation of the linear regression simulated values vs. observed values indicates a good correlation as confirmed by the values of the slope (b = 1.1) and intercept (a = 20.0).

The RMSE index value is fairly low, moreover, the percentage very low of GSD (4%) indicates how the model works well in the simulation of phenological data. Also the high value of EF index, equal to 0.83, confirms the predictive ability of the model. The CRM index value (-0.01) and MBE index values (1.60) confirm the goodness of this estimate and a slightest tendency to underestimate. The d-Index, with a value of 0.93, confirms the good correlation between observed and simulated data.

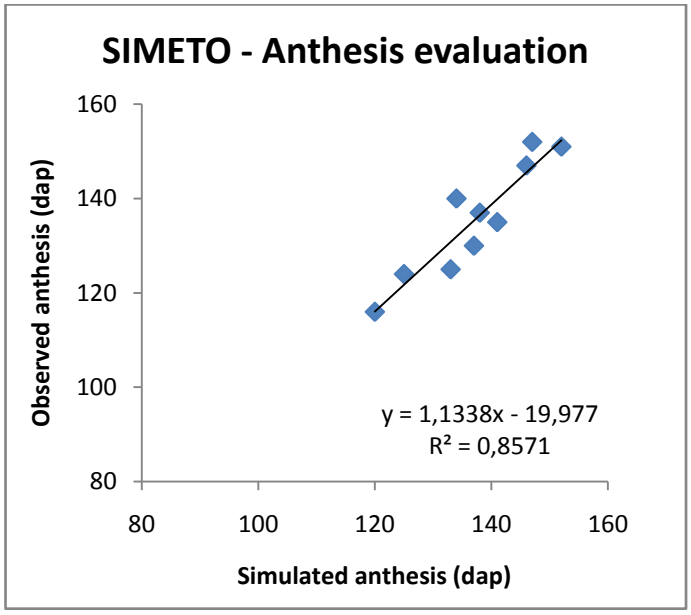

Figure 1.3.2 Evaluation of anthesis for Simeto by comparing observed and simulated values of anthesis (dap) for Ottava experimental site.

Santa Lucia:

The same analysis was performed also for Santa Lucia experimental site. Following are reported the statistical results (Table 1.3.2).

Table 1.3.2 CERES-Wheat evaluation results for Santa Lucia experimental site on grain yield (t ha^{-1}) and anthesis (dap=day after planting) for Simeto cultivar. Mean, standard deviation (SD), minimum, and maximum observed and simulated values are reported. Statistical analysis results are also shown.

SIMETO		YIELD (t ha^{-1})		ANTHESIS (dap)	
		OBS	SIM	OBS	SIM
Mean	**Mean**	5.1	4.1	126	128
Standard deviation	**SD**	1.6	1.3	19	20
Minimum	**Min**	2.2	1.9	87	83
Maximum	**Max**	7.3	6.1	146	147
Number of samples	**N**	14		9	
Pearson coefficient	**r**	0.80***		0.99***	
Coefficient of determination	**R^2**	0.64		0.97	
Root Mean Square Error	**RMSE**	1.42		4.19	
General standard Deviation	**GSD (%)**	28		3	
Modeling Efficiency	**EF**	0.18		0.94	
Mean Bias Error	**MBE**	-1.10		3.56	
Mean Absolute Error	**MAE**	1.10		2.44	
Coefficient of Residual Mass	**CRM**	0.21		-0.02	
Index of agreement	**d-Index**	0.79		0.99	

*p≤0.02; **p≤0.01; ***p≤0.001; ns=not significant.

OBS, observed values; SIM, simulated values.

The results for model evaluation at Santa Lucia experimental site show a difference tendency of the model that tends to underestimate the yield. Indeed the mean value for simulated yields is lower than the correspondent mean value of observed yields for the period considered. The value of standard deviation for simulated yields is lower than the standard deviation value for observed yields. This is probably due to the fact that, at Santa Lucia field, water tables frequently start to perch at about 70 cm soil depth and often reach the surface.

However, the r coefficient of Pearson, with a value of 0.80, is significant for $p < 0.001$ and the coefficient of determination R^2 explains 64% of the total variation. The Figure 1.3.3 shows the correlation of values for the simulated and observed data. The data show a high significant correlation, as also demonstrated by the parameters of the equation of the linear regression ($b = 0.97$, $a = 1.2$).

Taking into account the indices based on differences between expected data and measured data there is relatively low value of RMSE (1.4 t ha^{-1}). This, together with a low value of GSD (28%) confirms a good predictive efficiency of the model. The EF index, with a value of 0.18, is lower than the values of the others sites but having a positive value, indicates, however, that the mean of estimates values are better than the mean of the observations. The positive value of CRM and the negative value of MBE confirm the tendency of the model to underestimate the yields for this site. Finally, the index of agreement between simulated data and measured data (d-Index), showed a quite high value (0.79).

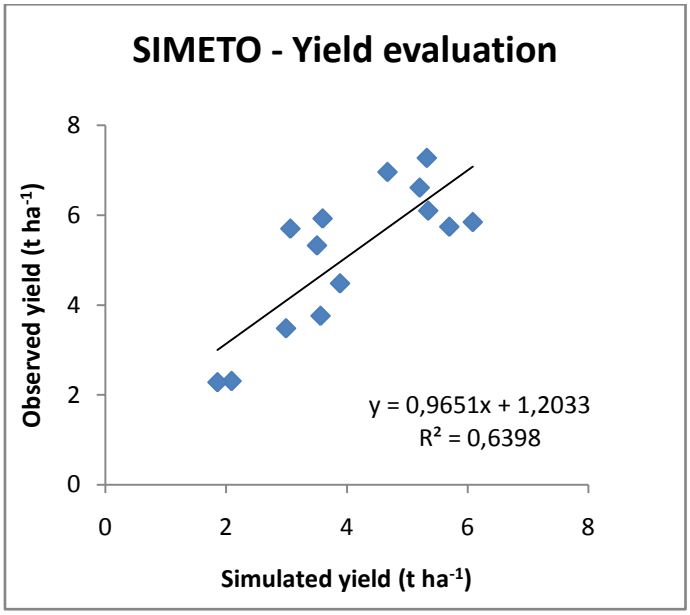

Figure 1.3.3 Evaluation of yield for Simeto by comparing observed and simulated values of yield (t ha^{-1}) for Santa Lucia experimental site.

The results for anthesis evaluation show a good correspondence between mean values of observed and simulated data.

The value of Pearson's r (r = 0.99) is significant for p <0.001. The coefficient of determination R^2 indicates that 97% of the total variation is explained by the model. The comparison between simulated data and observed data is shown in Figure 1.3.4.

The RMSE index value is fairly low, moreover, the percentage very low of GSD (3%) indicates how the model works well in the simulation of phenological data. Also the very high value of EF index, equal to 0.94, confirms the good predictive ability of the model. The values of CRM index (-0.02) and MBE index (3.56) confirm the goodness of the model to estimate anthesis, with a slight tendency to underestimate.

The d-Index value of 0.99, shows an almost perfect agreement between observed and simulated data.

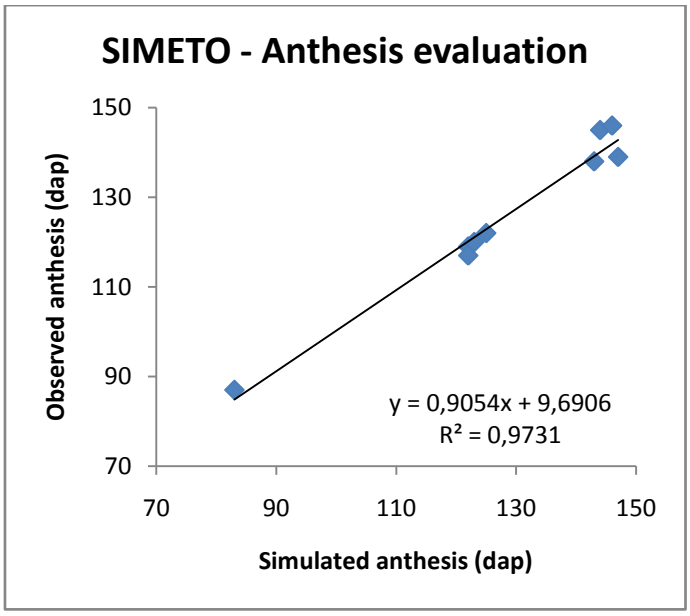

Figure 1.3.4 Evaluation of anthesis for Simeto by comparing observed and simulated values of anthesis (dap) for Santa Lucia experimental site.

1.4 Evaluation for Iride cultivar

The model evaluation for Iride cultivar was performed using experimental data of Ottava and Santa Lucia sites. The statistical results for yield and anthesis are listed in Table 1.4.1.

Ottava

Table 1.4.1 CERES-Wheat evaluation results for Ottava experimental site on grain yield (t ha^{-1}) and anthesis (dap=day after planting) for Iride cultivar. Mean, standard deviation (SD), minimum, and maximum observed and simulated values are reported. Statistical analysis results are also shown.

IRIDE		YIELD (t ha^{-1})		ANTHESIS (dap)	
		OBS	SIM	OBS	SIM
Mean	**Mean**	4.1	4.2	127	130
Standard deviation	**SD**	1.6	1.4	10	8
Minimum	**Min**	1.7	2.5	112	116
Maximum	**Max**	6.0	6.6	144	141
Number of samples	**N**	8		8	
Pearson coefficient	**r**	0.82*		0.91**	
Coefficient of determination	**R^2**	0.67		0.83	
Root Mean Square Error	**RMSE**	0.87		5.21	
General standard Deviation	**GSD (%)**	21		4	
Modeling Efficiency	**EF**	0.67		0.70	
Mean Bias Error	**MBE**	0.05		3.13	
Mean Absolute Error	**MAE**	0.70		4.32	
Coefficient of Residual Mass	**CRM**	-0.01		-0.02	
Index of agreement	**d-Index**	0.90		0.91	

*p≤0.02; **p≤0.01; ***p≤0.001; ns=not significant.

OBS, observed values; SIM, simulated values.

The results for Ottava experimental site confirm the good predictive ability of the model. Indeed, the mean value for simulated yields is very similar to the correspondent mean value of observed yields for the period considered. The value of standard deviation for simulated yields is a little bit lower than the standard deviation value for observed yields.

The r coefficient of Pearson, with a value of 0.82, is significant for p <0.02 and the coefficient of determination R^2 explains 67% of the total variation. The Figure 1.4.1 shows the correlation of values for the simulated and observed data. The data show a good correlation, as demonstrated by the parameters of the equation of the linear regression (b =0.93, a = 0.3).

Taking into account the indices based on differences between expected data and measured data there are relatively low values of RMSE (0.9 t ha^{-1}). This data confirm the good predictive

efficiency of the model, as further demonstrated by the GSD index value (21%), and EF index, (0.67). Thus, as regards the data predicted by the model for the cultivar Iride, the mean of estimate values are better than the mean of the observations. Among the indices based on simple differences, the value of CRM and MBE are close to zero, with respectively -0.01 and 0.05, that are indicatives of the good predictive capability of the model. Finally, the index of agreement between simulated data and measured data (d-Index), showed a high value (0.90).

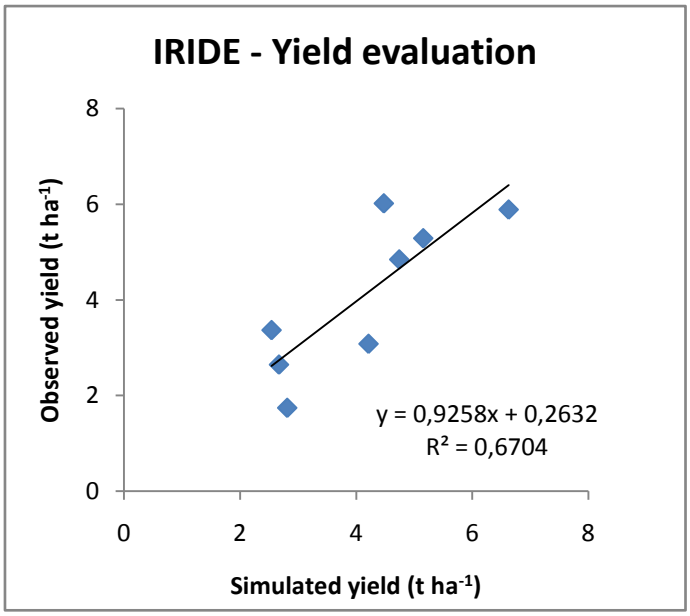

Figure 1.4.1 Evaluation of yield for Iride by comparing observed and simulated values of yield (t ha^{-1}) for Ottava experimental site.

The results for anthesis evaluation show that the mean values of observed data for anthesis is lower than the correspondent value for simulated data, with a little bit lower standard deviations for simulated values.

The value of Pearson coefficient r (r = 0.91) is significant for p <0.001, with a coefficient of determination R^2 of 0.83. The comparison between simulated data and observed data is shown in Figure 1.4.2. The equation of the linear regression simulated values vs. observed values indicates a good correlation as confirmed by the values of the slope (b = 1.2) and intercept (a = 24.9).

The RMSE index value is fairly low, moreover, the percentage very low of GSD (4%) indicates how the model works well in the simulation of phenological data. Also the high value of EF index, equal to 0.70, confirms the predictive ability of the model for anthesis. The slightly negative value of CRM index (-0.02) and the positive value of MBE index (3.13) confirm the goodness of this estimate and a slight tendency to underestimate. The d-Index, with a value of 0.91, confirms the good correlation between observed and simulated data.

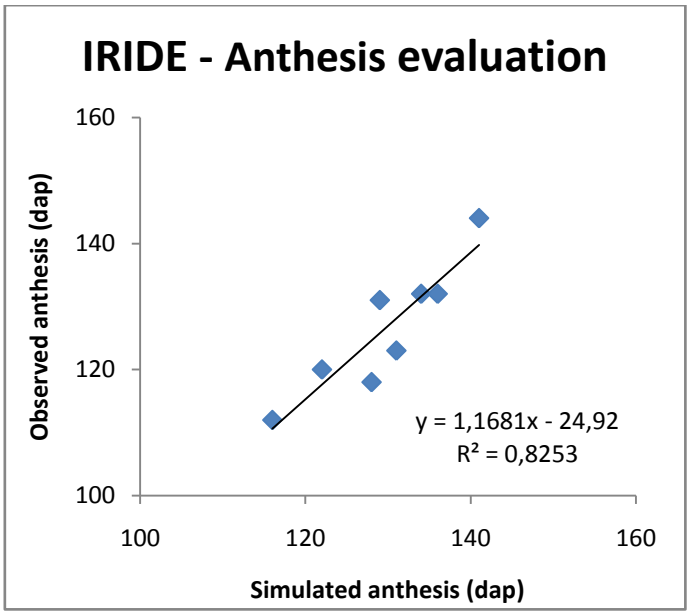

Figure 1.4.2 Evaluation of anthesis for Iride by comparing observed and simulated values of anthesis (dap) for Ottava experimental site.

Santa Lucia

In Table 1.4.2. the statistical results for Simeto at Santa Lucia site are shown.

Table 1.4.2 CERES-Wheat evaluation results for Santa Lucia experimental site on grain yield (t ha^{-1}) and anthesis (dap=day after planting) for Iride cultivar. Mean, standard deviation (SD), minimum, and maximum observed and simulated values are reported. Statistical analysis results are also shown.

IRIDE		YIELD (t ha^{-1})		ANTHESIS (dap)	
		OBS	SIM	OBS	SIM
Mean	**Mean**	6.4	4.9	122	123
Standard deviation	**SD**	1.9	1.5	14	19
Minimum	**Min**	2.3	2.0	95	81
Maximum	**Max**	8.8	6.4	141	143
Number of samples	**N**	10		9	
Pearson coefficient	**R**	0.83**		0.97***	
Coefficient of determination	**R^2**	0.68		0.93	
Root Mean Square Error	**RMSE**	1.8		6.02	
General standard Deviation	**GSD (%)**	28		5	
Modeling Efficiency	**EF**	0.04		0.80	
Mean Bias Error	**MBE**	-1.48		1.11	
Mean Absolute Error	**MAE**	1.55		4.44	
Coefficient of Residual Mass	**CRM**	0.23		-0.01	
Index of agreement	**d-Index**	0.76		0.96	

*p≤0.02; **p≤0.01; ***p≤0.001; ns=not significant.

OBS, observed values; SIM, simulated values.

The results shows that the mean value for simulated yields is higher than the correspondent mean value of observed yields for the period considered. As observed for Simeto results for Santa Lucia site, this can be justified considering that at Santa Lucia field water tables frequently start to perch at about 70 cm soil depth and often reach the surface. The value of standard deviation for simulated yields is lower than the standard deviation value for observed yields.

However, the r coefficient of Pearson, with a value of 0.83, is significant for $p < 0.01$ and the coefficient of determination R^2 explains 68% of the total variation. The Figure 1.4.3 shows the correlation of values for the simulated and observed data. The data show a good correlation, according to the parameters of the linear regression equation (b = 1.05, a = 1.2).

Taking into account the indices based on differences between expected data and measured data there are relatively low values of RMSE (1.9 t ha^{-1}). This data confirm the quite good predictive efficiency of the model, as further demonstrated by the GSD index value (28%). The very low value of EF index is due at the big difference between observed and simulated values. Indeed the model tend to underestimate, as confirmed by the values of CRM (0.23) and MBE (-

1.48) indices. Finally, the index of agreement between simulated data and measured data (d-Index), showed a rather satisfactory value (0.76).

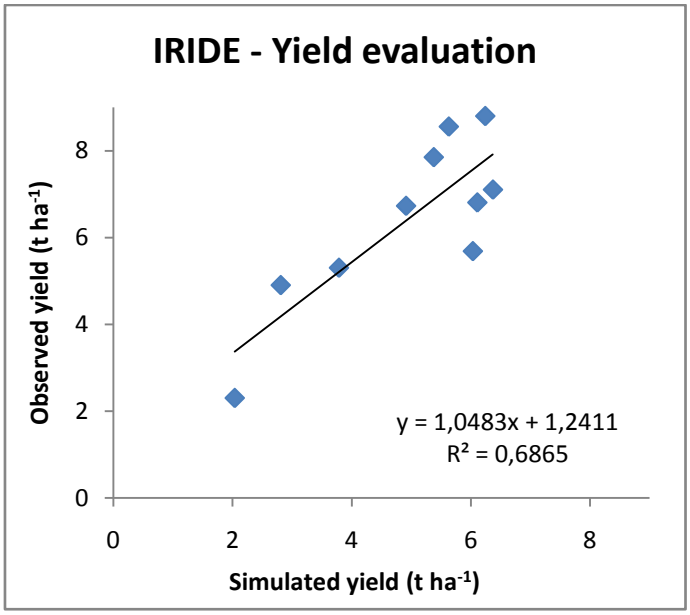

Figure 1.4.3 Evaluation of yield for Iride by comparing observed and simulated values of yield (t ha^{-1}) for Santa Lucia experimental site.

The results for anthesis evaluation show a good correspondence between mean values of observed and simulated data, with a little bit lower standard deviations for observed values.

The value of Pearson's r (r = 0.97) is significant for p <0.001. The coefficient of determination R^2 indicates that 93% of the total variation is explained by the model. The comparison between simulated data and observed data is shown in the graph of Figure 1.4.4. The equation of the linear regression simulated values vs. observed values indicates a good correlation as confirmed by the values of the slope (b = 0.7) and intercept (a = 31.4).

The RMSE index value is fairly low, moreover, the percentage low of GSD (5%) indicates how the model works well in the simulation of phenological data. Also the high value of EF index, equal to 0.80, confirms the predictive ability of the model for anthesis. The values of CRM (-0.01) and MBE (1.11) indices confirm the goodness of this estimate and a slight tendency to overestimate. The d-Index, with a value of 0.96 confirms the good correlation between observed and simulated data.

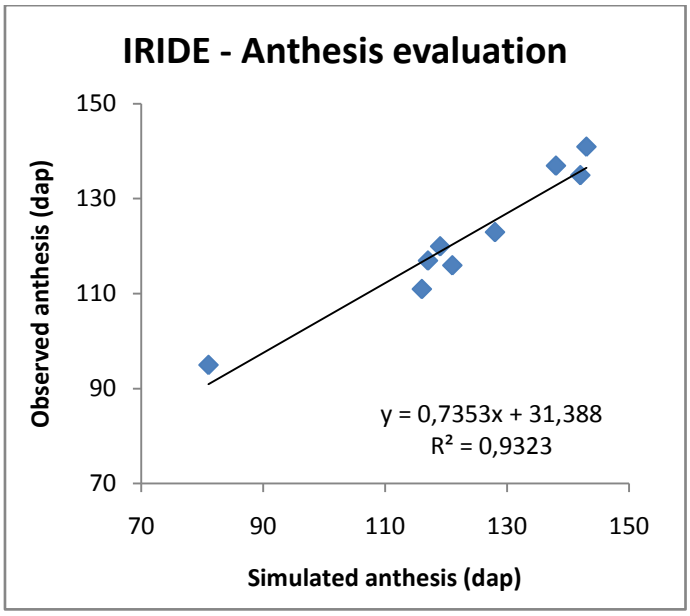

Figure 1.4.4 Evaluation of anthesis for Iride by comparing observed and simulated values of anthesis (dap) for Santa Lucia experimental site.

1.5 CERES-Wheat model validation

The results obtained for model calibration and evaluation are successful for anthesis for both cultivar at all experimental sites, as show by several statistical indices considered. So, the model can be considerated validated for anthesis.

The results for yield are also successful for both cultivar for Benatzu, Ussana and Ottava site, despite a general tendency of the model to overestimate the yield. On the contrary for Santa Lucia experimental site, the model tends to underestimate the yield. This is probably due, as already discussed, to the particular soil characteristics, that the model cannot reproduce. Anyway, despite the underestimation, the model is able to reproduce the observed trend in yield also for this site, and can be considerated validated also for yield simulation.

2. CLIMATE CHANGE SCENARIOS

In this section, results on the analysis performed on climate data and scenarios are described.

First, changes in maximum and minimum temperature (TEMP), solar radiation (SRAD) and daily precipitation (PREC) variables are shown. The future climatic datasets were obtained by projections of the three GCMs (Hadley, NCAR and ECHAM) for three climate change scenarios (low, middle and high) for three future periods (2025, 2050 and 2075).

Than for each of the experimental stations (Ussana/Benatzu, Ottava and Santa Lucia), and for the three future periods, monthly mean changes in PREC (mm), in mean TEMP (°C) and in SRAD (MJ m^{-2}) were analysed.

Results projected for each variables by the three GCMs considering the extremes (low and high) climate change scenarios are shown (the middle scenario results were not reported to improve the understanding of the graphs).

Percentage differences in annual and quarterly mean TEMP, SRAD and PREC for all three GCM, and for the three future periods considered, in comparison to current climate, were computed.

2.1 Ussana site

Precipitation

Figures 2.1.1 *a*, *b* and *c* show the results for projected precipitation for Ussana site.

A decrease in rainfall already for 2025 for the simulations with all three GCMs for all months was observed. As expected the GCMs simulations with the most pessimistic climate scenarios (high), produce a decrease almost double than those with the optimistic climate scenario (low).

The changes in precipitation projected by ECHAM and Hadley GCMs show more or less the same trend, but ECHAM simulates greater reductions than Hadley for the winter, spring and autumn monthly rainfall. The Hadley simulations show more sensitive decreases than ECHAM in precipitation only for the summer months (June, July and August). However, the rainfall for the summer months are not relevant for the wheat crop. In fact, in our environment, the grain filling phase is ended by the end of June, and generally, wheat is harvested in the period between late June to early July. So, the most effective rainfall for wheat crop are those fallen during the period from October to April-May.

In relation to this, it is interesting to consider that the NCAR projections show a different trend, with a slight increase in precipitation respect to actual values for March and November and no changes in precipitation for April, with both high and low climate change scenarios. This is very important for wheat crop that can take advantage of increases in precipitation during these months. Moreover, NCAR estimates higher reduction then Hadley and ECHAM in the expected rainfall for August, but, it is not relevant for wheat crop.

In general the GCMs simulations with low climate scenario estimate very low decreases in rainfall in particular for the winter months which are those most important for wheat crop.

The changes in precipitation projected by the GCMs for 2050 show the same trend of 2025, with decreases more marked than the 2025 in all cases. ECHAM simulations show higher reductions than Hadley simulations, except for summer months, where Hadley projections are more pessimistic. The increases in NCAR projections for March and November are double than the increases expected for 2025.

For 2075 projected changes in precipitations confirm the trends observed in the previous climatic periods. The highest decreases are projected by ECHAM with high climate scenario for autumn, winter and spring months. Increases, which are limited only to March and November with the NCAR, are more than double respect those projected for 2050.

Precipitation amount (mm) for present period:												
Year	*Jan*	*Feb*	*Mar*	*Apr*	*May*	*Jun*	*Jul*	*Aug*	*Sep*	*Oct*	*Nov*	*Dec*
427.8	**40.9**	**47.4**	**40.2**	**44.3**	**25.3**	**12.5**	**3.9**	**7.7**	**33.3**	**46.9**	**66.3**	**58.9**

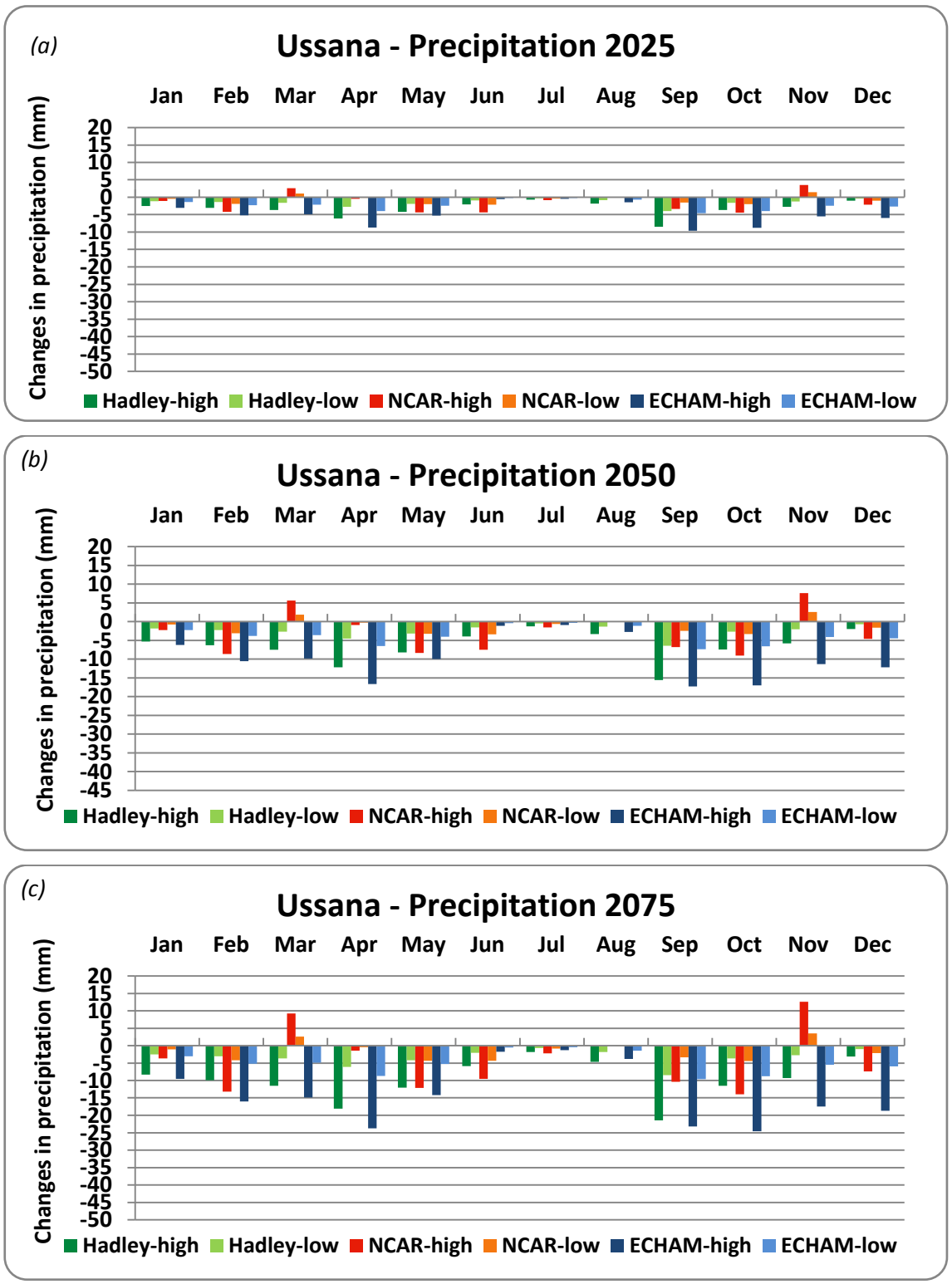

Figure 2.1.1 a, b, c. Monthly precipitation changes from present to future periods (2025, 2050, 2075), with three different GCMs and two extremes climate scenarios (high and low). In the table above the graphs reference values of annual and monthly precipitation amount for the current period are shown.

The results considering the middle scenario are summarized in Table 2.1.1.

The highest decreases in terms of annual changes (%) from actual values (now) are projected by ECHAM, and the lowest by NCAR.

Analysing the quarters that are most important for the crop development and growth (*JFM* and *AMJ*), this trend is confirmed. It is observed that for both the greater decreases in precipitation are projected by ECHAM. On the contrary the lower changes for these periods are projected by NCAR.

Table 2.1.1 Ussana – Annual and quarterly summarized changes in precipitation (%) from present to future periods with three GCMs and middle climate scenario.

	now (mm)	2025			2050			2075		
		ECHAM	HADLEY	NCAR	ECHAM	HADLEY	NCAR	ECHAM	HADLEY	NCAR
Year	**427.8**	-13.0	-10.1	-7.9	-24.7	-19.5	-15.5	-35.2	-28.3	-22.9
Jan-Feb-Mar	**147.3**	-9.0	-3.6	-4.2	-17.6	-7.2	-8.4	-25.8	-10.9	-12.5
Apr-May-Jun	**109.8**	-14.7	-10.1	-6.6	-27.7	-19.5	-12.9	-39.3	-28.4	-19.0
Jul-Aug-Sep	**24.0**	-11.1	-15.3	-16.5	-21.1	-28.7	-30.7	-29.5	-40.6	-42.9
Oct-Nov-Dec	**148.2**	-15.9	-10.1	-4.1	-29.7	-19.6	-8.1	-42.0	-28.4	-12.3

Temperature

In Figures 2.1.2 *a*, *b*, and *c* are shown the results for changes in monthly mean temperature projected by three GCMs and low and high climate scenarios for Ussana site.

The projections for 2025 show a similar pattern with all GCMs, both for low and high climate scenarios. However, the changes projected by ECHAM are a little bit lower than the others GCMs. For low climate scenarios, the monthly mean projection are less than 0.5°C for all GCMs. In high climate scenarios the estimated increase in mean temperature is about 1°C for all GCMs, and it reache about 1.3°C for August and September.

For 2050 the projected increases in monthly mean temperature vary from a value lower than 1°C with low emission scenario, for all GCMs, to 2°C with high climate scenario for Hadley and NCAR simulations, while the changes projected by ECHAM are a little bit lower in particular for the summer months.

For the period 2075 the projected increases range from 1°C (all GCMs with low climate scenario) to less than 3.5°C projected by NCAR and about 3.0°C by Hadley and ECHAM.

The higher increases are projected for the winter and spring months, i.e. during the development and growth period for wheat, but the increased temperature values for winter and spring months are generally about 3.0°C.

In Table 2.1.2 the summarized results for annual and quarterly changes in temperature projected by the three GCMs with the middle climate scenarios are shown.

The higher increases in annual temperature are projected by NCAR for all future periods.

Considering winter months the increases are similar for all GCMs, and considering the spring months the higher increases are projected by NCAR.

Table 2.1.2 Ussana – Annual and quarterly summarized changes in temperature (°C) from present to future periods with three GCMs and middle climate scenario.

	now (°C)	2025			2050			2075		
		ECHAM	HADLEY	NCAR	ECHAM	HADLEY	NCAR	ECHAM	HADLEY	NCAR
Year	16.9	0.6	0.7	0.7	1.3	1.4	1.4	2.0	2.1	2.2
Jan-Feb-Mar	10.3	0.6	0.6	0.6	1.2	1.2	1.3	1.9	1.8	1.9
Apr-May-Jun	14.6	0.5	0.5	0.6	1.1	1.1	1.3	1.6	1.7	2.0
Jul-Aug-Sep	24.2	0.7	0.8	0.8	1.4	1.7	1.7	2.1	2.6	2.6
Oct-Nov-Dec	18.4	0.7	0.8	0.8	1.5	1.6	1.6	2.3	2.4	2.4

Mean temperature (°C) for present period:												
Year	*Jan*	*Feb*	*Mar*	*Apr*	*May*	*Jun*	*Jul*	*Aug*	*Sep*	*Oct*	*Nov*	*Dec*
16.9	**9.9**	**10.0**	**11.7**	**13.8**	**18.2**	**22.2**	**24.8**	**25.3**	**22.7**	**18.8**	**14.0**	**11.1**

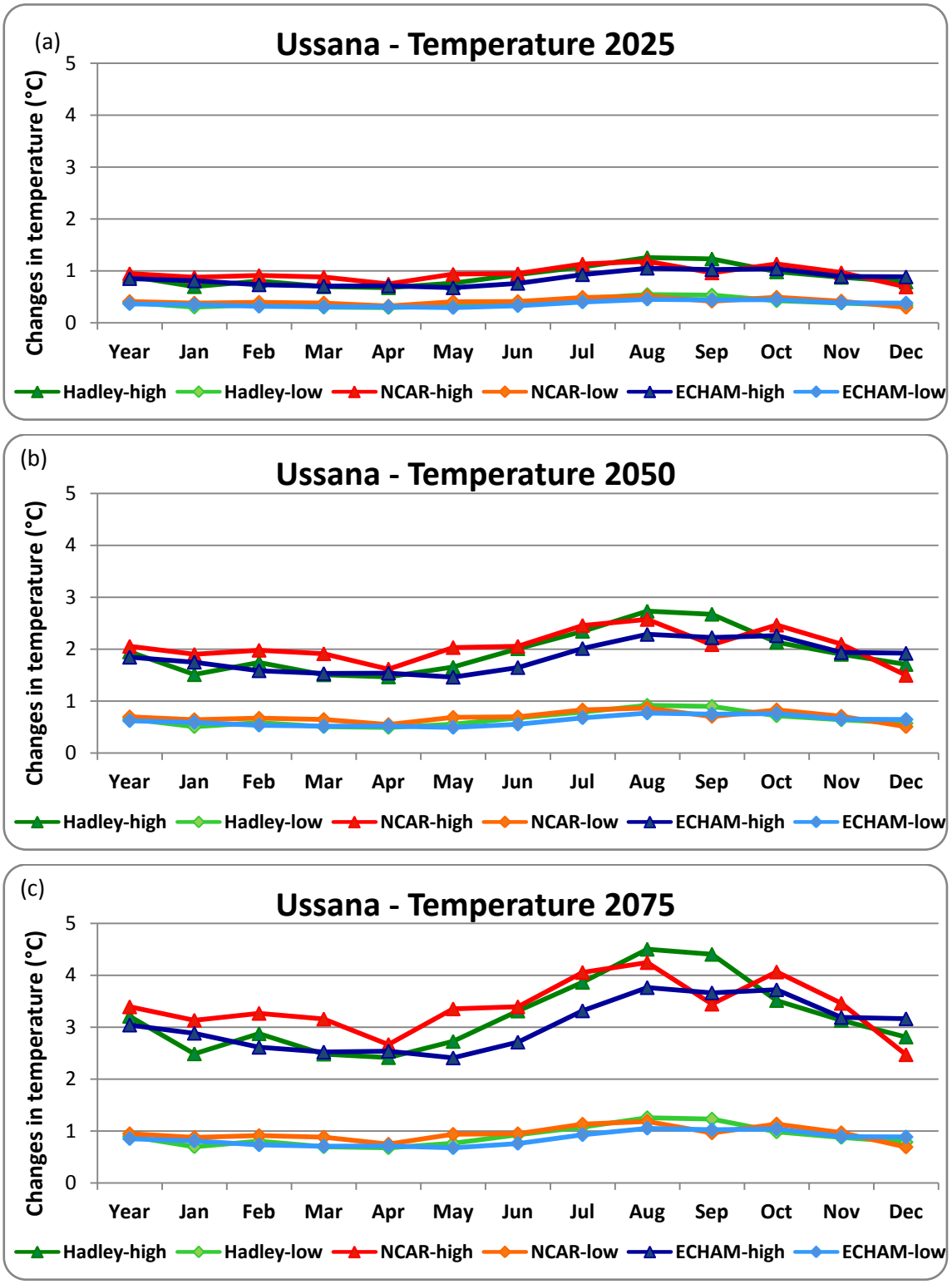

Figure 2.1.2 a, b, c. Annual and monthly temperature changes (°C) from present to future periods (2025, 2050, 2075), with three different GCMs and two extremes climate scenarios (high and low). In the table above the graphs reference values of annual and monthly mean values of temperature for current period are shown.

Solar radiation

In the Figures 2.1.3 *a, b,* and *c* the results for changes in monthly solar radiation amount (MJ m^{-2}) projected by three GCMs and low and high climate scenarios for Ussana site are shown.

Projections obtained by the three GCMs in increases for solar radiation are very different.

The changes projected by NCAR are greater than the changes projected by Hadley and ECHAM for January and February, in all three future periods considered, both with low and high climate scenarios. For the months from March to September Hadley provides the highest increases, whereas the highest increases for October and December are given by ECHAM. However, solar radiation availability is particularly important for crop growth during the first six months of the year.

Table 2.1.3 shows the summarized results for annual and quarterly changes (%) in solar radiation amount projected by the three GCMs with the middle climate scenarios respect to actual values. The higher increases in annual solar radiation are projected by Hadley for all future periods. Also considering winter (*JFM*) and spring (*AMJ*) months the higher increases are projected by Hadley for all future periods.

Table 2.1.3 Ussana – Annual and quarterly summarized changes in solar radiation (%) from present to future periods with three GCMs and middle climate scenario.

	now	2025			2050			2075		
	(MJ·m^{-2})	ECHAM	HADLEY	NCAR	ECHAM	HADLEY	NCAR	ECHAM	HADLEY	NCAR
Year	**5216.2**	0.7	1.1	0.7	1.3	2.3	1.4	2.1	3.6	2.2
Jan-Feb-Mar	**556.2**	1.3	0.3	1.1	2.6	0.6	2.3	4.0	1.0	3.5
Apr-May-Jun	**1573.8**	0.8	1.2	0.5	1.6	2.5	1.1	2.5	3.9	1.7
Jul-Aug-Sep	**2125.4**	0.3	1.6	0.6	0.6	3.2	1.3	0.9	4.9	1.9
Oct-Nov-Dec	**973.2**	0.9	0.9	0.8	1.8	1.9	1.7	2.8	2.9	2.5

Solar Radiation (MJ m^{-2}) amount for present period:												
Year	*Jan*	*Feb*	*Mar*	*Apr*	*May*	*Jun*	*Jul*	*Aug*	*Sep*	*Oct*	*Nov*	*Dec*
5216	**174**	**231**	**395**	**509**	**670**	**735**	**744**	**646**	**458**	**318**	**187**	**151**

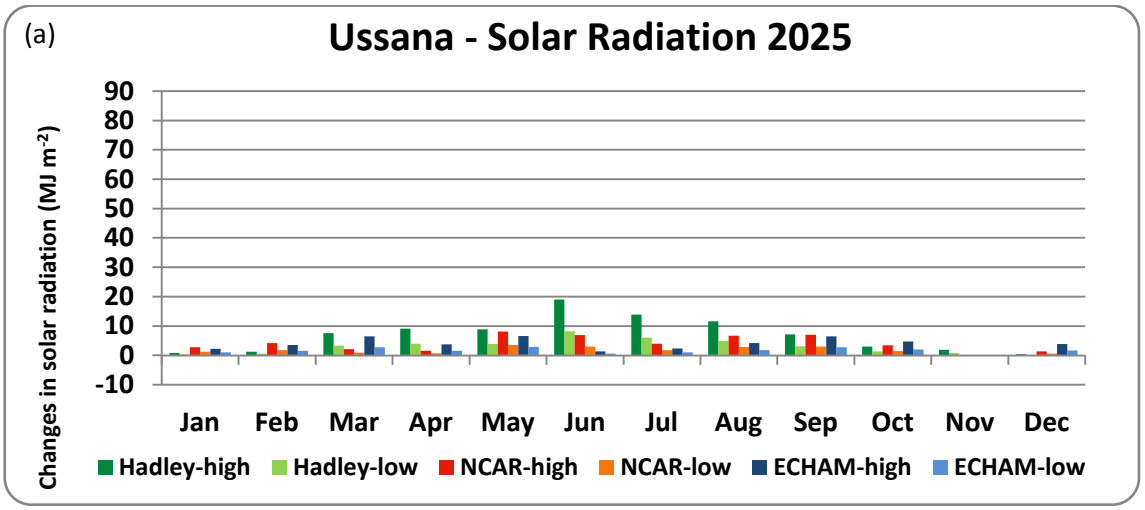

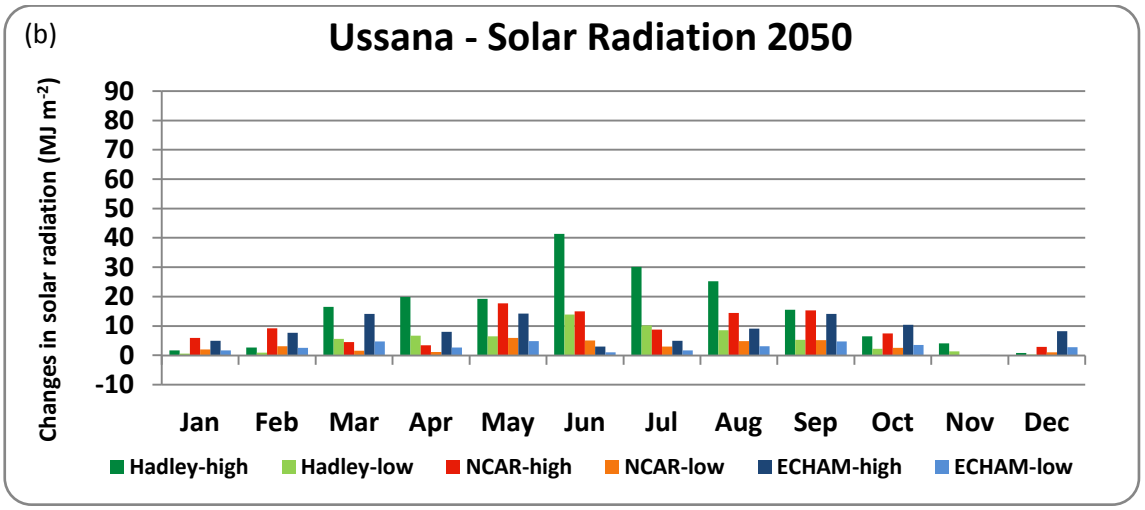

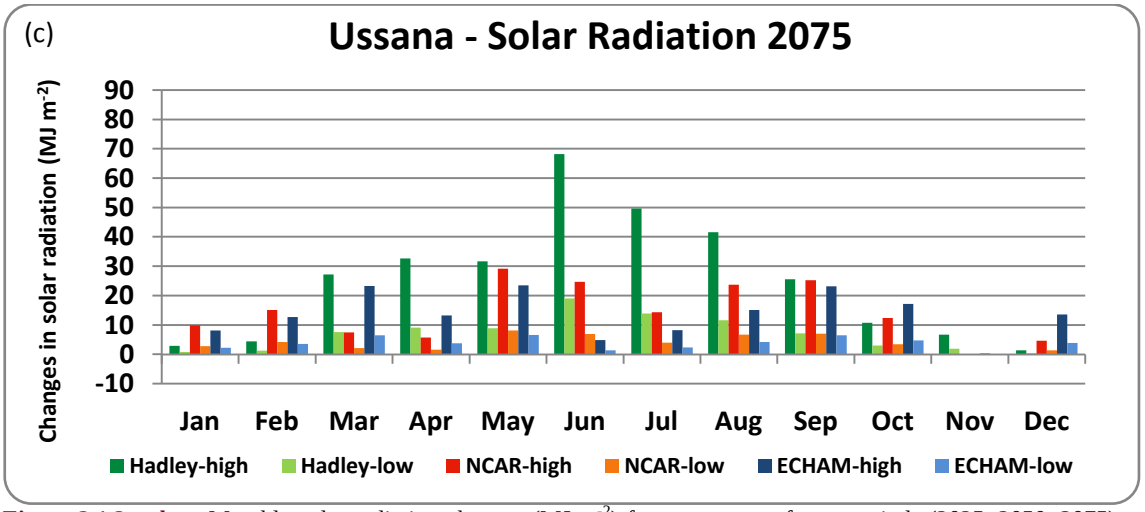

Figure 2.1.3 a, b, c. Monthly solar radiation changes (MJ m^{-2}) from present to future periods (2025, 2050, 2075), with three different GCMs and two extremes climate scenarios (high and low). In the table above the graphs reference values of annual and monthly mean values of temperature for present period are shown.

2.2 Ottava site

Precipitation

Figures 2.2.1 *a, b* and *c* show the results for projected changes in precipitation for Ottava site.

It is possible to observe a decrease in rainfall already for 2025 for the simulations with all three GCMs for all months. The GCMs simulations with the most pessimistic climate scenarios (high) show decreases more than double respect those projected with the optimistic climate scenario (low).

The larger decreases in precipitation are those designed by ECHAM for all months in all three future periods (2025, 2050, 2075); only for the months from May to September, the largest decreases in precipitation are projected by Hadley. NCAR provides rather significant increases in precipitation for March, August and November. This could have positive effects on the crop growth.

The precipitation changes projected for Ottava are also a little bit lower than those projected for Ussana site.

The summarized results considering the middle climate scenario are shown in Table 2.2.1.

The higher decreases in terms of annual changes (%) from actual values (now) are projected by ECHAM and the lower by NCAR for all future periods.

Considering further the quarters that are most important for the crop development and growth (*JFM* and *AMJ*), it is possible to observe that for both cases the greater decreases in precipitation are projected by ECHAM. On the contrary the lower changes for all future periods for *JFM* are those projected by Hadley and for *AMJ* are those projected by NCAR.

Table 2.2.1 Ottava – Annual and quarterly summarized changes in precipitation (%) from present to future periods with three GCMs and middle climate scenario.

	now (mm)	2025			2050			2075		
		ECHAM	HADLEY	NCAR	ECHAM	HADLEY	NCAR	ECHAM	HADLEY	NCAR
Year	555.9	-12.5	-10.6	-6.5	-23.8	-20.3	-12.7	-34.0	-29.5	-19.0
Jan-Feb-Mar	165.3	-8.4	-2.4	-3.4	-16.5	-4.9	-6.9	-24.2	-7.3	-10.3
Apr-May-Jun	133.9	-13.7	-10.9	-3.6	-26.0	-20.9	-7.3	-37.1	-30.3	-11.0
Jul-Aug-Sep	40.0	-13.3	-17.5	-14.0	-23.9	-32.4	-26.4	-32.4	-45.1	-37.7
Oct-Nov-Dec	219.1	-13.8	-9.7	-4.8	-26.1	-18.8	-9.5	-37.3	-27.4	-14.3

Precipitation amount (mm) for present period:												
Year	*Jan*	*Feb*	*Mar*	*Apr*	*May*	*Jun*	*Jul*	*Aug*	*Sep*	*Oct*	*Nov*	*Dec*
556	**49.9**	**44.0**	**44.3**	**50.7**	**38.8**	**17.5**	**6.1**	**16.5**	**41.3**	**86.3**	**89.0**	**71.4**

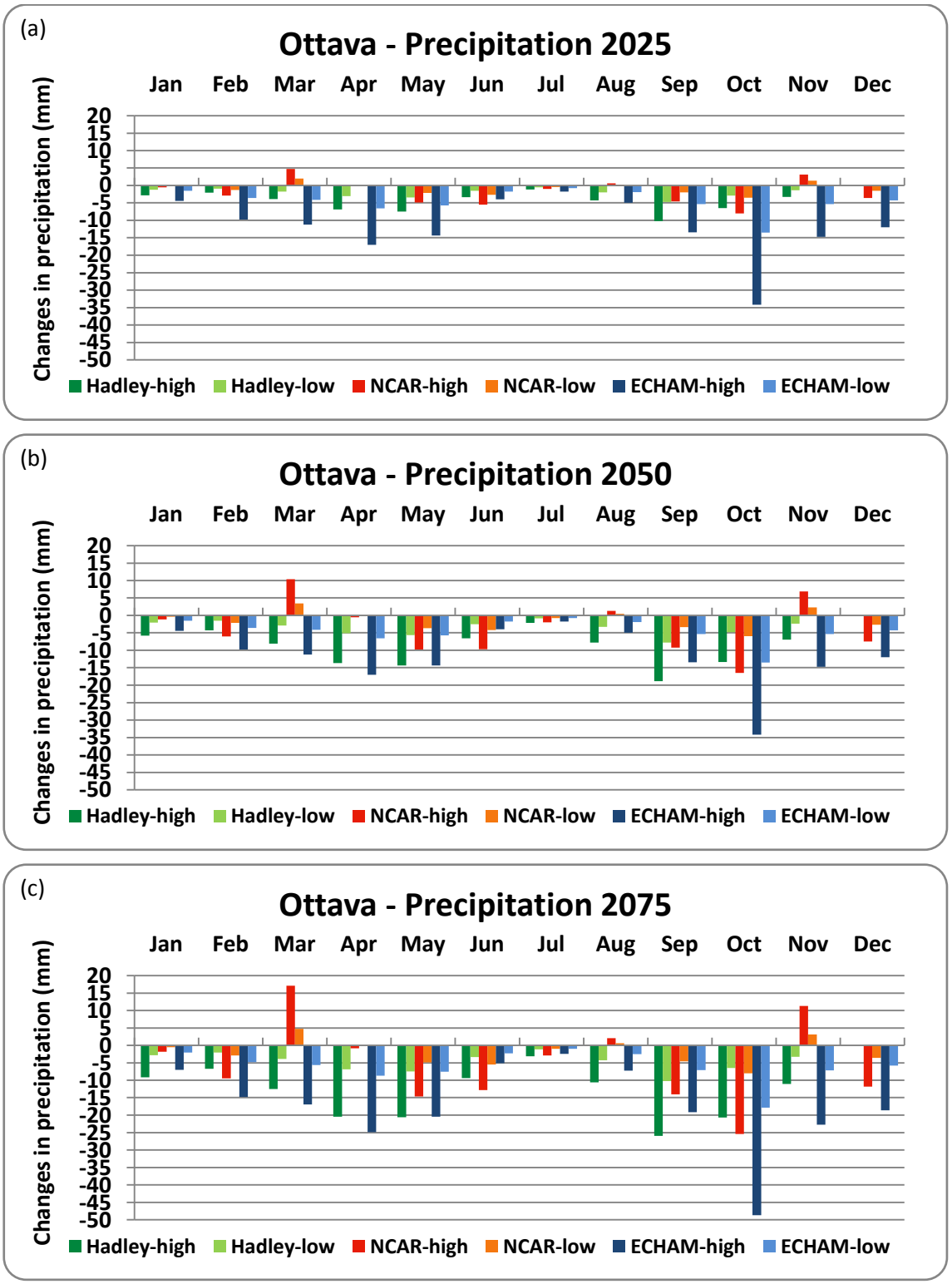

Figure 2.2.1 a, b, c. Precipitation changes from present to future periods (2025, 2050, 2075), with three different GCMs and two extremes climate scenarios (high and low). In the table above the graphs reference values of annual and monthly precipitation amount for present period are shown.

Temperature

In Figures 2.2.2 *a*, *b*, and *c* the results for changes in monthly mean temperature projected by three GCMs and low and high climate scenarios for Ottava site are shown.

For 2025 a similar projection with all GCM both for low and high climate scenarios isobtained. However, the changes projected by ECHAM are a little bit lower than the changes projected by NCAR and Hadley. The monthly mean projection for low climate scenarios are less than 0.5°C for all GCMs. With high climate scenario the estimated increase in monthly mean temperature is about 1°C for all GCMs, and it could reach about 1.4°C for August with Hadley, that estimates the higher increases for the summer months.

The projected increases in monthly mean temperature for 2050 are lower than 1°C with low emission scenario for all GCMs and could reach 3°C with high climate change scenario with Hadley for August, while the changes projected by ECHAM are the lower, in particular for the summer months. However, the mean annual change projected for 2050 is about 2°C for all GCMs with high climate change scenario.

For the period 2075 the projected increases estimated by all GCMs with low climate change scenario are very similar (≈1°C), while with the high climate change scenario the changes in monthly mean temperature are quite different among the GCMs. ECHAM provides smaller increases than Hadley and NCAR, and Hadley provides the higher increases especially for the summer months, reaching +5°C for August. However, in average the projected mean annual increase for 2075 is less than 3.5°C.

The Table 2.2.2 shows the summarized results for annual and quarterly changes in tempeature projected by the three GCMs with the middle climate scenarios.The annual changes in mean temperature are very similar among the three GCM, with a little bit higher increases projected by Hadley for 2050 and 2075. No particular differences are in winter and spring monthly temperatures for all GCMs, but for the summer months the differences between the GCMs are more evident.

Table 2.2.2 Ottava – Annual and quarterly summarized changes in temperature (°C) from present to future periods with three GCMs and middle climate scenario.

	now (°C)	2025			2050			2075		
		ECHAM	HADLEY	NCAR	ECHAM	HADLEY	NCAR	ECHAM	HADLEY	NCAR
Year	**16.2**	0.6	0.7	0.7	1.3	1.5	1.4	2.0	2.3	2.2
Jan-Feb-Mar	**10.1**	0.6	0.6	0.6	1.2	1.2	1.2	1.9	1.9	1.9
Apr-May-Jun	**13.9**	0.5	0.6	0.6	1.0	1.2	1.2	1.6	1.8	1.9
Jul-Aug-Sep	**23.0**	0.7	0.9	0.8	1.4	1.9	1.6	2.2	2.9	2.5
Oct-Nov-Dec	**17.7**	0.7	0.8	0.8	1.5	1.6	1.6	2.3	2.5	2.4

Mean temperature (°C) for present period:												
Year	*Jan*	*Feb*	*Mar*	*Apr*	*May*	*Jun*	*Jul*	*Aug*	*Sep*	*Oct*	*Nov*	*Dec*
16.2	**9.7**	**9.7**	**11.2**	**13.3**	**17.1**	**20.9**	**23.8**	**24.2**	**21.3**	**18.3**	**13.7**	**10.9**

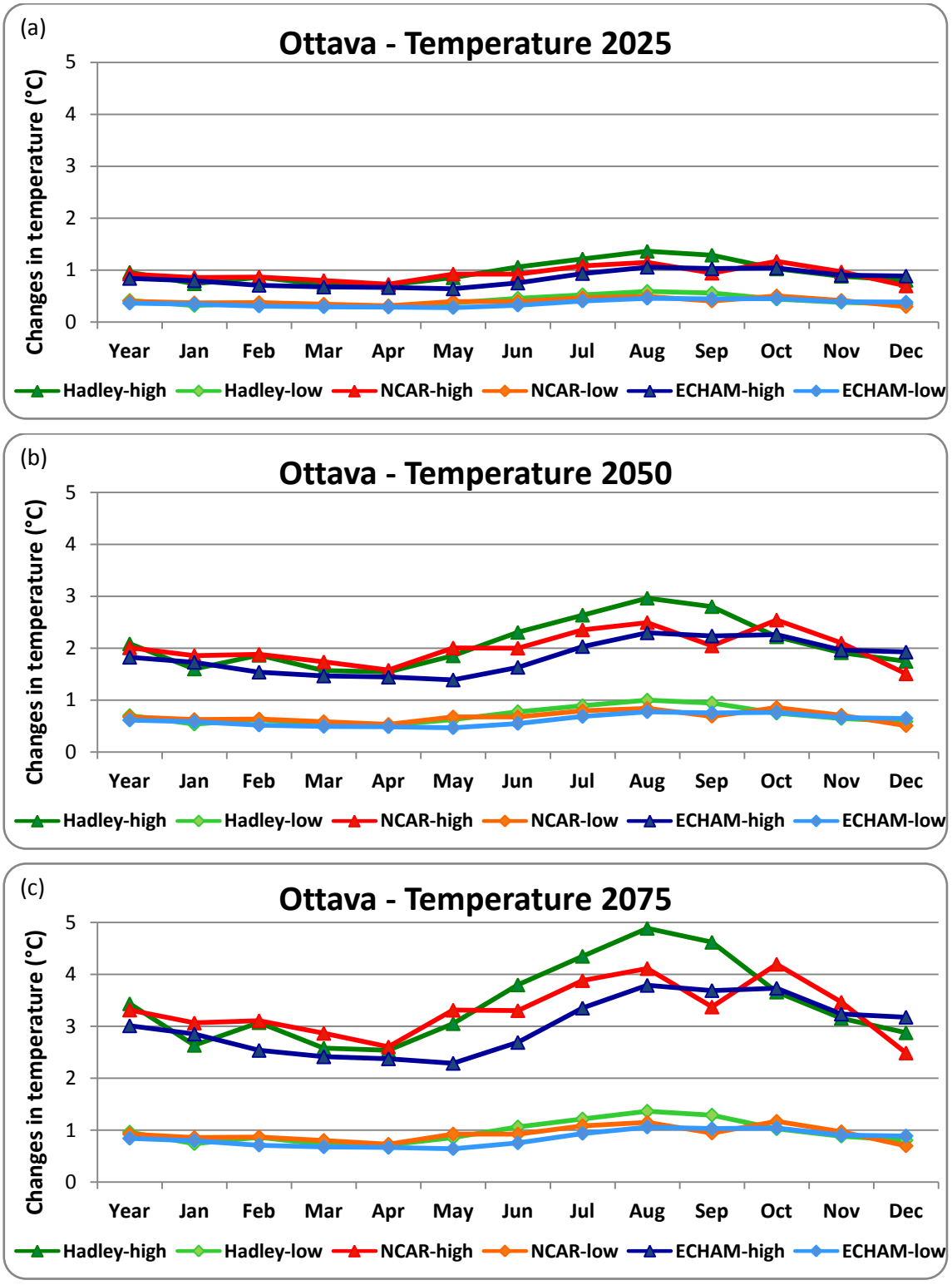

Figg. 2.2.2 a, b, c. Annual and monthly temperature changes (°C) from present to future periods(2025, 2050, 2075), with three different GCMs and two extremes climate scenarios (high and low). In the table above the graphs reference values of annual and monthly mean temperature for present period are shown.

Solar radiation

In Figures 2.2.3 *a*, *b*, and *c* the results for changes in monthly solar radiation amount (MJ m^{-2}) projected by three GCMs and low and high climate scenarios for Ottava site are shown.

Also for Ottava site, the projected increases in solar radiation are very different for the three GCMs.

The changes projected by the three GCMs for 2025 are similar and quite limited both in low and high climate scenarios. For 2050 and 2075 the projected increases in monthly solar radiation are more evident in particular with Hadley for spring months and NCAR for autumn and winter months. ECHAM estimates the lower increases for all future periods both for high and low climate scenarios.

Table 2.2.3 shows the annual and quarterly changes (%) in solar radiation amount projected by the three GCMs with the middle climate scenarios respect to te current climate. The higher increases in annual solar radiation are projected by Hadley for all future periods. Also considering spring (*AMJ*) and autumn (*OND*) months for all future periods, but considering winter (*JFM*) months the lower values are those projected by Hadley.

Table 2.2.3 Ottava – Annual and quarterly summarized changes in temperature (°C) from present to future periods with three GCMs and middle climate scenario.

	now	2025			2050			2075		
	(MJ·m^{-2})	ECHAM	HADLEY	NCAR	ECHAM	HADLEY	NCAR	ECHAM	HADLEY	NCAR
Year	**5032.3**	0.6	1.3	0.8	1.2	2.7	1.6	1.9	4.1	2.5
Jan-Feb-Mar	**513.9**	1.0	0.2	1.0	2.1	0.5	2.0	3.3	0.8	3.0
Apr-May-Jun	**1500.7**	0.7	1.7	0.5	1.5	3.4	1.0	2.3	5.3	1.6
Jul-Aug-Sep	**2057.9**	0.3	1.6	0.7	0.6	3.3	1.5	0.9	5.1	2.4
Oct-Nov-Dec	**972.3**	0.8	1.0	1.3	1.6	2.0	2.7	2.5	3.0	4.1

Solar Radiation (MJ m^{-2}) amount for present period:												
Year	*Jan*	*Feb*	*Mar*	*Apr*	*May*	*Jun*	*Jul*	*Aug*	*Sep*	*Oct*	*Nov*	*Dec*
5032	**161**	**218**	**375**	**485**	**640**	**702**	**728**	**628**	**462**	**315**	**184**	**134**

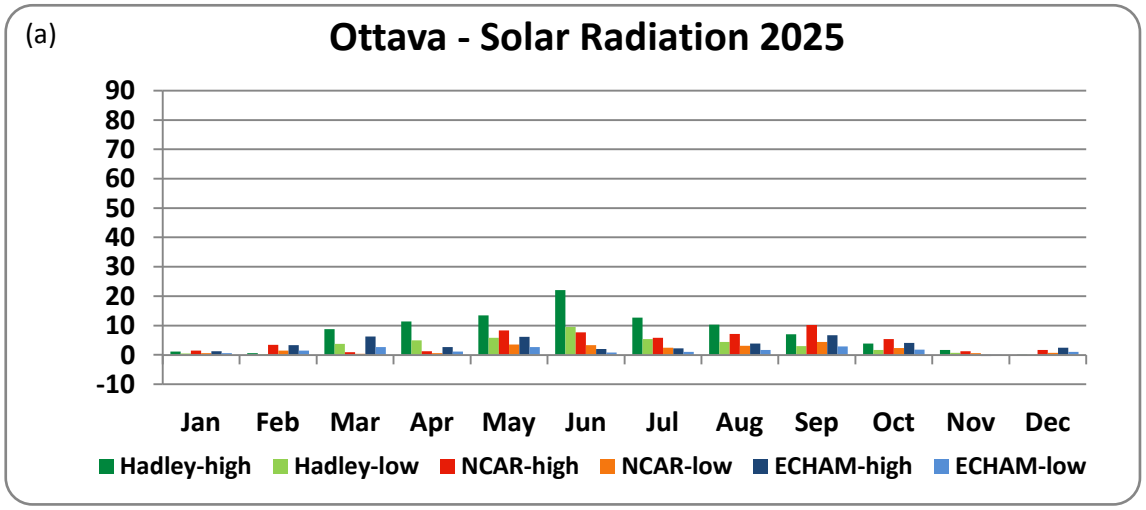

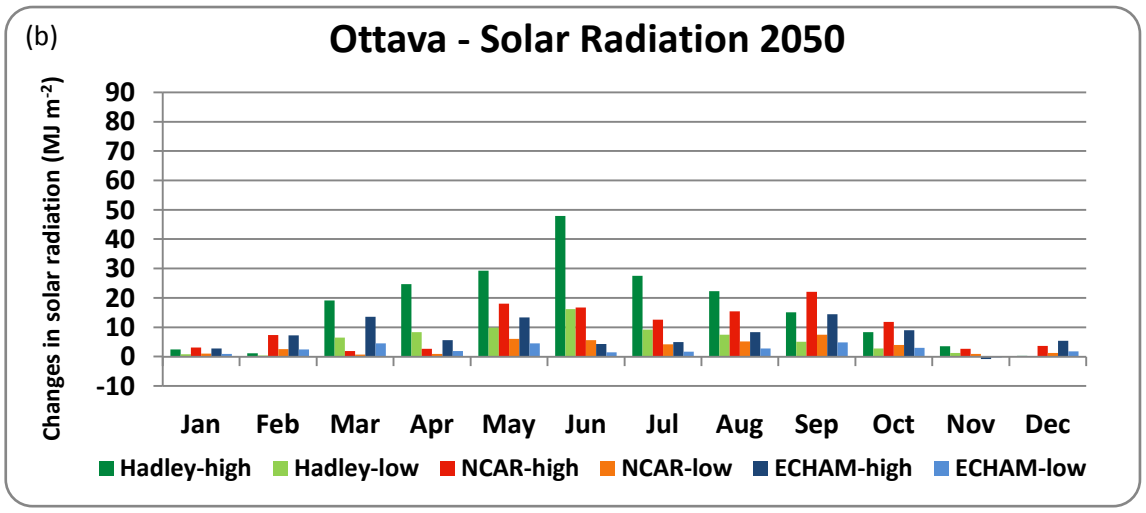

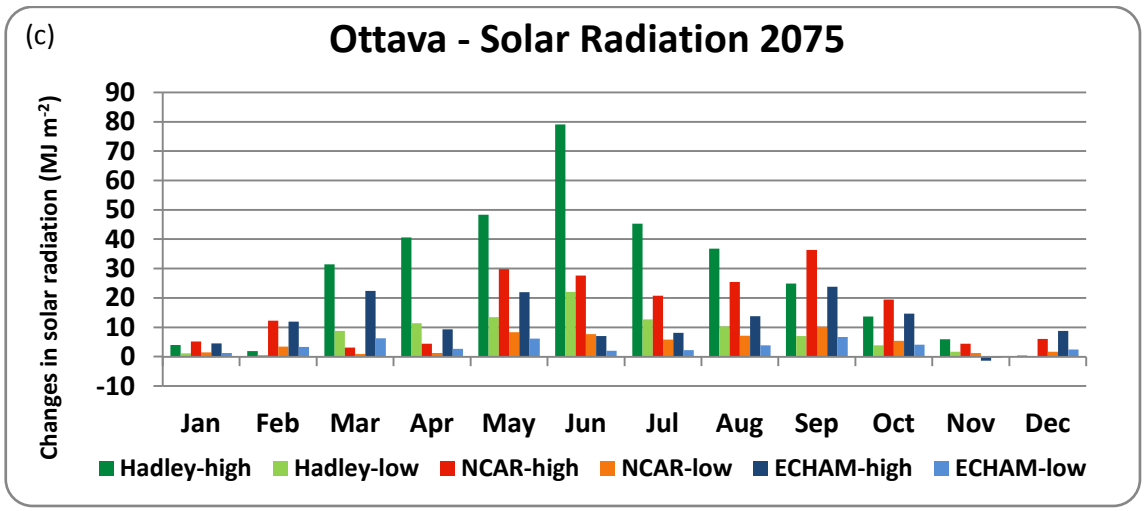

Figure 2.2.3 a, b, c. Solar radiation changes (%) from present to future periods (2025, 2050, 2075), with three different GCMs and two extremes climate scenarios (high and low). In the table above the graphs reference values of annual and monthly solar radiation amount (MJ m^{-2}) for present period are shown.

2.3 Santa Lucia site

Precipitation

For projected changes in precipitation for Santa Lucia site (Figures 2.3.1 *a*, *b* and *c*), it is possible to observe a decrease in rainfall already for 2025 for the simulations with all three GCMs for all months. The GCMs simulations with the most pessimistic climate scenarios (high) show decreases more than double respect those projected with the optimistic climate scenario (low).

Larger decreases in precipitation are those designed by ECHAM for all months in all three future periods (2025, 2050, 2075); only for the months from May to September, the largest decreases in precipitation are projected by Hadley. On the contrary NCAR provides significant increases in precipitation for March, August and November, in particular for 2050 and 2075. This could have positive effects for the crop. As for Ottava site, also for Santa Lucia it's possible to observe a little bit lower decreases in annual precipitation than Ussana site.

For the middle climate scenario (Table 2.3.1), the higher decreases in terms of annual changes (%) from actual values (now) are projected by ECHAM and Hadley, with very similar values of percentage changes for all future periods and the lower by NCAR.

Taking into consideration the quarters that are most important for the crop development and growth (*JFM* and *AMJ*), it is possible to observe that the greater decreases in precipitation are projected by ECHAM. Lower changes for all future periods are projected by Hadley for *JFM* and by NCAR for *AMJ*.

Table 2.3.1 Santa Lucia – Annual and quarterly summarized changes in temperature (°C) from present to future periods with three GCMs and middle climate scenario.

	now (mm)	2025			2050			2075		
		ECHAM	HADLEY	NCAR	ECHAM	HADLEY	NCAR	ECHAM	HADLEY	NCAR
Year	547.9	-10.7	-10.8	-7.6	-20.7	-20.9	-14.9	-30.0	-30.2	-21.9
Jan-Feb-Mar	176.9	-9.1	-3.6	-3.9	-17.6	-7.2	-7.7	-25.8	-10.8	-11.6
Apr-May-Jun	133.4	-12.8	-10.6	-5.3	-24.3	-20.4	-10.5	-34.8	-29.6	-15.6
Jul-Aug-Sep	30.5	-5.7	-17.5	-16.0	-10.8	-32.2	-30.1	-16.0	-44.9	-42.2
Oct-Nov-Dec	209.2	-15.1	-10.4	-4.7	-28.4	-20.1	-9.4	-40.3	-29.1	-14.2

Precipitation amount (mm) for present period:												
Year	*Jan*	*Feb*	*Mar*	*Apr*	*May*	*Jun*	*Jul*	*Aug*	*Sep*	*Oct*	*Nov*	*Dec*
548	**52.5**	**50.4**	**43.3**	**53.2**	**36.9**	**16.8**	**4.5**	**9.3**	**37.5**	**73.0**	**96.5**	**74.1**

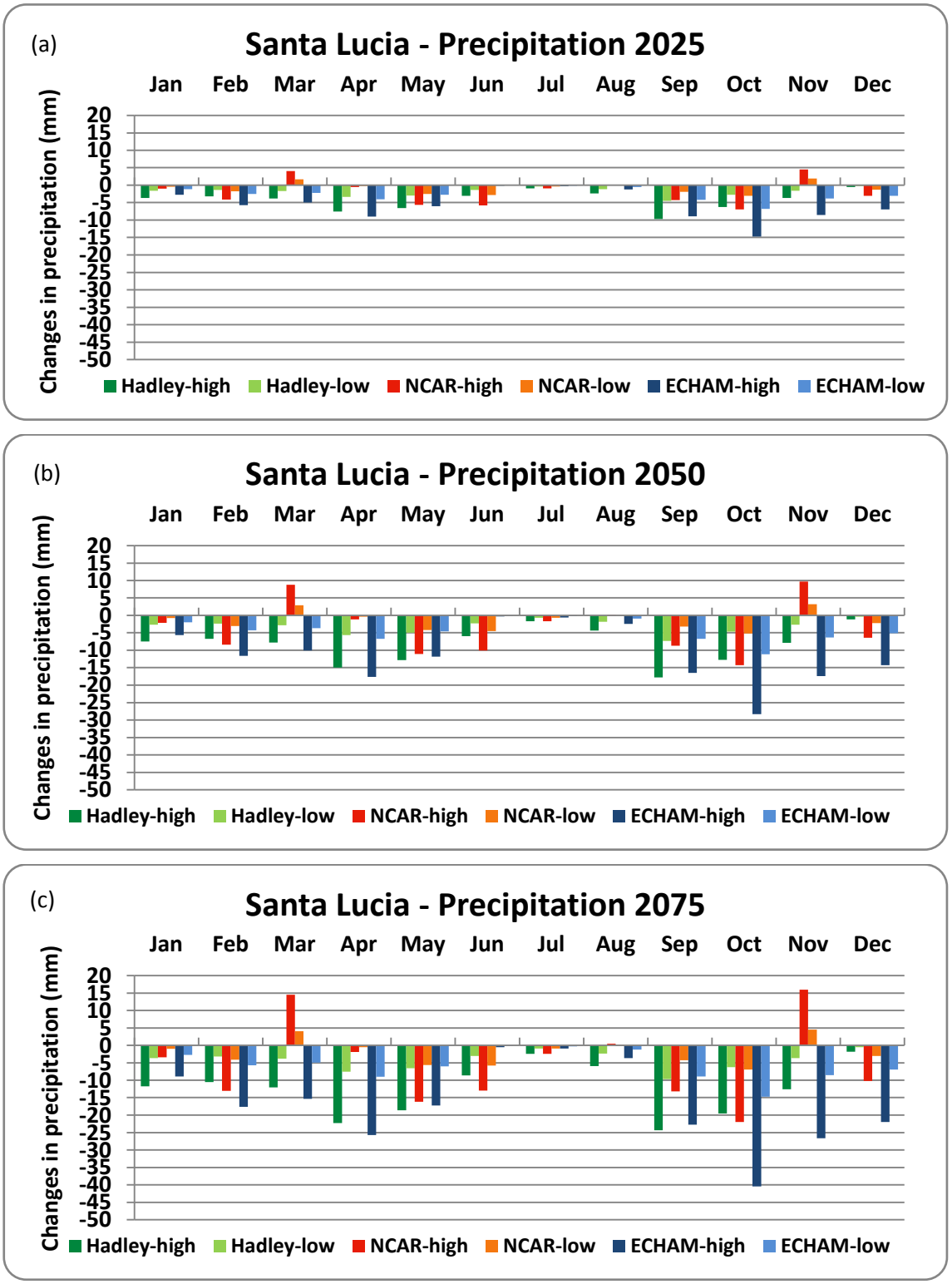

Figure 2.3.1 a, b, c. Precipitation changes from present to future periods (2025, 2050, 2075), with three different GCMs and two extremes climate scenarios (high and low). In the table above the graphs reference values of annual and monthly precipitation amount (mm) for present period are shown.

Temperature

Changes in monthly mean temperature projected by three GCMs and low and high climate scenarios for Santa Lucia site are shown in Figures 2.3.2 *a*, *b* and *c*.

The results for 2025 show similar projections with all GCM both for low and high climate scenarios. However the changes projected by ECHAM are a little bit lower than the changes projected by NCAR and Hadley. The monthly mean projection for low climate scenarios are less than 0.5°C for all GCMs. With high climate scenario the estimated increase in monthly mean temperature is about 1°C for all GCMs, and could reach about 1.3°C for August with Hadley, that estimates the higher increases for the summer months.

For 2050 the projected increases in monthly mean temperature are lower than 1°C with low emission scenario for all GCMs and could reach 3°C in August for Hadley considering high climate scenario, while the changes projected by ECHAM are the lower, in particular for the summer months. However, the annual mean change in precipitation projected for 2050 is about 2°C.

For the period 2075 the projected increases estimated by all GCMs with low climate scenario are very similar (≈1°C), while with the high climate scenario the changes in monthly mean temperature are quite different among the three GCMs. ECHAM provides smaller increases than Hadley and NCAR, while Hadley provides the higher increases especially for the summer months, and NCAR for winter and spring months. However, the annual mean change in precipitation projected for 2075 is less than 3.5°C.

Table 2.3.2 shows the summarized results for annual and quarterly changes in tempeature projected by the three GCMs with the middle climate scenarios.

The annual changes in mean temperature are very similar among the three GCMs, with a little bit lower increases projected by ECHAM for all future periods. In particular, increases in winter and spring are similar for all GCMs for the different future periods, with more evident differences between the GCMs in summer months.

Table 2.3.2 Santa Lucia – Annual and quarterly summarized changes in temperature (°C) from present to future periods with three GCMs and middle climate scenario.

	now (°C)	2025			2050			2075		
		ECHAM	HADLEY	NCAR	ECHAM	HADLEY	NCAR	ECHAM	HADLEY	NCAR
Year	**16.7**	0.6	0.7	0.7	1.3	1.4	1.4	1.9	2.2	2.2
Jan-Feb-Mar	**10.4**	0.6	0.6	0.6	1.2	1.2	1.2	1.9	1.8	1.9
Apr-May-Jun	**14.6**	0.5	0.5	0.6	1.0	1.1	1.3	1.6	1.7	2.0
Jul-Aug-Sep	**23.4**	0.6	0.9	0.8	1.3	1.7	1.6	2.0	2.7	2.5
Oct-Nov-Dec	**18.2**	0.7	0.8	0.8	1.5	1.6	1.6	2.3	2.5	2.4

Mean temperature (°C) for present period:												
Year	*Jan*	*Feb*	*Mar*	*Apr*	*May*	*Jun*	*Jul*	*Aug*	*Sep*	*Oct*	*Nov*	*Dec*
16.7	**9.9**	**10.2**	**11.8**	**13.9**	**18.0**	**21.6**	**24.2**	**24.5**	**21.8**	**18.7**	**14.0**	**11.0**

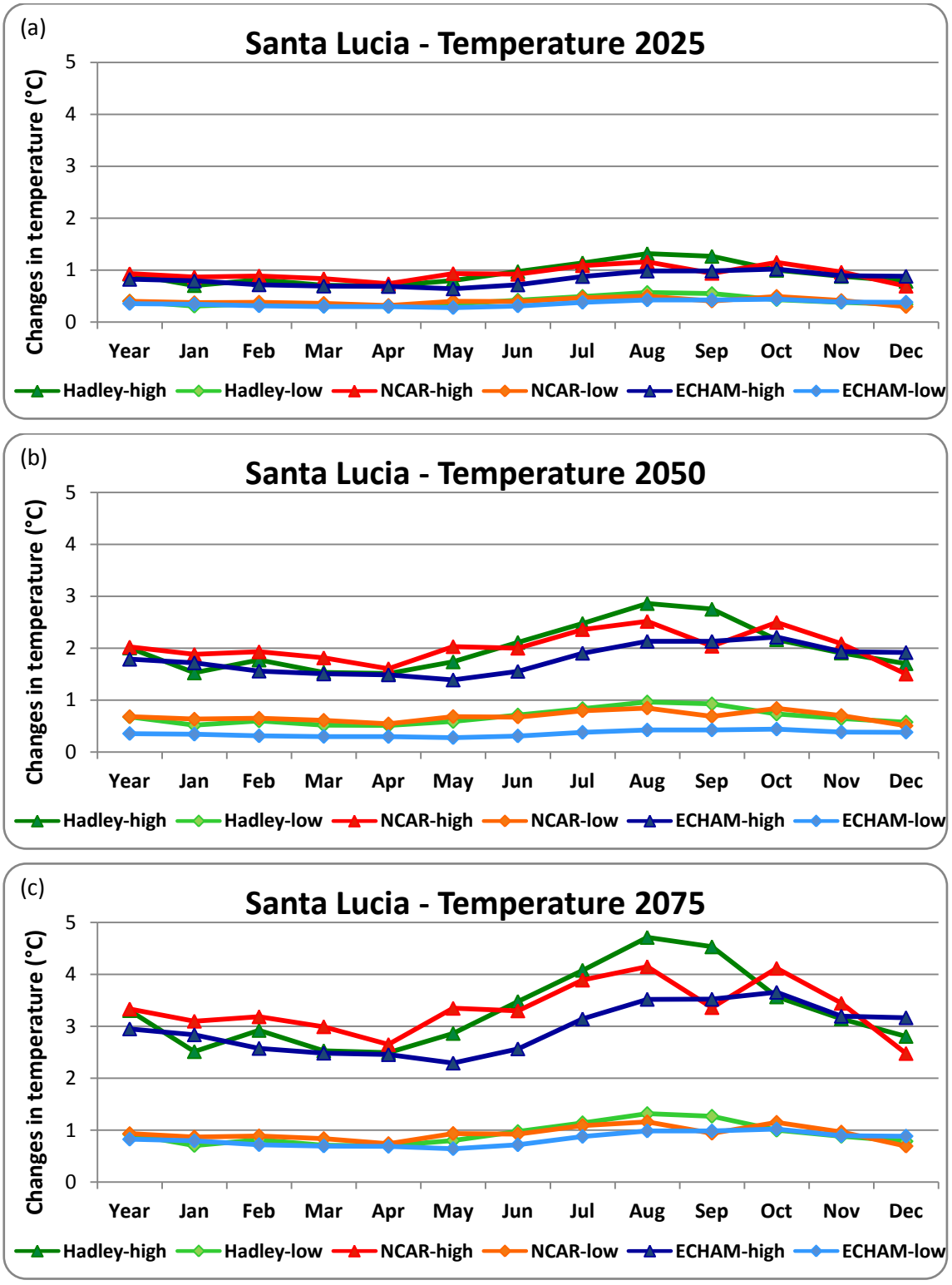

Figure 2.3.2 a, b, c. Temperature changes (°C) from present to future periods(2025, 2050, 2075), with three different GCMs and two extremes climate scenarios (high and low). In the table above the graphs reference values of annual and monthly mean temperature (°C) for present period are shown.

Solar radiation

Changes in monthly solar radiation amount (MJ m^{-2}) projected by three GCMs and low and high climate scenarios for Santa Lucia site are very different (Figures 2.3.3 *a*, *b*, and *c*).

The changes projected by NCAR are greater than the changes projected by Hadley and ECHAM for January, February, September and October in all three future periods considered, both with low and high climate scenarios. For the months from March until August Hadley provides the highest increases, while for December is ECHAM that provides the highest increases.

The Table 2.3.3 shows the summarized results for annual and quarterly changes (%) in solar radiation amount projected by the three GCMs with the middle climate scenarios respect to now. The higher increases in annual solar radiation are projected by Hadley for all future periods. Also considering spring (*AMJ*) months the higher increases are projected by Hadley for all future periods but for winter (*JFM*) Hadley estimates the lower increase.

Table 2.3.3 Santa Lucia – Annual and quarterly summarized changes in solar radiation amount (MJ m^{-2}) from present to future periods with three GCMs and middle climate scenario.

	now (MJ·m^{-2})	2025			2050			2075		
		ECHAM	HADLEY	NCAR	ECHAM	HADLEY	NCAR	ECHAM	HADLEY	NCAR
Year	**5904.2**	0.6	1.4	0.7	1.2	2.9	1.5	1.8	4.4	2.2
Jan-Feb-Mar	**718.8**	1.1	0.4	1.1	2.2	0.7	2.2	3.4	1.1	3.4
Apr-May-Jun	**1729.3**	0.7	1.5	0.5	1.5	3.2	1.1	2.3	4.9	1.6
Jul-Aug-Sep	**2281.1**	0.2	2.0	0.6	0.5	4.0	1.3	0.8	6.2	2.0
Oct-Nov-Dec	**1189.5**	0.8	1.0	1.0	1.5	2.1	2.1	2.4	3.2	3.2

Solar Radiation (MJ m^{-2}) amount for present period:												
Year	*Jan*	*Feb*	*Mar*	*Apr*	*May*	*Jun*	*Jul*	*Aug*	*Sep*	*Oct*	*Nov*	*Dec*
5904	**227**	**290**	**461**	**563**	**705**	**769**	**798**	**714**	**535**	**394**	**248**	**201**

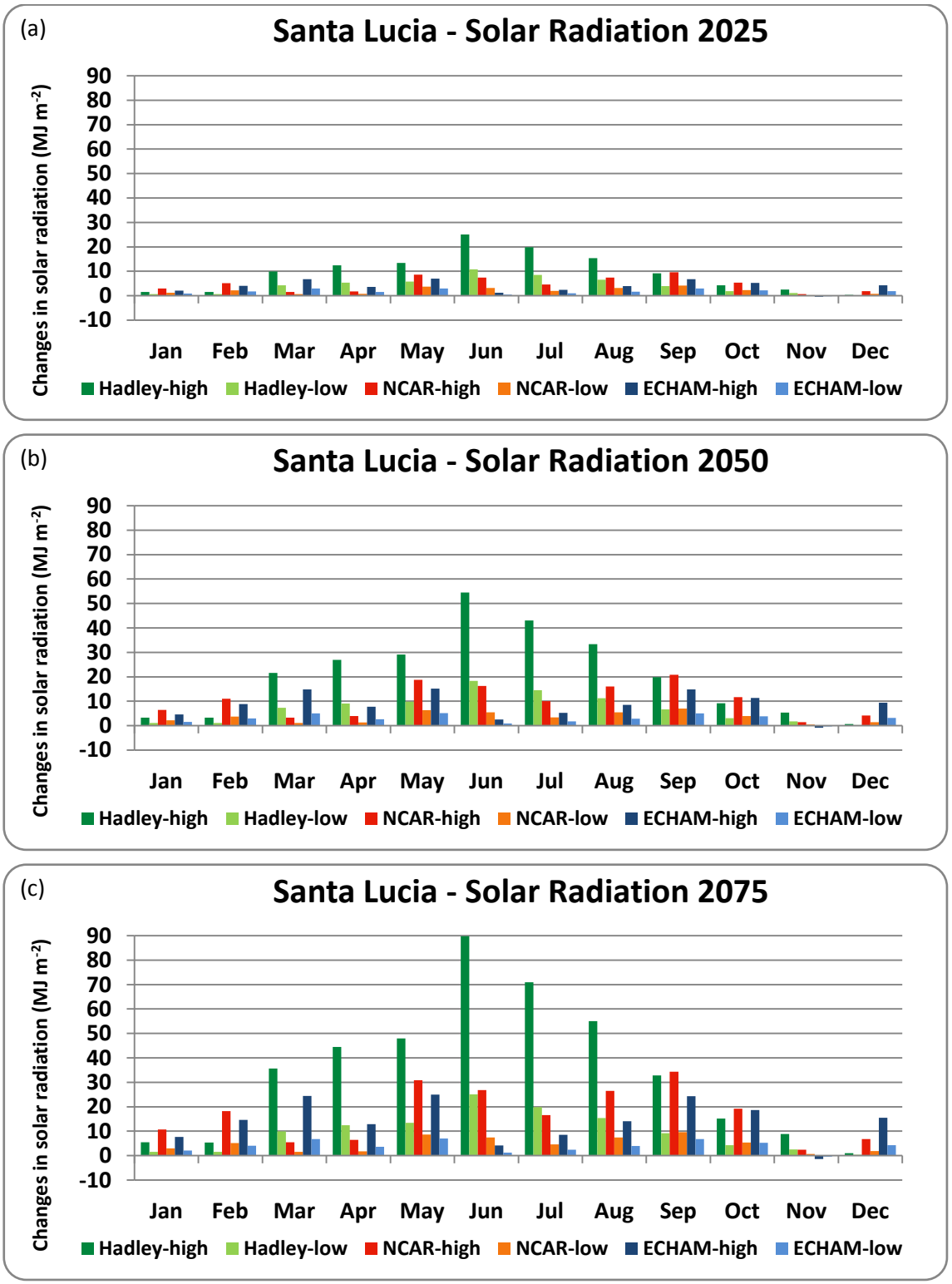

Figure 2.3.3 a, b, c. Solar radiation changes (%) from present to future periods (2025, 2050, 2075), with three different GCMs and two extremes climate scenarios (high and low). In the table above the graphs reference values of annual and monthly solar radiation amount (MJ m^{-2}) for present period are shown.

3. WEATHER GENERATOR VALIDATION

The validation of the weather generator was made in terms of crop model outputs by comparing yield and anthesis values obtained with synthetic and observed weather series for each cultivar and for each experimental site.

Results for Simeto cultivar, are shown in Table 3.1., and the results obtained considering Iride cultivar, are shown in Table 3.2.

Table 3.1 Weather Generator validation by comparing yield (t ha^{-1}) and anthesis (dap) for Simeto cultivar obtained with observed weather series (Obs. WS) and synthetic weather series (Synt. WS) for each experimental site. Results for t-test (α=0.05) and F-test (α=0.05) are reported.

	Ussana		**Benatzu**		**Ottava**		**Santa Lucia**	
	Anthesis	**Yield**	**Anthesis**	**Yield**	**Anthesis**	**Yield**	**Anthesis**	**Yield**
Obs. WS (N = 30)								
AVG	136.3	3.5	128.7	3.9	136.9	3.9	127.7	3.9
STD	5.0	1.1	4.8	1.3	5.2	1.2	5.2	1.5
Synt.WS (N=99)								
AVG	135.5	3.4	127.8	4.0	136.1	3.6	126.8	4.1
STD	5.6	1.3	5.2	1.6	5.3	1.0	5.1	1.6
P(T>t)	*0.51*	*0.71*	*0.39*	*0.89*	*0.45*	*0.12*	*0.43*	*0.52*
P(F>f)	*0.44*	*0.21*	*0.67*	*0.23*	*0.98*	*0.16*	*0.84*	*0.80*

Considering Simeto cultivar, the mean yields simulated with the synthetic weather series are lower than the mean yields simulated by observed weather series for Ussana and Ottava and higher for Benatzu and Santa Lucia. For anthesis, in all sites, mean values simulated with the synthetic weather series are slightly lower than those simulated by synthetic weather series. The standard deviations are generally higher for anthesis and yields simulated using synthetic weather series.

These difference are not so marked, which is confirmed by the statistical analysis.

In fact, the F-test indicates that the variances of yields and anthesis simulated with the two types of weather series are not statistically significantly different (α=0.05) in all comparison tests. The t-test shows that the means simulated with the two weather series for yields and anthesis are not statistically significantly different (α=0.05) for all comparisons.

Table 3.2 Weather Generator validation by comparing yield (t ha^{-1}) and anthesis (dap) for Iride cultivar obtained with observed weather series (Obs. WS) and synthetic weather series (Synt. WS) for each experimental site. Results for t-test (α=0.05) and F-test (α=0.05) are reported.

	Ussana		**Benatzu**		**Ottava**		**Santa Lucia**	
	Anthesis	**Yield**	**Anthesis**	**Yield**	**Anthesis**	**Yield**	**Anthesis**	**Yield**
Obs. WS (N = 30)								
AVG	128.1	4.0	123.3	4.6	128	4.6	124.1	4.7
STD	5.5	1.2	5.3	1.5	5.6	1.8	5.7	1.9
Synt. WS (N=99)								
AVG	127.7	4.0	122.9	4.6	127.6	4.2	123.4	4.8
STD	5.6	1.3	5.7	1.7	5.8	1.3	5.8	1.9
P(T>t)	*0.73*	*1.00*	*0.72*	*0.99*	*0.71*	*0.26*	*0.61*	*0.80*
P(F>f)	*0.91*	*0.46*	*0.72*	*0.32*	*0.88*	*0.03*	*0.95*	*0.85*

Considering Iride cultivar, the mean yields simulated with the synthetic weather series are very similar to those simulated by observed weather series for Ussana, Benatzu and Santa Lucia, while are lower than the mean yields simulated by observed series for Ottava site. The mean anthesis values simulated with the synthetic weather series are close to the mean values simulated by synthetic weather series in all sites. The values of standard deviations are generally higher for anthesis and yields simulated by synthetic weather series for all site, except for Ottava site, where the standard deviation for yield simulated by synthetic weather series is lower than standard deviation for yield simulated by observed weather series.

The F-test indicates that the variances of yields and anthesis simulated with the two weather series are statistically significantly different (α=0.05) only for Ottava site. However, the t-test shows that the means simulated with the two weather series for yields and anthesis are not statistically significantly different (α=0.05) for all comparisons. For Ottava site the result for t-test is relative to t-test for independent samples with unequal variance.

4. CLIMATE CHANGE IMPACT ASSESSMENT

In this section, results of climate change impact assessment on the two wheat cultivar (Simeto and Iride) for each experimental site are shown.

For each site the impact of climate change on yield and anthesis was evaluated, considering the three different GCMs and three climate change scenarios (low, mid and high).

Graphical comparison of yield (t ha^{-1}) and anthesis (dap) values for now and for the three future periods (2025, 2050 and 2075), considering separately the three GCMs with three climate change scenarios, was performed.

For yields, the effects of climate change impacts were analysed considering separately climate change impact without increasing in CO_2 concentration, and climate change with projected changes in CO_2 concentration. To make the interpretation of results easier, differences between yields simulated in all scenarios compared to those simulated using synthetic actual scenarios are also summarized as percentage changes.

For anthesis, the comparison was made only for fixed values of CO_2 because of the projected increases in CO_2 ambient concentration does not have effects on shift of the anthesis date.

A statistical analysis results are also reported in order to consider the statistical significant differences between the mean values of yield and anthesis from now to future periods.

4.1 USSANA

4.1.1 Simeto

Yield

The Figures 4.1.1.1 *a*, *b*, and *c*, show the results of climate change impact on yield (t ha^{-1}) for Simeto cultivar considering, separately for the three GCMs, the climate change scenarios with and without considering CO_2 concentration changes in atmosphere. The table 4.1.1.1 reports the correspondent changes in terms of percentage, from now to future periods.

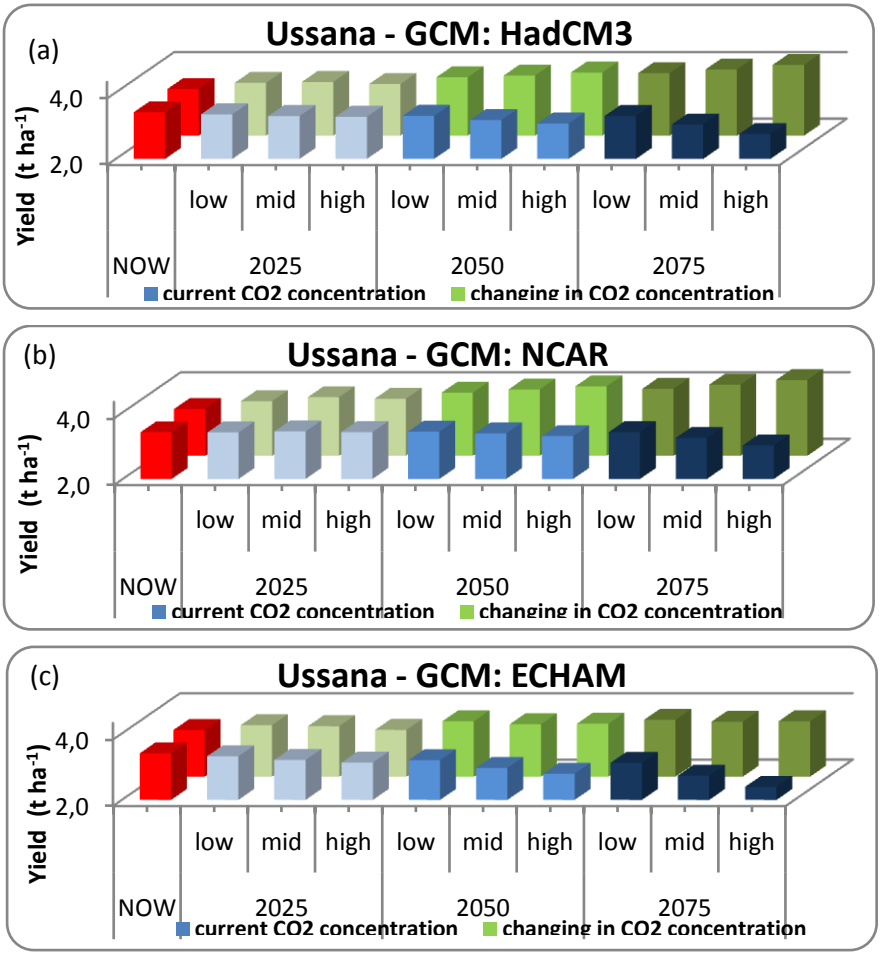

Figg. 4.1.1.1 a, b, c. Changes in yield (t ha^{-1}) from now to future periods, with current and future CO_2 concentration, with HadCM3 (a), NCAR (b) and ECHAM (c) GCMs and three climate scenarios (low, mid and high) for Simeto cultivar at Ussana site.

At the first analysis, the simulations for Simeto at Ussana site, without consider future increases in CO_2 concentration, show a slight reduction in yield for 2025 only for the simulation with ECHAM, in particular with high climate change scenario. The reduction in yield is evident for

Hadley starting from 2050 and for NCAR starting from 2075, in particular with mid and high climate change scenarios. However the higher decreases in yield are assumed with ECHAM. This could be justified considering the difference between the GCMs in particular in predicting the future patter of precipitation. NCAR provides lower reductions in precipitation respect to the others GCMs and, on the contrary, it provides increments in some months of the year, like March and November, that are very important for wheat crop in terms of water availability. ECHAM instead provides the highest decreases in precipitations.

As shown in Table 4.1.1.1, the higher reductions in the yield, without consider future changes in CO_2 concentration, are quite moderate with NCAR, but may reach -19% with Hadley and -29% with ECHAM, for 2075 considering high climate change scenario.

The simulations taking into account the projected changes in CO_2 concentration for future periods, with the three different climate change scenarios, show a general increase in yield from now to future periods. It means that the direct effect of CO_2 increase is able to compensate the decrease in yield due to indirect CO_2 effect, and it could also be able to induce an increase in mean production, particularly evident for the 2075 where the CO_2 is expected to reach values from 501 to 705, respectively for low and high climate change scenarios.

The increases in yield are progressive from now to future periods with all GCMs, especially with NCAR (25.7% for 2075 whit high climate change scenario), and more limited with ECHAM (7.8% for 2075 whit high climate change scenario). This is because the indirect effect of the increased CO_2, that causes changes in the climate regime projected by ECHAM, is so strong that it cannot be offset by expected increases in CO_2 atmospheric concentration.

Table 4.1.1.1. Changes (%) in yield from now to future periods, with current and future CO_2 concentration, for Hadley, NCAR and ECHAM GCMs and three climate scenarios (low, mid, high) for Simeto at Ussana site.

		Hadley		NCAR		ECHAM		Mean yield change considering CO_2 increases
		Current CO_2	Changing in CO_2	Current CO_2	Changing in CO_2	Current CO_2	Changing in CO_2	
2025	***low***	-1.8	5.4	-0.2	7.0	-2.7	4.3	**5.6**
	mid	-3.3	6.3	0.7	10.5	-5.9	3.4	**6.7**
	high	-4.0	4.4	0.1	9.1	-8.2	0.2	**4.6**
2050	***low***	-3.1	10.4	0.6	14.5	-6.1	7.8	**10.9**
	mid	-6.9	11.9	-1.0	17.3	-12.9	5.1	**11.4**
	high	-10.0	14.6	-3.4	20.1	-18.1	5.6	**13.4**
2075	***low***	-3.3	14.1	0.1	17.9	-8.5	9.1	**13.7**
	mid	-10.8	17.3	-5.1	21.5	-19.8	7.4	**15.4**
	high	-19.3	21.4	-11.8	25.7	-29.7	7.8	**18.3**

The mean changes of yield projected by the three GCMs, and considering the direct and indirect effects of CO_2, could range from 4.6 to 6.7 % for 2025, from 10.9 to 13.4 % for 2050 and from 13.7 to 18.6 % for 2075 for Simeto cultivar at Ussana site. The range of these result is comparable to that shown by other similar studies (Olesen and Bindi, 2002; Trnka *et al.*, 2004; Brassard and Singh, 2008) and studies from controlled, semi-controlled and open-field experiments (Kimball *et al.*, 2002).

The variability of the simulated yields (data not shown), expressed in terms of coefficient of variation (CV=Standard Deviation/ mean) decrease, considering all GCMs and climate change scenarios, from 41% to 37% respectively for simulations without consider the direct effect of CO_2 and considering the effect of CO_2. These changes could be related to the water stress that is negatively correlated to direct effect of CO_2. The increasing intensity of the water stress, due to indirect effect of CO_2 reduces the mean yields but enhances the variability of the yields. If both effects are combined the variability tends to decrease, due to the reduction of water stress in ambient with higher concentration of CO_2 (Zalud and Dubrovsky, 2002).

In the Table 4.1.1.2 are reported the statistical analysis using Student-Newman-Keuls (SNK) test.

Table 4.1.1.2 Mean yield (t ha^{-1}) comparison for now and future periods with different GCMs and climate scenarios for Simeto cultivar at Ussana site.

		Hadley[a] yield (t ha^{-1})		NCAR[a] yield (t ha^{-1})		ECHAM[a] yield (t ha^{-1})	
		Current CO_2	Changes in CO_2	Current CO_2	Changes in CO_2	Current CO_2	Changes in CO_2
Now		3.4 a	3.4 b	3.4 a	3.4 c	3.4 a	3.4 a
2025	**Low**	3.3 ab	3.6 ab	3.4 a	3.6 bc	3.3 ab	3.6 a
	Mid	3.3 ab	3.6 ab	3.4 a	3.8 abc	3.2 ab	3.5 a
	High	3.3 ab	3.6 ab	3.4 a	3.7 abc	3.1 ab	3.4 a
2050	**Low**	3.3 ab	3.8 ab	3.4 a	3.9 abc	3.2 ab	3.7 a
	Mid	3.2 ab	3.8 ab	3.4 a	4.0 ab	3.0 ab	3.6 a
	High	3.1 ab	3.9 ab	3.3 a	4.1 ab	2.8 bc	3.6 a
2075	**Low**	3.3 ab	3.9 ab	3.4 a	4.0 ab	3.1 ab	3.7 a
	Mid	3.1 ab	3.9 ab	3.2 a	4.1 ab	2.7 bc	3.7 a
	High	2.7 b	4.1 a	3.0 a	4.3 a	2.4 c	3.7 a

Means within each group (single GCM and different future periods) sharing the same letter do not differ significantly from one another (Student-Newman-Keuls test at $P \leq 0.05$).

[a] The two groups of yields, with current CO_2 and changes in CO_2 concentration, are evaluated separately.

The mean yield comparisons show a statistically significant difference only between now and 2075 with high climate change scenario for Hadley GCM, considering or not the direct effect of CO_2 concentration. Considering NCAR, there is not significantly comparison from now and

future scenarios without consider CO_2, while there are significant differences from the means of the yield projected for now and the mean projected by NCAR for 2050 with mid and high climate change scenarios, and for 2075 with all climate change scenarios. On the contrary, the mean projected by ECHAM does not show any significant change from now to future periods considering CO_2 effect, while without considering CO_2 increase it shows a significant difference from now to 2050 with high climate change scenario and to 2075 with mid and high climate change scenarios. This is obviously justified by the fact that if the mean yields are not significantly modified by climate change impact without CO_2, the positive effect of CO_2 fertilization could be more effective.

The non-significant differences found in the nearest future periods are due to the fact that climate change expected (as discussed in session 3) are not so catastrophic and the positive direct effect of CO_2, both on photosynthesis and water use efficiency is able to offset the negative effects associated with the increase of temperature and reduced precipitation.

Anthesis

The Figures 4.1.1.2 *a*, *b*, and c, show the results for climate change impact on anthesis date (difference in days from now to future periods) obtained for different future periods with the three GCMs and three climate change scenarios; in the Table 4.1.1.3 results for statistical analysis using SNK-test are reported.

An advancement of the anthesis phase occurrence can already be observed for the period 2025 with all GCMs, in particular with high climate change scenario. The anthesis date by 2050 might be about 6 days earlier than under present climate. This trend continues for 2075 time period when duration of the period to flowering stage might be about 9 days shorter than nowadays. The higher reduction is projected by NCAR GCM, probably due to the fact that NCAR projected the major increase in temperature in particular for the winter and spring months.

Considering the most pessimistic climate change scenarios, the date of anthesis might change from 4 to 14 days in advance respectively for 2025 and 2075 periods.

Analyzing the results by Student-Newman-Keuls test, the differences from now to future periods are significantly different in most of comparison both for now and future periods.

This means that increases in temperature from now to future periods are likely to significantly change the length of the entire reproductive cycle of wheat, even in the less pessimistic climate scenarios, without evident differences between the three GCMs.

This advance of anthesis date indicates a clear acceleration of the crop development that might leads, as a consequence, to a lower accumulation of dry matter.

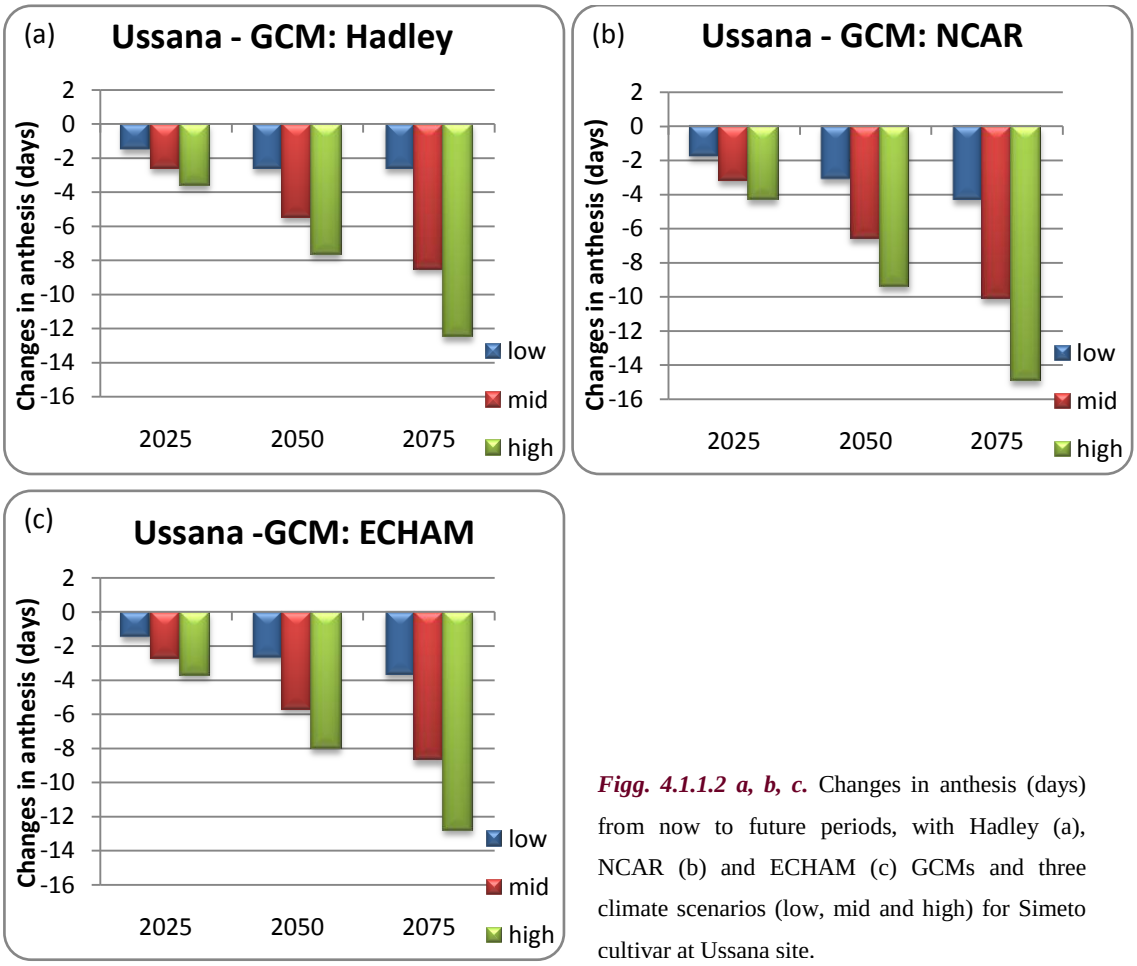

Figg. 4.1.1.2 a, b, c. Changes in anthesis (days) from now to future periods, with Hadley (a), NCAR (b) and ECHAM (c) GCMs and three climate scenarios (low, mid and high) for Simeto cultivar at Ussana site.

Table 4.1.1.3 Mean anthesis date (dap) comparison for now and future periods with different GCMs and climate scenarios for Simeto cultivar at Ussana site.

		Hadley		NCAR		ECHAM	
		Anthesis (dap)		Anthesis (dap)		Anthesis (dap)	
Now		136	a	136	a	136	a
2025	**Low**	134	ab	134	b	134	b
	Mid	133	bc	132	bc	133	bc
	High	132	c	131	c	132	c
2050	**Low**	133	bc	132	bc	133	bc
	Mid	130	d	129	d	130	d
	High	128	e	126	e	128	e
2075	**Low**	133	bc	131	c	132	c
	Mid	127	e	125	e	127	e
	High	123	f	121	f	123	f

Means within each group (single GCM and different future periods) sharing the same letter do not differ significantly from one another (SNK-test at P≤0.05).

4.1.2 Iride

Yield

The Figures 4.1.2.1 *a*, *b*, and *c*, show the results of climate change impact on yield (t ha^{-1}) for Iride cultivar considering, separately for the three GCMs, the climate change scenarios with and without considering CO_2 concentration changes in atmosphere. In the Table 4.1.2.1 are reported the correspond changes in terms of percentage from now to future periods.

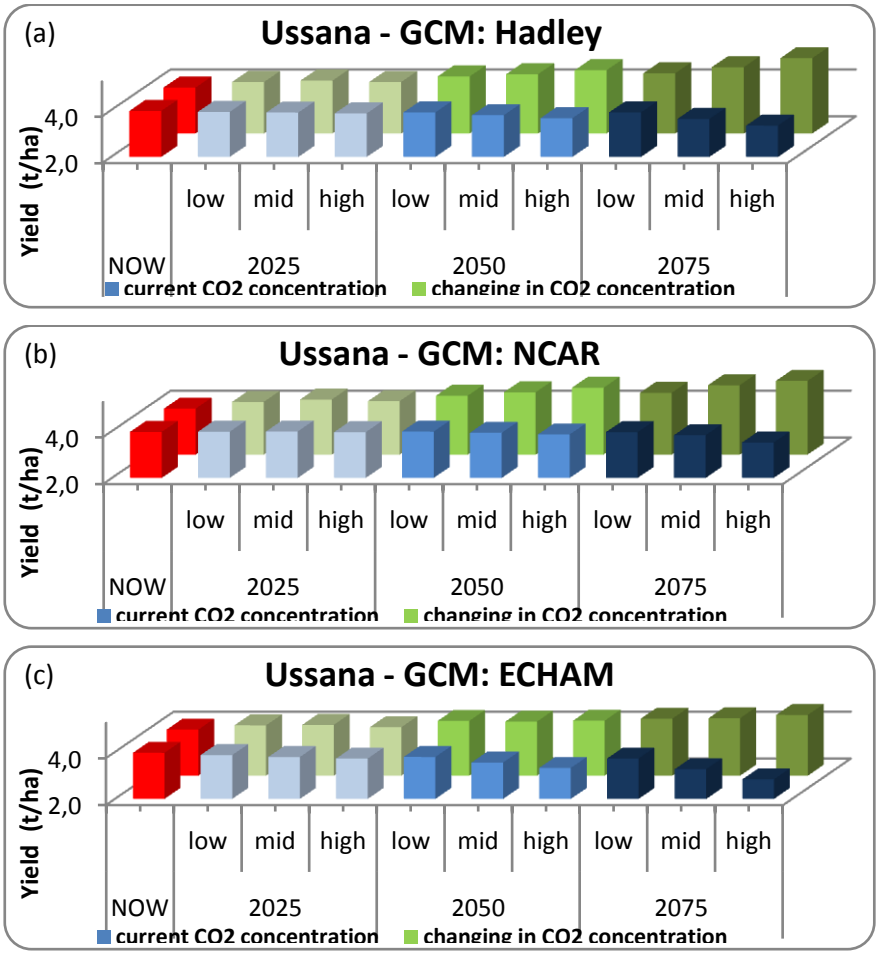

Figg. 4.1.2.1 a, b, c. Changes in yield (t ha^{-1}) from now to future periods, with current and future CO_2 concentration, with Hadley (a), NCAR (b) and ECHAM (c) GCMs and three climate scenarios (low, mid and high) for Iride cultivar at Ussana site.

For Iride at Ussana site, simulations, without consider future increases in CO_2 concentration, show a decrease in yield for 2025 close to zero for Hadley and NCAR GCMs, that could reach -6% for ECHAM projection with high climate change scenario. The reduction in yield are evident for Hadley starting from 2050 e for NCAR starting from 2075, in particular with mid

and high climate change scenarios. However the higher decreases in yield are assumed with ECHAM.

As evident in Table 4.1.2.1, the yield reductions, without consider future changes in CO_2 concentration, are quite low with NCAR, but may reach -16 % with Hadley and -29% with ECHAM, for 2075 considering high climate change scenario.

The simulations taking into account the projected changes in CO_2 concentration for future periods, with the three different climate scenarios, show a general increase in yield from now to future periods. The increases in yield are progressive from now to future periods with all GCMs, especially with Hadley (32%) and NCAR (30%), and more moderate with ECHAM (16%). This is because the indirect effect of the increased CO_2, that causes changes in the climate regime projected by ECHAM, is so strong that cannot be offset by the expected increases in CO_2 atmospheric concentration.

The results are very similar to those obtained for Simeto at the same site, but the increases in mean yield are higher for Iride than Simeto considering the changes in CO_2 concentration for the high climate change scenarios in all future periods, and in particular with Hadley and ECHAM.

The mean yield changes projected by the three GCM, considering the direct and indirect effects of CO_2, could range from 5.5 to 7.5 % for 2025, from 11.7 to 16.9 % for 2050 and from 14.7 to 25.8 % for 2075 for Iride cultivar at Ussana site.

Also for Iride the CV decrease, considering all GCMs and climate change scenarios, from 33% to 30% respectively for simulations without consider the direct affect of CO_2 and considering the effect of CO_2.

Table 4.1.2.1. Changes (%) in yield from now to future periods, with current and future CO_2 concentration, for Hadley, NCAR and ECHAM GCMs and three climate scenarios (low, mid and high) for Iride at Ussana site.

		Hadley		NCAR		ECHAM		Mean yield change considering CO_2 increases
		Current CO_2	Changing in CO_2	Current CO_2	Changing in CO_2	Current CO_2	Changing in CO_2	
2025	***low***	-1.0	6.0	0.2	7.2	-2.4	4.6	**5.9**
	mid	-1.7	7.6	0.4	9.7	-4.4	5.1	**7.5**
	high	-2.5	5.9	-0.3	8.1	-6.2	2.6	**5.5**
2050	***low***	-1.6	12.0	0.3	13.8	-4.4	9.3	**11.7**
	mid	-4.5	14.4	-1.0	17.5	-10.4	8.6	**13.5**
	high	-7.8	18.8	-2.8	22.4	-16.2	9.6	**16.9**
2075	***low***	-1.6	15.4	-0.3	16.9	-6.2	11.8	**14.7**
	mid	-8.5	22.0	-3.6	25.1	-17.6	12.2	**19.8**
	high	-15.8	31.7	-11.5	29.9	-28.5	15.7	**25.8**

However, the yield mean comparison by Student-Newman-Keuls test (Table 4.1.2.2) shows a statistically significant difference in means projected by Hadley only between now and 2075 with high climate scenario, without consider the direct effect of CO_2 concentration, and starting from 2050 considering the direct effect of CO_2. Considering the results obtained with NCAR, there are not significantly differences by comparing now and future scenarios without consider CO_2, while there are significantly differences from now for the mean projected by NCAR for 2050 with mid and high climate change scenarios, and for the mean yields projected for 2075 with all climate change scenarios.

On the contrary, the mean projected by ECHAM show a significantly change from now to future periods considering CO_2 effect only for 2075 with high climate change scenario, while without considering CO_2 increases, show a significant difference from now to 2050 with high climate scenario and to 2075 with mid and high climate scenarios. This is due to the fact that when the mean yields are significantly modified by climate change impact without CO_2, the positive effect of CO_2 fertilization could not be anymore evidence.

Table 4.1.2.2 Mean yield (t ha^{-1}) comparison for now and future periods with different GCMs and climate scenarios for Simeto cultivar at Ussana site.

		Hadley[a] yield (t ha^{-1})		**NCAR[a] yield (t ha^{-1})**		**ECHAM[a] yield (t ha^{-1})**	
		Current CO_2	**Changes in CO_2**	**Current CO_2**	**Changes in CO_2**	**Current CO_2**	**Changes in CO_2**
Now		4.0 a	4.0 d	4.0 a	4.0 e	4.0 a	3.4 b
2025	**Low**	3.9 a	4.2 cd	4.0 a	4.3 de	3.9 a	4.1 ab
	Mid	3.9 a	4.3 cd	4.0 a	4.4 cde	3.8 abc	4.2 ab
	High	3.9 a	4.2 cd	4.0 a	4.4 de	3.7 abcd	4.1 ab
2050	**Low**	3.9 a	4.4 bcd	4.0 a	4.5 bcd	3.8 ab	4.3 ab
	Mid	3.8 ab	4.5 bc	4.0 a	4.7 bcd	3.6 abcd	4.3 ab
	High	3.7 ab	4.7 bc	3.9 a	4.9 abc	3.3 bcd	4.3 ab
2075	**Low**	3.9 a	4.6 bc	4.0 a	4.6 abcd	3.7 abcd	4.3 ab
	Mid	3.6 ab	4.8 b	3.8 a	5.0 ab	3.3 bd	4.5 ab
	High	3.3 b	5.2 a	3.5 a	5.2 a	2.8 e	4.6 a

Means within each group (single GCM and different future periods) sharing the same letter do not differ significantly from one another (Student-Newman-Keuls test at $P \leq 0.05$).

[a] The two groups of yields, with current CO_2 and changes in CO_2 concentration, are evaluated separately.

Anthesis

The Figures 4.1.2.2 *a*, *b*, and c, show the results for climate change impact on anthesis date (difference in days from now to future periods) obtained for different future periods with the three GCMs and three climate change scenarios.

It is possible to observe a shortening of the duration of the period between sowing and anthesis phase already for 2025 with all GCMs, in particular with high climate scenario. The anthesis date by 2050 might have an advancement of about 7 days compared to present climate. This trend continues for 2075 time period when duration of the vegetation cycle until flowering might be about 10 days shorter than nowadays. As for Simeto, the higher reduction is projected by NCAR, because this GCM provides the major increase in temperature in particular for the winter and spring months.

Considering the most pessimistic climate scenarios, the date of anthesis might change from 5 to 15 days in advance respectively for 2025 and 2075 periods.

Generally, for Iride is expected a slightly reduction in anthesis phase duration than Simeto at Ussana site.

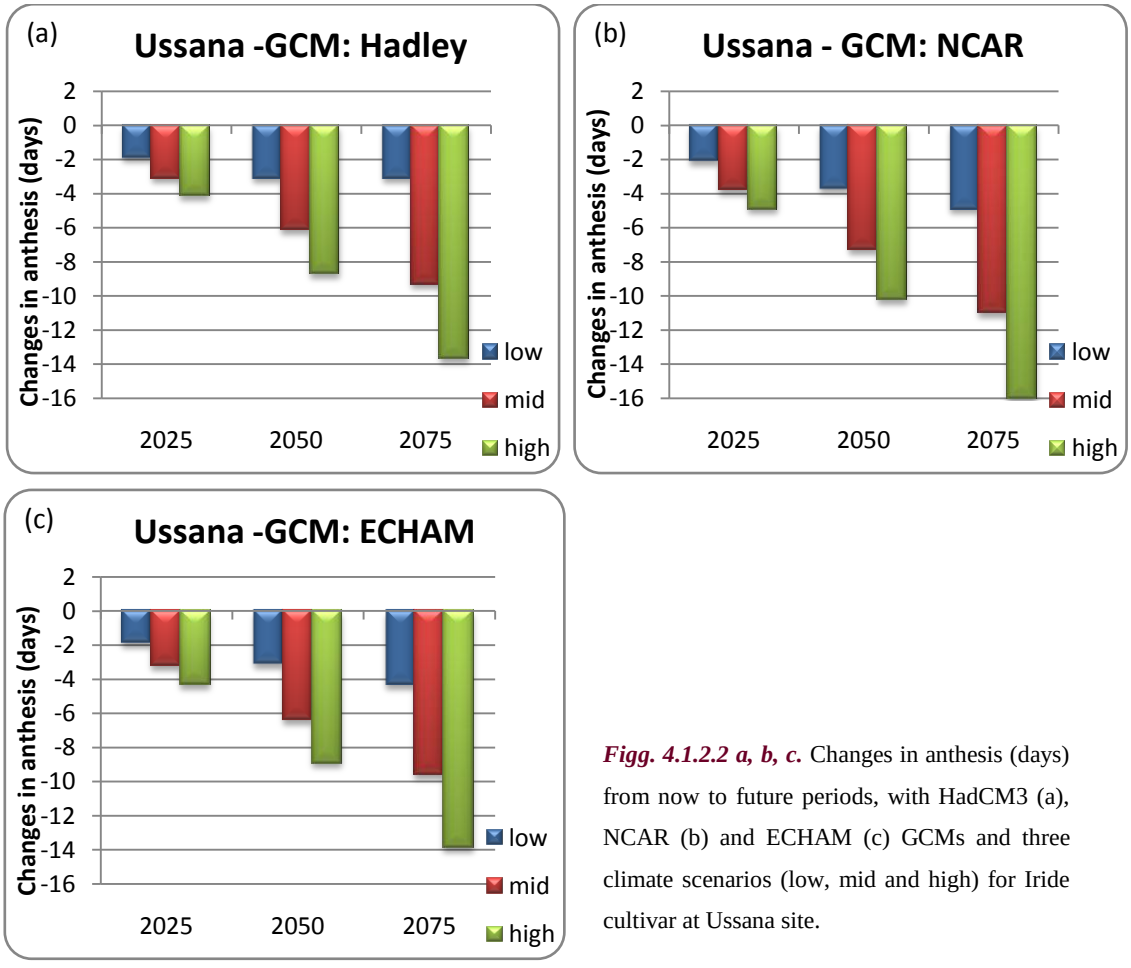

Figg. 4.1.2.2 a, b, c. Changes in anthesis (days) from now to future periods, with HadCM3 (a), NCAR (b) and ECHAM (c) GCMs and three climate scenarios (low, mid and high) for Iride cultivar at Ussana site.

Analyzing the results by Student-Newman-Keuls test, the difference from now to future periods are significantly different in most of comparison (see Table 4.1.2.3), both comparing now and future periods and comparing future periods together.

This means that the changes in temperature from now to future periods are likely to significantly change the length of the development phases for wheat, even with the less pessimistic climate scenarios, without evident differences between the three GCMs.

Table 4.1.2.3 Mean anthesis date (dap) comparison for now and future periods with different GCMs and climate scenarios for Iride cultivar at Ussana site.

		Hadley		NCAR		ECHAM	
		Anthesis (dap)		Anthesis (dap)		Anthesis (dap)	
Now		128	a	128	a	128	a
2025	**Low**	126	b	126	b	126	b
	Mid	125	bc	124	bc	125	bc
	High	124	c	123	c	123	c
2050	**Low**	125	bc	124	c	125	bc
	Mid	122	d	120	d	121	d
	High	119	e	118	e	119	e
2075	**Low**	125	bc	123	c	123	c
	Mid	118	e	117	e	118	e
	High	114	f	112	f	114	f

Means within each group (single GCM and different future periods) sharing the same letter do not differ significantly from one another (SNK-test at $P \leq 0.05$).

4.2 BENATZU

4.2.1 Simeto

Yield

The Figures 4.2.1.1 *a*, *b*, and *c*, show the results of climate change impact on yield (t ha^{-1}) for Simeto cultivar at Benatzu experimental site, considering, separately for the three GCMs, the climate change scenarios with and without considering CO_2 concentration changes. In the table 4.2.1.1 are reported the correspond changes in terms of percentage from now to future periods.

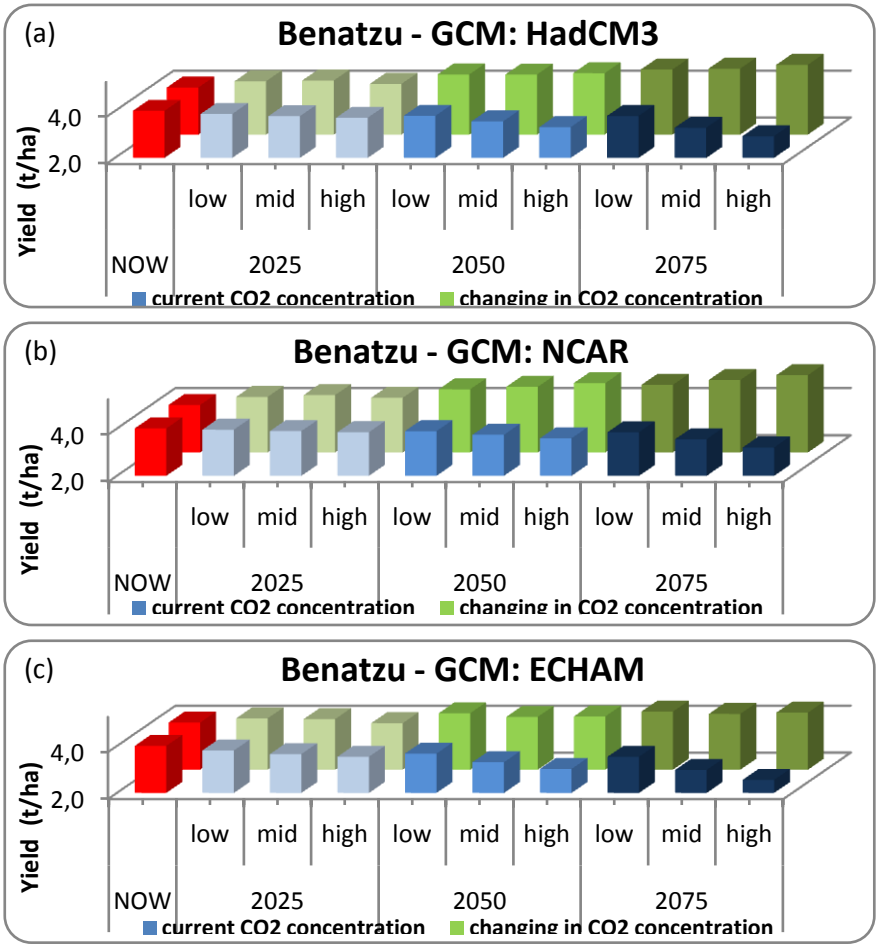

Figg. 4.2.1.1 a, b, c. Changes in yield (t ha^{-1}) from now to future periods, with current and future CO_2 concentration, with Hadley (a), NCAR (b) and ECHAM (c) GCMs and three climate scenarios (low, mid and high) for Simeto cultivar at Benatzu site.

The simulations for Simeto at Benatzu site, without consider future increases in CO_2 concentration, show a slight decrease in yield for 2025, in particular projected by ECHAM with high climate change scenario. The reductions in yield are evident for Hadley starting from 2050 e

for NCAR starting from 2075, in particular with high climate change scenarios. However the higher decreases in yield are projected by ECHAM.

The yield reductions, without consider future changes in CO_2 concentration, may reach –20% with NCAR, -27% with Hadley and -36% with ECHAM, for 2075 considering high climate change scenario (Table 4.2.1.1).

In general, all the simulations that take into account the projected changes in CO_2 concentration for future periods, with the three different climate scenarios, show an increase in yield from now to future periods. The increases in yield are progressive from now to future periods, especially with NCAR (32%) and Hadley (24%), and more moderate with ECHAM (11%). This is because the indirect effect of the increased CO_2, that causes changes in the climate regime projected by ECHAM, is so strong that cannot be offset by expected increases in CO_2 atmospheric concentration.

Comparing to results obtained for Simeto at Ussana site, at Benatzu site is possible to observe a greater decrease in yield without considering the direct effect of CO_2 and a greater increase in yields considering direct CO_2 effect. This is probably due to the different soil characteristics, particularly related to the greater nutrients availability in Benatzu soil than in Ussana that might explain the higher increase in yield due to direct effect of CO_2.

The mean yield changes projected by the three GCM, considering the direct and indirect effects of CO_2, could range from 3.6 to 7.2 % for 2025, from 13 to 15 % for 2050 and from 17 to 22 % for 2075 for Simeto cultivar at Benatzu site.

At Benatzu site, the mean CV for yields simulated by all GCMs and climate change scenarios, is higher than the CV for yields at Ussana. Also in this site the CV decrease from 43% to 41% respectively for simulation without consider the direct affect of CO_2 and considering the effect of CO_2.

However the yield mean comparison by Student-Newman-Keuls test (Table 4.2.1.2) shows a statistically significant difference in means projected by Hadley only between now and 2075 with mid and high climate change scenarios, without consider the direct effect of CO_2 concentration, and for 2075 with high climate change scenario considering the direct effect of CO_2. NCAR provides significant changes in yield only for 2075 with high climate change scenario without consider CO_2 effect and starting from 2050 considering CO_2 changes. Considering the results obtained with ECHAM, there are not significantly differences by comparing now and future scenarios considering CO_2, while there are significantly differences from now for the mean projected by ECHAM with mid and high climate change scenarios for 2050 and 2075.

Table 4.2.1.1. Changes (%) in yield from now to future periods, with current and future CO_2 concentration, for Hadley, NCAR and ECHAM GCMs and three climate scenarios (low, mid and high) for Simeto at Benatzu site.

		Hadley		NCAR		ECHAM		Mean yield change considering CO_2 increases
		Current CO_2	Changing in CO_2	Current CO_2	Changing in CO_2	Current CO_2	Changing in CO_2	
2025	***low***	-3.3	6.7	-1.4	8.5	-5.0	4.5	**6.6**
	mid	-5.7	7.5	-2.9	10.5	-8.8	3.7	**7.2**
	high	-7.4	3.9	-4.0	7.6	-11.7	-0.6	**3.6**
2050	***low***	-5.3	13.9	-2.9	16.5	-8.2	10.0	**13.5**
	mid	-11.2	13.9	-6.8	19.1	-17.4	6.0	**13.0**
	high	-17.3	15.3	-10.5	23.1	-24.6	6.5	**15.0**
2075	***low***	-5.5	19.2	-4.0	21.2	-11.6	11.7	**17.3**
	mid	-18.1	20.1	-11.5	26.5	-25.8	9.2	**18.6**
	high	-27.1	24.2	-20.2	31.5	-36.2	10.6	**22.1**

Table 4.2.1.2 Mean yield (t ha^{-1}) comparison for now and future periods with different GCMs and climate scenarios for Simeto cultivar at Benatzu site.

		Hadley[a] yield (t ha^{-1})				NCAR[a] yield (t ha^{-1})				ECHAM[a] yield (t ha^{-1})			
		Current CO_2		Changes in CO_2		Current CO_2		Changes in CO_2		Current CO_2		Changes in CO_2	
Now		4.0	c	4.0	a	4.0	a	4.0	d	4.0	E	4.0	a
2025	**Low**	3.9	bc	4.3	ab	4.0	a	4.4	bcd	3.8	De	4.2	a
	Mid	3.8	bc	4.3	ab	3.9	a	4.4	bcd	3.7	De	4.2	a
	High	3.7	bc	4.2	ab	3.8	a	4.3	cd	3.5	Bcde	4.0	a
2050	**Low**	3.8	bc	4.6	ab	3.9	a	4.7	abcd	3.7	Cde	4.4	a
	Mid	3.6	bc	4.6	ab	3.7	ab	4.8	abc	3.3	Bcd	4.3	a
	High	3.3	abc	4.6	ab	3.6	ab	4.9	abc	3.0	Abc	4.3	a
2075	**Low**	3.8	bc	4.8	ab	3.8	a	4.9	abc	3.5	Bcde	4.5	a
	Mid	3.3	ab	4.8	ab	3.5	ab	5.1	ab	3.0	Ab	4.4	a
	High	2.9	a	5.0	b	3.2	b	5.3	a	2.6	a	4.4	a

Means within each group (single GCM and different future periods) sharing the same letter do not differ significantly from one another (Student-Newman-Keuls test at $P \leq 0.05$).

[a] The two groups of yields, with current CO_2 and changes in CO_2 concentration, are evaluated separately.

Anthesis

The Figures 4.2.1.2 *a*, *b*, and c, show the results for climate change impact on anthesis date (difference in days from now to future periods) obtained for different future periods with the three GCMs and three climate change scenarios.

Also in this case, an advancement of the anthesis date occurrences progressively marked is observed for all GCMs, in particular with high climate scenario, but already evident for the period 2025. The anthesis date by 2050 might be about 6 days earlier than under present climate. This trend continues for 2075 time period when duration of the reproductive season might be about 9 days shorter than nowadays. The higher reduction is projected by NCAR, presumably because of it provides the major increase in temperature in particular for the winter and spring months.

Considering the most pessimistic climate change scenarios, the date of anthesis might change from 4 to 14 days in advance respectively for 2025 and 2075 periods.

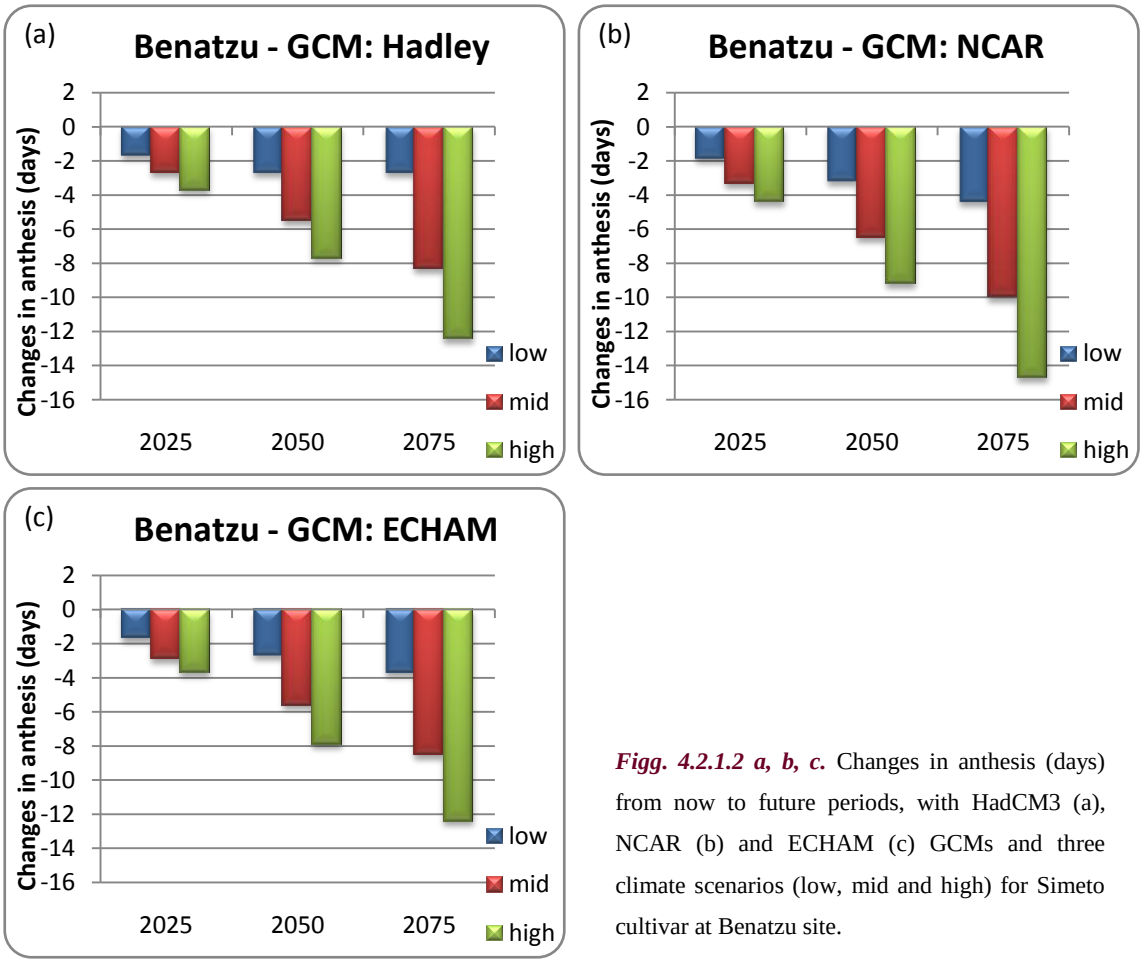

Figg. 4.2.1.2 a, b, c. Changes in anthesis (days) from now to future periods, with HadCM3 (a), NCAR (b) and ECHAM (c) GCMs and three climate scenarios (low, mid and high) for Simeto cultivar at Benatzu site.

Analyzing the results by Student-Newman-Keuls test, the difference from now to future periods are significantly different in most of comparison (see Table 4.2.1.3), both comparing now and future periods and comparing future periods together.

This means that the changes in temperature from now to future periods are likely to significantly change the length of the vegetative phase for wheat, even with the less pessimistic climate scenarios, without evident differences between the three GCMs.

Table 4.2.1.3 Mean anthesis date (dap) comparison for now and future periods with different GCMs and climate scenarios for Simeto cultivar at Benatzu site.

		Hadley		NCAR		ECHAM	
		Anthesis (dap)		Anthesis (dap)		Anthesis (dap)	
Now		128	a	128	a	128	a
2025	**Low**	126	b	126	b	126	b
	Mid	125	bc	125	bc	125	bc
	High	124	c	123	c	124	c
2050	**Low**	125	bc	125	bc	125	bc
	Mid	122	d	121	d	122	d
	High	120	e	119	e	120	e
2075	**Low**	125	bc	123	c	124	c
	Mid	120	e	118	e	119	e
	High	115	f	113	f	115	f

Means within each group (single GCM and different future periods) sharing the same letter do not differ significantly from one another (SNK-test at P≤0.05).

4.2.2 Iride

The Figures 4.2.2.1 *a*, *b*, and *c*, show the results of climate change impact on yield (t ha^{-1}) for Iride cultivar considering, separately for the three GCMs, the climate change scenarios with and without considering CO_2 concentration changes. In the table 4.2.2.1 are reported the correspond changes in terms of percentage from now to future periods.

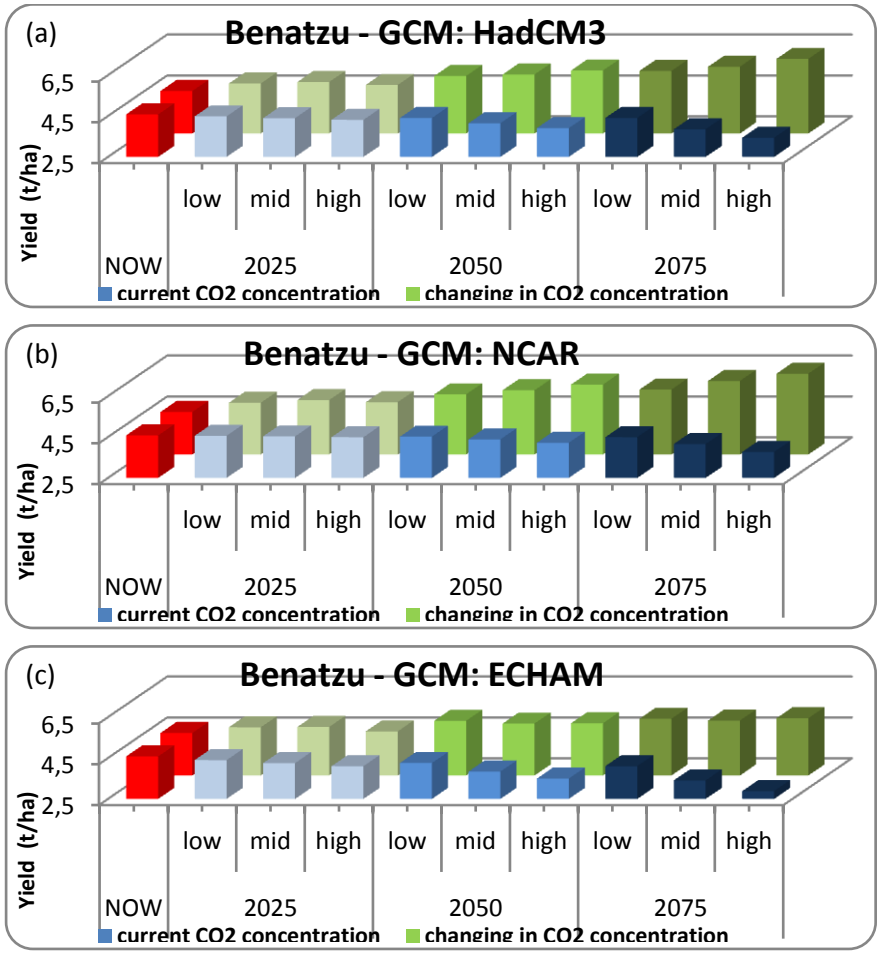

Figg. 4.2.2.1 a, b, c. Changes in yield (t ha^{-1}) from now to future periods, with current and future CO_2 concentration, with Hadley (a), NCAR (b) and ECHAM (c) GCMs and three climate scenarios (low, mid and high) for Iride cultivar at Benatzu site.

As for Simeto, the simulations for Iride at Benatzu site, without consider future increases in CO_2 concentration, show higher decrease in yield for all future periods than those projected for Iride at Ussana site. The reduction in yield are evident for Hadley starting from 2050 e for NCAR starting from 2075, in particular with mid and high climate change scenarios. However, the higher decreases in yield are assumed with ECHAM.

As shown in Table 4.2.2.1, the yield reductions, without consider future changes in CO_2 concentration, are quite modest with NCAR, but may reach -25 % with Hadley and -37% with ECHAM, for 2075 considering high climate change scenario.

The simulations taking into account the projected changes in CO_2 concentration for future periods, with the three different climate scenarios, show a general increase in yield from now to future periods. The increases in yield are progressive from now to future periods with all GCMs, especially with Hadley and NCAR, and more content with ECHAM. This is because the indirect effect of the increased CO_2, that causes changes in the climate regime projected by ECHAM, is so strong that cannot be offset by expected increases in CO_2 atmospheric concentration.

The results are very similar to those obtained for Simeto at this site, but the increases in mean yield are higher for Iride than Simeto considering the changes in CO_2 concentration for all future periods, and climate change scenarios.

The mean yield changes projected by the three GCM, considering the direct and indirect effects of CO_2, could range from 6.2 to 9.6 % for 2025, from 15.9 to 20.5 % for 2050 and from 20.2 to 30.3 % for 2075 for Iride cultivar at Benatzu site.

Compared to results obtained for Iride at Ussana site, it is possible to observe a greater increase in yields considering direct and indirect CO_2 effect than those projected for Ussana site. As in the Simeto response, this is probably due to the differences in soil characteristics, particularly related to the greater nutrients availability in Benatzu soil than in Ussana. This might explain the higher increase in yield due to direct effect of CO_2 at Benatzu site.

Also for Iride at Benatzu site, the mean CV for yields simulated by all GCMs and climate change scenarios, decreases from 39% to 34% respectively for simulation without consider the direct affect of CO_2 and considering the effect of CO_2.

However the yield mean comparison by Student-Newman-Keuls test (Table 4.2.2.2) shows a statistically significant difference in means projected by Hadley only between now and 2075 with mid and high climate scenario, without consider the direct effect of CO_2 concentration, and starting from 2050 considering the direct effect of CO_2. Considering the results obtained with NCAR, there is significantly difference by comparing now and future scenarios without consider CO_2 only for 2075 with high climate change scenario, while there are significantly differences from now for the mean projected by NCAR for the mean yields projected for 2050 and 2075 with all climate change scenario. In the opposite the means projected by ECHAM do not show a significantly change from now to future periods considering CO_2 effect, while without considering CO_2 increases, show a significant difference from now to 2050 with mid and high climate scenario and to 2075 with mid and high climate scenarios.

Table 4.2.2.1. Changes (%) in yield from now to future periods, with current and future CO_2 concentration, for Hadley, NCAR and ECHAM GCMs and three climate scenarios (low, mid and high) for Iride at Benatzu site.

		Hadley		NCAR		ECHAM		Mean yield change considering CO_2 increases
		Current CO_2	Changing in CO_2	Current CO_2	Changing in CO_2	Current CO_2	Changing in CO_2	
2025	***low***	-2.1	8.0	-0.4	9.9	-4.0	6.1	**8.0**
	mid	-4.0	9.6	-1.1	12.7	-7.2	6.5	**9.6**
	high	-5.8	6.4	-1.9	10.5	-10.4	1.7	**6.2**
2050	***low***	-3.8	16.0	-1.3	18.8	-7.0	13.0	**15.9**
	mid	-9.4	17.6	-4.3	23.2	-16.2	10.0	**17.0**
	high	-14.6	21.9	-7.9	29.3	-23.7	10.4	**20.5**
2075	***low***	-3.8	21.5	-1.9	24.0	-10.4	15.2	**20.2**
	mid	-15.9	25.9	-9.2	33.2	-25.7	13.2	**24.1**
	high	-24.9	34.3	-17.7	40.9	-37.1	15.7	**30.3**

Table 4.2.2.2 Mean yield (t ha^{-1}) comparison for now and future periods with different GCMs and climate scenarios for Iride cultivar at Benatzu site.

		Hadley[a] yield (t ha^{-1})				NCAR[a] yield (t ha^{-1})				ECHAM[a] yield (t ha^{-1})			
		Current CO_2		Changes in CO_2		Current CO_2		Changes in CO_2		Current CO_2		Changes in CO_2	
Now		4.6	a	4.6	d	4.6	a	4.6	d	4.6	a	4.6	a
2025	**Low**	4.5	ab	4.9	cd	4.6	a	5.0	cd	4.4	ab	4.9	a
	Mid	4.4	ab	5.0	bcd	4.5	a	5.2	cd	4.3	ab	4.9	a
	High	4.3	ab	4.9	cd	4.5	a	5.1	cd	4.1	ab	4.7	a
2050	**Low**	4.4	ab	5.3	bc	4.5	a	5.4	bc	4.3	ab	5.2	a
	Mid	4.1	ab	5.4	bc	4.4	a	5.6	bc	3.8	bc	5.0	a
	High	3.9	abc	5.6	abc	4.2	ab	5.9	ab	3.5	c	5.1	a
2075	**Low**	4.4	ab	5.6	abc	4.5	a	5.7	bc	4.1	ab	5.3	a
	Mid	3.9	bc	5.8	ab	4.2	ab	6.1	ab	3.4	c	5.2	a
	High	3.4	c	6.1	a	3.8	b	6.5	a	2.9	d	5.3	a

Means within each group (single GCM and different future periods) sharing the same letter do not differ significantly from one another (Student-Newman-Keuls test at $P \leq 0.05$).

[a] The two groups of yields, with current CO_2 and changes in CO_2 concentration, are evaluated separately.

Anthesis

The Figures 4.2.2.2 *a*, *b*, and c, show the results for climate change impact on anthesis date obtained for different future periods with the three GCMs and three climate change scenarios.

The effect of a shortening of the sowing-anthesis phase duration, also for this case, is already evident for the period 2025, and more with all the other cases. The anthesis date by 2050 might happen about 6 days before than under present climate. This trend continues for 2075 time period when the anthesis stage might occur about 9 days earlier than nowadays. As for Simeto, the higher reduction is projected by NCAR GCM, because of NCAR provides the major increase in temperature in particular for the winter and spring months.

Considering the most pessimistic climate scenarios, the date of anthesis might change from 5 to 15 days in advance respectively for 2025 and 2075 periods.

Generally, for Iride is expected a more evident reduction in the anthesis phase duration than in Simeto also for Benatzu site.

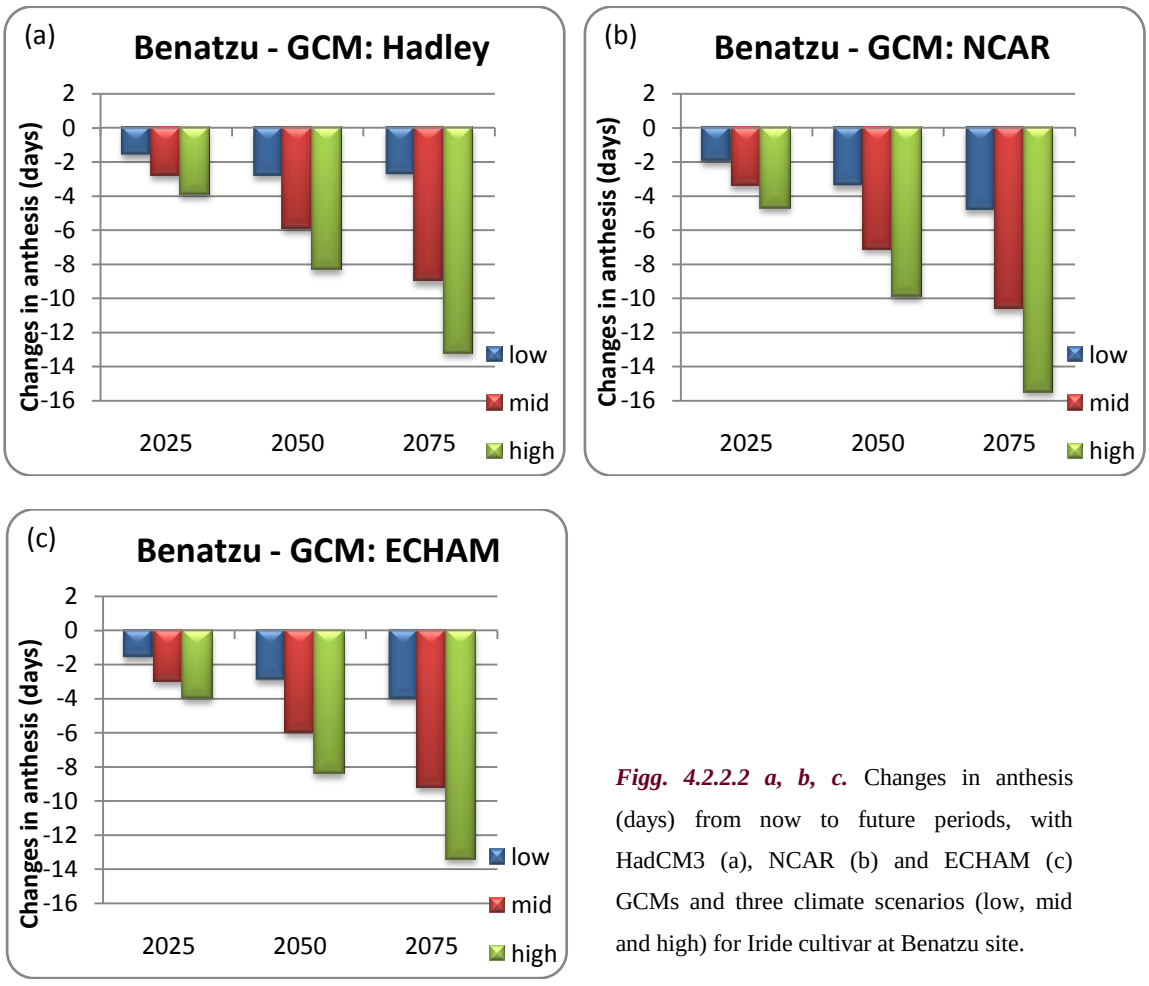

Figg. 4.2.2.2 a, b, c. Changes in anthesis (days) from now to future periods, with HadCM3 (a), NCAR (b) and ECHAM (c) GCMs and three climate scenarios (low, mid and high) for Iride cultivar at Benatzu site.

The Student-Newman-Keuls test, give significant differences from now to future periods in most of comparison (see Table 4.2.2.3), both comparing now and future periods and comparing future periods together.

This confirm that the expected means that the changes in temperature from now to future periods are likely to significantly change the time occurrence for wheat anthesis, even with the less pessimistic climate scenarios, also for Iride cultivar.

Table 4.2.2.3 Mean anthesis date (dap) comparison for now and future periods with different GCMs and climate scenarios for Iride cultivar at Benatzu site.

		Hadley		NCAR		ECHAM	
		Anthesis (dap)		Anthesis (dap)		Anthesis (dap)	
Now		123	a	123	a	123	a
2025	**Low**	121	b	121	b	121	b
	Mid	120	bc	120	bc	120	bc
	High	119	c	118	c	119	c
2050	**Low**	120	bc	120	bc	120	bc
	Mid	117	d	116	d	117	d
	High	115	e	113	e	115	e
2075	**Low**	120	bc	118	c	119	c
	Mid	114	e	112	e	114	e
	High	110	f	107	f	110	f

Means within each group (single GCM and different future periods) sharing the same letter do not differ significantly from one another (SNK-test at $P \leq 0.05$).

4.3 OTTAVA

4.3.1 Simeto

Yield

The Figures 4.3.1.1 *a*, *b*, and *c*, show the results of climate change impact on yield (t ha^{-1}) for Simeto cultivar considering, separately for the three GCMs, the climate scenario with and without considering CO_2 concentration changes. In the table 4.3.1.1 are reported the correspondent changes in terms of percentage from now to future periods.

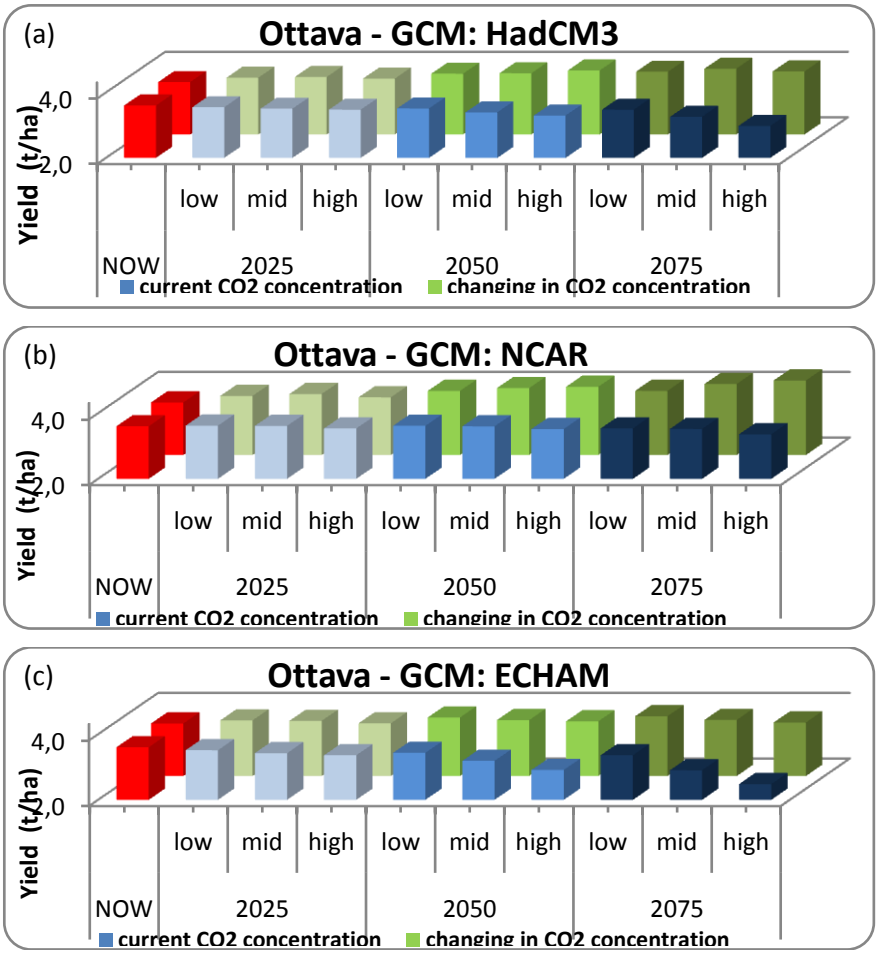

Figg. 4.3.1.1 a, b, c. Changes in yield (t ha^{-1}) from now to future periods, with current and future CO_2 concentration, with Hadley (a), NCAR (b) and ECHAM (c) GCMs and three climate scenarios (low, mid and high) for Simeto cultivar at Ottava site.

The results of simulations for Simeto at Ottava site, show the same trend observed for the other sites but with smaller variations in mean yields. Without consider future increases in CO_2 concentration, it is possible to observe a decrease in yield for 2025 close to zero, that could reach -

7% for simulations with ECHAM for high climate change scenario. The reduction in yield are evident for Hadley starting from 2050 e for NCAR starting from 2075, in particular with high climate change scenarios. However, the higher decreases in yield are assumed with ECHAM, that could reach -31% respect to now.

As shown in Table 4.3.1.1, the yield reductions, without consider future changes in CO_2 concentration, are quite low with NCAR, but may reach -17% with Hadley and -31% with ECHAM, for 2075 considering high climate change scenario.

The simulations taking into account the projected changes in CO_2 concentration for future periods, with the three different climate scenarios, show a general increases in yield from now to future periods, but lower than that provided for Simeto in the other sites. The higher increases in yield is projected by NCAR (17%) for 2075 with high climate change scenario, and the lower increase is projected by ECHAM for all future periods.

The mean yield changes projected by the three GCM, considering the direct and indirect effects of CO_2, could range from 2.5 to 4.6 % for 2025, from 7.3 to 8.3 % for 2050 and from 8.3 to 10 % for 2075. This may be probably due to the lower annual values of solar radiation at this site.

The mean CV for yields simulated by all GCMs and climate change scenarios, decreases from 319% to 29% respectively for simulation without consider the direct affect of CO_2 and considering the effect of CO_2.

Table 4.3.1.1 Changes (%) in yield from now to future periods, with current and future CO_2 concentration, for Hadley, NCAR and ECHAM GCMs and three climate scenarios (low, mid, high) for Simeto at Ottava site.

		Hadley		NCAR		ECHAM		Mean yield change considering CO_2 increases
		Current CO_2	Changing in CO_2	Current CO_2	Changing in CO_2	Current CO_2	Changing in CO_2	
2025	***low***	-1.5	3.7	0.5	5.5	-2.5	2.6	**4.0**
	mid	-2.7	4.3	0.3	7.2	-5.0	2.2	**4.6**
	high	-3.6	3.0	-1.9	4.3	-6.8	0.1	**2.5**
2050	***low***	-2.5	7.1	0.4	9.8	-4.7	5.1	**7.3**
	mid	-5.9	7.5	-0.1	12.1	-11.5	2.8	**7.5**
	high	-8.6	9.9	-2.4	13.3	-19.2	1.8	**8.3**
2075	***low***	-3.6	8.8	-1.9	9.8	-6.8	6.1	**8.3**
	mid	-9.6	11.3	-2.3	15.6	-19.5	3.0	**10.0**
	high	-17.3	9.0	-6.8	18.6	-31.2	0.8	**9.5**

Indeed the yield mean comparison by Student-Newman-Keuls test (Table 4.3.1.2) shows a statistically significant difference in means projected by Hadley, without consider the direct effect of CO_2 concentration, only between now and 2075 with high climate scenario, and considering the direct effect of CO_2 there are no significant changes in the mean yields for future periods compared to now. Considering the results obtained with NCAR, there are not significantly differences by comparing now and future scenarios without consider CO_2, while there are significantly differences from now for the mean projected by NCAR for 2075 with mid and high climate change scenarios.

In the opposite the mean projected by ECHAM show a significantly change from now to 2050, with high climate scenario and to 2075 with mid and high climate scenarios, while without considering CO_2 increases, there are not significantly differences from now to future periods.

Table 4.3.1.2 Mean yield (t ha^{-1}) comparison for now and future periods with different GCMs and climate scenarios for Simeto cultivar at Ottava site.

		Hadley[a]				**NCAR[a]**				**ECHAM[a]**			
		yield (t ha^{-1})				**yield (t ha^{-1})**				**yield (t ha^{-1})**			
		Current CO_2		**Changes in CO_2**		**Current CO_2**		**Changes in CO_2**		**Current CO_2**		**Changes in CO_2**	
Now		3.6	a	3.6	a	3.6	a	3.6	c	3.6	A	3.6	A
2025	**Low**	3.6	a	3.7	a	3.6	a	3.8	abc	3.5	A	3.7	A
	Mid	3.5	a	3.8	a	3.6	a	3.9	abc	3.4	A	3.7	A
	High	3.5	a	3.7	a	3.5	a	3.8	bc	3.4	A	3.6	A
2050	**Low**	3.5	a	3.9	a	3.6	a	4.0	abc	3.4	A	3.8	A
	Mid	3.4	a	3.9	a	3.6	a	4.0	abc	3.2	Ab	3.7	A
	High	3.3	ab	4.0	a	3.5	a	4.1	abc	2.9	B	3.7	A
2075	**Low**	3.5	a	3.9	a	3.5	a	4.0	abc	3.4	A	3.8	A
	Mid	3.3	ab	4.0	a	3.5	a	4.2	ab	2.9	B	3.7	A
	High	3.0	b	3.9	a	3.4	a	4.3	a	2.5	C	3.6	A

Means within each group (single GCM and different future periods) sharing the same letter do not differ significantly from one another (Student-Newman-Keuls test at $P \leq 0.05$).

[a] The two groups of yields, with current CO_2 and changes in CO_2 concentration, are evaluated separately.

Anthesis

The Figures 4.3.1.2 *a*, *b*, and c, show the results for climate change impact on anthesis date (difference in days from present to future periods) obtained for different future periods with the three GCMs and three climate change scenarios.

As with other experimental sites, it is possible to observe a shortening of the anthesis phase duration from sowing already for the period 2025 with all GCMs, in particular with high climate scenario. The date of anthesis in 2050 might be about 5 days before than under present climate.

This trend continues for 2075 time period when duration of the season might be about 8 days shorter than nowadays. The lower shortening of the anthesis phase provided for Ottava for 2075 may be justified considering the higher mean annual value of temperature that characterized this site. As for the other sites the higher reduction is projected by NCAR, because of NCAR provides the major increase in temperature in particular for the winter and spring months.

Considering the most pessimistic climate scenarios, the date of anthesis might change from 4 to 12 days in advance respectively for 2025 and 2075 periods.

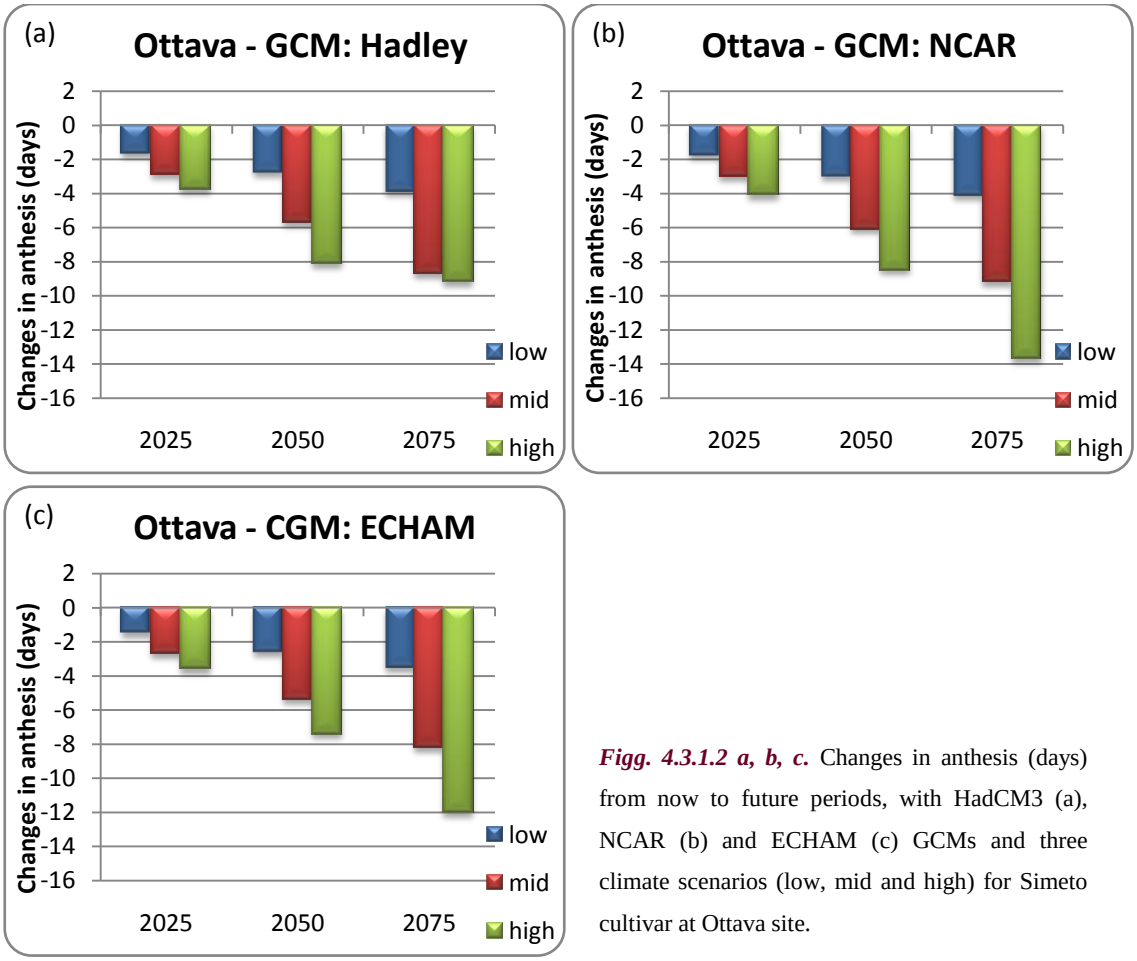

Figg. 4.3.1.2 a, b, c. Changes in anthesis (days) from now to future periods, with HadCM3 (a), NCAR (b) and ECHAM (c) GCMs and three climate scenarios (low, mid and high) for Simeto cultivar at Ottava site.

Analysis by Student-Newman-Keuls test, show significant differences from now to future periods in most of comparison (see Table 4.3.1.3), both comparing now and future periods and comparing future periods together.

This means that the changes in temperature from now to future periods, despite involving minor's reductions in the duration of the anthesis phase, are still likely to significantly change the length of the reproductive period for wheat, even with the less pessimistic climate scenarios, without evident differences between the three GCMs.

Table 4.3.1.3 Mean anthesis date (dap) comparison for now and future periods with different GCMs and climate scenarios for Simeto cultivar at Ottava site.

		Hadley		NCAR		ECHAM	
		Anthesis (dap)		Anthesis (dap)		Anthesis (dap)	
Now		136	a	136	a	136	a
2025	**Low**	134	b	134	b	134	b
	Mid	133	bc	133	bc	133	bc
	High	132	c	132	c	133	c
2050	**Low**	133	bc	133	bc	134	bc
	Mid	130	d	130	d	131	d
	High	128	e	128	e	129	e
2075	**Low**	132	c	132	c	133	c
	Mid	127	e	127	e	128	e
	High	127	e	122	f	124	f

Means within each group (single GCM and different future periods) sharing the same letter do not differ significantly from one another (SNK-test at $P \leq 0.05$).

4.3.2 Iride

Yield

The the results of climate change impact on yield (t ha^{-1}) for Iride cultivar are shown in Figures 4.3.2.1 *a*, *b*, and *c*, considering, separately for the three GCMs, the climate change scenarios with and without considering CO_2 concentration changes in atmosphere. In the Table 4.3.2.1 are reported the correspond changes in terms of percentage from now to future periods.

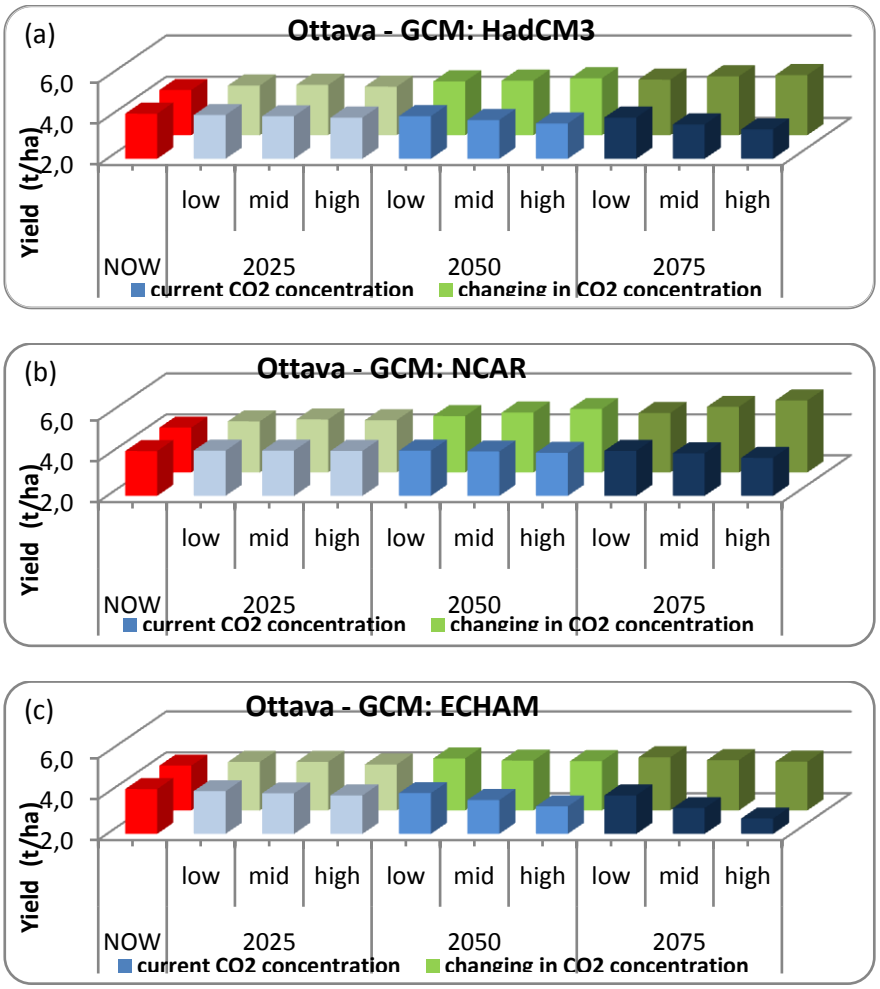

Figg. 4.3.2.1 a, b, c. Changes in yield (t ha^{-1}) from now to future periods, with current and future CO_2 concentration, with Hadley (a), NCAR (b) and ECHAM (c) GCMs and three climate scenarios (low, mid and high) for Iride cultivar at Ottava site.

The simulations for Iride at Ottava site, without consider future increases in CO_2 concentration, show decrease in yield for 2025 close to zero for all GCMs, and could reach -7.4% only for simulation with ECHAM and high climate change scenario. The reduction in yield is evident for Hadley starting from 2050 e for NCAR starting from 2075, in particular with high

climate change scenarios. However the higher decreases in yield are assumed with ECHAM for all three future periods.

As shown in Table 4.3.2.1, the yield reductions, without consider future changes in CO_2 concentration, are lower with NCAR, and may reach -18 % with Hadley and -34% with ECHAM, for 2075 considering high climate change scenario.

The simulations taking into account the projected changes in CO_2 concentration for future periods, with the three different climate scenarios, show a general increase in yield from now to future periods. The increases in yield are progressive with all GCMs, especially with NCAR (32%) and Hadley (17%), but are less than 5% with ECHAM.

The results are very similar to those obtained for Simeto at this site, but the increases in mean yield are slightly higher for Iride than Simeto considering the changes in CO_2 concentration for all future periods.

The mean yield changes projected by the three GCM for Iride cultivar at Ottava site, considering the direct and indirect effects of CO_2, could range from 4.6 to 6.6 % for 2025, from 10.6 to 13.5 % for 2050 and from 13 to 17.9 % for 2075.

Also for Iride at Ottava site, the mean CV for yields simulated by all GCMs and climate change scenarios, decreases from 33% to 30% respectively for simulation without consider the direct affect of CO_2 and considering the effect of CO_2.

Table 4.3.2.1. Changes (%) in yield from now to future periods, with current and future CO_2 concentration, for Hadley, NCAR and ECHAM GCMs and three climate scenarios (low, mid and high) for Iride at Ottava site.

		Hadley		NCAR		ECHAM		Mean yield change considering CO_2 increases
		Current CO_2	Changing in CO_2	Current CO_2	Changing in CO_2	Current CO_2	Changing in CO_2	
2025	***low***	-1.6	5.2	0.5	7.3	-2.5	4.3	**5.6**
	mid	-3.0	6.0	0.5	9.6	-5.0	4.4	**6.6**
	high	-4.6	3.9	0.2	8.6	-7.4	1.3	**4.6**
2050	***low***	-2.8	9.9	0.5	13.5	-4.8	8.4	**10.6**
	mid	-7.4	10.9	-0.5	17.5	-12.8	5.9	**11.5**
	high	-11.4	13.6	-2.0	21.7	-20.3	5.3	**13.5**
2075	***low***	-4.6	12.1	0.2	17.1	-7.4	9.7	**13.0**
	mid	-12.6	15.9	-2.6	24.2	-22.2	6.4	**15.5**
	high	-18.3	17.4	-7.9	31.7	-34.4	4.6	**17.9**

The yield mean comparison by Student-Newman-Keuls test (Table 4.3.2.2) shows a statistically significant difference in means projected by Hadley, without consider the direct effect

of CO_2 concentration, only between now and 2075 with high climate scenario and, considering the direct effect of CO2, for 2075 with mid and high climate change scenario. Considering the results obtained with NCAR, there are not significantly differences by comparing now and future scenarios without consider CO_2, while there are significantly differences from now for the mean projected by NCAR for 2050 and 2075 with all climate change scenarios.

In the opposite the mean projected by ECHAM without considering CO_2 increases, show a significantly change from now to 2050 with high climate scenario and to 2075 with mid and high climate scenarios, while considering CO_2 effect there are not statistically significant differences from now and future periods.

Table 4.3.2.2 Mean yield (t ha^{-1}) comparison for now and future periods with different GCMs and climate scenarios for Iride cultivar at Ottava site.

		Hadley[a]				NCAR[a]				ECHAM[a]			
		yield (t ha^{-1})				yield (t ha^{-1})				yield (t ha^{-1})			
		Current CO_2		Changes in CO_2		Current CO_2		Changes in CO_2		Current CO_2		Changes in CO_2	
Now		4.2	a	4.2	b	4.2	a	4.2	e	4.2	A	4.2	A
2025	**Low**	4.1	a	4.4	ab	4.2	a	4.5	de	4.1	Ab	4.4	A
	Mid	4.1	a	4.4	ab	4.2	a	4.6	cde	4.0	Ab	4.4	A
	High	4.0	a	4.4	ab	4.2	a	4.6	cde	3.9	Ab	4.3	A
2050	**Low**	4.1	a	4.6	ab	4.2	a	4.8	bcd	4.0	Ab	4.5	A
	Mid	3.9	ab	4.7	ab	4.2	a	4.9	bcd	3.7	Bc	4.4	A
	High	3.7	ab	4.8	ab	4.1	a	5.1	abc	3.3	C	4.4	A
2075	**Low**	4.0	a	4.7	ab	4.2	a	4.9	bcd	3.9	Ab	4.6	A
	Mid	3.7	ab	4.9	a	4.1	a	5.2	ab	3.3	C	4.5	A
	High	3.4	b	4.9	a	3.9	a	5.5	a	2.8	D	4.4	A

Means within each group (single GCM and different future periods) sharing the same letter do not differ significantly from one another (Student-Newman-Keuls test at $P \leq 0.05$).

[a] The two groups of yields, with current CO_2 and changes in CO_2 concentration, are evaluated separately.

Anthesis

The Figures 4.3.2.2 *a*, *b*, and c, show the results for climate change impact on anthesis date (difference in days from now to future periods) obtained for different future periods with the three GCMs and three climate change scenarios.

As already observed for the other sites it is possible to observe a shortening of the anthesis phase duration already for the period 2025 with all GCMs. This trend continues for 2050 time period when duration of the vegetation season might be about 6 days shorter than nowadays and

for 2075 time period when duration of the vegetation season might be about 9 days shorter than nowadays.

As for Simeto, the higher reduction is projected by NCAR, but for Iride is expected a little bit higher reduction in anthesis phase duration than Simeto at Ottava site.

Considering the most pessimistic climate scenarios, the date of anthesis might change from 4 to 13 days in advance respectively for 2025 and 2075 periods.

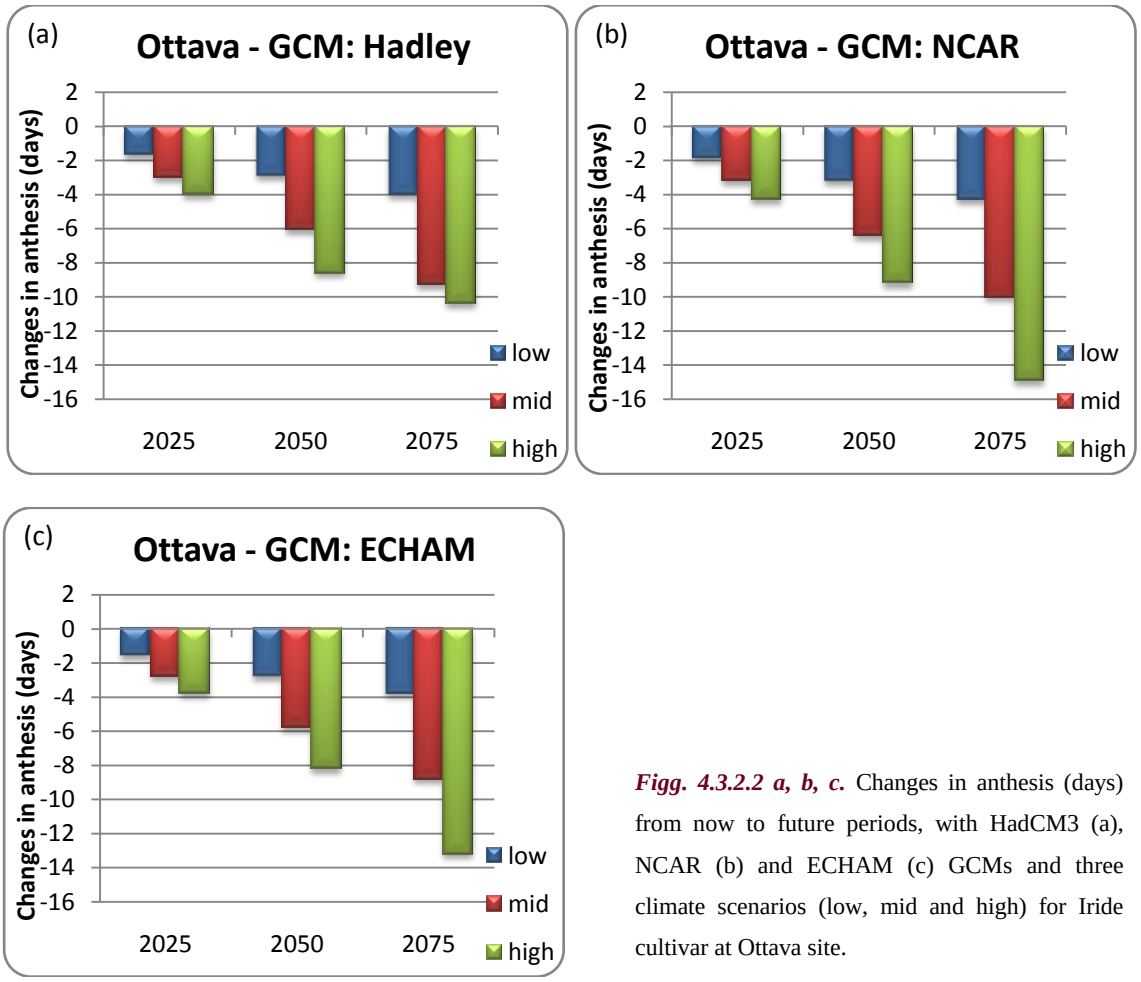

Figg. 4.3.2.2 a, b, c. Changes in anthesis (days) from now to future periods, with HadCM3 (a), NCAR (b) and ECHAM (c) GCMs and three climate scenarios (low, mid and high) for Iride cultivar at Ottava site.

Also for Iride the mean anthesis date analyzed by Student-Newman-Keuls test, show significant differences from now to future periods in most of comparison (see Table 4.3.2.3), both comparing now and future periods and comparing future periods together.

Table 4.3.2.3 Mean anthesis date (dap) comparison for now and future periods with different GCMs and climate scenarios for Iride cultivar at Ottava site.

		Hadley		NCAR		ECHAM	
		Anthesis (dap)		Anthesis (dap)		Anthesis (dap)	
Now		128	a	128	a	128	a
2025	**Low**	126	bc	126	b	126	b
	Mid	125	bc	124	bc	125	bc
	High	124	b	123	c	124	c
2050	**Low**	125	c	124	bc	125	bc
	Mid	122	d	121	d	122	d
	High	119	c	118	e	119	e
2075	**Low**	124	ef	123	c	124	c
	Mid	118	f	118	e	119	e
	High	117	e	113	f	114	f

Means within each group (single GCM and different future periods) sharing the same letter do not differ significantly from one another (SNK-test at $P \leq 0.05$).

4.4 SANTA LUCIA

4.4.1 Simeto

Yield

The Figures 4.4.1.1 *a*, *b*, and *c*, show the results of climate change impact on yield (t ha^{-1}) for Simeto cultivar considering, separately for the three GCMs, the climate scenarios with and without considering CO_2 concentration changes in atmosphere. In the Table 4.4.1.1 are reported the correspond changes in terms of percentage from now to future periods.

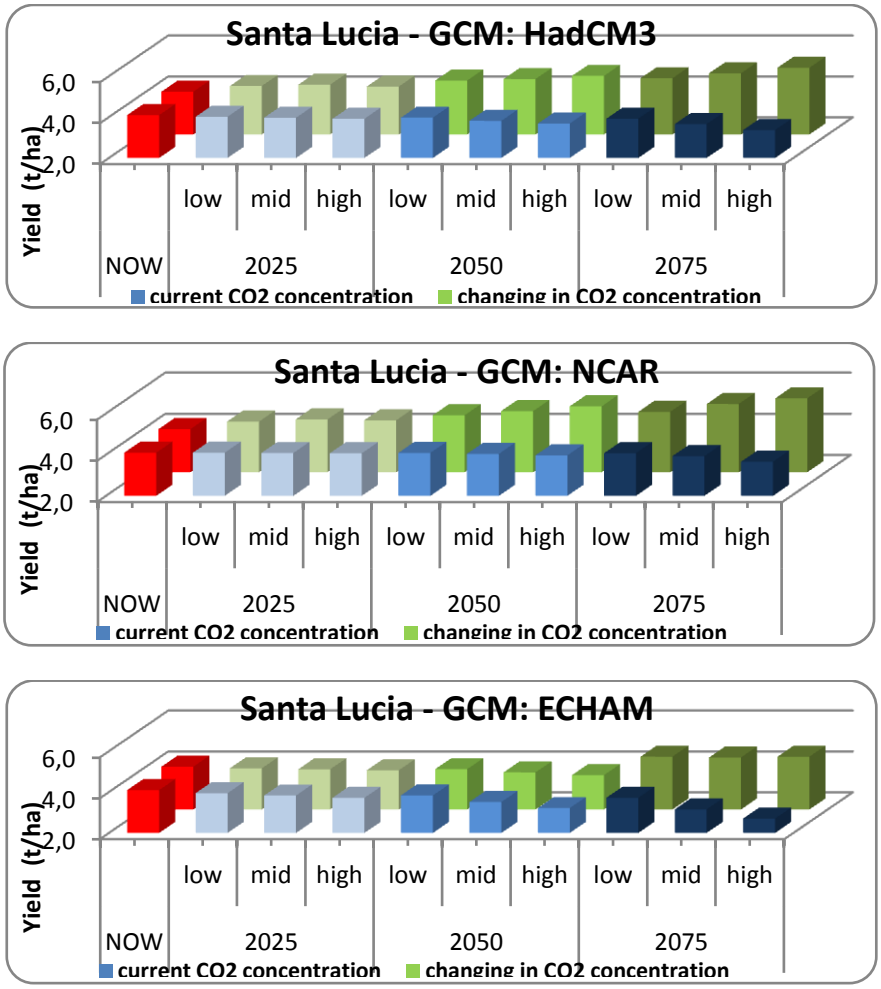

Figg. 4.4.1.1 a, b, c. Changes in yield (t ha^{-1}) from now to future periods, with current and future CO_2 concentration, with Hadley (a), NCAR (b) and ECHAM (c) GCMs and three climate scenarios (low, mid and high) for Simeto cultivar at Santa Lucia site.

For Simeto at Santa Lucia experimental site, simulations show that, without consider future increases in CO_2 concentration, the magnitude of decrease in yield depends on the GCM, climate

scenario and period considered: close to zero for NCAR and Hadley in 2025, while is more evident for simulation with ECHAM for high climate change scenario (-9%). The reductions in yield are evident for Hadley starting from 2050 e for NCAR starting from 2075, in particular with mid and high climate change scenarios. However, the higher decreases in yield are projected by ECHAM for all three future periods.

As evident in Table 4.4.1.1, the yield reductions, without consider future changes in CO_2 concentration, are quite low with NCAR (-11%), but may reach -18 % with Hadley and -34% with ECHAM, for 2075 considering high climate change scenario.

The simulations taking into account the projected changes in CO_2 concentration for future periods, with the three different climate scenarios, show a general increase in yield from now to future periods. The increases in yield are progressive from now to future periods with all GCMs, especially with Hadley and NCAR, and more moderate with ECHAM. This is probably due to the fact that the indirect effect of the increased CO_2 projected by ECHAM is so strong that cannot be offset by the expected increases in CO_2 atmospheric concentration.

The results are very similar to those obtained for Simeto in the other experimental sites.

The mean yield changes projected by the three GCMs, considering the direct and indirect effects of CO_2, could range from 4 to 5.6 % for 2025, from 8.9 to 12 % for 2050 and from 16.1 to 25.7 % for 2075 for Simeto at Santa Lucia site.

Table 4.4.1.1. Changes (%) in yield from now to future periods, with current and future CO_2 concentration, for Hadley, NCAR and ECHAM GCMs and three climate scenarios (low, mid and high) for Simeto at Santa Lucia site.

		Hadley		NCAR		ECHAM		Mean yield change considering CO_2 increases
		Current CO_2	Changing in CO_2	Current CO_2	Changing in CO_2	Current CO_2	Changing in CO_2	
2025	***low***	-1.9	6.8	0.0	8.9	-3.7	-1.9	4.6
	mid	-3.1	8.4	-0.4	11.5	-6.5	-3.1	5.6
	high	-4.4	6.1	-0.7	10.4	-9.2	-4.4	4.0
2050	***low***	-3.0	13.3	-0.2	16.4	-6.3	-3.0	8.9
	mid	-6.8	15.1	-1.4	21.4	-14.2	-6.8	9.9
	high	-10.1	18.9	-3.2	27.0	-21.5	-10.1	12.0
2075	***low***	-4.4	16.0	-0.7	20.4	-9.2	11.9	16.1
	mid	-10.7	21.9	-4.1	29.8	-23.0	10.9	20.9
	high	-17.9	28.6	-10.8	36.5	-34.0	11.8	25.7

The Student-Newman-Keuls test (Table 4.4.1.2) shows a statistically significant difference in means projected by Hadley only between now and 2075 with high climate scenario, without consider the direct effect of CO_2 concentration, and starting from 2050 considering the direct effect of CO_2. Considering the results obtained with NCAR, there are not significantly differences by comparing now and future scenarios without consider direct effect of CO_2, while there are significantly differences from now for the mean projected by NCAR for 2050 and 2075 with all climate change scenarios.

Conversely, the means projected by ECHAM, without consider the direct effect of CO_2, show a significantly decrease in 2050 with high climate scenario and in 2075 with mid and high climate scenarios, while, considering both direct and indirect effect of CO_2, the means projected by ECHAM for all future periods with all climate change scenarios show no significant differences respect to actual .

The mean CV for yields simulated by all GCMs and climate change scenarios, decreases from 39% to 33% respectively for simulation without consider the direct affect of CO_2 and considering the effect of CO_2.

Table 4.4.1.2 Mean yield (t ha^{-1}) comparison for now and future periods with different GCMs and climate scenarios for Simeto cultivar at Santa Lucia site.

		Hadley[a]				**NCAR[a]**				**ECHAM[a]**			
		yield (t ha^{-1})				**yield (t ha^{-1})**				**yield (t ha^{-1})**			
		Current CO_2		**Changes in CO_2**		**Current CO_2**		**Changes in CO_2**		**Current CO_2**		**Changes in CO_2**	
Now		4.1	a	4.1	d	4.1	a	4.1	d	4.1	a	4.1	A
2025	**Low**	4.0	ab	4.4	cd	4.1	a	4.5	cd	3.9	a	4.3	A
	Mid	4.0	ab	4.4	bcd	4.1	a	4.6	cd	3.8	a	4.3	A
	High	4.0	ab	4.3	cd	4.1	a	4.5	cd	3.7	ab	4.2	A
2050	**Low**	4.0	ab	4.6	bcd	4.1	a	4.8	bc	3.8	a	4.5	A
	Mid	3.8	ab	4.7	abc	4.0	a	5.0	bc	3.5	abcd	4.4	A
	High	3.7	ab	4.9	abc	4.0	a	5.2	ab	3.2	bd	4.4	A
2075	**Low**	3.9	ab	4.8	abc	4.1	a	4.9	bc	3.7	abc	4.6	A
	Mid	3.7	ab	5.0	ab	4.0	a	5.3	ab	3.2	bd	4.5	A
	High	3.4	b	5.3	a	3.7	a	5.6	a	2.7	e	4.6	A

Means within each group (single GCM and different future periods) sharing the same letter do not differ significantly from one another (Student-Newman-Keuls test at $P \leq 0.05$).

[a] The two groups of yields, with current CO_2 and changes in CO_2 concentration, are evaluated separately.

Anthesis

The Figures 4.4.1.2 *a*, *b*, and c, show the results for climate change impact on anthesis date (difference in days from now to future periods) obtained for different future periods with the three GCMs and three climate change scenarios for Simeto at Santa Lucia site.

As for the other site, it is possible to observe a shortening of the duration of the period between sowing and anthesis phase already for the period 2025 with all GCMs, in particular with high climate change scenario. The anthesis date by 2050 might have an advancement of about 6 days compared to present climate. This trend continues for 2075 time period when duration of the vegetation cycle until flowering might be about 8 days shorter than nowadays. The higher reduction is projected by NCAR.

Considering the most pessimistic climate scenarios, the date of anthesis might change from 4 to 9 days in advance respectively for 2025 and 2075 periods.

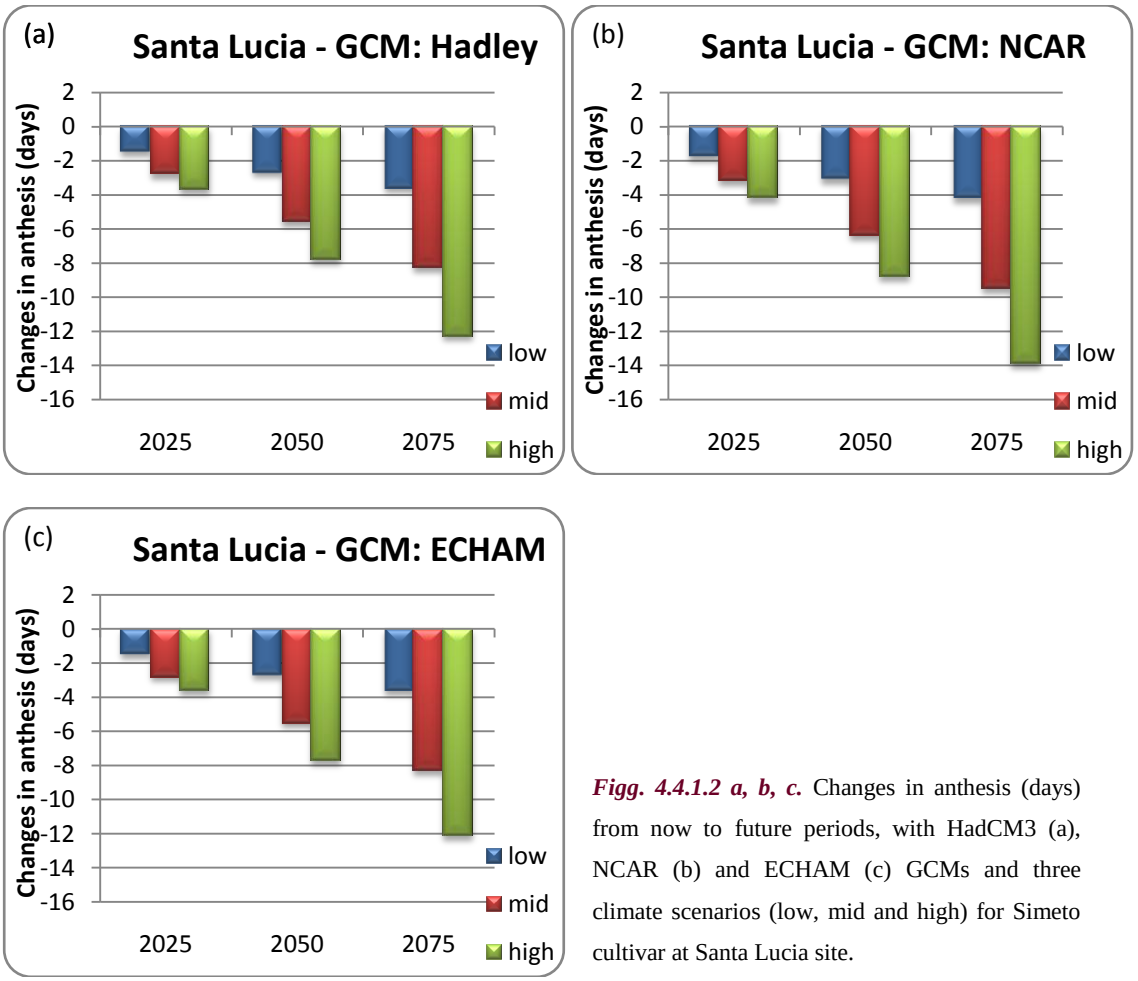

Figg. 4.4.1.2 a, b, c. Changes in anthesis (days) from now to future periods, with HadCM3 (a), NCAR (b) and ECHAM (c) GCMs and three climate scenarios (low, mid and high) for Simeto cultivar at Santa Lucia site.

Analyzing results by Student-Newman-Keuls test, the difference from now to future periods are significantly different in most of comparison (see Table 4.4.1.3), both comparing now and future periods and comparing future periods together.

Table 4.4.1.3 Mean anthesis date (dap) comparison for now and future periods with different GCMs and climate scenarios for Simeto cultivar at Santa Lucia site.

		Hadley		NCAR		ECHAM	
		Anthesis (dap)		Anthesis (dap)		Anthesis (dap)	
Now		127	a	127	a	127	a
2025	**Low**	125	b	125	b	125	b
	Mid	124	bc	124	bc	124	bc
	High	123	c	123	c	123	c
2050	**Low**	124	bc	124	bc	124	bc
	Mid	121	d	120	d	121	d
	High	119	e	118	e	119	e
2075	**Low**	123	c	117	e	123	c
	Mid	119	e	113	f	119	e
	High	115	f	123	c	115	f

Means within each group (single GCM and different future periods) sharing the same letter do not differ significantly from one another (SNK-test at $P \leq 0.05$).

4.4.2 Iride

Yield

The Figures 4.4.2.1 *a*, *b*, and *c*, show the results of climate change impact on yield (t ha^{-1}) for Iride cultivar considering, separately for the three GCMs, the climate scenarios with and without considering CO_2 concentration changes in atmosphere. In the Table 4.4.2.1 are reported the correspond changes in terms of percentage from now to future periods.

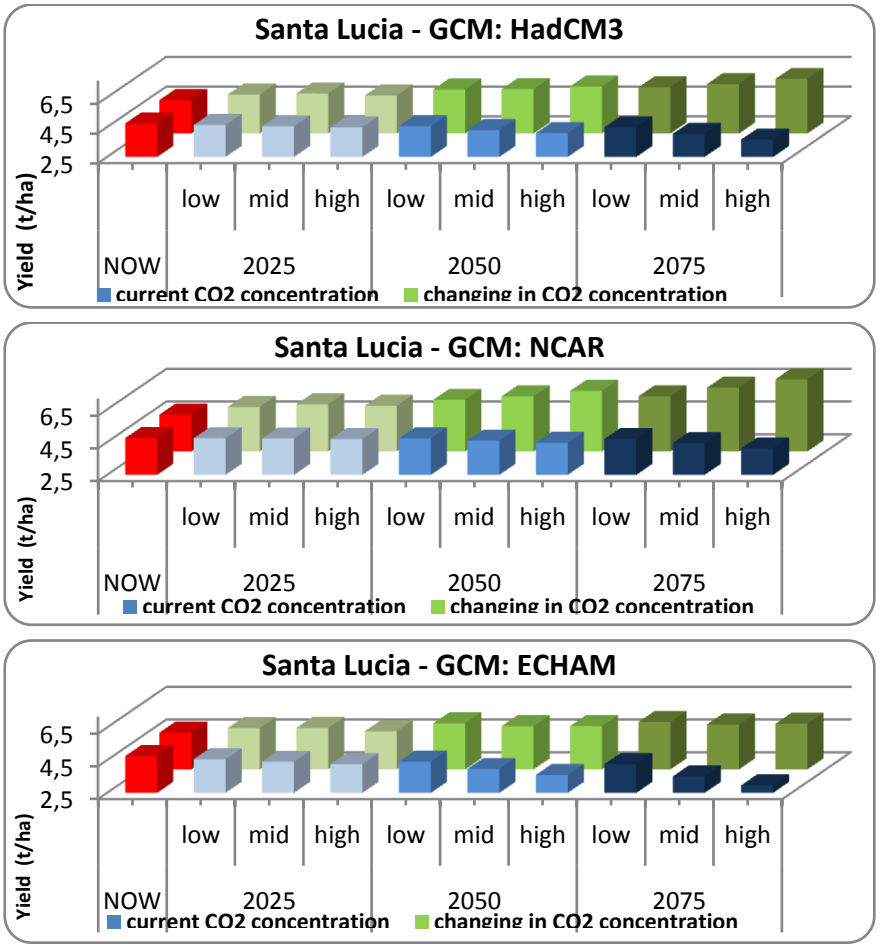

Figg. 4.4.2.1 a, b, c. Changes in yield (t ha^{-1}) from now to future periods, with current and future CO_2 concentration, with Hadley (a), NCAR (b) and ECHAM (c) GCMs and three climate scenarios (low, mid and high) for Iride cultivar at Santa Lucia site.

The results obtained for Iride at Santa Lucia site, without consider future increases in CO_2 concentration, show a decrease in yield for 2025 close to zero for NCAR, while the mean yields projected by Hadley and ECHAM, for high climate change scenario, could reach -5.6% and -10% respectively. The reductions in yield are evident for NCAR only for 2075, in particular with mid

and high climate change scenarios. However, the higher decreases in yield are assumed with ECHAM.

As evident in Table 4.4.2.1, the yield reductions, without consider future changes in CO_2 concentration, are moderates with NCAR, but may reach -22 % with Hadley and -37% with ECHAM, for 2075 considering the most pessimistic climate change scenario.

The simulations taking into account the projected changes in CO_2 concentration for future periods, with the three different climate scenarios, show a general increase in yield from now to future periods. The increases in yield are progressive from now to future periods with all GCMs, especially with Hadley and NCAR, and more moderate with ECHAM. As already noted for Simeto variety, this is probably due to the fact that the indirect effect of the increased CO_2, that causes changes in the climate regime, as projected by ECHAM, is so strong that cannot be offset by expected increases in CO_2 atmospheric concentration.

The results are very similar to those obtained for Simeto at the same site, but the increases in mean yield are higher for Iride than Simeto considering the changes in CO_2 concentration for the high climate change scenarios in all future periods, and in particular with Hadley and ECHAM.

The mean yield changes projected by the three GCM, considering the direct and indirect effects of CO_2, could range from 6.6 to 7.9 % for 2025, from 15.3 to 19.4 % for 2050 and from 18.5 to 28.9 % for 2075 for Iride cultivar at Santa Lucia site.

The mean CV for yields simulated by all GCMs and climate change scenarios, decreases from 42% to 34% respectively for simulation without consider the direct affect of CO_2 and considering the effect of CO_2.

Table 4.4.2.1. Changes (%) in yield from now to future periods, with current and future CO_2 concentration, for Hadley, NCAR and ECHAM GCMs and three climate scenarios (low, mid and high) for Iride at Santa Lucia site.

		Hadley		NCAR		ECHAM		Mean yield change considering CO_2 increases
		Current CO_2	Changing in CO_2	Current CO_2	Changing in CO_2	Current CO_2	Changing in CO_2	
2025	***low***	-2.1	7.9	-0.2	10.0	-4.0	5.9	7.9
	mid	-4.0	9.3	-0.5	13.3	-7.3	6.1	9.6
	high	-5.6	6.4	-1.3	11.4	-10.3	1.9	6.6
2050	***low***	-3.8	15.0	-0.3	19.1	-7.1	12.0	15.3
	mid	-9.4	15.5	-3.3	23.6	-16.6	8.3	15.8
	high	-13.6	19.1	-5.9	30.7	-24.2	8.5	19.4
2075	***low***	-5.6	18.0	-1.3	23.6	-10.3	13.8	18.5
	mid	-14.7	22.6	-6.4	34.8	-26.2	10.6	22.7
	high	-22.8	29.9	-13.4	45.5	-37.7	11.4	28.9

The Student-Newman-Keuls test (Table 4.4.2.2), give significant differences in means projected by Hadley only between now and 2075 with high climate scenario, without consider the direct effect of CO_2 concentration, and starting from 2050 considering the direct effect of CO_2. Considering the results obtained with NCAR, there are not significantly differences by comparing now and future scenarios without consider CO_2, while there are significantly differences from now for the mean projected by NCAR for 2050 and for 2075 with all climate change scenarios.

In the opposite the means projected by ECHAM show a significantly change from now to future periods without consider CO_2 effect already for 2050 with mid and high climate change scenario, and also for mid and high climate change scenarios for 2075, while considering CO_2 increases, there are not significant differences from now to future periods. This is due to the fact that when the mean yields are significantly modified by climate change impact without CO_2, the positive effect of CO_2 fertilization could not be anymore evidence.

Table 4.4.2.2. Mean yield (t ha^{-1}) comparison for now and future periods with different GCMs and climate scenarios for Iride cultivar at Santa Lucia site.

		Hadley[a]				NCAR[a]				ECHAM[a]			
		yield (t ha^{-1})				yield (t ha^{-1})				yield (t ha^{-1})			
		Current CO_2		Changes in CO_2		Current CO_2		Changes in CO_2		Current CO_2		Changes in CO_2	
Now		4.8	a	4.8	c	4.8	a	4.8	e	4.8	a	4.8	A
2025	**Low**	4.7	a	5.1	bc	4.7	a	5.2	de	4.6	ab	5.0	A
	Mid	4.6	a	5.2	bc	4.7	a	5.4	de	4.4	ab	5.0	A
	High	4.5	a	5.1	bc	4.7	a	5.3	de	4.3	ab	4.8	A
2050	**Low**	4.6	a	5.5	abc	4.7	a	5.7	cd	4.4	ab	5.3	A
	Mid	4.3	ab	5.5	abc	4.6	a	5.9	bcd	4.0	bc	5.1	A
	High	4.1	ab	5.7	ab	4.5	a	6.2	bc	3.6	c	5.2	A
2075	**Low**	4.5	a	5.6	ab	4.7	a	5.9	bcd	4.3	ab	5.4	A
	Mid	4.1	ab	5.8	ab	4.4	a	6.4	ab	3.5	c	5.3	A
	High	3.7	b	6.2	a	4.1	a	7.0	a	3.0	d	5.3	A

Means within each group (single GCM and different future periods) sharing the same letter do not differ significantly from one another (Student-Newman-Keuls test at $P \leq 0.05$).

[a] The two groups of yields, with current CO_2 and changes in CO_2 concentration, are evaluated separately.

.

Anthesis

The Figures 4.4.2.2 *a*, *b*, and c, show the results for climate change impact on anthesis date (difference in days from now to future periods) obtained for different future periods with the three GCMs and three climate change scenarios for Iride at Santa Lucia site.

As for the other experimental sites it is possible to observe a shortening of the anthesis phase duration from sowing already for the period 2025 with all GCMs. The anthesis date by 2050 might be about 5 days before than under present climate. This trend continues for 2075 time period when duration of the season might be about 8 days shorter than nowadays. As for Simeto, the higher reduction is projected by NCAR.

Considering the most pessimistic climate scenarios, the date of anthesis might change from 3 to 13 days in advance respectively for 2025 and 2075 periods.

Generally, for Iride is expected a more evident reduction in the anthesis phase duration than in Simeto at Santa Lucia site.

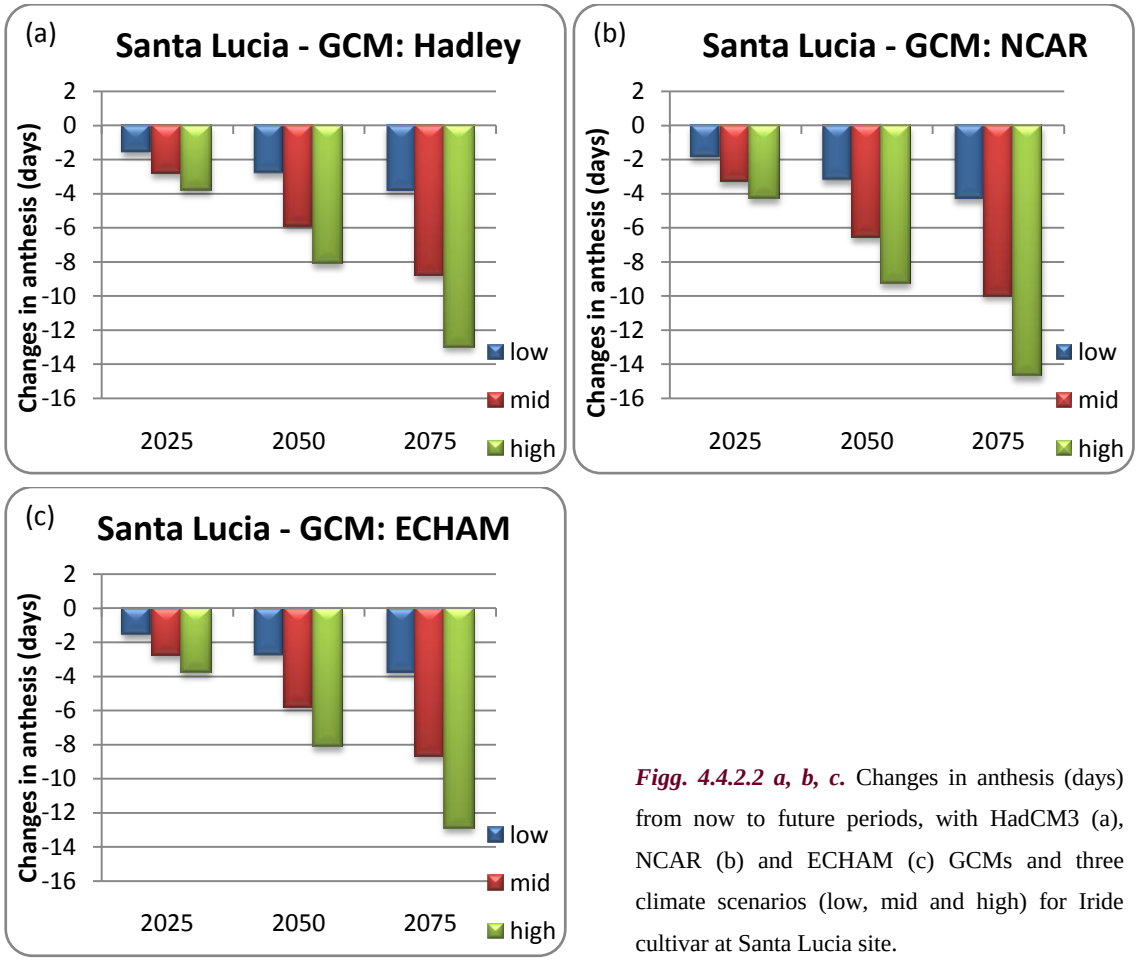

Figg. 4.4.2.2 a, b, c. Changes in anthesis (days) from now to future periods, with HadCM3 (a), NCAR (b) and ECHAM (c) GCMs and three climate scenarios (low, mid and high) for Iride cultivar at Santa Lucia site.

The Student-Newman-Keuls test, give significant differences from now to future periods in most of comparison (see Table 4.4.2.3), both comparing now and future periods and comparing future periods together.

Table 4.4.2.3 Mean anthesis date (dap) comparison for now and future periods with different GCMs and climate scenarios for Iride cultivar at Santa Lucia site.

		Hadley		NCAR		ECHAM	
		Anthesis (dap)		Anthesis (dap)		Anthesis (dap)	
Now		123	a	123	a	123	a
2025	**Low**	122	b	122	b	122	b
	Mid	121	bc	120	bc	121	bc
	High	120	c	119	c	120	c
2050	**Low**	121	bc	120	bc	121	bc
	Mid	118	d	117	d	118	d
	High	115	e	114	e	115	e
2075	**Low**	120	c	119	c	120	c
	Mid	115	e	113	e	115	e
	High	110	f	109	f	111	f

Means within each group (single GCM and different future periods) sharing the same letter do not differ significantly from one another (SNK-test at $P \leq 0.05$).

5. ADAPTATION STRATEGIES EVALUATION

For the evaluation of the possible application of adaptation strategies for durum wheat, in this thesis a simple experiment was performed. Results of the crop simulations for a 'Climate Change plus Adaptation' scenarios for the two wheat cultivars (Simeto and Iride) at each experimental site are shown in this section.

For each site the effects of adapatation strategies, in terms of changes in sowing date, on yield and anthesis were evaluated. The analysis was conducted considering the three different GCMs previously described, and only the middle climate change scenario.

A graphical comparison of changes in yield (t ha^{-1}) and anthesis (days) values between now and future periods (2025, 2050 and 2075) was performed, considering separately the three GCMs, with and wihtout adaptation strategies.

A statistical analysis of results is also reported in order to consider the statistical significant differences between the mean values of yield and anthesis in the different future periods, with and without considering adaptation strategies.

5.1 USSANA

5.1.1 Simeto

Yield

Figures 5.1.1.1 *a*, *b* and *c*, show, separately for the three GCMs, the ratio of yield for middle climate change scenarios, with and without adaptation, to baseline yields (t ha^{-1}), for Simeto, under future projected climate change conditions.

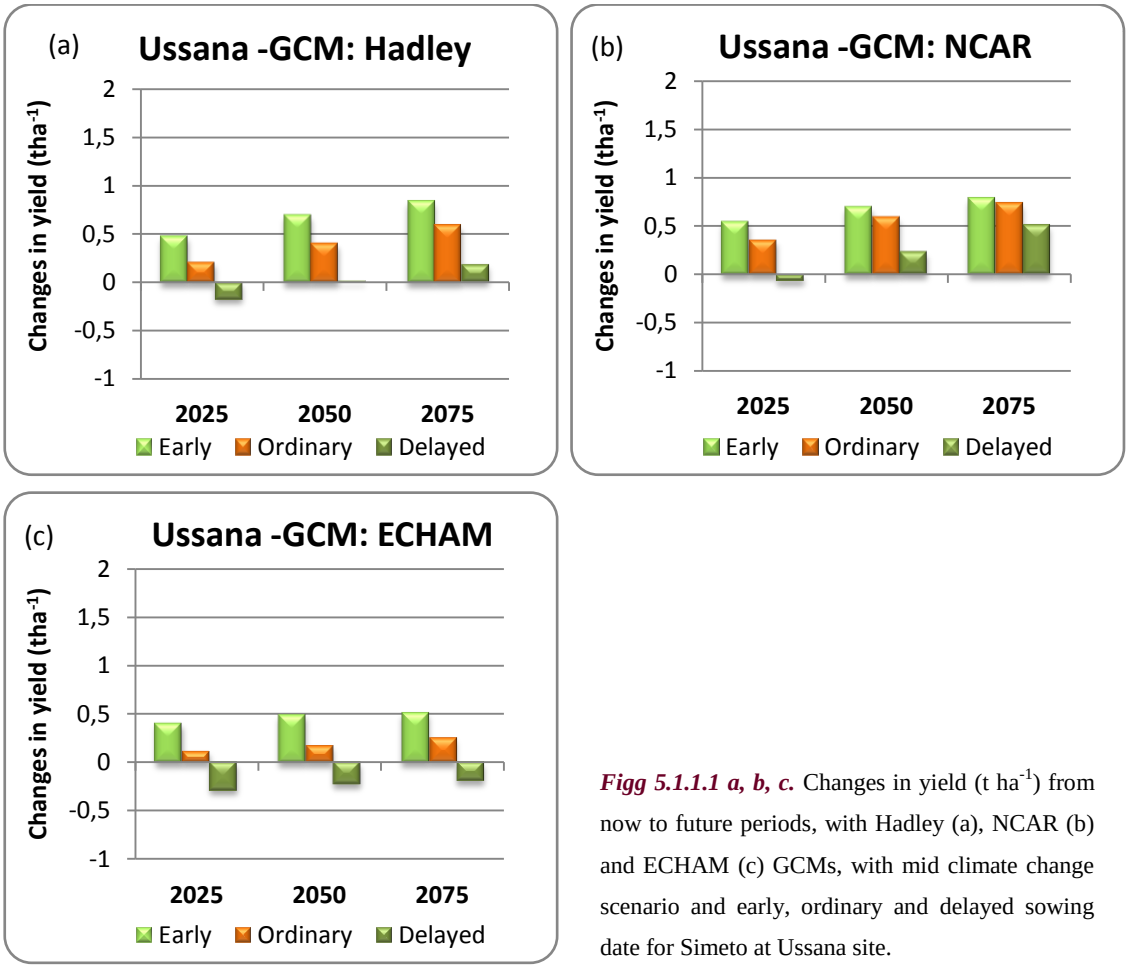

Figg 5.1.1.1 a, b, c. Changes in yield (t ha^{-1}) from now to future periods, with Hadley (a), NCAR (b) and ECHAM (c) GCMs, with mid climate change scenario and early, ordinary and delayed sowing date for Simeto at Ussana site.

The simulations show a evident differences in yield by comparing the middle climate change scenario with and without change in sowing date, in particular for 2025. For the other two future periods, the differences from middle climate change scenarios without adaptation and the scenarios with adaptation are more moderate. Although there are different results for each GCM, the anticipation of the crop cycle, through an early sowing, always involves an increase in yields. The yield tends to increase respect to the scenario without adaptation, considering early sowing

date, in particular for ECHAM and Hadley projections. On the contrary, the yield tends to decrease respect to the scenario without adaptation, considering delayed sowing date.

The differences in yields, projected by the three GCMs, could be justified considering, in particular, the difference between the GCMs in prediction the future pattern of precipitation. Indeed, NCAR provides the increases in precipitation for November and March. In particular the increase in precipitation for November, and in general the lower reduction in annual precipitation projected by NCAR, respect to the others GCMs, could explain the differences in the trend of NCAR.

However, the mean yield comparisons by SNK-test (Tab. 5.1.1.1) show a statistically significant difference only between now and climate change scenarios with early sowing date for 2050 a 2075, for Hadley and NCAR projections, while no significant difference is highlighted for ECHAM, between now and climate change scenarios with early or delayed sowing date.

Despite the increase in yield projected by the model for a early sowing date, these differences are not significant in any case if compared to the ordinary sowing date.

Table 5.1.1.1 Mean yield (t ha^{-1}) comparison for now and future periods, with three GCMs for mid climate change scenario without adaptation (CC mid) and climate change scenarios with adaptation (early and delayed sowing date) for Simeto at Ussana site.

		Hadley		NCAR		ECHAM	
		Yield (t ha^{-1})		Yield (t ha^{-1})		Yield (t ha^{-1})	
Now		3.4	cde	3.4	b	3.4	abc
2025	**CC (mid)**	3.6	bcde	3.8	ab	3.5	abc
	CC (mid) +A (early)	3.9	abcd	3.9	a	3.8	ab
	CC (mid) +A (delayed)	3.2	e	3.3	b	3.1	c
2050	**CC (mid)**	3.8	abcd	4.0	a	3.6	abc
	CC (mid) +A (early)	4.1	ab	4.1	a	3.9	a
	CC (mid) +A (delayed)	3.4	de	3.6	ab	3.2	c
2075	**CC (mid)**	4.0	abc	4.1	a	3.7	abc
	CC (mid) +A (early)	4.2	a	4.2	a	3.9	a
	CC (mid) +A (delayed)	3.6	bcde	3.9	a	3.2	bc

Means within each group (single GCM and different future periods) sharing the same letter do not differ significantly from one another (SNK-test at P≤0.05).

Anthesis

The Figures 5.1.1.2 *a*, *b*, and *c*, show the effects of changing in planting date on anthesis date (difference in days from now to future periods), under future climate change scenarios, considering separately the three GCMs with middle climate change scenario.

It is possible to observe a longer duration of the period from sowing to anthesis if the date of sowing is advanced by 30 days respect to the ordinary sowing date, for all future periods and particularly for 2025, as projected by all GCMs.

On the contrary, if the sowing date is delayed by 30 days, the duration of the period from sowing to anthesis, is projected to decrease for all future periods.

The differences in projection of the three GCMs are quite similar for anthesis, respect the projections of the three GCMs for yield. This is justified by the fact that anthesis is closely dependent on temperature (and for temperature the GCMs provide similar changes), while the yield is related to the effect of different variable combination.

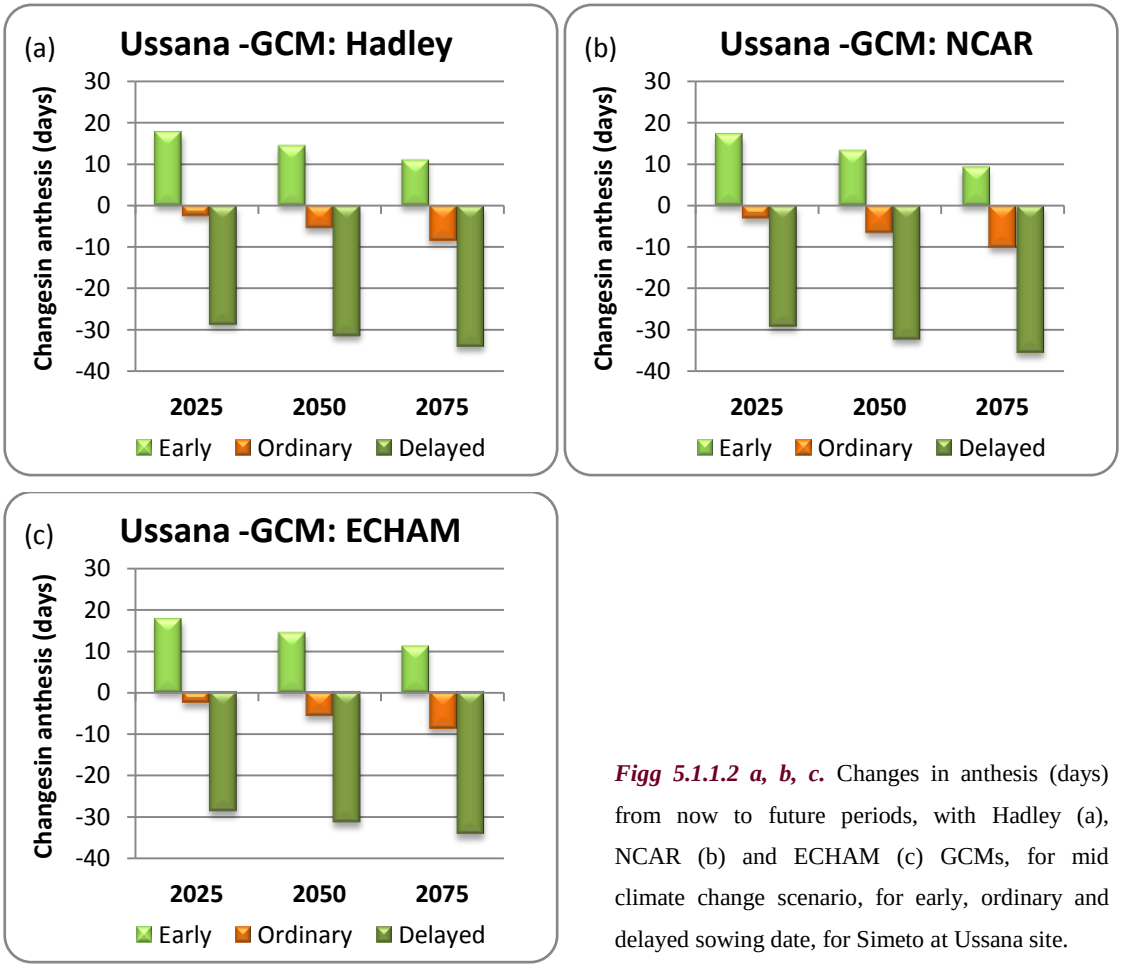

Figg 5.1.1.2 a, b, c. Changes in anthesis (days) from now to future periods, with Hadley (a), NCAR (b) and ECHAM (c) GCMs, for mid climate change scenario, for early, ordinary and delayed sowing date, for Simeto at Ussana site.

The statistical analysis performed with SNK-test (Table 5.1.1.2) shows significantly differences from now to future climate change scenarios either with or without adaptation strategies, and also comparing the same future period with or without change in planting date. This means that changes in planting date are likely to significantly change the length of the phase from

sowing to anthesis under climate change conditions. This partially justifies the higher yield highlighted in the previous analysis.

Table 5.1.1.2 Mean anthesis (dap) comparison for now and future periods, with three GCMs for mid climate change scenario without adaptation (CC mid) and climate change scenarios with adaptation (early and delayed sowing date) for Simeto at Ussana site.

		Hadley	NCAR	ECHAM
		Anthesis (days)	**Anthesis (days)**	**Anthesis (days)**
Now		136 d	136 d	136 d
2025	**CC (mid)**	133 e	132 e	133 e
	CC (mid) +A (early)	153 a	153 a	153 a
	CC (mid) +A (delayed)	107 h	106 h	107 h
2050	**CC (mid)**	130 f	129 f	130 f
	CC (mid) +A (early)	150 b	149 b	150 b
	CC (mid) +A (delayed)	104 i	103 i	104 i
2075	**CC (mid)**	127 g	125 g	127 g
	CC (mid) +A (early)	147 c	145 c	147 c
	CC (mid) +A (delayed)	102 j	100 j	101 j

Means within each group (single GCM and different future periods) sharing the same letter do not differ significantly from one another (SNK-test at $P \leq 0.05$).

5.1.2 Iride

Yield

Figures 5.1.2.1 *a, b* and *c*, show, separately for the three GCMs, the ratio of yield for middle climate change scenarios, with and without adaptation, to baseline yields (t ha^{-1}), for Iride, under future projected climate change conditions.

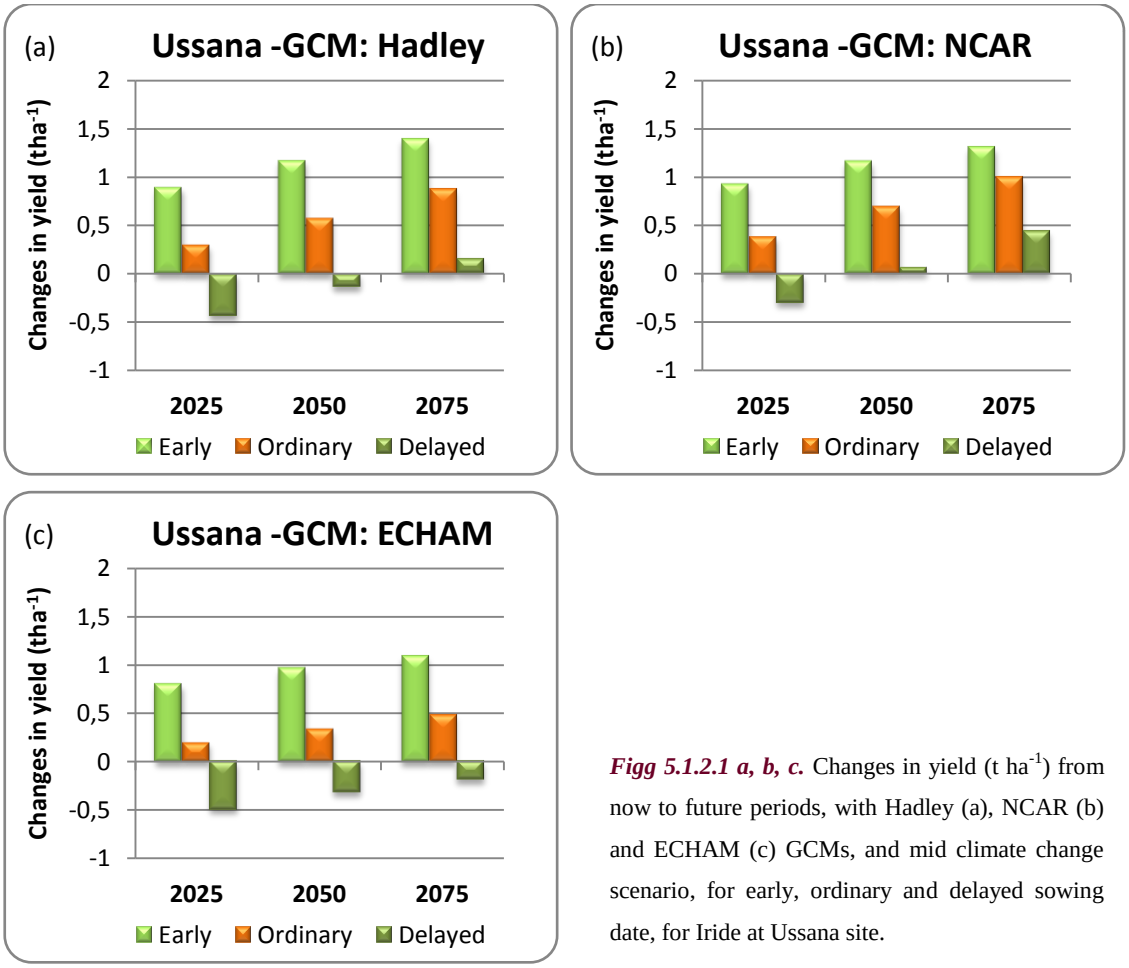

Figg 5.1.2.1 a, b, c. Changes in yield (t ha^{-1}) from now to future periods, with Hadley (a), NCAR (b) and ECHAM (c) GCMs, and mid climate change scenario, for early, ordinary and delayed sowing date, for Iride at Ussana site.

For Iride it is possible to observe similar trends than those observed for Simeto at the same site, but for Iride are projected higher mean changes in yield considerind early sowing date, while the ratio of reduction in yield for simulations with delayed sowing date are similar to that projected for Simeto.

The mean yield comparisons by SNK-test (Tab. 5.1.2.1) show statistically significant differences between yield projected by all three GCMs for now and climate change scenarios with early sowing date for all future periods. It means that for Iride an early sowing date may be in the future a valide adaptation strategies to benefit for the effects of climate change.

Table 5.1.2.1 Mean yield (t ha^{-1}) comparison for now and future periods, with three GCMs for mid climate change scenario without adaptation (CC mid) and climate change scenarios with adaptation (early and delayed sowing date) for Iride at Ussana site.

		Hadley		NCAR		ECHAM	
		Yield (t ha^{-1})		Yield (t ha^{-1})		Yield (t ha^{-1})	
Now		4.0	e	4.0	de	4.0	def
2025	**CC (mid)**	4.3	de	4.4	cd	4.2	cde
	CC (mid) +A (early)	4.9	bc	4.9	ab	4.8	ab
	CC (mid) +A (delayed)	3.5	f	3.7	e	3.5	g
2050	**CC (mid)**	4.5	cd	4.7	bc	4.3	cd
	CC (mid) +A (early)	5.1	ab	5.1	a	4.9	a
	CC (mid) +A (delayed)	3.8	ef	4.0	de	3.6	fg
2075	**CC (mid)**	4.8	bc	5.0	ab	4.5	bc
	CC (mid) +A (early)	5.4	a	5.3	a	5.1	a
	CC (mid) +A (delayed)	4.1	de	4.4	cd	3.8	efg

Means within each group (single GCM and different future periods) sharing the same letter do not differ significantly from one another (SNK-test at P≤0.05).

Anthesis

The Figures 5.1.2.2 *a, b,* and *c,* show the effects of changing in planting date on anthesis date (difference in days from now to future periods), under future climate change scenarios, considering separately the three GCMs with middle climate change scenario.

Similarly to Simeto, for Iride it is possible to observe a longer duration of the period from sowing to anthesis if the date of sowing is advanced by 30 days respect to the ordinary sowing date, for all future periods and particularly for 2025, as projected by all GCMs, but for Iride the duration of the period from sowing to anthesis is some days shorter than that one projected for Simeto.

On the contrary, if the sowing date is delayed by 30 days, the duration of the period from sowing to anthesis, is projected to decrease for all future periods.

Also for Iride, the differences in projection of the three GCMs are quite similar for anthesis, respect the projections of the three GCMs for yield.

The statistical analysis performed with SNK-test (Tab. 5.1.2.2) show significantly differences from now to future climate change scenarios either with or without adaptation strategies, and also comparing the same future period with or without change in planting date. This partially justifies the higher yield highlighted in the previous analysis.

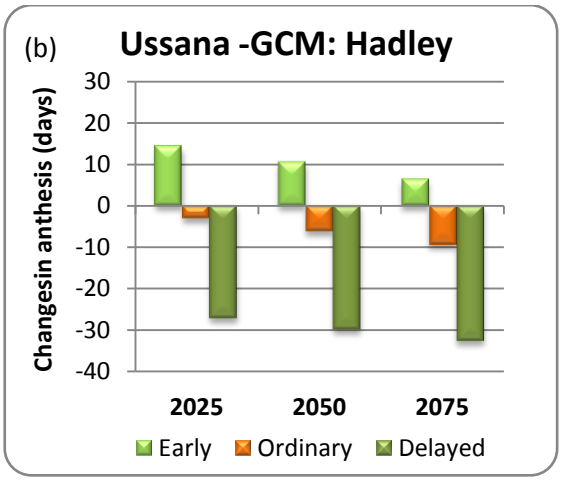

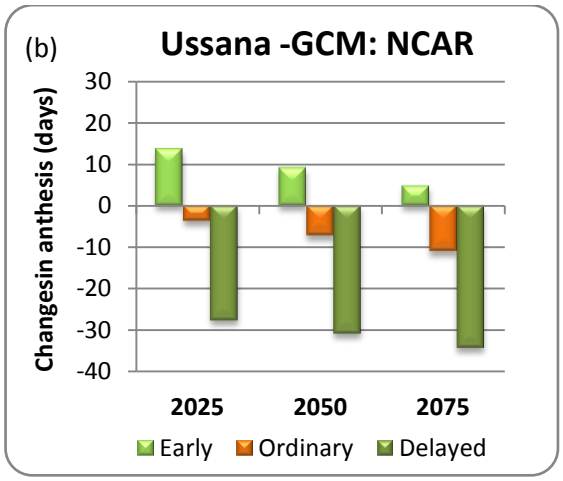

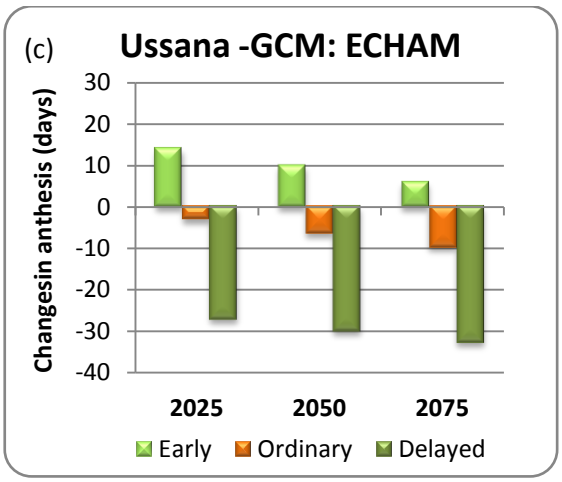

Figg 5.1.2.2 a, b, c. Changes in anthesis (days) from now to future periods, with Hadley (a), NCAR (b) and ECHAM (c) GCMs, for mid climate change scenario, for early, ordinary and delayed sowing date, for Iride at Ussana site.

Table 5.1.2.2 Mean anthesis (dap) comparison for now and future periods, with three GCMs for mid climate change scenario without adaptation (CC mid) and climate change scenarios with adaptation (early and delayed sowing date), for Iride at Ussana site.

		Hadley	NCAR	ECHAM
		Anthesis (days)	Anthesis (days)	Anthesis (days)
Now		128 d	128 d	128 d
2025	**CC (mid)**	125 e	124 e	125 e
	CC (mid) +A (early)	142 a	141 a	142 a
	CC (mid) +A (delayed)	101 h	100 h	101 h
2050	**CC (mid)**	122 f	120 f	121 f
	CC (mid) +A (early)	138 b	137 b	138 b
	CC (mid) +A (delayed)	98 i	97 i	98 i
2075	**CC (mid)**	118 g	117 g	118 g
	CC (mid) +A (early)	134 c	133 c	134 c
	CC (mid) +A (delayed)	95 j	93 j	95 j

Means within each group (single GCM and different future periods) sharing the same letter do not differ significantly from one another (SNK-test at P≤0.05).

5.2 BENATZU

5.2.1 Simeto

Yield

Figures 5.2.1.1 *a*, *b* and *c*, show, separately for the three GCMs, the ratio of yield for middle climate change scenarios, with and without adaptation, to baseline yields (t ha^{-1}), for Simeto, under future projected climate change conditions.

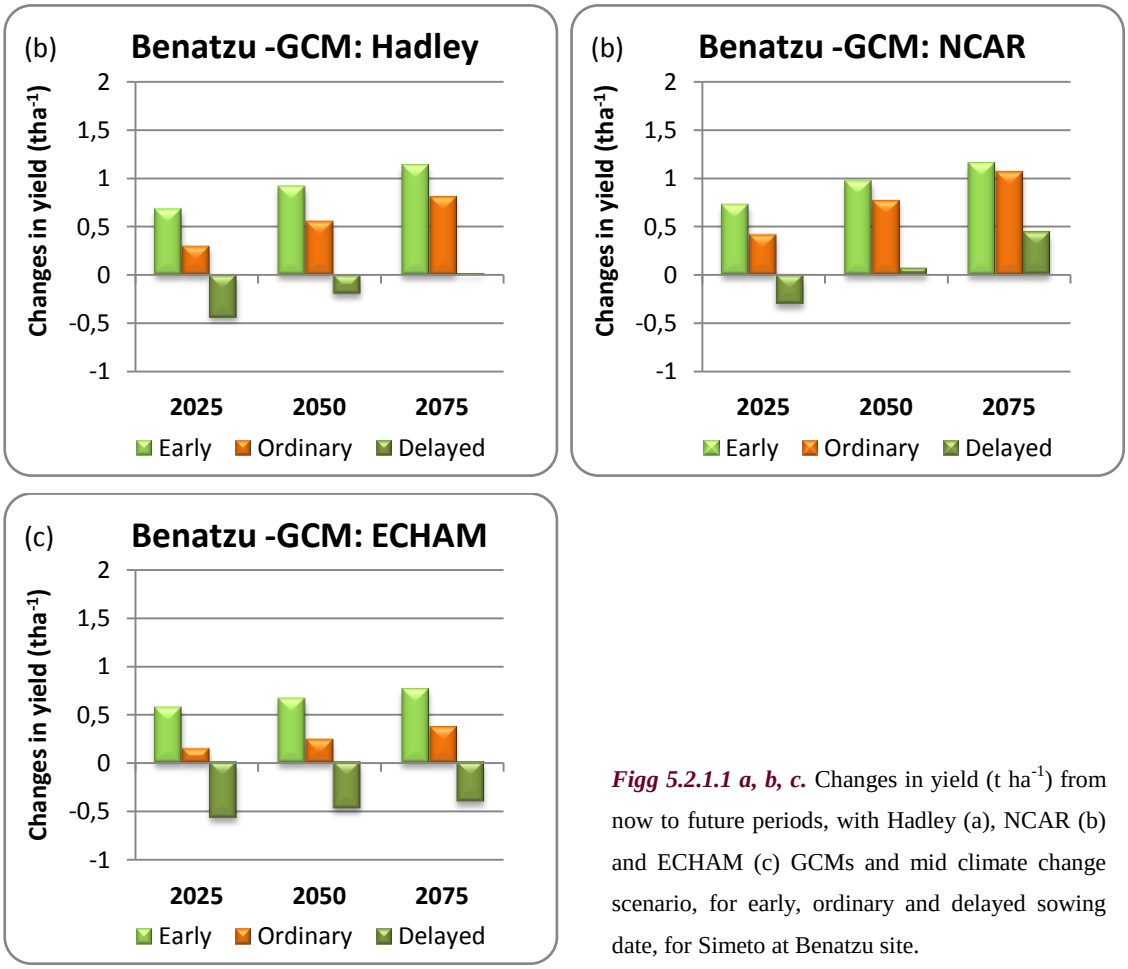

Figg 5.2.1.1 a, b, c. Changes in yield (t ha^{-1}) from now to future periods, with Hadley (a), NCAR (b) and ECHAM (c) GCMs and mid climate change scenario, for early, ordinary and delayed sowing date, for Simeto at Benatzu site.

Also at Benatzu site, the simulations for Simeto show a evident differences in yield by comparing the middle climate change scenario with and without change in sowing date, in particular for 2025 with ECHAM and Hadley. The differences are more moderate with NCAR. For the others two future periods, the differences from middle climate change scenarios without adaptation and the scenarios with adaptation are more moderate. The yield tends to increase respect to the scenario without adaptation, considering early sowing date, and tends to decrease respect to

the scenario without adaptation, considering delayed sowing date. The lowest differences between ordinary sowing and early or delayed sowing are those projected by NCAR.

However, the mean yield comparisons by SNK-test (Tab. 5.2.1.1) show a statistically significant difference only between now and climate change scenarios with early sowing date for 2050 a 2075, for Hadley and NCAR projections, while no significant difference is highlighted for EHCAM, between now and climate change scenarios with early or delayed sowing date.

Despite the increase in yield projected by the model for a early sowing date, these differences are not significant in any case if compared with the ordinary sowing date. While statistically significant differences between yield projected for a delayed sowing date compared to the ordinary sowing are highlighted.

Table 5.2.1.1 Mean yield (t ha^{-1}) comparison for now and future periods, with three GCMs for mid climate change scenario without adaptation (CC mid) and climate change scenarios with adaptation (early and delayed sowing date) for Simeto at Benatzu site.

		Hadley		NCAR		ECHAM	
		Yield (t ha^{-1})		Yield (t ha^{-1})		Yield (t ha^{-1})	
Now		4.0	cdef	4.0	cd	4.0	abc
2025	**CC (mid)**	4.3	bcde	4.4	bc	4.2	abc
	CC (mid) +A (early)	4.7	abc	4.7	ab	4.6	a
	CC (mid) +A (delayed)	3.6	f	3.7	d	3.4	c
2050	**CC (mid)**	4.6	abcd	4.8	ab	4.3	ab
	CC (mid) +A (early)	4.9	ab	5.0	ab	4.7	a
	CC (mid) +A (delayed)	3.8	ef	4.1	cd	3.5	bc
2075	**CC (mid)**	4.8	ab	5.1	ab	4.4	a
	CC (mid) +A (early)	5.1	a	5.2	a	4.8	a
	CC (mid) +A (delayed)	4.0	def	4.4	bc	3.6	bc

Means within each group (single GCM and different future periods) sharing the same letter do not differ significantly from one another (SNK-test at $P \leq 0.05$).

Anthesis

The Figures 5.2.1.2 *a*, *b*, and *c*, show the effects of changing in planting date on anthesis date (difference in days from now to future periods), under future climate change scenarios, considering separately the three GCMs with middle climate change scenario for Simeto at Benatzu site.

Also for this site it is possible to observe a longer duration of the period from sowing to anthesis if the date of sowing is advanced by 30 days respect to the ordinary sowing date, for all future periods and particularly for 2025, as projected by all GCMs.

On the contrary, if the sowing date is delayed by 30 days, the duration of the period from sowing to anthesis, is projected to decrease for all future periods.

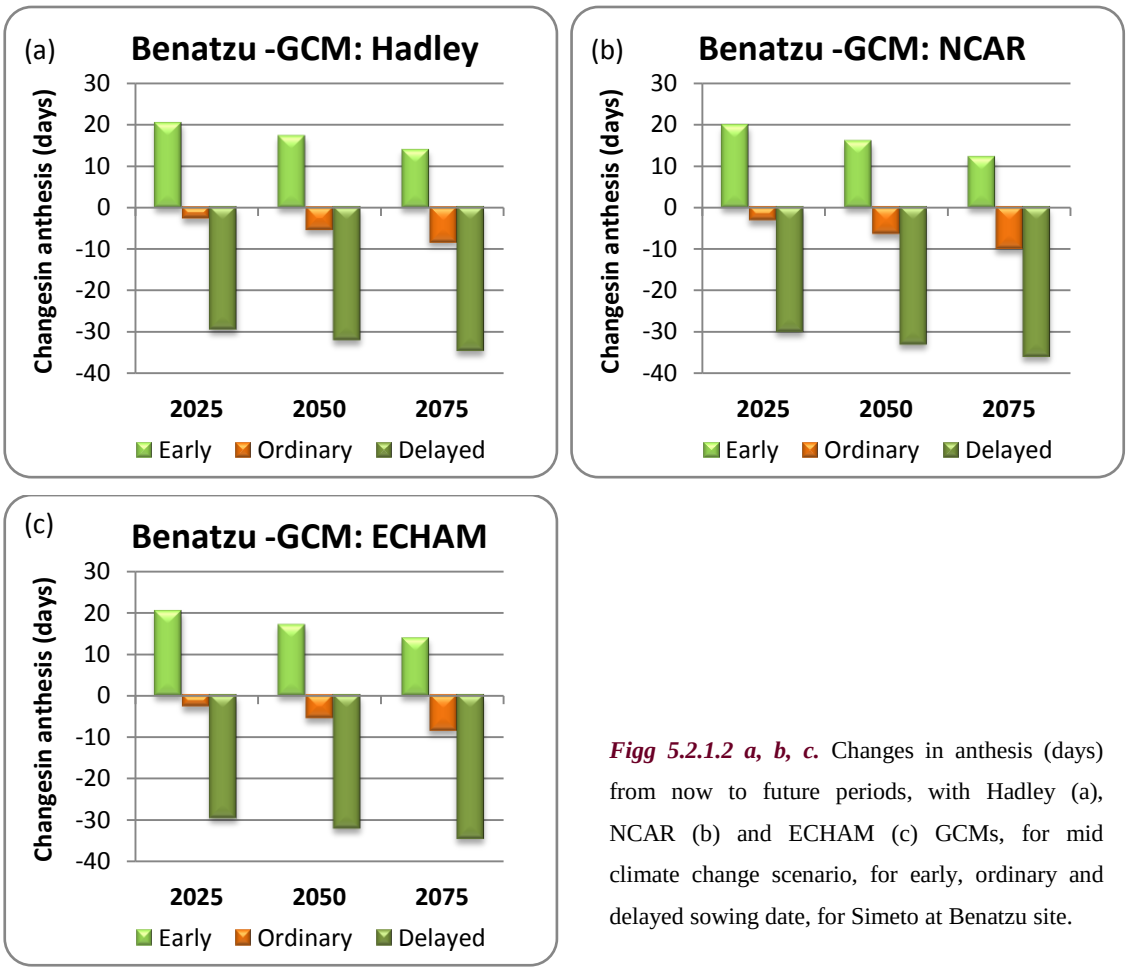

Figg 5.2.1.2 a, b, c. Changes in anthesis (days) from now to future periods, with Hadley (a), NCAR (b) and ECHAM (c) GCMs, for mid climate change scenario, for early, ordinary and delayed sowing date, for Simeto at Benatzu site.

The statistical analysis performed with SNK-test show (Tab. 5.2.1.2) significantly differences from now to future climate change scenarios both with and without adaptation strategies, and also comparing the same future period with or without change in planting date. This means that changes in planting date are likely to significant change the length of the period from sowing to anthesis under climate change conditions. This partially justifies the higher yield highlighted in the previous analysis.

Table 5.2.1.2 Mean anthesis (dap) comparison for now and future periods, with three GCMs for mid climate change scenario without adaptation (CC mid) and climate change scenarios with adaptation (early and delayed sowing date) for Simeto at Benatzu site.

		Hadley		NCAR		ECHAM	
		Anthesis (days)		Anthesis (days)		Anthesis (days)	
Now		128	d	128	d	128	d
2025	**CC (mid)**	125	e	125	e	125	e
	CC (mid) +A (early)	148	a	148	a	148	a
	CC (mid) +A (delayed)	98	h	98	h	98	h
2050	**CC (mid)**	122	f	121	f	122	f
	CC (mid) +A (early)	145	b	144	b	145	b
	CC (mid) +A (delayed)	96	i	95	i	96	i
2075	**CC (mid)**	120	g	118	g	119	g
	CC (mid) +A (early)	142	c	140	c	142	c
	CC (mid) +A (delayed)	93	j	92	j	93	j

Means within each group (single GCM and different future periods) sharing the same letter do not differ significantly from one another (SNK-test at $P \leq 0.05$).

5.2.2 Iride

Yield

Figures 5.2.2.1 *a, b* and *c*, show, separately for the three GCMs, the ratio of yield for middle climate change scenarios, with and without adaptation, to baseline yields (t ha^{-1}), for Iride, under future projected climate change conditions.

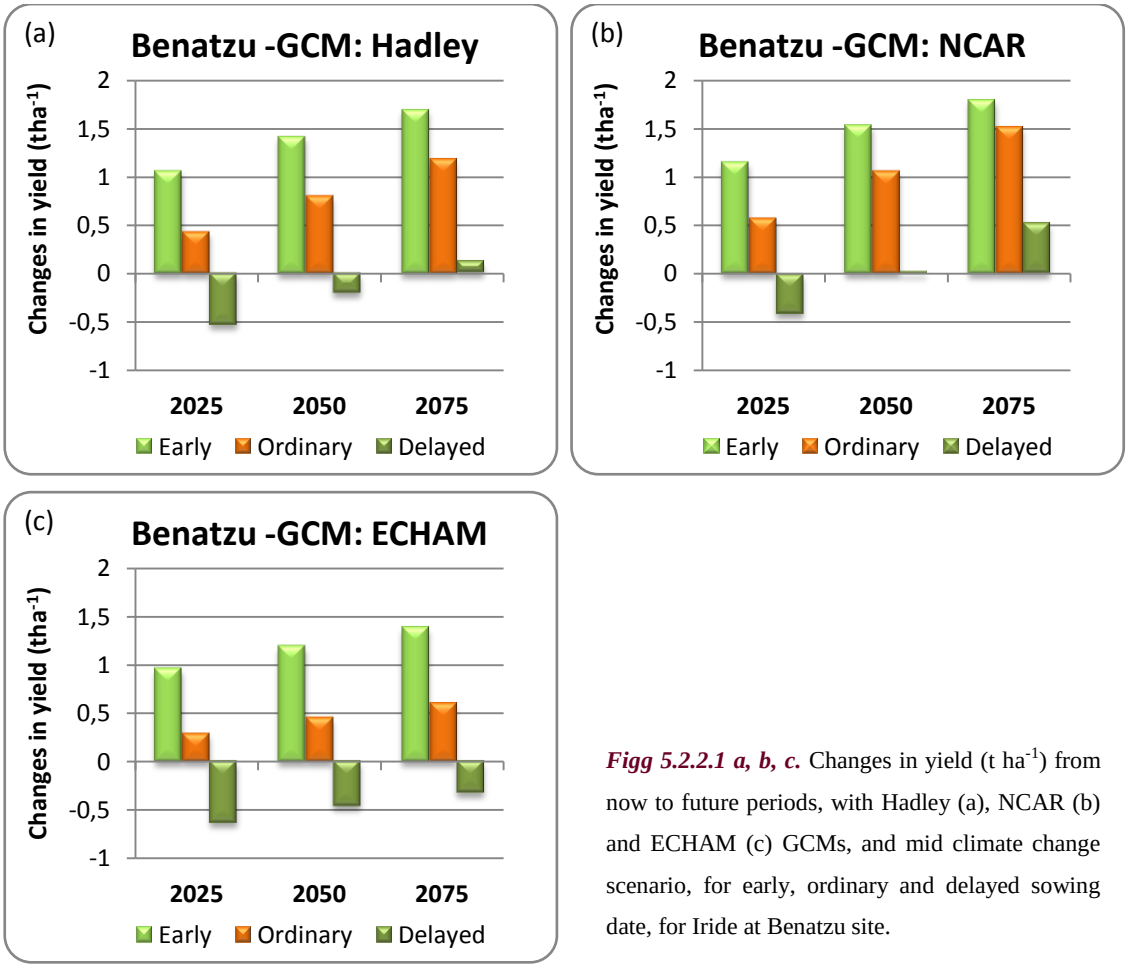

Figg 5.2.2.1 a, b, c. Changes in yield (t ha^{-1}) from now to future periods, with Hadley (a), NCAR (b) and ECHAM (c) GCMs, and mid climate change scenario, for early, ordinary and delayed sowing date, for Iride at Benatzu site.

Also for this site, the yield simulations for Iride show the same trend observed for Simeto, but for Iride are projected higher mean changes in yield considering early sowing date, while the ratio of reduction in yield for simulations with delayed sowing date are similar to that projected for Simeto.

The mean yield comparisons by SNK-test (Tab. 5.2.2.1) show a statistically significant difference between now and climate change scenarios with early sowing date for the three future periods, whit all GCMs projections. Furthermore, there are statistically significant differences between early and ordinary sowing date for 2025 and 2050 for Hadley projections and for all future

periods for ECHAM projections and only for 2025 for NCAR, that confirms also in this case the more moderate changes in yield in responce to adaptation strategies respect to those projected by the others GCMs.

Table 5.2.2.1 Mean yield (t ha^{-1}) comparison for now and future periods, with three GCMs for mid climate change scenario without adaptation (CC mid) and climate change scenarios with adaptation (early and delayed sowing date) for Iride at Benatzu site.

		Hadley		NCAR		ECHAM	
		Yield (t ha^{-1})		Yield (t ha^{-1})		Yield (t ha^{-1})	
Now		4.6	efg	4.6	de	4.6	de
2025	**CC (mid)**	5.0	de	5.2	c	4.9	cd
	CC (mid) +A (early)	5.6	bc	5.7	b	5.5	ab
	CC (mid) +A (delayed)	4.1	g	4.2	e	3.9	f
2050	**CC (mid)**	5.4	cd	5.6	b	5.0	bcd
	CC (mid) +A (early)	6.0	ab	6.1	ab	5.8	a
	CC (mid) +A (delayed)	4.4	fg	4.6	e	4.1	ef
2075	**CC (mid)**	5.8	abc	6.1	ab	5.2	bc
	CC (mid) +A (early)	6.3	a	6.4	a	6.0	a
	CC (mid) +A (delayed)	4.7	ef	5.1	cd	4.3	ef

Means within each group (single GCM and different future periods) sharing the same letter do not differ significantly from one another (SNK-test at P≤0.05).

Anthesis

The Figures 5.2.2.2 *a*, *b*, and *c*, show the effects of changing in planting date on anthesis date (difference in days from now to future periods), under future climate change scenarios, considering separately the three GCMs with middle climate change scenario.

Also for this site, it is possible to observe for Iride a longer duration of the period from sowing to anthesis, if the date of sowing is advanced by 30 days respect to the ordinary sowing date, for all future periods and particularly for 2025, as projected by all GCMs, but for Iride the duration of the period from sowing to anthesis is few days shorter than that projected for Simeto for the same site.

On the contrary, if the sowing date is delayed by 30 days, the duration of the period from sowing to anthesis, is projected to decrease for all future periods.

Also for Iride, the differences in projection of the three GCMs are quite similar for anthesis, respect the projections of the three GCMs for yield.

The statistical analysis performed with SNK-test (Tab. 5.2.2.2) show significantly differences from now to future climate change scenarios both with and without adaptation strategies, and also comparing the same future period with or without change in planting date. This partially justifies the higher yield highlighted in the previous analysis.

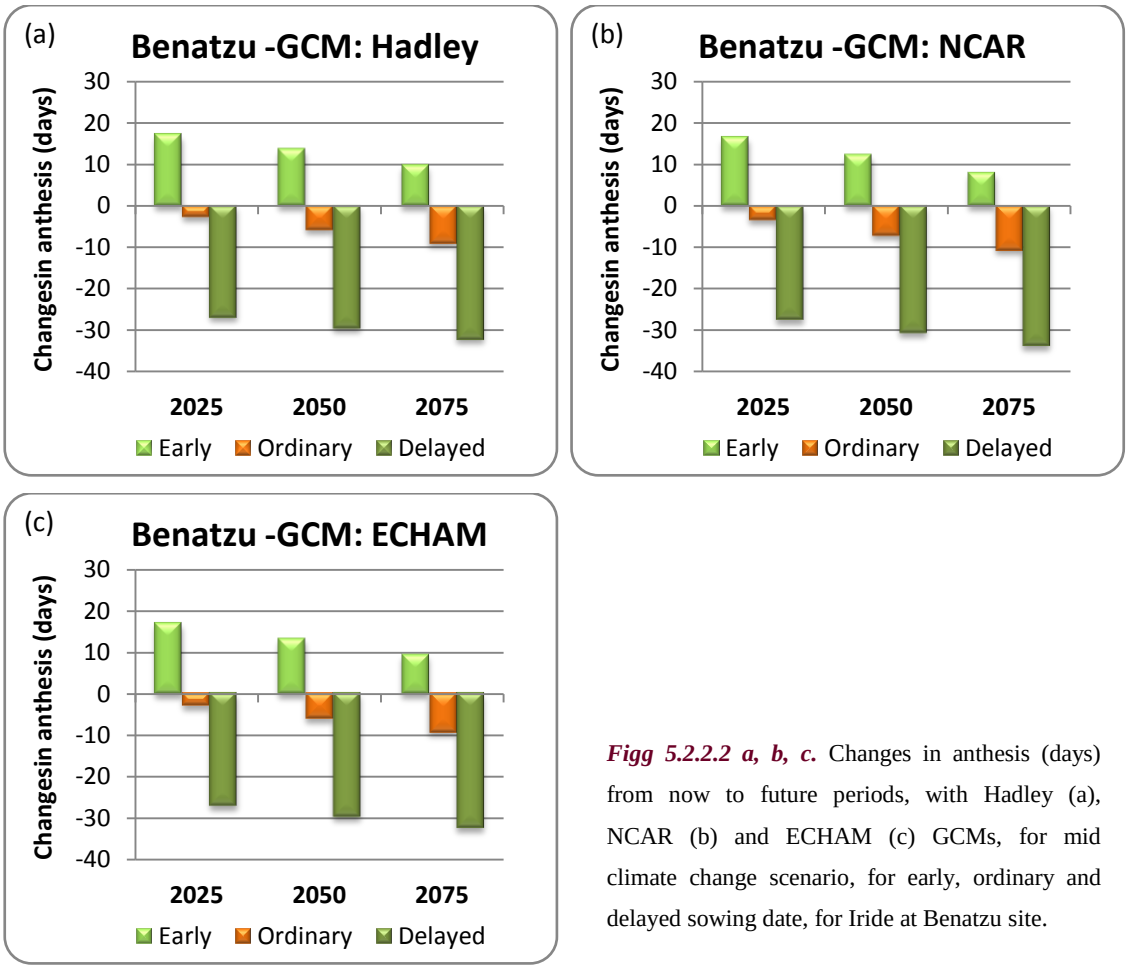

Figg 5.2.2.2 a, b, c. Changes in anthesis (days) from now to future periods, with Hadley (a), NCAR (b) and ECHAM (c) GCMs, for mid climate change scenario, for early, ordinary and delayed sowing date, for Iride at Benatzu site.

Table 5.2.2.2 Mean anthesis (dap) comparison for now and future periods, with three GCMs for mid climate change scenario without adaptation (CC mid) and climate change scenarios with adaptation (early and delayed sowing date) for Iride at Benatzu site.

		Hadley	NCAR	ECHAM
		Anthesis (days)	Anthesis (days)	Anthesis (days)
Now		123 d	123 d	123 d
2025	**CC (mid)**	120 e	119 e	120 e
	CC (mid) +A (early)	140 a	139 a	140 a
	CC (mid) +A (delayed)	96 h	95 h	96 h
2050	**CC (mid)**	117 f	116 f	117 f
	CC (mid) +A (early)	137 b	135 b	136 b
	CC (mid) +A (delayed)	93 i	92 i	93 i
2075	**CC (mid)**	114 g	112 g	114 g
	CC (mid) +A (early)	133 c	131 c	132 c
	CC (mid) +A (delayed)	91 j	89 j	91 j

Means within each group (single GCM and different future periods) sharing the same letter do not differ significantly from one another (SNK-test at P≤0.05).

5.3 OTTAVA

5.3.1 Simeto

Yield

Figures 5.3.1.1 *a*, *b* and *c*, show, separately for the three GCMs, the ratio of yield for middle climate change scenarios, with and without adaptation, to baseline yields (t ha^{-1}), for Simeto, under future projected climate change conditions.

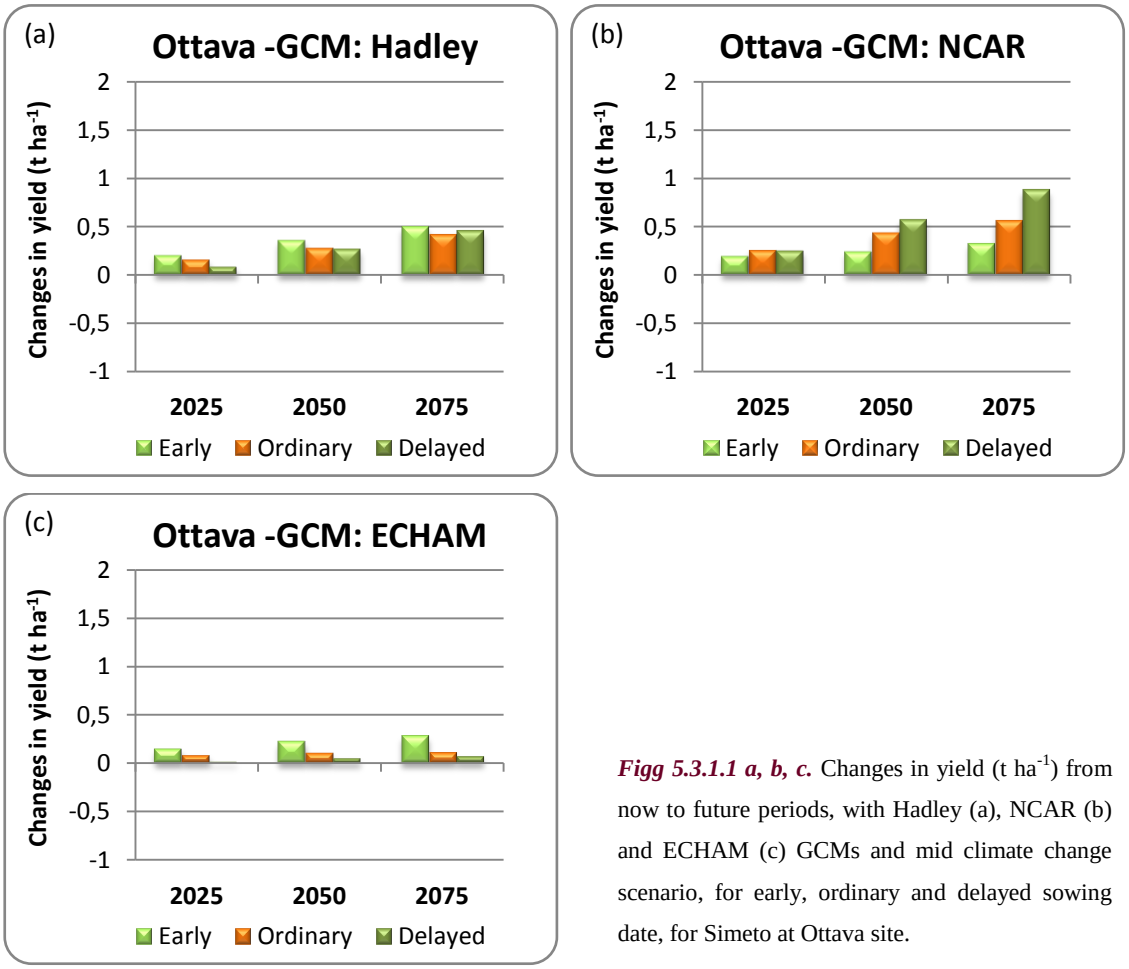

Figg 5.3.1.1 a, b, c. Changes in yield (t ha^{-1}) from now to future periods, with Hadley (a), NCAR (b) and ECHAM (c) GCMs and mid climate change scenario, for early, ordinary and delayed sowing date, for Simeto at Ottava site.

The results of simulation for Simeto at Ottava experimental site show a different trend respect to those observed in the previous analysis.

Generally, it is possible to observe changes close to zero for mean yield projected by Hadley and ECHAM, for all future periods. It is interesting to note the trend shown by the NCAR projections, that appears opposite respect to all previous analysis, showing a higher increase in yield for delayed instead of early sowing, respect to the ordinary sowing.

The mean yield comparison by SNK-test (Tab. 5.3.1.1) does not show statistically significant differences between now and climate change scenarios with early or delayed sowing date for all future periods, for Hadley and ECHAM projections, while significant difference is highlighted for NCAR, for 2050 and 2075, between now and climate change scenarios with delayed sowing date.

Table 5.3.1.1 Mean yield (t ha^{-1}) comparison for now and future periods, with three GCMs for mid climate change scenario without adaptation (CC mid) and climate change scenarios with adaptation (early and delayed sowing date) for Simeto at Ottava site.

		Hadley	NCAR	ECHAM
		Yield (t ha^{-1})	Yield (t ha^{-1})	Yield (t ha^{-1})
Now		3.6 a	3.6 c	3.6 a
2025	**CC (mid)**	3.8 a	3.9 bc	3.7 a
	CC (mid) +A (early)	3.8 a	3.8 bc	3.7 a
	CC (mid) +A (delayed)	3.7 a	3.9 bc	3.6 a
2050	**CC (mid)**	3.9 a	4.0 bc	3.7 a
	CC (mid) +A (early)	4.0 a	3.8 bc	3.8 a
	CC (mid) +A (delayed)	3.9 a	4.2 ab	3.6 a
2075	**CC (mid)**	4.0 a	4.2 ab	3.7 a
	CC (mid) +A (early)	4.1 a	3.9 bc	3.9 a
	CC (mid) +A (delayed)	4.1 a	4.5 a	3.7 a

Means within each group (single GCM and different future periods) sharing the same letter do not differ significantly from one another (SNK-test at P≤0.05).

Anthesis

The Figures 5.3.1.2 *a, b,* and *c*, show the effects of changing in planting date on anthesis date (difference in days from now to future periods), under future climate change scenarios, considering separately the three GCMs with middle climate change scenario.

Also for this site it is possible to observe a longer duration of the period from sowing to anthesis if the date of sowing is advanced by 30 days respect to the ordinary sowing date, for all future periods and particularly for 2025, as projected by all GCMs.

On the contrary, if the sowing date is delayed by 30 days, the duration of the period from sowing to anthesis, is projected to decrease for all future periods.

The statistical analysis performed with SNK-test (Tab. 5.3.1.2) show significantly differences from now to future climate change scenarios either with or without adaptation strategies, and also comparing the same future period with or without change in planting date.

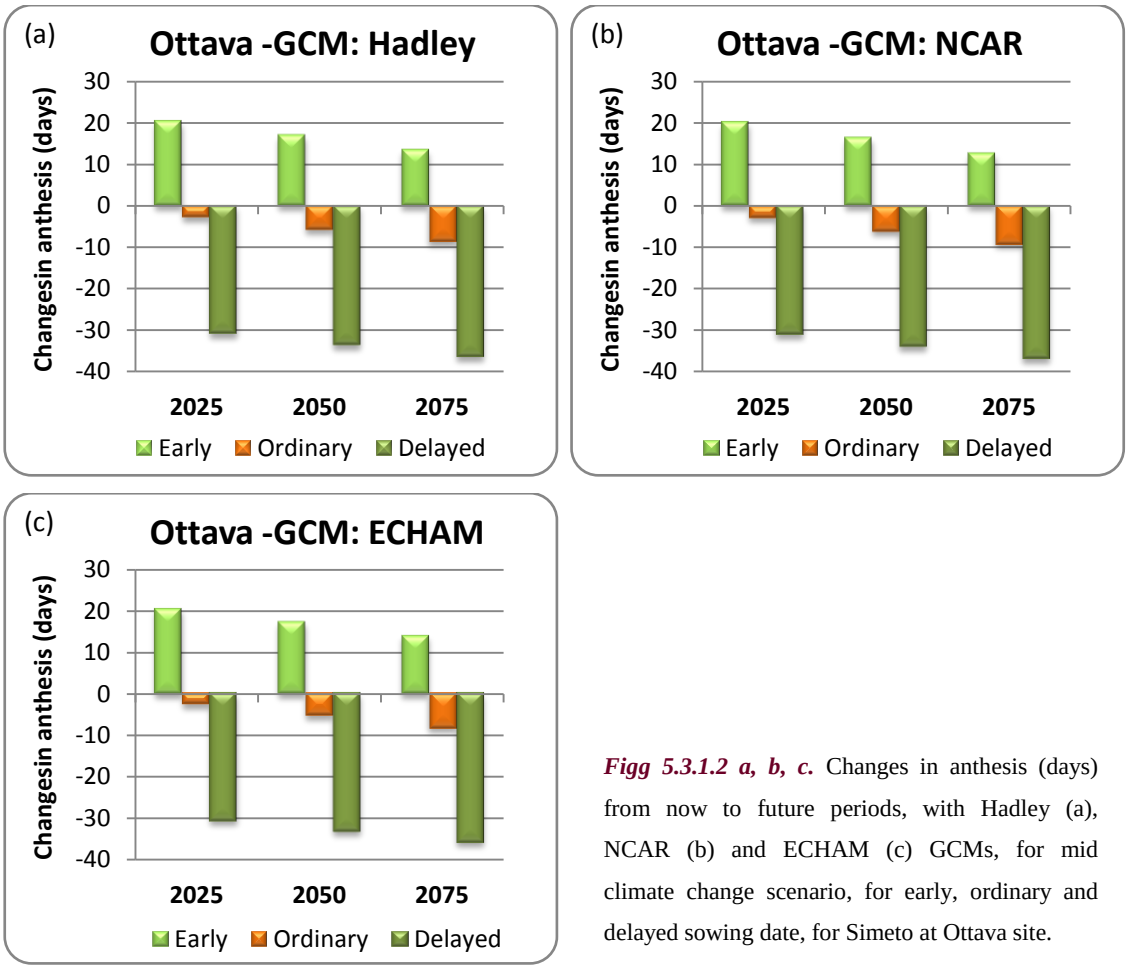

Figg 5.3.1.2 a, b, c. Changes in anthesis (days) from now to future periods, with Hadley (a), NCAR (b) and ECHAM (c) GCMs, for mid climate change scenario, for early, ordinary and delayed sowing date, for Simeto at Ottava site.

Table 5.3.1.2 Mean anthesis (dap) comparison for now and future periods, with three GCMs for mid climate change scenario without adaptation (CC mid) and climate change scenarios with adaptation (early and delayed sowing date) for Simeto at Ottava site.

		Hadley	NCAR	ECHAM
		Anthesis (days)	**Anthesis (days)**	**Anthesis (days)**
Now		136 d	136 d	136 d
2025	**CC (mid)**	133 e	133 e	133 e
	CC (mid) +A (early)	156 a	156 a	157 a
	CC (mid) +A (delayed)	105 h	105 h	105 h
2050	**CC (mid)**	130 f	130 f	131 f
	CC (mid) +A (early)	153 b	153 b	154 b
	CC (mid) +A (delayed)	103 i	102 i	103 i
2075	**CC (mid)**	128 g	127 g	128 g
	CC (mid) +A (early)	150 c	149 c	150 c
	CC (mid) +A (delayed)	100 j	99 j	100 j

Means within each group (single GCM and different future periods) sharing the same letter do not differ significantly from one another (SNK-test at P≤0.05).

5.3.2 Iride

Yield

Figures 5.3.2.1 *a*, *b* and *c*, show, separately for the three GCMs, the ratio of yield for middle climate change scenarios, with and without adaptation, to baseline yields (t ha^{-1}), for Iride, under future projected climate change conditions.

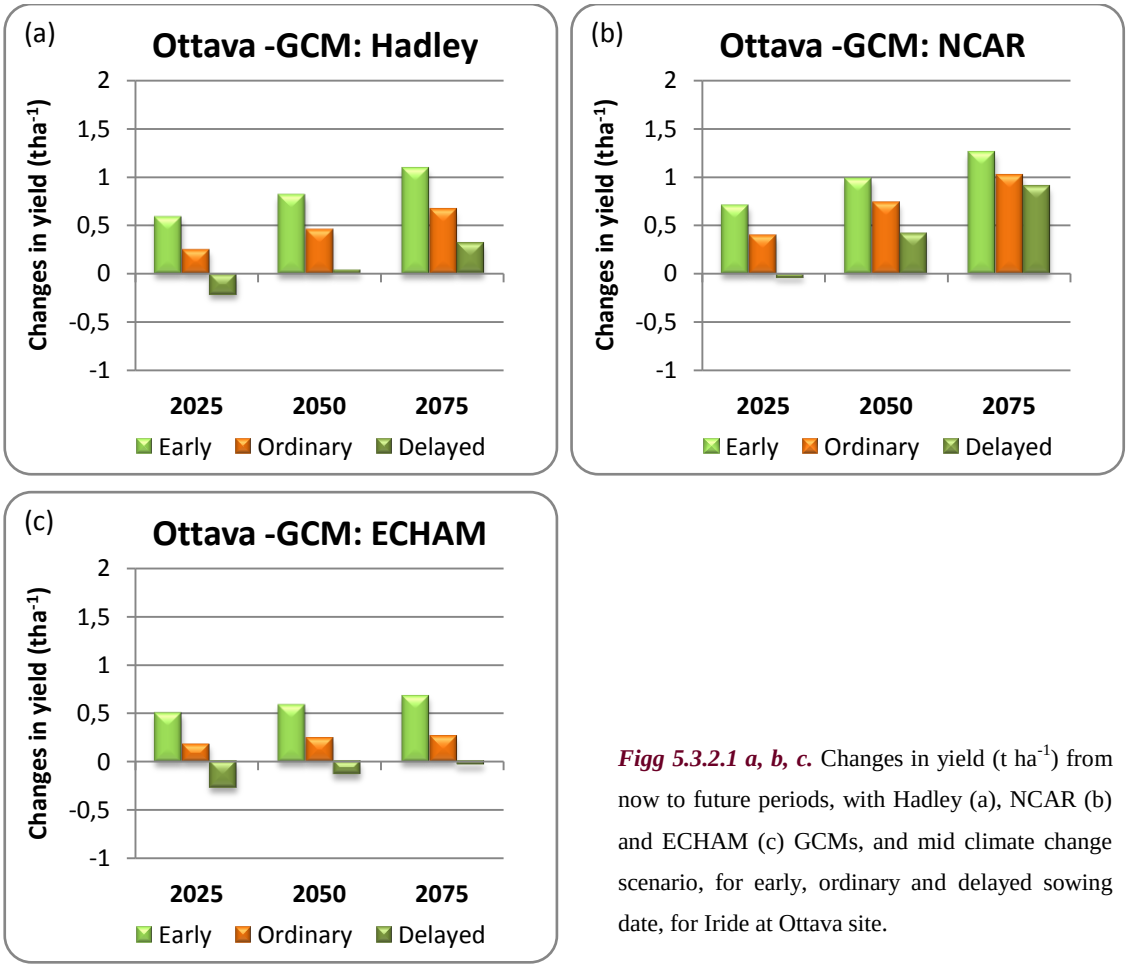

Figg 5.3.2.1 a, b, c. Changes in yield (t ha^{-1}) from now to future periods, with Hadley (a), NCAR (b) and ECHAM (c) GCMs, and mid climate change scenario, for early, ordinary and delayed sowing date, for Iride at Ottava site.

On the contrary than for Simeto, the simulations for Iride at Ottava site show the same trend observed in the previous analysis for yield. The yield tends to increase respect to the scenario without adaptation, considering early sowing date, in particular for ECHAM and Hadley projections. On the contrary, the yield tends to decrease respect to the scenario without adaptation, considering delayed sowind date. Indeed, NCAR provides more moderate changes in yield, both for early and delayed sowing date.

In this case the mean yield comparisons by SNK-test (Tab. 5.3.2.1) show a statistically significant difference between now and climate change scenarios with early sowing date for all future periods for Hadley and NCAR projections, and for 2050and 2075 for ECHAM projections. But these differences are not significant in any case if compared with the ordinary sowing date.

Table 5.3.2.1 Mean yield (t ha^{-1}) comparison for now and future periods, with three GCMs for mid climate change scenario without adaptation (CC mid) and climate change scenarios with adaptation (early and delayed sowing date) for Iride at Ottava site.

		Hadley		NCAR		ECHAM	
		Yield (t ha^{-1})		Yield (t ha^{-1})		Yield (t ha^{-1})	
Now		4.2	cd	4.2	d	4.2	bc
2025	**CC (mid)**	4.4	bcd	4.6	cde	4.4	abc
	CC (mid) +A (early)	4.8	ab	4.9	bc	4.7	ab
	CC (mid) +A (delayed)	4.0	d	4.2	de	3.9	c
2050	**CC (mid)**	4.7	bc	4.9	abc	4.4	abc
	CC (mid) +A (early)	5.0	ab	5.2	ab	4.8	a
	CC (mid) +A (delayed)	4.2	cd	4.6	cd	4.1	c
2075	**CC (mid)**	4.9	ab	5.2	ab	4.5	abc
	CC (mid) +A (early)	5.3	a	5.5	a	4.9	a
	CC (mid) +A (delayed)	4.5	bcd	5.1	abc	4.2	c

Means within each group (single GCM and different future periods) sharing the same letter do not differ significantly from one another (SNK-test at $P \leq 0.05$).

Anthesis

The Figures 5.3.2.2 *a, b,* and *c*, show the effects of changing in planting date on anthesis date (difference in days from now to future periods), under future climate change scenarios, considering separately the three GCMs with middle climate change scenario.

Also for Ottava site, it is possible to observe for Iride a longer duration of the period from sowing to anthesis, if the date of sowing is advanced by 30 days respect to the ordinary sowing date, for all future periods, and particularly for 2025, as projected by all GCMs. However, for Iride the duration of the period from sowing to anthesis is few days shorter than that one projected for Simeto for the same site.

Also for Iride, the differences in projection of the three GCMs are quite similar for anthesis, respect the projections of the three GCMs for yield.

The statistical analysis performed with SNK-test (Tab. 5.3.2.2) show significantly differences from now to future climate change scenarios, both with and without adaptation strategies, and also comparing the same future period with or without change in planting date. This partially justifies the higher yield pointed out in the previous analysis.

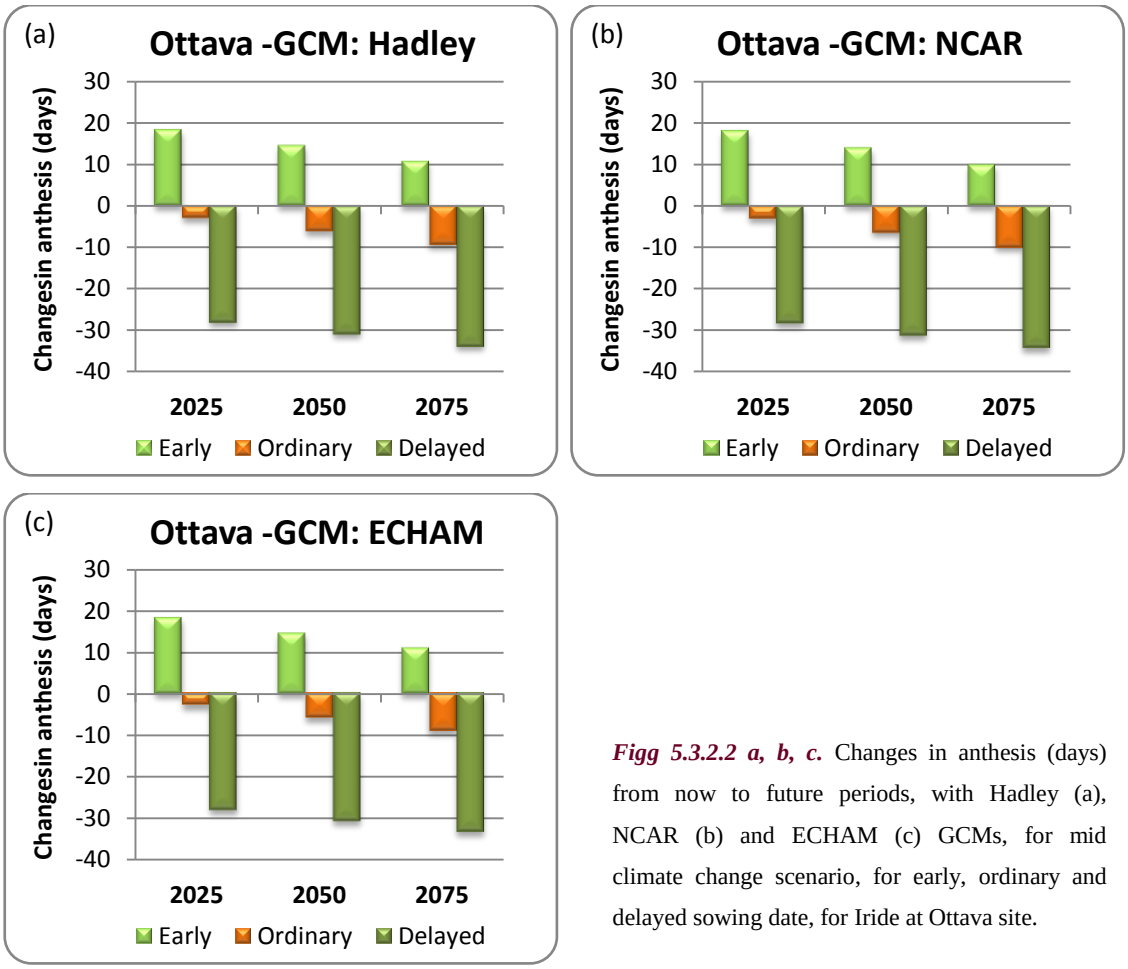

Figg 5.3.2.2 a, b, c. Changes in anthesis (days) from now to future periods, with Hadley (a), NCAR (b) and ECHAM (c) GCMs, for mid climate change scenario, for early, ordinary and delayed sowing date, for Iride at Ottava site.

Table 5.3.2.2 Mean anthesis (dap) comparison for now and future periods, with three GCMs for mid climate change scenario without adaptation (CC mid) and climate change scenarios with adaptation (early and delayed sowing date), for Iride at Ottava site.

		Hadley	NCAR	ECHAM
		Anthesis (days)	Anthesis (days)	Anthesis (days)
Now		128 d	128 d	128 d
2025	**CC (mid)**	125 e	124 e	125 e
	CC (mid) +A (early)	146 a	146 a	146 a
	CC (mid) +A (delayed)	100 h	99 h	100 h
2050	**CC (mid)**	122 f	121 f	122 f
	CC (mid) +A (early)	142 b	142 b	142 b
	CC (mid) +A (delayed)	97 i	96 i	97 i
2075	**CC (mid)**	118 g	118 g	119 g
	CC (mid) +A (early)	138 c	138 c	139 c
	CC (mid) +A (delayed)	94 j	93 j	94 j

Means within each group (single GCM and different future periods) sharing the same letter do not differ significantly from one another (SNK-test at P≤0.05).

5.4 SANTA LUCIA

5.4.1 Simeto

Yield

Figures 5.4.1.1 *a*, *b* and *c*, show, separately for the three GCMs, the ratio of yield for middle climate change scenarios, with and without adaptation, to baseline yields (t ha^{-1}), for Simeto, under future projected climate change conditions.

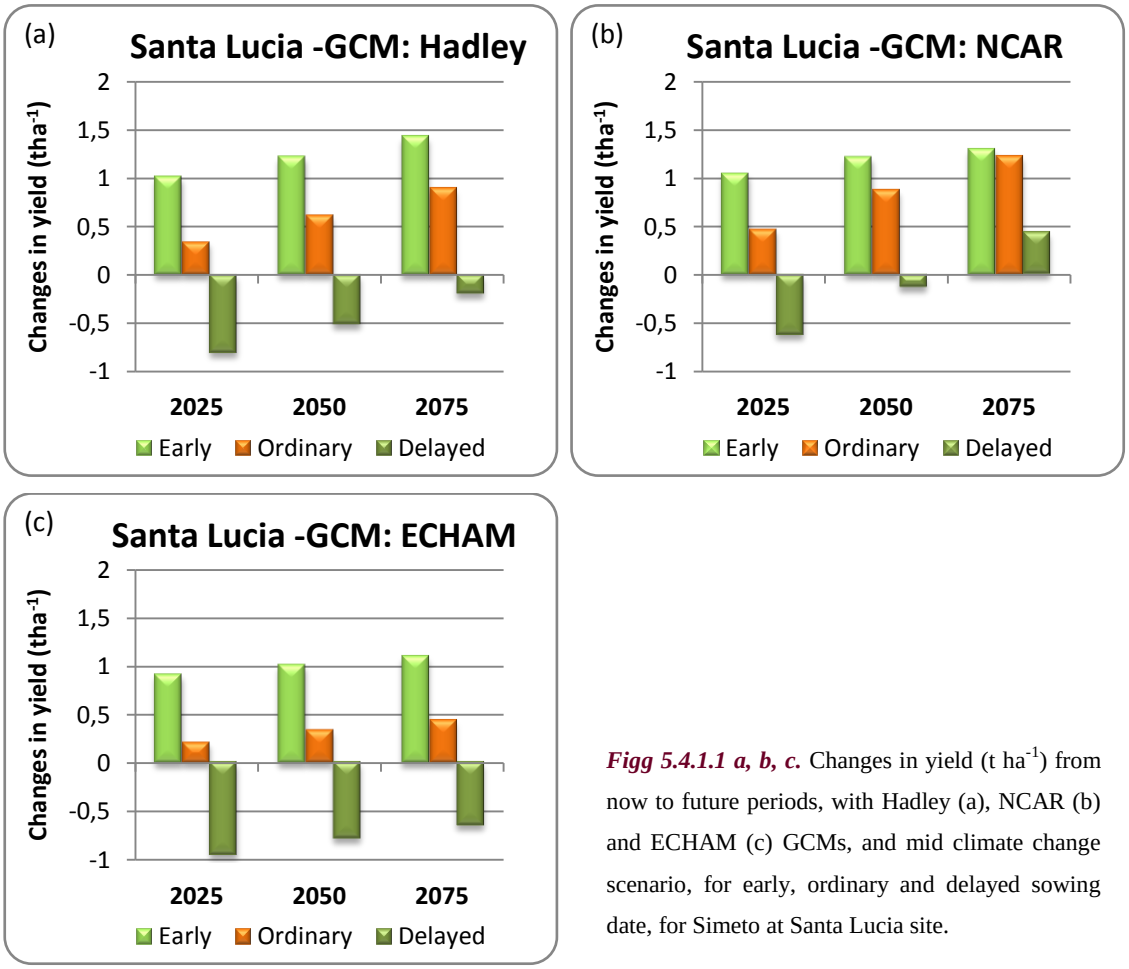

Figg 5.4.1.1 a, b, c. Changes in yield (t ha^{-1}) from now to future periods, with Hadley (a), NCAR (b) and ECHAM (c) GCMs, and mid climate change scenario, for early, ordinary and delayed sowing date, for Simeto at Santa Lucia site.

Also in this case, the simulations for yields, considering early sowing date, show a increase respect to the scenario without adaptation, in particular for ECHAM and Hadley projections. On the contrary, the yield tends to decrease respect to the scenario without adaptation, considering delayed sowing date. While NCAR provides the more moderate changes between scenarios with or without adaptation strategy.

However, the mean yield comparisons by SNK-test (Tab. 5.4.1.1) for Simeto, at santa Lucia site, show a statistically significant difference between now and climate change scenarios

with early sowing date for all future periods, with all GCMs. Moreover, significant differences are shown also comparing yield projected by the model for a early sowing date than those projected with the ordinary sowing date. This means that for this site and this cultivar, the earlier sowing date might be a usefull adaptation strategy in responce to climate change.

Table 5.4.1.1 Mean yield (t ha^{-1}) comparison for now and future periods, with three GCMs for mid climate change scenario without adaptation (CC mid) and climate change scenarios with adaptation (early and delayed sowing date) for Simeto at Santa Lucia site.

		Hadley		NCAR		ECHAM	
		Yield (t ha^{-1})		Yield (t ha^{-1})		Yield (t ha^{-1})	
Now		4.1	ef	4.1	d	4.1	b
2025	**CC (mid)**	4.4	de	4.6	c	4.3	b
	CC (mid) +A (early)	5.1	abc	5.1	a	5.0	a
	CC (mid) +A (delayed)	3.3	h	3.5	e	3.1	c
2050	**CC (mid)**	4.7	cd	5.0	ab	4.4	b
	CC (mid) +A (early)	5.3	ab	5.3	a	5.1	a
	CC (mid) +A (delayed)	3.6	gh	4.0	d	3.3	c
2075	**CC (mid)**	5.0	bc	5.3	a	4.5	b
	CC (mid) +A (early)	5.5	a	5.4	a	5.2	a
	CC (mid) +A (delayed)	3.9	fg	4.5	b	3.4	c

Means within each group (single GCM and different future periods) sharing the same letter do not differ significantly from one another (SNK-test at P≤0.05).

Anthesis

The Figures 5.4.1.2 *a*, *b*, and *c*, show the effects of changing in planting date on anthesis date (difference in days from now to future periods), under future climate change scenarios, considering separately the three GCMs with middle climate change scenario.

Again, also for this site it is possible to observe a longer duration of the period from sowing to anthesis if the date of sowing is advanced by 30 days respect to the ordinary sowing date, for all future periods and all GCMs. On the contrary, if the sowing date is delayed by 30 days, the duration of the period from sowing to anthesis, is projected to decrease for all future periods.

The statistical analysis performed with SNK-test (Tab. 5.4.1.2) show significantly differences from now to future climate change scenarios both with and without adaptation strategies, and also comparing the same future period with or without change in sowing date.

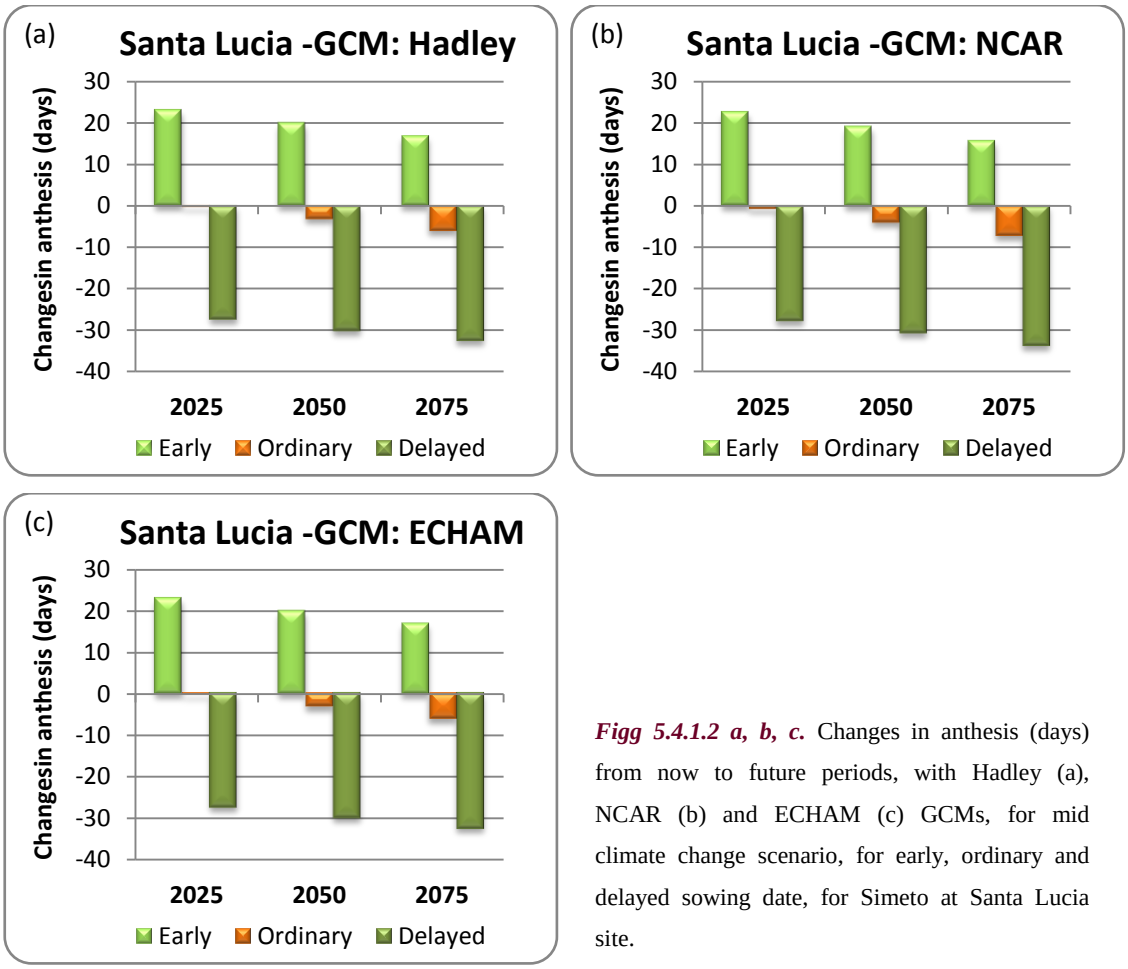

Figg 5.4.1.2 a, b, c. Changes in anthesis (days) from now to future periods, with Hadley (a), NCAR (b) and ECHAM (c) GCMs, for mid climate change scenario, for early, ordinary and delayed sowing date, for Simeto at Santa Lucia site.

Table 5.4.1.2 Mean anthesis (dap) comparison for now and future periods, with three GCMs for mid climate change scenario without adaptation (CC mid) and climate change scenarios with adaptation (early and delayed sowing date), for Simeto at Santa Lucia site.

		Hadley	NCAR	ECHAM
		Anthesis (days)	Anthesis (days)	Anthesis (days)
Now		125 d	125 d	125 d
2025	**CC (mid)**	124 d	124 d	124 d
	CC (mid) +A (early)	148 a	147 a	148 a
	CC (mid) +A (delayed)	97 g	97 g	97 g
2050	**CC (mid)**	121 e	120 e	121 e
	CC (mid) +A (early)	144 b	144 b	145 b
	CC (mid) +A (delayed)	94 h	94 h	95 h
2050	**CC (mid)**	118 f	117 f	119 f
	CC (mid) +A (early)	141 c	140 c	142 c
	CC (mid) +A (delayed)	92 i	91 i	92 i

Means within each group (single GCM and different future periods) sharing the same letter do not differ significantly from one another (SNK-test at P≤0.05).

5.4.2 Iride

Yield

Figures 5.4.2.1 *a, b* and *c*, show, separately for the three GCMs, the ratio of yield for middle climate change scenarios, with and without adaptation, to baseline yields (t ha^{-1}), for Iride, under future projected climate change conditions.

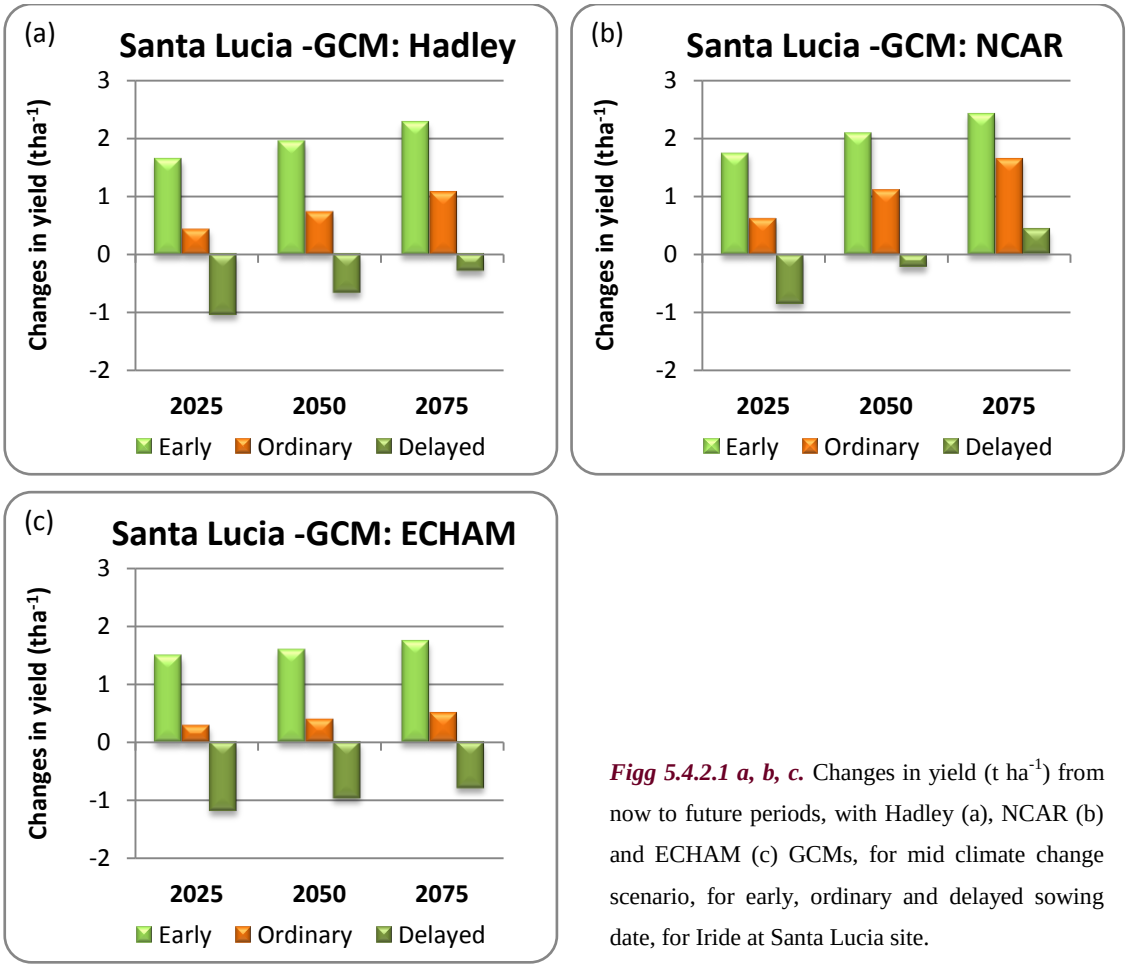

Figg 5.4.2.1 a, b, c. Changes in yield (t ha^{-1}) from now to future periods, with Hadley (a), NCAR (b) and ECHAM (c) GCMs, for mid climate change scenario, for early, ordinary and delayed sowing date, for Iride at Santa Lucia site.

Also for this site, the yield simulations for Iride show the same trend observed for Simeto, but for Iride are projected higher mean changes in yield considering early sowing date, while the ratio of reduction in yield for simulations with delayed sowing date are similar to that projected for Simeto.

The mean yield comparisons by SNK-test (Tab. 5.4.2.1) show a statistically significant difference between now and climate change scenarios with early sowing date for the three future periods, whit all GCMs projections. Furthermore, there are statistically significant differences also between early and ordinary sowing date for all future periods fand all climate change scenarios.

Table 5.4.2.1 Mean yield (t ha^{-1}) comparison for now and future periods, with three GCMs for mid climate change scenario without adaptation (CC mid) and climate change scenarios with adaptation (early and delayed sowing date).

		Hadley		NCAR		ECHAM	
		Yield (t ha^{-1})		Yield (t ha^{-1})		Yield (t ha^{-1})	
Now		4.8	ef	4.8	ef	4.8	b
2025	**CC (mid)**	5.2	de	5.4	d	5.0	b
	CC (mid) +A (early)	6.4	b	6.5	b	6.2	a
	CC (mid) +A (delayed)	3.7	h	3.9	g	3.6	c
2050	**CC (mid)**	5.5	cd	5.9	c	5.1	b
	CC (mid) +A (early)	6.7	ab	6.9	ab	6.3	a
	CC (mid) +A (delayed)	4.1	gh	4.5	f	3.8	c
2050	**CC (mid)**	5.8	c	6.4	b	5.3	b
	CC (mid) +A (early)	7.0	a	7.2	a	6.5	a
	CC (mid) +A (delayed)	4.5	fg	5.2	de	4.0	c

Means within each group (single GCM and different future periods) sharing the same letter do not differ significantly from one another (SNK-test at P≤0.05).

Anthesis

The Figures 5.4.2.2 *a, b,* and *c*, show the effects of changing in planting date on anthesis date (difference in days from now to future periods), under future climate change scenarios, considering separately the three GCMs with middle climate change scenario.

Also for this site, it is possible to observe for Iride a longer duration of the period from sowing to anthesis, if the date of sowing is advanced by 30 days respect to the ordinary sowing date, for all future periods and particularly for 2025, as projected by all GCMs, but for Iride the duration of the period from sowing to anthesis is few days shorter than that projected for Simeto for the same site.

Also for Iride, the differences in projection of the three GCMs are quite similar for anthesis, respect the projections of the three GCMs for yield.

The statistical analysis performed with SNK-test (Tab. 5.4.2.2) show significantly differences from now to future climate change scenarios both with and without adaptation strategies, and also comparing the same future period with or without change in planting date.

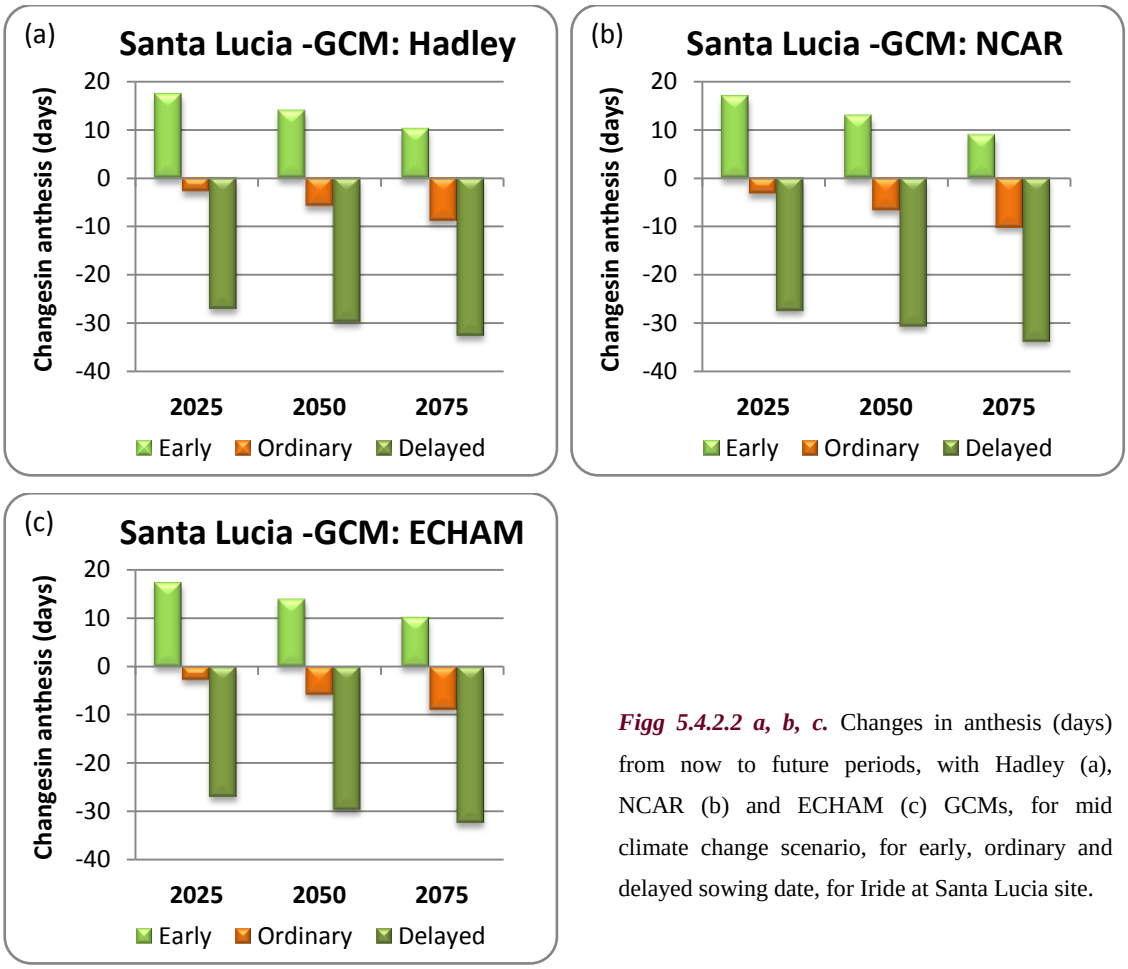

Figg 5.4.2.2 a, b, c. Changes in anthesis (days) from now to future periods, with Hadley (a), NCAR (b) and ECHAM (c) GCMs, for mid climate change scenario, for early, ordinary and delayed sowing date, for Iride at Santa Lucia site.

Table 5.4.2.2 Mean anthesis (dap) comparison for now and future periods, with three GCMs for mid climate change scenario without adaptation (CC mid) and climate change scenarios with adaptation (early and delayed sowing date), for Iride at Santa Lucia site.

		Hadley	NCAR	ECHAM
		Anthesis (days)	Anthesis (days)	Anthesis (days)
Now		123 d	123 d	123 d
2025	**CC (mid)**	121 e	120 e	121 e
	CC (mid) +A (early)	141 a	140 a	141 a
	CC (mid) +A (delayed)	96 h	96 h	96 h
2050	**CC (mid)**	118 f	117 f	118 f
	CC (mid) +A (early)	137 b	136 b	137 b
	CC (mid) +A (delayed)	94 i	93 i	94 i
2050	**CC (mid)**	115 g	113 g	115 g
	CC (mid) +A (early)	134 c	132 c	134 c
	CC (mid) +A (delayed)	91 j	90 j	91 j

Means within each group (single GCM and different future periods) sharing the same letter do not differ significantly from one another (SNK-test at P≤0.05).

DISCUSSION AND CONCLUSIONS

Performance of CERES-Wheat model

The results of the analysis performed in this study confirm the good performance of the CERES-Wheat model when applied in Mediterranean areas. In the first part of this thesis, the model was successfully calibrated and validated as far as the simulation of grain yield and anthesis is concerned.

As major results, the model tends to slightly overestimate the yield in all sites, except for Santa Lucia, where the model tends to underestimate. This is probably due to the particular soil characteristics of this site, in which water table frequently start to perch at about 70 cm soil depth and sometimes reach the surface, as already was pointed out in the description of the results.

Moreover, the general overestimation of the variables, obtained for all site with different environmental and soil conditions, could be partially explained considering that the model does not take into account the effect of pests and diseases. Such effects, which are very important in actual experimental conditions and may affect the yield, in fact, are not included in the model equations (St'astna *et al.*, 2002; Ghaffari *et al.*, 2002, Trnka *et al.*, 2004).

However, major difficulties to obtain a satisfactory calibration of the model, and thus good performance in the validation phase, are related to the size of the datasets available for the study. In fact, the process of crop model application requires, in general, a collection of large data sets, which must include weather, soil, and crop management data, collected over long time periods. Furthermore, data used to evaluate crop models are generally designed for other purposes than the model evaluation and collected from experiments that are carried out to reach different final goals. This was also the case of this study, where crop and management data come from the collection of the Italian durum wheat network for cultivar evaluation (http://www. cerealicoltura.it).

Moreover, data set somehow do not contain the input data necessary for crop model functioning (e.g. solar radiation, initial condition at planting date, detailed information about phenological phases, etc..). In this case, this information, had to be estimated, with the obvious limitations that this may cause.

Climate change impact assessment

The methodological approach for assessing the climate change impact that was used in this thesis shows several strengths. In particular, the method for developing climate change scenarios that was applied allows to explore a wide range of possible future changes in climate and consequently, to give a more likely crop impact assessment.

The choice of reproducing weather series representing the changed climate through a generator, was supported by the necessity to have site specific weather series that well reproduce local climate variability. The results obtained in the validation of the weather generator, that was performed comparing statistical properties of crop model output simulated using observed weather data versus outputs obtained with synthetic weather series (generated by weather generator) for actual period, showed no statistical differences by mean comparison. Consequently, the use of CERES-Wheat coupled with synthetic weather series provides an efficient and reliable method for assessing the impacts on agricultural production.

It is essential to highlight that the analysis carried out with multiple climate change scenarios take into account the uncertainties still present in the study of climate change impact. Based on this consideration reported by several researches, in this study it was considered the effects of several different scenarios obtained by the combination of three GCMs and three values of ΔT_G (obtained by combining three levels of climate sensitivities and four emission scenarios).

Furthermore, the pattern scaling technique applied in this work allowed to consider uncertainties in the climate change pattern (differences between individual GCMs and internal uncertainty of a given GCM) and uncertainty in estimating the global mean temperature.

In particular, for each experimental site, 27 climate change scenarios, 9 for each future period, were developed. This approach has allowed exploring a wide range of variability in future climate projections. A wide range of values for the climatic variables, such as temperature, precipitation and solar radiation, projected by the three GCMs with different emission scenarios and values of climate sensitivity, for all experimental sites studied in Sardinia was obtained. The differences between CGMs are quite evident, in particular for precipitation pattern. The major diversity is that, while Hadley and especially ECHAM show an evident reduction in precipitations for future periods respect to present period, NCAR provides the lower decreases and conversely an increase in November and March for all future periods.

Also the crop response to projected climate change scenarios still contains many uncertainties. Many studies have highlighted that many complex processes and interactions affect crop yield under climate change conditions. Among them, the direct impact of atmospheric composition on crops has received, in recent years, much attention, from both experimentalists and modellers. In particular, the effect of the increased carbon dioxide concentration was investigated.

Many recent studies modelling the impact of climate change on crops have simulated the effects of elevated CO_2, showing a general increase in yield due to an higher CO_2 concentration in atmosphere. However, Long *et al.* (2006) consider that crop models tends to overestimate the effect of CO_2 on plant growth and yield, as a result of the CO_2-related model parameters are mainly derived from controlled and semi-controlled experiments, which typically show a higher CO_2 response than observed under field conditions. Conversely, Tubiello *et al.* (2007), argued that, despite the number of free air carbon dioxide enrichment (FACE) experiments available to validate

crop models under field conditions is still limited, there is growing evidence that crop models are able to reproduce the observed crop responses in the FACE experiments.

In this study were explored separately direct and indirect effects of different CO_2 concentrations projected for the future periods to estimate the effect linked to it.

The results obtained show that the indirect effect of CO_2 concentration, related to changed weather conditions, is, in general, negative. The yields decrease from the lower value of 1.2% projected for 2025 with the low climate change scenario, to the higher value of 27.8% projected for 2075 with high climate change scenario, for Simeto cultivar, considering the ranges of mean values projected by the three GCMs for different climate change scenarios, in the present concentration of ambient CO_2. Similarly, for Iride cultivar, decreases from 1.1% projected for 2025 with the low climate change scenario, to 26.6% projected for 2075 with high climate change scenario, are obtained. The differences between GCMs and also between sites are rather evident, but considering the mean values projected for the four experimental sites, it is possible observe decreases in yield from 3-6% for 2025, to 11-18% for 2075, for Simeto, and from 2-4% for 2025, to 10-16% for 2075 for Iride cultivar.

Hence, results for climate change impact assessment, for the four sites considered in this study, show a general decrease in yields without considering the direct effect of CO_2 for both cultivars, particularly due to a reduction in precipitation and an increase in temperature. The increased temperature will shorten the period of the growing season anticipating the phenological phase occurrences, and will not allow an optimal development of the crop. In fact, the results obtained for climate change impact on anthesis date, show an advancement of anthesis phase occurrence: from the lower value of 2 days projected for 2025 to 15 days projected for 2075, for both cultivars studied. The simultaneous decrease of precipitation and increase of temperature and solar radiation sums will further reduce the yields through intensifying the water stress.

Despite similar trend patterns at individual climate change scenarios and time periods, there is a significant influence of the site-specific conditions that play an important role in determination of climate change impact on yields. The higher decreases are projected for both varieties for Benatzu (South of Sardinia) site and the lower for Ottava (North of Sardinia) site.

Since the magnitude of the indirect effect is closely related to the site-specific climatic conditions and the climate change scenario employed, the comparison with other studies has only limited information value. Nevertheless, it should be noted that Trnka *et al.* (2004) report that, using seven GCMs and two emission scenarios for three future periods, the reduction in wheat yield could reach up to 25%, if the direct effect of CO_2 concentration is not considered. Ghaffary *et al.*, (2002), show a decrease in wheat yield from 3 to 9%, considering an increase in temperature of 2 and 4°C respectively. Similarly, Cesaraccio et al., (2008), using incremental scenarios of increased temperature (from 1 to 6 °C) and decreased precipitation (from 5 to 30%), for two experimental sites in the South of Sardinia, report a decrease in wheat yield variable from 2 to

38%. Also Brassard and Singh, using two GCMs and two emission scenarios, for seven location in Southern Québec, show a decrease in wheat yield that could reach more than 40%, without consider direct effect of increase in CO_2 concentration. The decreases were attributed mainly to shortened crop growth phases due to increased temperatures and an increased evapotraspiration demand caused both by the higher temperature and by increased solar radiation sums. An overview of 17 experimental studies (Amthor, 2001) shows that wheat yield reacted to the increased temperature sums (1.1-4°C) with yield reduction of 0.5-48%.

Combination of the changed climatic conditions and increased CO_2 concentration on crop yields may lead to the inverse trend. In fact, the results obtained in this study, considering both direct and indirect effect of CO_2 concentration, show a mean increase in wheat yield in all sites for the two cultivars, especially for Iride. It could be expected a mean increase by 5% for 2025 and by 16% for 2075, for Simeto variety and by 7% for 2025 and by 21% for 2075 for Iride variety.

It means that the positive effects of increase in CO_2 concentration may dominate over the negative effect of changed weather conditions. The magnitude of the direct effect of increased CO_2 concentration on yield is a result of a superposition of two mechanisms: on one hand the intensified photosynthesis activity, and, on the other hand, greater water use efficiency. In fact, a higher CO_2 concentration reduce stomatal aperture and stomatal density, which causes a reduction in stomatal conductance and thus transpiration (Olesen and Bindi, 2002). An average reduction of 20% of stomatal conductance has been found with a doubling of the current CO_2 concentration (Drake *et al.,* 1997), and CERES-models are able to consider this important factor, as already reported in methodology. The values obtained for 2075 are generally higher that the other projections because the water stress is higher and the positive effect on yield of improved water use efficiency is more pronounced. The differences recorded between sites are evident and are justified by differences in weather and soil conditions. In particular, soils with a good nutrient supply (e.g., Santa Lucia and Benatzu), show a highest response for increased CO_2 concentration.

Similar results were obtained by other authors. For example, Trnka *et al*. (2004) report that the wheat yields tend to increase in the range of 7.5-25.3% from 2025 to 2100 (using 7 GCMs-based scenarios). Brassard and Singh (2008), considering the CO_2 fertilisation effect, report a changes in wheat yield ranging from 5.8 to 47.3%, and a mean value of 14.8%, for several climate change scenarios. Ghaffary *et al.,* report that the combined direct and indirect increased CO_2 concentration effects may cause increases in yield under all climate change scenarios considered. An overview of climate change impact studies for a number of grain crops in Europe, (Olesen and Bindi, 2002), shows, for rainfed wheat in South Europe region, that the yield may change from +18% to -16% as consequence of the climate change scenarios used. Tubiello *et al.,* 2002, using two GCMs, report a mean reduction in wheat yield from 10 to 40%, although the direct effect of increased CO_2 concentration was included. These results, however, are related to rainfed wheat and therefore affected by changes in water stress, which may differ for individual sites and climate

scenarios. It is, also, difficult to compare results obtained in studies that differ for crop simulation models, GCMs and emission scenarios used to climate change impact assessment. The crop response to CO_2 increase depends strongly on management practices. For example, Tubiello and Ewert (2002), considering the interaction between water stress and CO_2, showed that for a range of models and observations, water-stressed crops did show a greater percentage increase in yield under elevated CO_2. The contrary is true for nitrogen limitation, because well fertilized crops respond more positively to CO_2 than less fertilized ones, with a higher production of dry matter (Tubiello *et al.*, 2000).

It is also known that the CO_2 fertilization effect is usually stronger at higher temperatures (Goudrian and Zadoks, 1995). It seems that the highest CO_2 fertilisation effect should be found where growing season temperature increases are the greatest. But for each crop it necessary to carefully consider the competing interaction between temperature and CO_2 fertilisation.

In fact, regarding CO_2 effects, it is still necessary to better understand the possible interactions with the effects of elevated CO_2 and other factors, such as different climate variables, soil and crop management (Ewert *et al.*, 2007).

Adaptation strategies evaluation

Considering the adaptation strategies, it is possible to observe that the decrease of the mean yield, due to the indirect effect of increased CO_2 concentration, may be reduced if the wheat is sown one month earlier (compared to the sowing date of the representative year). Indeed, the earlier planting date would cause an additional increase in wheat yield and could be an efficient adaptation strategy for this region.

In particular for Simeto cultivar, it was possible to observe a longer growing season, postponing the phenological phases occurrence (from a mean value for the four sites of 4 days in 2025 to 10 days in 2075), with a mean increase in yield from 15% in 2025 to 22% for 2075. Also for Iride it was obtained a longer growing season, delaying the phenological phases occurrence (from a mean value for the four sites of 5 days in 2025 to 11 days in 2075), with a mean increase in yield of 23% in 2025 and of 34% in 2075.

To conclude, it may be stated that the results are in good agreement with the rules governing the growth and development of the crop. Specifically, the increases or decreases of yields may be logically explained by effects of a changed weather regime and changed ambient CO_2 concentration on the duration of growing period, water stress occurrence and photosynthesis rate.

More efforts are necessary to improve knowledge about application of CERES-Model for taking in to account water stress in the Mediterranean area.

Study to investigate all these aspects should be made afterward, and the same methodology explained in this thesis might be applied in subsequent works to clarify some aspect of the mechanism either on the impacts of climate change and possible adaptation strategies application.

REFERENCES

ACC/SCN (United Nations Administrative Committee on Coordination/Standing Committee on Nutrition), 2004. Fifth report on the world nutrition situation: Nutrition for improved development outcomes. Geneva, Switzerland.

Acock, B., Allen, L.H. Jr., 1985. Crop responses to elevated carbon dioxide concentrations. In: Strain B.R., Cure J.D. (eds) Direct effects of increasing carbon dioxide on vegetation. DOE/ERB0238. U.S. Department of Energy, Washington DC, pp 53–97.

Acock, B., Reddy, V.R., 1997. Designing an object-oriented structure for crop models. Ecol. Modelling 94, 33–44.

Acock, B., Reynolds, J.F., 1997. Introduction: modularity in plant models. Ecol. Modelling 94, 1-6.

Adger W.N., Arnell N.W., Tompkins E.L., 2005. Successful adaptation to climate change across scales. Glob Environ Change 15:77–86.

Aggarwal, P.K., Roetter, R.P., Kalra, N., Van Keulen, H., Hoanh, C.T. and Van Laar, H.H. (eds.), 2001. Land use analysis and planning for sustainable food security: with an illustration for the state of Haryana, India. Indian Agricultural Research Institute, New Delhi, International Rice Research Institute, Los Baños, Wageningen University and Research centre, Wageningen, 167 pp.

Ainsworth, E.A. and Long, S.P., 2005. What have we learned from 15 years of free-air CO2 enrichment (FACE)? A meta-analysis of the responses of photosynthesis, canopy properties and plant production to rising CO2. New Phytologist 165: 351-372.

Alexandrov, V. A.: 1997, 'Vulnerability of agronomic systems in Bulgaria', Climatic Change 36, 135–149.

Alexandrov V.A., Hoogenboom G., 2000. The impact of climate variability and change on crop yield in Bulgaria. Agric For Meteorol 104:315–327.

Alexandrov, V., Eitzinger, J., Cajic, V., Oberforster, M., 2002. Potential impact of climate change on selected agricoltural crops in northeastern Austria. Global Change Biology, 8, 372-389.

Amthor, J.S., (2001). Effects of atmospheric CO2 concentration on wheat yield: review of results from experiments using various approaches to control CO_2 concentration. Field Crops Res. 73, 1–34.

Arnell, N.W., Cannell, M.G.R., Hulme, M., Kovats, R.S., Mitchell, J.F.B., Nicholls, R.J., Parry, M.L., Livermore, M.T.J. and White, A., 2002. The Consequences of CO2 Stabilisation for the Impacts of Climate Change. Climatic Change, 53, (4), 413-446.

Arnold, C.D., Elliot, W.J., 1996. CLIGEN Weather generator predictions of seasonal wet and dry spells in Uganda. Trans. ASAE 39 (3), 969–972.

Asseng S, Van Herwaarden A, Setter TL, Palta JA (2003)The impact of crop modelling on plant physiological research and breeding—an example. In: Solutions for a better environment. Proceedings of the 11th Australian Agronomy Conference. Geelong, Victoria, Australia. 2–6 February 2003. Published on CDROM ISBN 0-9750313-0-9. p 4

Audsley, E. & Pearn, K.R. & Simota, C. & Cojocaru, G. & Koutsidou, E. & Rounsevell, M.D.A. & Trnka, M. & Alexandrov, V., 2006. "What can scenario modelling tell us about future European scale land use, and what not?" , Environmental Science & Policy, vol. 9, page 148-162.

Autrique, E., Nachit, M.M., Monneveux, P., Tanksley, S.D. and Sorrells, M.E., 1996. Genetic diversity in durum wheat based on RFLPs, morphophysiological traits, and coefficient of parentage. Crop Sci. 36, 735–742.

Baenziger P., Graybosch R., Van Sanford D., and Berzonsky W., 2009. Winter and Specialty Wheat M.J. Carena (ed.), Cereals, pp. 251-265. DOI: 10.1007/978-0-387-72297-9, Springer Science + Business Media, LLC 2009.

Baffaut, C., Nearing, M.A., Nicks, A.D., 1996. Impact of CLIGEN parameters on WEPP-predicted average annual soil loss. Trans. ASAE 39 (2), 447–457.

Bagnara, D., Scarascia Mugnozza, G.T., 1975. Outlook in breeding for yield in durum wheat. In: Scarascia Mugnozza, G. T. (Ed.), Genetics and Breeding of Durum Wheat, pp. 249-274.

Belaid, A. (2000) Durum wheat in WANA: Production, trade and gains from technological change. In: C. Royo, M.M. Nachit, N. Di Fonzo and J.L. Araus (Eds.), Durum Wheat Improvement in the Mediterranean Region: New challenges. Options Méditerranéennes. Series A. 40, 63–70.

Barrett, D.J., Gifford, R.M., (1999). Increased C-gain by an endemic Australian pasture grass at elevated atmospheric CO2 concentration when supplied with non-labile inorganic phosphorous. Aust. J. Plant Physiol. 26, 443–451.

Bechhofer, R.E., Santner, T.J. and Goldsman, D.M., 1995. Design and Analysis of Experiments for Statistical Selection, Screening, and Multiple Comparisons. Wiley, New York.

Bellocchi G., Maestrini C., Fila G., Fontana F., 2002. Assessment of the effects of climate change and elevated CO_2: a case study in Northern Italy. VII European Society for Agronomy Congress, Cordoba, Spain. 15–18 July 2002, 763–764.

Bender J., Hertstein U., Black C.R., 1999. Growth and yield responses of spring wheat to increasing carbon dioxide, ozone and physiological stresses: a statistical analysis of 'ESPACE-wheat', results. Eur J Agron 10:185–195.

Beniston, M., Stephenson D.B., Christensen O.B., Ferro C.A.T., Frei C., Goyette S., Halsnaes K., Holt T., Jylhä K., Koffi B., Palutikof J., Schöll R., Semmler T. and Woth K., 2007. Future extreme events in European climate: an exploration of regional climate model projections. Climatic Change, 81, S71-S95.

Bindi, M., Ferrini, F. and Miglietta, F., 1992. 'Climatic change and the shift in the cultivated area of olive trees', J. Agric. Mediterranea 22, 41–44.

Bongaarts J., 1994. Can the growing human population feed itself? Sci Am 270(3):18–24.

Boogaard, H.L., C.A. van Diepen, R.P. Rtter, J.M.C.A. Cabrera & H.H. van Laar, 1998. User's guide for the WOFOST 7.1 crop growth simulation model and WOFOST Control Center 1.5. DLO-Winand Staring Centre, Wageningen, Thecnical Document 52, 144 pp.

Boote, K.J., Loomis, R.S. (Eds.), 1991. Modeling crop photosynthesis — from biochemistry to canopy. CSSA Special Publication Number 19. Crop Science Society of America, Madison, WI.

Boote, K.J., Jones, J.W., Pickering, N.B., 1996. Potential uses and limitations of crop models. Agron. J. 88, 704–716.

Boote, K.J., Jones, J.W., Hoogenboom, G., 1997. Simulation of crop growth: CROPGRO model. In: Peart, R.M., Curry, R.B. (Eds.), Agricultural Systems Modeling. Marcel Dekker, New York, pp. 651–692.

Bosello F., Carraro C. and De Cian E. (2009), An Analysis of Adaptation as a Response to Climate Change, Copenhagen Consensus Center, available on line at: http://fixtheclimate.com

Bouman, B.A.M., van Keulen, H., van Laar, H.H., Rabbinge, R., 1996. The School-of-de-Wit crop growth simulation models: a pedigree and historical overview. Agricultural Systems 52 (2-3), 171–198.

Brassard, J.P. and Singh, B., 2008. Impacts of climate change and CO2 increase on agricultural production and adaptation options for Southern Que´bec, Canada. Mitig Adapt Strateg Glob Change. 13:241–265.

Brisson, N., Gary, C., Justes, E., Roche, R., Mary, B., Ripoche, D., Zimmer, D., Sierra, J., Bertuzzi, P., Burger, P., Bussie`re, F., Cabidoche, Y.M., Cellier, P., Debaeke, P., Gaudille`re, J.P., He´nault, C., Maraux, F., Seguin, B., Sinoquet, H., 2003. An overview of the crop model STICS. European Journal of Agronomy 18, 309-332.

Brisson N., Wery, J., and Boote K., 2006. Fundamental concepts of crop models illustrated by a comparative approach. In: Working with Dynamic Crop Models, chapter 9: 257-279.

Bryant, C.R., Smit, B., Brklacich, M., Johnston, T., Smithers, J., Chiotti, Q. and Singh, B., 2000. Adaptation in Canadian agriculture to climatic variability and change. Clim. Change 45, 181–201.

Brown, J.K.M., 2002. Yield penalties of disease resistance in crops. Current Opinion in Plant Biology 5: 339-344.

Brown R.A., Rosenberg N.J., 1997. Sensitivity of crop yield and water use to change in a range of climatic factors and CO2 concentrations: a simulation study applying EPIC to the central USA. Agric Forest Meteor 83:171–203.

Bruinsma, J. (ed.), 2003: World agriculture: towards 2015/2030, FAO, London: Earthscan.

Carbone G.J., Kiechle W., Locke C., Mearns L.O., McDaniel L., Downton M.W., 2003. Response of soybean and Sorghum to varying spatial scales of climate change scenarios in the South-eastern United States. Clim Change 60:73–98.

Carter, T. R., Saarikko, R. A. and Niemi, K. J., 1996. 'Assessing the risks and uncertainties of regional crop potential under a changing climate in Finland', Agric. Food Sci. Finland 3, 329–349.

Cesaraccio C., Dettori M., Duce P., Spano D., Motroni A., Mereu V. (2008). Using Long-Term Data and Crop Modelling to Assess Climate Change Impacts on Durum Wheat Production in the Mediterranean. Proceedings of the X Congress of ESA, Bologna.

Challinor A.J., Wheeler T.R., Craufurd P.Q., Ferro C.A.T., Stephenson D.B., 2007a. Adaptation of crops to climate change through genotypic responses to mean and extreme temperatures. Agric Ecosyst Environ 119:190–204.

Challinor A.J., Wheeler T.R., Garforth C., Craufurd P.Q., Kassam A., 2007b. Assessing the vulnerability of food crop systems in Africa to climate change. Clim Change 83:381–399.

Chiotti, Q.P. and Johnston, T., 1995. Extending the boundaries of climate change research: A discussion on agriculture. J. Rural Stud. 11(3), 335–350.

Chmielewski, F.M., Muller A., Bruns E., 2004. Climate changes and trends in phenology of fruit trees and field crops in Germany, 1961–2000. Agricult For Meteorol 121(1–2):69–78.

Clark, W.C., Crutzen, P.J. and. Schellnhuber, H.J., 2004. Science for global sustainability: toward a new paradigm. Earth System Analysis for Sustainability, Schellnhuber H.-J., Crutzen P.J., Clark W.C., Claussen M. and Held H., Eds., MIT Press, Cambridge, Massachusetts, 1-28.

Coakley, S.M., Scherm, H., Chakraborty, S., 1999. Climate change and plant disease management. Annual Review of Phytopathology 37, 399±426.

Cooper P., 2004. Coping with climatic variability and adapting to climate change: rural water management in dry-land areas. International Development Research Centre, London.

COPA COGECA 2003: Assessment of the impact of the heat wave and drought of the summer 2003 on agriculture and forestry. http://www.copa-cogeca.be/en/ 2003.

Cure, J.D., Acock, B., 1986. Crop responses to carbon dioxide doubling: a literature survey. Agr. For. Meteorol. 38, 127-145.

Dettori, M., 2006. Tesi di Dottorato.

Di Fonzo, N., Ravaglia, S., DeAmbrogio, E., Blanco, A. and Troccoli, A., 2005. Durum wheat improvement in Italy. In: C. Royo, M.N. Nachit, N. Di Fonzo, J.L. Araus, W.H. Pfeiffer and G.A. Slafer (Eds.), Durum Wheat Breeding: Current Approaches and Future Strategies. Food Products Press, New York, pp. 825–881.

Donatelli, M., 1995. Sistemi nella gestione integrate delle colture. Appunti dalle lezioni. Pubblicazione speciale dell'Istituto Sperimentale Agronomico, ISA-Sezione Modena, pp.133.

Donatelli, M., and G.S. Campbell. 1998. A simple model to estimate global solar radiation. In: Proc. 5th ESA Congress, Nitra, Slovak Republic, 2:133-134.

Donatelli, M., Bellocchi, G., Fontana, F., 2003. RadEst 3.00: software to estimate daily radiation data from commonly available meteorological variables. Eur. J. Agron., 18, 369-372.

Downing, T.E., Barrow, E.M., Brooks, R.J., Butterfield, R.E., Carter, T.R., Hulme, M., Olesen, J.E., Porter, J.R., Schellberg, J., Semenov, M.A., Vinther, F.P., Wheeler, T.R., Wolf, J., 2000. Quantification of uncertainty in climate change impact assessment. In: Downing, T.E., Harrison, P.A., Butterfield, R.E., Lonsdale, K.G. (Eds.), Climate Change, Climatic Variability and Agriculture in Europe. Environmental Change Unit. University of Oxford, UK, pp. 415–434.

Drake, B.G., Gonzalez-Meler, M.A., Long, S.P., 1997. More efficient plants: a consequence of rising atmospheric CO2? Ann. Rev. Plant Physiol. Plant Mol. Biol. 48, 609–639.

Dubrovsky, M., 1997. Creating daily weather series with use of weather generator. Environmetrics 8 (5), 409–424.

Dubrovsky, M., Zalud, Z. and Stastna, M., 2000. Sensitivity of CERES-Maize yields to statistical structure of daily weather series. Climatic Change 46, 447- 472.

Dubrovsky ,M., Buchtele, J., Zalud, Z., 2004. High-frequency and low-frequency variability in stochastic daily weather generator and its effect on agricultural and hydrologic modeling. Climatic Change 63: 145-179.

Dubrovsky, M., Nemesova, I., Kalvova, J., 2005. Uncertainties in climate change scenarios for the Czech Republic. Climate Research 29, 139-156.

Dubrovský M. 2009. Linking the climate change scenarios and weather generators with agroclimatological models. Seminar in Sassari, May 25 – June 5, 2009.

Drake, B.G., Gonzales-Meler, M.A., Long, S.P., 1997. More efficient plants: a consequence of rising atmospheric CO_2? Annu. Rev. Plant Physiol. Mol. Biol. 48, 609–939.

Easterling, W.E., 1996. Adapting North American Agriculture to Climate Change in Review, Agricultural and Forest Meteorology 80 (1), 1-54.

Easterling, W.E., Crosson, P.R., Rosenberg, N.J., McKenney, M.S., Katz, L.A. and Lemon, K.M., 1993. Agricultural impacts of and responses to climate change in the Missouri-Iowa-Nebraska-Kansas region. Clim. Change 24(1–2), 23–62.

Easterling, W. and Apps M., 2005. Assessing the consequences of climate change for food and forest resources: a view from the IPCC. Climatic Change (2005) 70: 165–189.

Ewert, F., Rodriguez, D., Jamieson, P., et al., 2002. Effects of elevated CO_2 and drought on wheat: testing crop simulation models for different experimental and climatic conditions. Agriculture, Ecosystems and Environment 93: 249–266.

Ewert F., Rounsevell M.D.A., Reginster I., Metzger M.J., Leemans R., 2005. Future scenarios of European agricultural land use. I: estimating changes in crop productivity. Agric Ecosyst Environ 107:101–116 doi:10.1016/j.agee.2004.12.003.

Ewert F, Porter JR, Rounsevell MD. 2007. Crop models, CO2, and climate change. Science 315, 459–460.

Fageria, N.K., 1992. Maximizing Crop Yields. Marcel Dekker, New York.

Falcon, W.P. and Naylor, R.L., 2005. Rethinking food security for the twenty-first century. American Journal of Agricultural Economics, 87, 1113-1127.

Fankhauser, S.: 1996. The potential costs of climate change adaptation, in J.B. Smith, N. Bhatti, G. Menzhulin, R. Bennioff, M. Budyko, M. Campos, B. Jallow and F. Rijsberman (eds.), Adapting to Climate Change: An International Perspective, New York, Springer, pp. 80–96.

FAO, 2005. Impact of Climate Change, Pests and Diseases on Food Security and Poverty Reduction. Special event background document for the 31st Session of the Committee on World Food Security. Rome. 23-26 May 2005.

FAO, 2007. Adaptation to climate change in agriculture, forestry and fisheries: Perspective, framework and priorities. INTERDEPARTENTAL WORKING GROUP ON CLIMATE CHANGE. Rome 2007.Available on: http://www.fao.org.

FAO, 2008. Expert Meeting on Climate Change Adaptation and Mitigation, Option for Decision Makers. Rome, 5-7 March 2008.

FAO, 2009. Crop Prospects and Food Situation. No. 3, July 2009. Available on http://www.fao.org/giews/.

Farrar, J. F., 1996. Sinks, integral parts of a whole plant. J. Exp. Bot. 47, 1273–1280.

Fischer G., Shah M., Velthuizen H., Nachtergael F.O., 2001. Global agro-ecological assessment for agriculture in the 21st century. International Institute for Applies Systems Analysis. IIASA Publications, Vienna Austria.

Fischer, G., Shah M. and van Velthuizen H., 2002a. Climate change and agricultural vulnerability, IIASASpecial Report commissioned by the UN for theWorld Summit on Sustainable Development, Johannesburg 2002. International Institute forApplied SystemsAnalysis, Laxenburg,Austria, 160 pp.

Fischer, G., H. van Velthuizen, M. Shah and F.O. Nachtergaele, 2002b. Global agro-ecological assessment for agriculture in the 21st century:methodology and results. Research Report RR-02-02. ISBN 3-7045-0141-7., International Institute forApplied SystemsAnalysis, Laxenburg,Austria, 119 pp.

Fischer, G., Shah, M., Tubiello, F.N., van Velthuizen, H., 2005. Socio-economic and climate change impacts on agriculture: an integrated assessment, 1990–2080. Phil. Trans. R. Soc. B 360 (1463), 2067–2083.

Flessa H., Ruser R., Do¨rsch, Kamp P.T., Jimenez M.A., Munch J.C., Beese F., 2002. Integrated evaluation of greenhouse gas emissions (CO2, CH4, N2O) from two farming systems in southern Germany. Agric Ecosys Environ 91:175–189.

Frankel, O.H., Brown, A.H.D. and Burdon, J.J., 1995. The Conservation of Plant Biodiversity. Cambridge: Cambridge University Press.

Friend, A.D., 1998. Parameterisation of a global daily weather generator for terrestrial ecosystem modelling. Ecol. Modelling 109 (2), 121–140.

Füssel H.M. and Klein R.J.T., 2006: Climate Change Vulnerability Assessments: An Evolution of Conceptual Thinking, Climatic Change, 75, 301-329.

Ghaffari, A., Cook, H.F., and Lee, H.C., 2002. Climate change and winter wheat management. A modelling scenario for south-eastern England. Climatic Change 55: 509-533.

GAIM Task Force, 2002. GAIM's Hilbertian questions. Research GAIM: Newsletter of the Global Analysis, Integration and Modelling Task Force, 5, 1-16.

Gbetibouo G.A., Hassan R., 2005. Measuring the economic impact of climate change on major South African filed crops: a Ricardian approach. Glob Planet Change 47:143–152.

Geng, S., Penning de Vries, F.W.T., Supit, I., 1986. A simple method for generating daily rainfall data. Agric. For. Meteorol. 36, 363–376.

Gifford, R.M., Barrett, D.L., Lutze, J.L., (2000). The effects of elevated CO2 on the C:N and C:P mass ratios of plant tissues. Plant Soil 224, 1–14.

Goldammer, J.G., Price, C., 1998. Potential impacts of climate change on fire regimes in the tropics based on MAGICC and a GISS GCM-derived lightning model. Clim Change 39:273–296.

Gordon, H.B., and O'Farrell, S.P., 1997. Transient climate change in the CSIRO coupled model with dynamic sea ice. Monthly Weather Review, 125(5):875–907.

Gordon, C., Cooper, C.A. Senior, Banks, H., Gregory, J.M., Johns, T.C., Mitchell, J.F.B., and Wood, R.A., 2000. The simulation of SST, sea ice extents and ocean heat transports in aversion of the Hadley Centre coupled model without flux adjustments. Climate Dynamics,16:147-168.

Goudriaan J, Zadoks JC (1995) Global climate change: modeling the potential responses of agro-ecosystems with special reference to crop protection. Environ Pollut 87:215–224

Gregory P.J., Ingram J.S.I., Brklacich M., 2005. Climate change and food security. Philos Trans R Soc Lond, B 360(1463):2139–2148.

Grignac, P., 1965. Contribution a l'étude du Triticum durum Desf. Paris: The`se Fac. De Toulouse.

Gualdi, S., Guilyardi, E., Navarra, A., Masina, S. and Delecluse, P., (2003a): The interannual variability in the tropical Indian Ocean as simulated by a CGCM, Clim. Dyn., 20, 567–582.

Gualdi, S., Navarra, A., Guilyardi, E., and Delecluse, P., (2003b): Assessment of the tropical Indo-Pacific climate in the SINTEX CGCM, Ann. Geophys., 46, 1 – 26.

Guenni, L.: 1994, 'Spatial Interpolation of the Parameters of StochasticWeatherModels', in Paoli, G. (ed.), Climate Change, Uncertainty and Decision Making, Institute for Risk Research, University of Waterloo, Ontario and IGBP-BAHC, Berlin, pp. 61–79.

Guerena, A., Ruiz-Ramos, M., Diaz-Ambrona, C.H., Conde, J.R. and Minguez M.I., 2001. Assessment of Climate Change and Agriculture in Spain Using Climate Models. Agronomy Journal, 93: 237-249.

Guilyardi, E., Delecluse, P., Gualdi, S. and Navarra, A., (2003): Mechanisms for ENSO phase change in a coupled GCM, J. Clim., 16, 1141–1158.

Hafner, S., 2003. Trends in maize, rice and wheat yields for 188 nations over the past 40 years: A prevalence of linear growth. Agriculture, Ecosystems and Environment, 97, 275-283.

Haile, M., 2005. Weather patterns, food security and humanitarian response in sub-Saharan Africa. Philos Trans R Soc Lond B 360(1463):2169–2182.

Harrison, P.A. and Butterfield, R.E. and Gawith, M.J., 1995. Effects on winter wheat, sunflower, onion and grassland in Europe, in P. A. Harrison, R. Butterfield and T. E. Downing (eds.), Climate Change and Agriculture in Europe: Assessment of Impacts and Adaptations. Research Report No. 9, Environmental Change Unit, University of Oxford, UK, pp. 330–388.

Harrison, P.A. and Butterfield, R.E., 2000. Modelling climate change impacts on wheat, potato and grapevine in Europe, in Downing, T.E., Harrison, P. A., Butterfield, R. E. and Lonsdale, K. G. (eds.), Climate Change, Climate Variability and Agriculture in Europe: An Integrated Assessment, Research Report 21, Environmental Change Unit, University of Oxford, pp. 367–390.

Harvey, L.D.D., Gregory, J., Hoffert, M., Jain, A. and 5 others, 1997. An introduction to simple climate models used in the IPCC Second Assessment Report. IPCC Tech Paper 2, Intergovernmental Panel on Climate Change, Geneva.

Heidhues, F., Atsain, A., Nyangito, H., Padilla, M., Gershi, G. and Le Vallee, J.C., 2004. Development strategies and food and nutrition security in Africa: An assessment. (= 2020 Discussion Paper 38), International Food Policy Research Institute (IFPRI), Washington D.C.

Hildén, M., H. Lehtonen, I. Bärlund, K. Hakala, T. Kaukoranta and S. Tattari, 2005. The Practice and Process of Adaptation in Finnish Agriculture. FINADAPT Working Paper 5, Finnish Environment Institute Mimeographs 335, Helsinki, 28 pp.

Hodges, T. (Ed.), 1991. Predicting Crop Phenology. CRC Press, Boca Raton, FL.

Hodges, T., Johnson, S.L., Johnson, B.S., 1992. A modular structure for crop simulation models: implemented in the SIMPOTATO model. Agron. J. 84, 911–915.

Holdridge, L.R., 1947. Determination of world plant formations from simple climatic data. Science, 105, 367– 368.

Holdridge, L. R., 1967. Life Zone Ecology. Tropical Science Centre, San Jose, Costa Rica.

Hoogenboom, G.J., Jones, W., Boote, K.J., 1992. Modeling growth, development and yield of grain legumes using SOYGRO, PNUTGRO, and BEANGRO: A Review. Transactions of the American Society of Agricultural Engineers. 35: 2043-2056.

Hoogenboom, G., 2000. Contribution of agrometeorology to the simulation of crop production and its applications. Agricultural and Forest Meteorology 103 (2000) 137–157.

Hoogenboom, G., P.W. Wilkens, P.K. Thornton, J.W. Jones, and L.A. Hunt. 1995. Advances in the development and application of DSSAT. p. 201–202. In GUEREN˜ A et al.,.: Climate Change and agriculture in Spain using climate models, Agron. J. 93:237–249 (2001).

Houghton, J. T., Y. Ding, D. J. Griggs, M. Noguer, P. J. van der Linden, and D. Xiaosu, Eds., 2001: Climate Change 2001: The Scientific Basis: Contributions of Working Group I to the Third Assessment Report of the Intergovernmental Panel on Climate Change. Cambridge University Press, 881 pp.

Hsiao, T.C., Jackson, R.B., 1999. Interactive effects of water stress and elevated CO2 on growth, photosynthesis, and water use efficiency. In: Luo Y, Mooney HA (eds) Carbon dioxide and environmental stress. Academic Press, New York, pp 3–31.

Hulme, M., Wigley, T.M.L., Barrow, E.M., Raper, S.C.B., Centella, A., Smith, S., Chipanshi, A.C., 2000. Using a climate scenario generator for vulnerability and adaptation assessments: MAGICC and SCENGEN Version 2.4 Workbook. Climatic Research Unit, Norwich.

Hunt, L.A., S. Pararajasingham, J.W. Jones, G. Hoogenboom, D.T Imamura, and R.M. Ogoshi. 1993. Gencalc: Software to facilitate the use of crop models for analyzing field experiments. Agron. J. 85:1090–1094.

Hunt, L.A., 1994. Data requirements for crop modeling. In: Uhlir, P.F., Carter, G.C. (Eds.), Crop Modeling and Related Environmental Data. A Focus on Applications for Arid and Semiarid Regions in Developing Countries. CODATA, Paris, France, pp. 15–25.

Hunt, L.A., Boote, K.J., 1998. Data for model operation, calibration, and evaluation. In: Tsuji, G.Y., Hoogenboom, G., Thornton, P.K. (Eds.), Understanding Options for Agricultural Production. Kluwer Academic Publishers, Dordrecht, Netherlands, pp. 9–39.

Hunt, L.A., J.W.White, and G. Hoogenboom. 2001. Agronomic data: Advances in documentation and protocols for exchange and use.Agric. Syst. 70:477–492.

Idso K.E., Idso S.B., 1994. Plant responses to atmospheric CO2 enrichment in the face of environmental constraint: a review of the past 10 years' research. Agric Forest Meteor 69:153–203.

Iglesias, A., Rosenzweig, C., and Pereira D., 1999. Agricultural impacts of climate change in Spain:developing tools for a spatial analysis. Global Environmental Change, 10: 69-80.

IPCC, 2001a. Climate change 2001: the scientific assessment. Intergovernmental Panel on Climate Change. Cambridge University Press, Cambridge UK, 845 pp.

IPCC, 2001b. Climate change 2001: Impacts, adaptation, and vulnerability. Contribution of working group II to the Third Assessment Report of the Intergovernmental Panel on Climate Change. Cambridge University Press, Cambridge.

IPCC, 2001c. Climate change 2001: mitigation. Intergovernmental Panel on Climate Change. Cambridge University Press. Cambridge, UK, 1076 pp.

IPCC, 2007. Fourth IPCC Assessment Report (AR4): Climate Change 2007. Cambridge University Press.

Jablonski, L.M., Wang, X., Curtis, P.S., 2002. Plant reproduction under elevated CO2 conditions: A meta-analysis of reports on 79 crop and wild species. New Phytologist 156 (1): 9-26.

Jamieson, P.D., Semenov, M.A., Brooking, I.R., Francis, G.S., 1998. Sirius: a mechanistic model of wheat response to environmental variation. Europ J Agronomy, 8:161-179.

Jimoh, O.D., Webster, P., 1997. The optimum order of a Markov chain model for daily rainfall in Nigeria. J. Hydrol. 185, 45–69.

Jones, P.G., Thornton, P.K., 1997. Spatial and temporal variability of rainfall related to a third-order Markov model. Agric. For. Meteorol. 86 (1-2), 127–138.

Jones JW, Keating BA, Porter CH, 2001. Approaches to modular model development. Agric Syst 70:421–443

Jones, P.D., Lister D.H., Jaggard K.W. and Pidgeon J.D., 2003. Future climate impact on the productivity of sugar beet (Beta vulgaris L.) in Europe. Climatic Change, 58, 93-108.

Jones, J.W., Tsuji, G.Y., Hoogenboom, G., Hunt, L.A., Thornton, P.K.,. Wilkens, P.W., Imamura, D.T., Bowen, W.T., Singh, U., 1998. Decision support system for agrotechnology transfer DSSAT v3. In: Tsuji, G.Y.,

Hoogenboom, G., Thornton, P.K. (Eds.), Understanding Options for Agricultural Production. Kluwer Academic Publishers, Dordrecht, Netherlands, pp. 157–177.

Jones J.W., Hoogemboom G., Porter C.H., Boote K.J., Batchelor W.D., Hunt L.A., Wilkens P.W., Singh U., Gijsman A.J., Ritchie J.T., 2003. Europ. J. Agronomy, 18: 235-265.

Jones J. W., Boote K. J., Hoogenboom G., 2007. Computer Simulation of Crop Growth and Management Responses. Summer Course 2007 June 11-15, June 22 July 23-27.

Johnson, G.L., Hanson, C.L., Hardegree, S.P., Ballard, E.B., 1996. Stochastic weather simulation overview and analysis of two commonly used models. J. Appl. Meteorol. 35 (10), 1878–1896.

Kharin, V.V., and F.W. Zwiers, 2000: Changes in the extremes in an ensemble of transient climate simulation with a coupled atmosphere-ocean GCM, Journal of Climate, 13, 3760-3788.

Kenny, G. J., Harrison, P. A., Olesen, J. E. and Parry, M. L.: 1993, 'The effects of climate change on land suitability of grain maize, winter wheat and cauliflower in Europe', Eur. J. Agron. 2, 325–338.

Kimball, B.A., 1983. Carbon dioxide and agricultural yield: an assemblage and analysis of 430 prior observations. Agron J. 75:779–788.

Kimball, B.A., Idso S.B., 1983. Increasing atmospheric CO2. Effects on crop yield, water use and climate Agric Water Manage 7:55–72

Kimball, B.A., Kobayashi, K., Bindi, M., (2002). Responses of agricultural crops to free-air CO2 enrichment. Adv. Agron. 77, 293-368.

Komor, E., Orlich, G., Weig, A. and Kockenberger, W., 1996. Phloem loading – not metaphysical, only complex: Towards a unified model of phloem loading. J. Exp. Bot. 47, 1155–1164.

Kont, A., Jaagus, J., Aunap, R., 2003. Climate change scenarios and the effect of sea-level rise for Estonia. Global Planet Change 36:1–15.

Loague and Green, 1991 K. Loague and R.E. Green, Statistical and graphical methods for evaluating solute transport models: overview and application, J. Contam. Hydrol. **7** (1991), pp. 51–73.

Long, S.P., Ainsworth, E.A., Leakey, A.D.B., Nosberger, J., Ort, D.R., 2006. Food for thought: lower-than-expected crop yield stimulation with rising CO_2 concentrations. Science 312, 1918–1921.

Ludwig, F., Asseng, S., 2006. Climate change impacts on wheat production in a Mediterranean environment in Western Australia. Agricultural Systems, 90: 159–179.

LULUCF, 2000. IPCC special reports: land use, land-use change, and forestry. Watson RT, Noble IR, Bolin B, Ravindranath NH, Verardo DJ, Dokken DJ (eds) (2000) Cambridge University Press, Cambridge, 324 pp.

Maccaferri, M., Sanguineti, M.C., Donini, P. and Tuberosa, R., 2003. Microsatellite analysis reveals a progressive widening of the genetic basis in the elite durum wheat germplasm. Theor. Appl. Genet. 107, 783–797.

Maccaferri, M., Sanguineti, M.C., Donini, P., Porcedu, E. and Tuberosa, R., 2005. A retrospective analysis of genetic diversity in durum wheat elite germplasm based on microsatellite analysis: a case study. In: C. Royo, M.N. Nachit, N. Di Fonzo, J.L. Araus, W.H. Pfeiffer and G.A. Slafer (Eds.), Durum Wheat Breeding: Current Approaches and Future Strategies. Food Products Press, New York, pp. 99–142.

MacKey, J., 2005. Wheat: Its concept, evolution and taxonomy. In: C. Royo, M. Nachit, N. Di Fonzo, J.L. Araus, W.H. Pfeiffer and G.A. Slafer (Eds.), Durum Wheat Breeding: Current Approaches and Future Strategies. Food Products Press, New York, pp. 3–61.

Madec, G., Delecluse, P., Imbard, I. and Levy, C., (1999), OPA 8.1 Ocean General Circulation Model reference manual, Note du Pôle de modélisation,, Inst. Pierre-Simon Laplace (IPSL), France, No. 11, 91 pp.

Manning W.J., Tiedemann A.V., 1995. Climate change: potential effects of increased atmospheric carbon dioxide (CO2), ozone (O3) and ultraviolet-B (uv-B) radiation on plant diseases. Environ Pollut 88: 219–245.

Martynov, S.P., Dobrotvorskaya, T.V. and Pukhalskiy, V.A., 2005. Analysis of genetic diversity of spring durum wheat (Triticum durum Desf.) cultivars released in Russia in 1929–2004. Russ. J. Genet. 41, 1113–1122.

Maytín C.E., Acevedo M.F., Jaimez R., Andressen R., Harwell M.A., Robock A., Azkcar A., 1995. Potential effects of global climatic change on the phenology and yield of maize in Venezuela. Climatic Change 29:189–211.

Mavromatis, T. And Jones, P.D., 1999. Evaluation of HadCM2 and direct use of daily GCM data in impact assessment studies. Climatic Change 41: 583-614.

Mavromatis, T. And Jones, P.D., 1998. Comparison of climate change scenario construction methodologies for impact assessment studies. Agricultural and Forest Meteorology 91: 51-67.

McCarthy (eds.): Climate Change 2001–Impacts, Adaptations and Mitigation of Climate Change: Scientific–Technical Analyses. Contribution of Working Group II to the Third Assessment Report of the Intergovernmental Panel on Climate Change, United Nations Environment Programme, World Meteorological Organization, Cambridge University Press.

McCown, R.L., Hammer, G.L., Hargreaves, J.N.G., Holzworth, D.P., Freebairn, D.M., 1996. APSIM: a novel software system for model development, model testing and simulation in agricultural systems research. Agric. Systems 50, 255–271.

McKinsey&Company, 2009: Pathways to a Low-Carbon Economy. Version 2 of the Global Greenhouse Gas Abatement Curve.

Mearns L.O., Rosenzweig C., Goldberg R., 1992. Effect of changes in interannual climatic variability on CERESwheat yields: sensitivity and 2 × CO2 general circulation model studies. Agric For Meteorol 62:159–189.

Mearns L.O., Rosenzweig C. and Goldberg R., 1997. Mean and variance change in climate scenarios: methods, agricultural applications, and measures of uncertainty, Clim. Change 35 (1997), pp. 367–396.

Meehl, G.A. and C. Tebaldi, 2004. More intense, more frequent, and longer lasting heatwaves in the 21st Century. Science, 305, 994-997.

van Meijl H., van Rheenen T., Tabeau A., Eickhout B., 2006. The impact of different policy environments on agricultural land use in Europe. Agric Ecosyst Environ 114:21–38.

Mendelsohn R., Dinar A., 1999. Climate Change, Agriculture, and Developing Countries: Does Adaptation Matter? World Bank Research Observer (14), 277-293.

Mereu V., Iocola I., Spano D., Murgia V., Duce P., Cesaraccio C., Tubiello F.N., Fischer G. Land suitability and potential yield variations of wheat and olive crops determined by climate change in Italy. Atti del X Congresso della Società Europea di Agronomia, Bologna 2008.

Mergoum M., Singh P.K., Anderson J.A., Pena R. J., Singh R.P., Xu S.S., and Ransom J.K., 2009. Spring Wheat Breeding, pp.127-156. M.J. Carena (ed.), Cereals, DOI: 10.1007/978-0-387-72297-9, Springer Science + Business Media, LLC 2009.

Milly, P.C.D., Wetherald, R.T., Dunne, K.A., Delworth, T.L., 2002. Increasing risk of great floods in a changing climate. Nature 415:514–517.

Mitchell, J.F.B., Manabe, S., Meleshko, V., Tokioka, T., 1990. Equilibrium climate change and its implications for the future. In: Houghton JT, Jenkins GJ, Ephraums JJ (eds) Climate change: the IPCC scientific assessment. report prepared by Working Group I. Cambridge University Press, Cambridge, p 131–164.

Mitchell, D. and Ingco M., 1993. The World Food Outlook, The World Bank, Washington, DC.

Mizina, S.V., Smith, J.B., Gossen, E., Spiecker, K.F. and Witkowski, S.L., 1999. An evaluation of adaptation options for climate change impacts on agriculture in Kazakhstan. Miti. & Adapt. Strat. for Glob. Change 4, 25–41.

Monteith, J.L., 1996. The quest for balance in crop modeling. Agron. J. 88, 695–697.

Moragues, M., Zarco-Herna´ndez, J., Moralejo, M.A. and Royo, C. (2006) Genetic diversity of glutenin protein subunits composition in durum wheat landraces [Triticum turgidum ssp. turgidum convar. durum (Desf.) MacKey] from the Mediterranean basin. Genet. Resour. Crop Evol. 53, 993–1002.

Moragues, M., Moralejo, M., Sorrells, M.E. and Royo, C. (2007) Dispersal of durum wheat [Triticum turgidum L. ssp. turgidum convar. durum (Desf.) MacKey] landraces across the Mediterranean basin assessed by AFLPs and microsatellites. Genet. Resour. Crop Evol. 54, 1133–1144.

Moriondo, M., Bindi, M., 2005. Cambiamenti climatici e ambiente vitivinicolo: impatto e strategie di adattamento. Rapporto finale per ARSIA.

Moriondo, M., Bindi, M. 2006. Comparison of temperatures simulated by GCMs, RCMs and statistical downscaling: potential application in studies of future crop development. Clim Res 30: 149–160.

Moriondo, M., Bindi, M. 2007. Impact of climate change on the phenology of typical Mediterranean crops. Italian Journal of Agrometeorology, 3: 5-12.

Murphy J., 1999. An evaluation of statistical and dynamical techniques for downscaling local climate. J Climate 12: 2256–2284.

Nonhebel S., 1996. Effects of temperature rise and increase in CO_2 concentration on simulated wheat yields in Europe. Clim Change 34:73–90.

OECD–FAO. 2008. OECD–FAO Agricultural Outlook 2008–2017. Paris.

Olesen, J.E., and Bindi, M., 2004. Agricultural impacts and adaptations to climate change in Europe. Farm Policy Journal 1 (3): 36-46.

Olesen, J.E., and Bindi, M., 2002. Consequences of climate change for European agricultural productivity, land use and policy. European Journal of Agronomy 16: 239-262.

Olesen, J.E., Jensen, T., Petersen, J., 2000. Sensitivity of field-scale winter wheat production in Denmark to climate variability and climate change. Clim. Res. 15, 221-238.

Olesen, J.E., Carter T.R., Díaz-Ambrona C.H., Fronzek S., Heidmann T., Hickler T., Holt T., Mínguez M.I., Morales P., Palutikof J., Quemada M., Ruiz-Ramos M., Rubæk G., Sau F., Smith B., Sykes M., 2007. Uncertainties in projected impacts of climate change on European agriculture and terrestrial ecosystems based on scenarios from regional climate models. Climatic Change, 81, S123-S143.

Parry, M.L. and Carter, T.R., 1989. An assessment of the effects of climatic change on agriculture. Clim. Change 15, 95–116.

Parry, M.L., Arnell, N.W. McMichael, A.J. Nicholls, R.J. Martens, P. Kovats, R.S. Livermore, M.T. Rosenzweig, C. Iglesias, A. Fischer, G., 2001. Millions at Risk: Defining Critical Climate Change Threats and Targets. Global Environmental Change, 11:181-183.

Parry, M.L., Rosenzweig C., Iglesias A., Livermore M. and Fischer G., 2004. Effects of climate change on global food production under SRES emissions and socio-economic scenarios. Global Environ. Change, 14, 53-67.

Parry M., Rosenzweig C., Livermore M., 2005. Climate change, global food supply and risk of hunger. Phil. Trans. R. Soc. B (2005) 360, 2125–2138.

Paustian K., Elliot E.T., Killian K., 1998. Modeling soil carbon in relation to management and climate change in some agro-ecosystems in central North America. In: Lal R et al (eds) Soil processes and the carbon cycle. CRC Press, Boca Raton FL, pp 459–471.

Pecetti, L. and Annicchiarico, P., 1998. Agronomic value and plant type of Italian durum wheat cultivars from different eras of breeding. Euphytica 99, 9–15.

Peiris, D. R., Crawford, J. W., Grashoff, C., Jefferies, R. A., Porter, J. R. and Marshall, B., 1996. A simulation study of crop growth and development under climate change. Agric. Forest Meteorol. 79, 271–287.

Peiris, D.R., McNicol, J.W., 1996. Modelling daily weather with multivariate time series. Agric. For. Meteorol. 79, 219–231.

Penning de Vries, F.W.T., van Laar, H.H. (Eds.), 1982. Simulation of plant growth and production. Simulation Monographs. Centre for Agricultural Publishing and Documentation (Pudoc). Wageningen, Netherlands.

Penning de Vries, F.W.T., Jansen, D.M., ten Berge, H.F.M., Bakema, A., 1989. Simulation of ecophysiological processes of growth of several annual crops. Simulation Monographs. Centre for Agricultural Publishing and Documentation (Pudoc). Wageningen, Netherlands.

Petr, J., 1991. Weather and Yield. Elsevier, Amsterdam, Netherlands.

Pickering N.B., Hansen J.W., Wells C.M., Chan V.K., Godwin D.C. WeatherMan: A utility for managing and generating daily weather data. Agron. J. 1994;86:332-337.

Polsky C., Easterling E., 2001. Adaptation to climate variability and change in the US Great Plains: a multi-scale analysis of Ricardian climate sensitivities. Agric Ecosyst Environ 85(1–3):133–144.

Poorter H., 1993. Interspecific variation in the growth response of plants to an elevated ambient CO2 concentration. Vegetation 104/105:77–97.

Porter C, Jones JW, Braga R (2000) An approach for modular crop model development. International Consortium for Agricultural Systems Applications, Honolulu, HI, p 13. Available from http://icasa.net/modular/index.html.

Racsko P, Szeidl L & Semenov MA (1991) A serial approach to local stochastic weather models. Ecological Modelling, 57:27-41

Rasse et al., 2000 D.P. Rasse, J.T. Ritchie, W.W. Wilhelm, J. Wei and E.C. Martin, Simulating Inbred–Maize yields with CERES-IM, Agron. J. 92 (2000), pp. 672–678.

Reilly J., 1995. Climate change and global agriculture: recent findings and issues. Am J Agric Econ 77:727–733.

Reilly, J. and Schimmelpfennig, D., 1999. Agricultural impact assessment, vulnerability, and the scope for adaptation. Clim. Change 43, 745–788.

Reilly J., Tubiello F., McCarl B., Abler D., Darwin R., Fuglie K., Hollinger S., Izaurralde C., Jagtap S., Jones J., Mearns L., Ojima D., Paul E., Paustian K., Riha S., Rosenberg N., Rosenzweig C., 2003. US Agriculture and climate change: new results. Clim Change 57:43–69.

Richardson, C.W., 1981. Stochastic simulation of daily precipitation, temperature, and solar radiation. Water Resources Res. 17 (1), 182–190.

Richardson, C.W., 1985. Weather simulation for crop management models. Trans. ASAE 28 (5), 1602–1606.

Riethoven, J.J.M., ten Berge, H.F.M., Drenth, H. (Eds.), 1995. Software development in the SARP project: a guide to applications and tools. SARP Research Proceedings. DLO Research Institute for Agrobiology and Soil Fertility, Wageningen, Netherlands, p. 301.

Riha et al., 1996. S.J. Riha, D.S. Wilks and P. Simeons, Impacts of temperature and precipitation variability on crop model predictions, Clim. Change 32, pp. 293–311.

Rinaldi, M., 2004. Water availability at sowing and nitrogen management of durum wheat: a seasonal analysis with the CERES-Wheat model. Field Crops research 89: 27-37.

Rither, G.M. and Semenov, M.A., 2004. Modelling impact of Climate Change on wheat yields in England and wales: assessing drought risks. Agricultural Systems. 84, 1: 77-97.

Ritchie, J.T., Otter, S., 1985. Description and performance of CERES-Wheat: a user-oriented wheat yield model. In: ARS Wheat Yield Project. ARS-38. Natl Tech Info Serv, Springfield, Missouri, pp. 159_/175.

Ritchie J.T., Godwin D.C. and Otter S., 1985. CERES-wheat: A user-oriented wheat yield model. Preliminary documentation. Michigan State University, MI.

Ritchie, J.T., Singh, U., Godwin, D.C., Bowen, W.T., 1998. Cereal growth, development and yield. In: Tsuji, G.Y., Hoogenboom, G., Thornton, P.K. (Eds.), Understanding Options for Agricultural Production. Kluwer Academic Publishers, Dordrecht, The Netherlands, pp. 79-98.

Roetter R.P. and Van Keulen H., 2008. Food Security, in: Science for Agriculture and Rural Development in Low-income Countries, Cap.III: 27–56. © Springer Science + Business Media B.V.

Royo C., Elias E.M., Manthey, F. A., 2009. Durum Wheat Breeding, pp: 199-226. M.J. Carena (ed.), Cereals. DOI: 10.1007/978/-0-387-72297-9, Springer Science + Business Media, LLC 2009.

Rosenzwieg, C. and Parry, M.L., 1994. Potential impact of climate change on world food supply. Nature 367, 133–138.

Rosenzweig C., Hillel D., 1998. Climate change and the global harvest: potential impacts of the greenhouse effect on agriculture. Oxford University Press, New York, NY, 324 pp.

Rosenzweig C., Iglesias A., Yang X.B., Epstein P.R., Chivian E., 2001. Climate change and extreme weather events. Implications for food production, plant diseases, and pests. Global Change and Human Health, Vol. 2, NO. 2: 90-104.

Rosenzweig C., Iglesias A., Yang X.B., Epstein P.R., Chivian E., 2002a. Climate change and extreme weather events: implications for food production, plant diseases, and pests. Global Change Human Health 2(2):90–104.

Rosenzweig C., Tubiello F.N., Goldberg R., Mills E., Bloomfield J., 2002b. Increased crop damage in the US from excess precipitation under climate change. Global Environ Change 12:197–202.

Rosenzweig C., Strzepek K.M., Major D.C., Iglesias A., Yates D.N., McCluskey A., Hillel D., 2004. Water resources for agriculture in a changing climate: international case studies. Global Environ Change 14:345–360.

Rosenzweig C., Yang X.B., Anderson P., Epstein P., Vicarelli M., 2005. Agriculture: Climate Change, crop pest and diseases. In Climate Change Futures: Health, Ecological and Economic Dimensions. P. Epstein and E. Mills, Eds. The Center for Health and the Global Medical School, pp.70-77.

Rosenzweig C. and Tubiello F.N., 2007. Adaptation and mitigation strategies in agriculture: an analysis of potential synergies. Mitig Adapt Strat Glob Change 12:855–873.

Salinger M.J., Stigter C.J., Das H.P., 2000. Agro meteorological adaptation strategies to increasing climate variability and climate change. Agric For Meteorol 103:167–184.

Santer, B.D., Wigley, T.M.L., Schlesinger, M.E., Mitchell, J.F.B., 1990. Developing climate scenarios from equilibrium GCM results. Report No.47, Max Planck Institute für Meteorologie, Hamburg.

Scarascia-Mugnozza, G.T., Bagnara, D. and Bozzini, A., 1972. Mutagenesis applied to durum wheat: results and perspectives. In: Induced mutations and Plant Improvement, IAEA, Vienna, pp. 183-197.

Schär, C., Vidale P.L., Lüthi D., Frei C., Häberli C., Liniger M.A. and Appenzeller C., 2004. The role of increasing temperature variability in European summer heatwaves. Nature, 427, 332-336.

Schmidt, G.M., Smajstrla, A.G., Zazueta, F.S., 1996. Parametric uncertainty in stochastic precipitation models — wet day amounts. Trans. ASAE 39 (6), 2093–2103.

Schmidt, G.M., Smajstrla, A.G., Zazueta, F.S., 1997. Long-term variability of monthly total precipitation. Trans. ASAE 40 (4), 1029–1039.

Semenov, M.A., and Porter, J.R., 1995. Climatic variability and the modelling of crop yields. Agricultural and Forest Meteorology 73: 265-283.

Semenov, M.A. and Barrow, E.M., 1997. Use of a stochastic weather generator in the development of climate change scenarios, Clim. Change 35 (1997), pp. 397–414.

Semenov, M.A., Brooks, R.J., Barrow, E.M., Richardson, C.W., 1998. Comparison of WGEN and LARS-WG stochastic weather generators for diverse climate. Clim. Res. 10 (2), 95–107.

Simmons A.J., Burridge D.M., Jarraud M., Girard C., Wergen W., 1989. The ECMWF medium-range prediction models. Development of the numerical formulations and the impact of increased resolution. Meteor.Atmos.Phys., 40, 28-60.

Sinclair T.S. and Seligman N., 2000. Criteria for publishing papers on crop modeling. Field Crops Res. 68, 165-172.

Singh B., El Maayar M., André P., Bryant C., Thouez J-P., 1998. Impacts of a GHG-induced climate change on crop yields: effects of acceleration in maturation, moisture stress and optimal temperature. Climatic Change 38:51–86.

Sirotenko, O. D., Abashina, H. V. and Pavlova, V. N., 1997. Sensitivity of the Russian agriculture to changes in climate, CO2 and tropospheric ozone concentrations and soil fertility. Climatic Change 36, 217–232.

Skinner, M.W., Smit, B., Dolan, A.H., Bradshaw, B. and Bryant, C.R., 2001. Adaptation Options to Climate Change in Canadian Agriculture: An Inventory and Typology, (Department of Geography Occasional paper No. 25.). Guelph: University of Guelph, 36 pp.

Skovmand, B., Warburton, M.L., Sullivan, S.N. and Lage, J., 2005. Managing and collecting genetic resources. In: C. Royo, M. Nachit, N. Di Fonzo, J.L. Araus, W.H. Pfeiffer and G.A. Slafer (Eds.), Durum Wheat Breeding: Current Approaches and Future Strategies. Food Products Press, New York, pp. 143–163.

Smit, B., McNabb, D. and Smithers, J., 1996. Agricultural adaptation to climatic variation. Climatic Change 33, 7–29.

Smit, B., Burton, I., Klein, R.J.T. and Street, R., 1999. The science of adaptation: A framework for assessment. Miti. & Adaptation Strat. for Glob. Change 4, 199–213.

Smit, B., O. Pilifosova, I. Burton, B. Challenger, S. Huq, R.J.T. Klein and G.Yohe, 2001. Adaptation to climate change in the context of sustainable development and equity. Climate Change 2001: Impacts, Adaptation, and Vulnerability. Contribution of Working Group II to the Third Assessment Report of the Intergovernmental Panel on Climate Change, J.J.McCarthy,O.F. Canziani,N.A. Leary, D.J. Dokken and K.S. White, Eds., Cambridge University Press, Cambridge, 879-906.

Smith, J.B. and Lenhart, S.S., 1996. Climate change adaptation policy options. Clim. Res. 6, 193–201.

Smith, J.B. and M. Hulme, 1998: Climate change scenarios. In: UNEP Handbook on Methods for Climate Change Impact Assessment and Adaptation Studies [Feenstra, J.F., I. Burton, J.B. Smith, and R.S.J. Tol (eds.)], United Nations Environment Programme, Nairobi, Kenya, and Institute for Environmental Studies, Amsterdam, pp. 3-1 - 3-40.

Smith B., Skinner M., 2002. Adaptation options in agriculture to climate change: a topology. Mitig Adapt Strateg Glob Change 7:85–114.

Smith J.B., Klein R.J.T., Huq S., 2003. Climate change, adaptive capacity, and development. Imperial College Press, London, 347 pp.

Smith B., Wandel J., 2006. Adaptation, adaptive capacity and vulnerability. Glob Environ Change 16:282–292.

Smithers, J. and Smit, B., 1997. Agricultural system response to environmental stress, in B. Ilbery, Q. Chiotti and T. Rickard (eds.), Agricultural Restructuring and Sustainability: A geographical perspective, Wallingford, CAB International, pp. 167–183.

Solomon D., Lehmann J., Zech W., 2000. Land use effects of soil organic matter properties of chromic luvisols in semi-arid northern Tanzania: carbon, nitrogen, lignin and carbohydrates. Agr Ecos Env 78:203–213.

Southworth J., Randolph J.C., Habeck M., Doering O.C., Pfeifer R.A., Rao D.G., Johnston J.J., 2000. Consequences of future climate change and changing climate variability on maize yields in the Midwestern United States. Agric Ecosyst Environ 82:139–158.

SRES, 2000. Emission Scenarios. A Special Report of IPCC, WG III. Summary for Policymakers.

St'astna, M., Trnka, M., Kren, J., Dubrovsky, M., Zalud, Z., 2002. Rostlinna Vybroba, 48 (3):125-132.

Stern, N., 2006. The economics of climate change. The Stern Review. Cambridge University Press, UK.

Stern, N., 2007: Stern Review on The Economics of Climate Change. HM Treasury, London: http://www.hm-treasury.gov.uk/sternreview_index.htm.

Stockle, C.O., and Donatelli M., 1994. CropSyst, a cropping system model: water/nitrogen budgets and crop yield. Agricultural Systems 46, 335-359.

von Storch H., Zwiers F., 1999. Statistical Analysis in Climate Research. Cambridge University Press, Cambridge,UK.

Tao F., Yokozawa M., Xu Y., Hayashi Y., Zhang Z., 2006. Climate changes and trends in phenology and yields of field crops in China, 1981–2000. Agric For Meteorol 138:82–92.

Timlin, D., Pachepsky, Y.A., Acock, B., 1996. Agronomic models: a design for a modular, generic soil simulator to interface with plant models. Agron. J. 88, 162–169.

Timmermann, R., Goosse, H., Madec, G., Fichefet, T., Etheb, C. and Dulière, V. , (2005): On the representation of high latitude processes in the ORCA-LIM global coupled sea ice– ocean model. Ocean Modell., 8, 175-201.

Tingem M. and Rivington M., 2009. Adaptation for crop agriculture to climate change in Cameroon: Turning on the heat. Mitig Adapt Strateg Glob Change (2009) 14:153–168.

Tol, R.S.J., Fankhauser, S. and Smith, J.B., 1998. The scope for adaptation to climate change: What can we learn from the impact literature?. Gl. Envir. Change 8(2), 109–123.

Tol, R.S.J., 2005: Emission abatement versus development as strategies to reduce vulnerability to climate change: an application of FUND, Environment and Development Economics, 10 (05): 615-629.

Trnka, M., Eitzinger J., Kapler P., Dubrovski M. Semerádová D., Zalud Z., and Formayer H., 2007. Effect of Estimated Daily Global Solar Radiation Data on the Results of Crop Growth Models. Sensors 2007, 7, 2330-2362.

Trnka, M., Dubrovski M. and Zalud Z., 2004. Climate change impacts and adaptation strategies in spring barley production in the Czech Republic. Climatic Change, 64, 227-255.

Trnka, M., Dubrovski, M., Semeradova, D., and Zalud, Z., 2004. Projections of uncerteinties in climate change scenarios into expected winter wheat yields. Theoretical ana Applied Climatology, 77, 229-249.

Tsuji, G.Y., Uehara, G., Balas, S. (Eds.), 1994. DSSAT version 3. University of Hawaii, Honolulu, Hawaii.

Tubiello F. N., Donatelli, M., Rosenzweig, C., Stockle C. O., 2000. Effects of climate change and eleveted CO_2 on cropping systems: model predictions at two Italian locations. European Journal of Agronomy 13 179–189.

Tubiello F.N., Ewert F., 2002. Modeling the effects of elevated CO_2 on crop growth and yield: a review. Eur J Agron 18(1–2): 57–74.

Tubiello F.N., Jagtap S., Rosenzweig C., Goldberg R., Jones J.W., 2002. Effects of climate change on US crop production from the National Assessment. Simulation results using two different GCM scenarios. Part I: Wheat, Potato, Corn, and Citrus, Climate Res 20(3):259–270.

Tubiello, F.N. and Fischer G., 2006. Reducing climate change impacts on agriculture: global and regional effects of mitigation, 2000-2080. Techol. Forecast. Soc., doi: 10.1016/j.techfore.2006.05.027.

Tubiello FN, Amthor JS, Boote KJ, Donatelli M, Easterling W, Fischer G, Giord RM, Howden M, Reilly J, Rosenzweig C. 2007. Crop response to elevated CO2 and world food supply a comment on ‘food for thought.’ by Long et al., Science 312:1918–1921, 2006. European Journal of Agronomy 26, 215–223.

Tubiello, F.N. and Rosenzweig C., 2008. Developing climate change impact metrics for agriculture. The Integral Assessment Journal *Bridging Sciences & Policy*. Vol.8, Iss.1, pp.165-184.

Tuck, G., Glendining, M.J., Smith, P., House, J.I., Wattenbach, M., 2006. The potential distribution of bioenergy crops in Europe under present and future climate. Biomass Bioener. 30, 83-197.

United Nations Framework Convention on Climate Change (UNFCCC): 1992, United Nations Framework Convention on Climate Change: Text, Geneva, World Meteorological Organization and United Nations Environment Program.

United Nations Framework Convention on Climate Change (UNFCCC): 1998, 'The Kyoto Protocol to the UNFCCC', in UNFCCC, Report of the Conference of the Parties Third Session, Kyoto, UNFCCC, pp. 4–29.

Verdin J., Funk C., Senay G., Choularton R., 2005. Climate science and famine early warning. Philos Trans R Soc Lond, B 360(1463):2155–2168.

Verheyen, R., 2005. Climate Change Damage and International Law: Prevention, Duties and State Responsibility.Martinus Nijhoff, Netherlands, 418 pp.

Valke, S., Terray, L., Piacentini, A., 2000. The OASIS coupled user guide version 2.4, Technical Report TR/ CMGC/00-10, CERFACS.

Waldman, S.E., Rickman, R.W., 1996. MODCROP: a crop simulation framework. Agron. J. 88, 170–175.

Wallach D., 2006. Evaluating crop models, Chapter 2 in: Working with Dynamic Crop Models. Edited by Wallach D., Makowski D., and Jones W. Elsevier B.V.

Wallis, T.W.R., and Griffiths, J.F. (1995). An assessment of the weather generator (WXGEN) used in the erosion/productivity impact calculator (EPIC). Agriculture for Meteorology. 73, 115-133.

Webb L.B., Wheton P.H., Barlow E.W.R., 2008. Climate change and winegrape quality in Australia. Clim Res 36:99–111.

Weiske, A., Vabitsch, A., Olesen, J.E., Schelde, K., Michel, J., Friedrich, R., Kaltschmitt, M., 2006. Mitigation of greenhouse gas emissions in European conventional and organic dairy farming. Agric. Ecosyst. Environ. 112, 221-232.

West TO, Marland G (2002) A synthesis of carbon sequestration, carbon emissions,and net carbon flux in agriculture: comparing tillage practices in the United States. Agr Ecosys Environ 91:217–232

Wheaton, E.E. and McIver, D.C., 1999. A framework and key questions for adapting to climate variability and change. Miti. & Adapt. Strat. for Glob. Change 4, 215–225.

Whetton P.H., Fowler A.M., Haylock M.R., Pittock A.B., 1993. Implications of climate change due to the enhanced greenhouse effect on floods and droughts in Australia. Climate Change 25, 289-317.

Wheeler, T. R., Ellis, R. H., Hadley, P., Morison, J. I. L., Batts, G. R. and Daymond, A. J., 1996. Assessing the effects of climate change on field crop production. Aspects Appl. Biol. 45, 49–54.

Wilbanks, T. J., 2005: Issues in developing a capacity for integrated analysis of mitigation and adaptation, Environmental Science & Policy, 8 (6), 541-547.

Wilbanks T.J., Leiby P., Perlack R. J., Ensminger T., Wright S.B., 2007. Toward an integrated analysis of mitigation and adaptation: some preliminary findings. Mitig Adapt Strat Glob Change (2007) 12:713–725.

Wilks D., 1999. Interannual variability and extrem-value characterisitcs of several stochastic daily precipitation models. Water Resour Res 34: 2995–3008.

Willmott CJ, 1981. On the validation of models. Physical Geography 2, 184-194.

Willmott CJ, 1982. Some comments on the evaluation of model performance. Bull. Am. Meteorol. Soc. 63: 1309-1313.

de Wit, C.T., Goudriaan, J., 1974. Simulation of ecological processes. Simulation monographs. Centre for Agricultural Publishing and Documentation (Pudoc). Wageningen, Netherlands.

Wolf, J. and van Diepen, C. A.: 1995, 'Effects of climate change on grain maize yield potential in the European Community', Climatic Change 29, 299–331.

Wolf J., 1996. Effects of nutrient supply (NPK) on spring wheat response to elevated atmospheric CO_2. Plant Soil 185:113–123.

Xevi et al., 1996 E. Xevi, J. Gilley and J. Feyen, Comparative study of two crop yield simulation models, Agric. Water Manage. **30** (1996), pp. 155–173.

Žalud, Z. and Dubrovský, M.: 2002, 'Modelling Climate Change Impacts on Maize Growth and Development', Theor. Appl. Climatol. 72, 1–2, 85–102.

Zorita E., von Storch H., 1999. The analog method as a simple statistical downscaling technique: comparison with more complicated methods. J Climate 12: 2474–2489.

ACKNOWLEDGMENTS

Throughout my three years of Ph.D. I had the pleasure and honour to get to know many special people, who have contributed to enrich my knowledge and experience background and whom I wish now to thank with sincere affection.

First of all, Professor Donatella Spano, whose precious supervision, suggestions and continuous confrontation supported every step of this work and whose great generosity has guided my personal and professional growth, by assigning me ever-new challenges and responsibilities.

A special thank to Dr. Carla Cesaraccio, whose distinctive passion and scientific uprightness have been by my side along this way, and with whom I have shared so many times of discussion, always stimulating and constructive.

I would like to thank the Chair of Department of Economics and Woody Plant Ecosystems, Professor Piero Deidda, and the Head of CNR-Ibimet di Sassari, Dr. Pierpaolo Duce, for allowing me to enhance my experience also by offering me a chance to compare it to other professional and cultural cases.

A warm and due thank to Dr. Martin Dubrovsky, for his simplicity and professionalism with which he introduced me to the wonderful world of climate scenarios and their issues; for his kindness and hospitality, which made my stay in the Czech Republic more pleasant and for giving me an opportunity to meet and cooperate with his inspiring workgroup, with special reference to Professor Zdenek Zalud, Dr. Mirek Trnka and Dr. Petr Hlavinka of Mendel University of Agriculture and Forestry in Brno.

Another special thank goes to Dr. Gianluca Carboni, my colleague and friend, with whom I often shared doubts and problems and whose distinct professionalism has been able to provide me with some valuable advice and actual aid to face the many difficulties arisen during the development of this work.

So many more people should be mentioned here, such as Dr. Andrea Motroni, Dr. Marco Dettori, Pierpaolo Zara, Dr. Ileana Iocola and all those who shared their experiences and knowledge with me, allowing me to improve my professional progress.

I also would like to thank all my colleagues and friends, Dr. Valentina Bacciu, Dr. Michele Salis, Dr. Stefania Pisanu and Dr. Serena Marras, Dr. Costantino Sirca, Dr. Luca Mercenaro, Dr. Annapaola Chergia, Dr. Marina Carta and Dr. Pasquangela Muresu, Pierpaolo Pani and Dr. Rita Marras and all those whom I am probably not mentioning now, but who were present during these

three years and with whom I have shared both work and leisure; each of them was able to motivate me with their passion and dedication for this special world of research.

I would like to thank Tore, Cipriano, Francesca and those who have endured my moments of daily discouragement: my old friends Mariangela, Paola, Alessio, and even those whom I may have lost on my way…thank you for letting me enjoy a better experience!

My final thanks are, last but not least, for my family – my beloved parents, for whom no thanking word would ever be enough, and my brother Pierpaolo, who have always been there with their love, to share with me the good and bad times that I had to face during these years, by offering me their precious advice and, most of all, by encouraging and supporting every choice of mine unconditionally.

RINGRAZIAMENTI

Durante questi tre anni di dottorato ho avuto il piacere e l'onore di conoscere tante persone speciali che hanno arricchito il mio bagaglio di conoscenze e di esperienza e che ora vorrei ringraziare con sincero affetto.

Prima fra tutte la Prof. Donatella Spano, che con la sua preziosa guida, i suggerimenti e il continuo confronto, ha sostenuto ogni fase di questo lavoro e con grande generosità ha guidato la mia crescita personale e professionale, affidandomi sempre nuove sfide e responsabilità.

Un ringraziamento speciale alla Dr. Carla Cesaraccio, che con la passione e il rigore scientifico che la contraddistinguono mi ha affiancato in questo percorso e con la quale ho condiviso tanti momenti di discussione, sempre stimolanti e costruttivi.

Al direttore del Dipartimento di Economia e Sistemi Arborei, il Prof. Piero Deidda e al direttore del CNR-Ibimet di Sassari, Dr. Pierpaolo Duce, per avermi permesso di arricchire questa esperienza anche grazie al confronto con altre realtà professionali e culturali.

Un sentito e doveroso ringraziamento al Dr. Martin Dubrovsky, per la professionalità e al tempo stesso la semplicità con cui mi ha introdotto nel magnifico mondo degli scenari climatici e delle loro problematiche. Per la gentilezza e l'ospitalità con cui ha allietato il mio soggiorno in Repubblica Ceca e per avermi dato l'opportunità di incontrare e collaborare con il suo stimolante gruppo di lavoro. Mi riferisco in particolare al Prof. Zdenek Zalud, al Dr. Mirek Trnka e al Dr.Petr Hlavinka della Mendel University of Agriculture and Forestry di Brno.

Un ringraziamento speciale al, collega e amico, Dr. Gianluca Carboni, con cui ho condiviso spesso dubbi e problematiche e che , con grande professionalità, ha saputo darmi preziosi consigli e concreti aiuti per affrontare i diversi problemi incontrati in questo lavoro.

Ancora tantissime sarebbero le persone da citare, tra cui il Dr. Andrea Motroni, il Dr. Marco Dettori, Pierpaolo Zara, la Dr. Ileana Iocola e tutti coloro che hanno condiviso con me le loro esperienze e conoscenze permettendomi di migliorare la mia crescita professionale.

Ringrazio ancora tutti i colleghi e amici, la Dr. Valentina Bacciu, il Dr. Michele Salis, la Dr. Stefania Pisanu e la Dr. Serena Marras, il Dr. Costantino Sirca, il Dr. Luca Mercenaro, la Dr. Annapaola Chergia, la Dr. Marina Carta e la Dr. Pasquangela Muresu, Pierpaolo pani e la Dr. Rita Marras, e tutti i coloro di cui ora forse sto dimenticando i nomi ma che sono stati presenti in questi 3 anni e con cui ho condiviso momenti di lavoro e di divertimento, persone che con le loro differenze mi hanno tutte trasmesso passione e dedizione per questo speciale mondo della ricerca.

Ringrazio Tore, Cipriano, Francesca e chi ha sopportato i frequenti momenti di quotidiano sconforto, gli amici di sempre Mariangela, Paola, Alessio, e anche quelli che ho perso per strada.. perché grazie a loro quest'esperienza è stata più bella!

Un ringraziamento finale, ma non ultimo, va alla mia famiglia, ai miei amati genitori… per i quali nessuna parola è grande abbastanza, e a mio fratello Pierpaolo, che con il loro amore sono stati sempre presenti, hanno condiviso con me i momenti belli e meno belli che in questi anni mi sono trovata ad affrontare, dandomi preziosi consigli ma soprattutto incoraggiando e sostenendo incondizionatamente ogni mia scelta.